Effects of oestrogenic chemicals on the liver

Stephanie Kristin Meyer

BSc, MRes.

Thesis submitted for the degree of Doctor of Philosophy

Newcastle University

Faculty of Medical Sciences

Institute of Cellular Medicine

March 2017

Abstract

Our environment and diet contains a variety of man-made endocrine disrupting chemicals which may pose a significant health threat for wildlife and humans. In particular, there is increasing concern regarding the adverse effects caused by xenoestrogens which are believed to trigger many endocrine-related diseases. Since high systemic levels of oestrogens are cholestatic, it was investigated whether xenoestrogens are able to cause adverse hepatic effects *in vivo* in mouse models and whether these effects are mediated by interaction with the murine oestrogen receptors (ERs).

The food dye tartrazine has previously been shown to activate the human ERα and intraperitoneal injection caused cholestasis in mice. In this study, tartrazine failed to activate murine ERα and two murine ERβ variants *in vitro* suggesting that cholestasis occurred independent of the ERs. Data indicate, however, that tartrazine, its major metabolites and a contaminant inhibited murine dopamine sulfotransferase. Considering the role of sulfotransferases in bile acid secretion, these findings suggest that impairment of bile acid sulfation and subsequent secretion may be a key event in tartrazine-mediated cholestasis. Oral exposure to tartrazine caused inflammation in the liver and gastrointestinal tract *in vivo* in mice without evidence of cholestatic effects.

Several soil extracts prepared from soil samples collected from around an urban landfill site activated human and murine ERα and two murine ERβ variants *in vitro*. Pooled oestrogenic soil extracts had mild cholestatic effects in a mouse model. Given the cholestatic features of the liver disease primary biliary cholangitis (PBC), which is linked to exposure to xenobiotics associated with a toxic environment and proximities to waste sites, environmental xenoestrogens could be a component of a xenobiotic insult that triggers PBC.

These findings indicate that if significant exposure to environmental xenoestrogens occurs, they can have adverse hepatic effects and may be part of a trigger process in cholestatic liver diseases.

Acknowledgements

First and foremost I would like to thank my supervisors Professor Matthew Wright, Dr Paul Jowsey and Professor Peter Blain for their support and motivation over the past four years. I owe an extended gratitude to Professor Matthew Wright who was always extremely enthusiastic, knowledgeable and helpful and offered invaluable assistance, encouragement and guidance throughout my PhD.

I would like to thank all the members of 'Team Wright' past and present: Emma Fairhall, Ally Leitch, Anne Lakey, Rod Figueiredo, Fouzeyyah Alsaeedi, Hussein Al-Sammak, Izzy Swidenbank and especially Philip Probert who has helped me in numerous ways with lab work. I will miss the Team Wright nights out! Huge thanks also to the MTC crew Preeti Singh-Aresh, Eliona Tsefou, Daniel Erskine, Lina Patterson and Israa Al-Banaa for their office banter and endless supply of cake and chocolate which fuelled me on long days in the lab. I couldn't have wished for a better office to work in!

I am also indebted to my friends outside the lab for their abundant support and who have helped to keep me sane. Preeti, Bala, James and Fadi, I could always count on you to cheer me up on bad days and celebrate the good ones.

Importantly, I would like to express my deepest gratitude to my family for their unconditional love and support with everything I do. It would not have been possible to complete this thesis without them.

Finally, I would like to thank Brendan for his tremendous support and patience over the past four years. Without his encouragement and love none of this would have been possible.

Publications and Abstracts

Publications

Meyer, S.K., Probert, P.M., Lakey, Leitch A.C., A.K., Blake, L.I., Jowsey, P.A., Cooke, M.P., Blain, P.G., Wright M,C, Environmental xenoestrogens super-activate a variant murine ER beta in cholangiocytes. *Toxicological Sciences.* Advance online publication. doi: 10.1093/toxsci/kfw234

Meyer, S.K., Probert, P.M., Lakey, A.K., Axon, A.A., Williams, F.M., Jowsey, P.A., Blain, P.G., Kass, G.E.N., Wright, M.C. Cholestatic effects of tartrazine (E102) are associated with an inhibition in sulfotransferases in the mouse. *Manuscript submitted*.

Probert, P.M.E., **Meyer, S.K**., Alsaeedi, F., Axon, A.A., Fairhall, E.A., Wallace, K., Charles, M., Oakley, F., Jowsey, P.A., Blain., P.G., Wright, M.C. An expendable donor-free supply of functional hepatocytes for toxicology. *Toxicology Research*, 203-222 (2015).

Abstracts

Meyer, S.K., Charles, M., Jowsey, P.A., Blain, P.G., Wright, M.C. No role for the estrogen receptor in pancreatic progenitor B-13 cell line trans-differentiation to functional hepatocyte-like cells (B13/H). British Toxicology Society Annual Congress 2014

Meyer, S.K., Axon, A.A., Jowsey, P.A., Williams, F.J., Blain, P.G., Wright, M.C. Tartrazine is not an activator of the mouse oestrogen ERα and ERβ receptors. *Toxicology letters*, S180 (2014).

Meyer, S.K., Axon, A.A., Jowsey, P.A., Williams, F.J., Blain, P.G., Wright, M.C. Tartrazine is not an activator of the mouse oestrogen ERα and ERβ receptors. North East Postgraduate Conference 2014

Meyer, S.K., Axon, A.A., Jowsey, P.A., Williams, F.J., Blain, P.G., Wright, M.C. Investigating if tartrazine is an activator of the mouse oestrogen receptors to establish whether an experimental mouse model is suitable for studying potential adverse effects. British Toxicology Society Annual Congress 2015

Meyer, S.K., Axon, A.A., Probert, P.M.E., Jowsey, P.A., Williams, F.J., Blain, P.G., Wright, M.C., Investigating hepatic and gastrointestinal effects of tartrazine in an experimental mouse model. EFSA's second scientific conference 2015

Declaration

I hereby declare that this thesis has been composed by myself and has not been accepted in application of a degree. All work was performed by myself unless otherwise stated. All sources of information have been acknowledged appropriately by means of a reference.

Stephanie Meyer

Table of Contents

List of Figures

List of Tables

List of Abbreviations

2-OADC	2-oxoacid dehydrogenase complex
aa	Amino acid
ABC	ATP-binding cassette
ADI	Acceptable daily intake
AF-1	Activation function -1
AF-2	Activation function -2
ALD	Alcoholic liver disease
ALP	Alkaline phosphatase
ALT	Alanine transaminase
AMA	Antimitochondrial antibody
ANIT	Alpha-naphthyl isothiocyanate
AP-1	Activator protein-1
ATP	Adenosine triphosphate
BCKD	Ketoacid dehydrogenase
BEC	Biliary epithelial cell
BPA	Bisphenol A
BSA	Bovine serum albumin
BSEP	Bile salt export pump
CAR	Constitutive androstane receptor
cDNA	complementary DNA
CK19	Cytokeratin 19
CV	Central vein
CYP450	Cytochrome P450
DBD	DNA binding domain
DMEM	Dulbecco's Modified Eagles Medium
DMSO	Dimethyl sulfoxide
DNA	Deoxyribonucleic acid
DTT	Dithiothreitol
E1	Oestrone
E2	17β-oestradiol

E3	Oestriol
EDC	Endocrine disrupting chemical
EE	Ethinyl oestradiol
ER	Oestrogen receptor
ERE	Oestrogen response element
ERR	Oestrogen related receptors
FBS	Foetal bovine serum
FMO	Flavin containing monooxygenase
GAPDH	Glyceraldehyde 3-phosphate dehydrogenase
GF	Growth factor
GFP	Green fluorescent protein
GFR	Growth factor receptor
GI	Gastrointestinal
H&E	Haematoxylin and eosin
hBEC	Human biliary epithelial cell
HBSS	Hank's Balanced Salt Solution
hER	Human oestrogen receptor
HRP	Horseradish peroxidase
HSC	Hepatic stellate cells
i.p.	Intraperitoneal
ICI	ICI182,780
IVIS	*In vivo* imaging system
KGD	Ketoglutarate dehydrogenase
LBD	Ligand binding domain
LDS	Lithium dodecyl sulfate
LPS	Lipopolysaccharide
MAPK	Mitogen-activated protein kinase
mBEC	Mouse biliary epithelial cell
MDR	Multidrug resistance protein
mER	Mouse oestrogen receptor
mERα	Mouse oestrogen receptor α
mERbv1	Mouse oestrogen receptor β transcript variant 1

mERbv2	Mouse oestrogen receptor β transcript variant 2
Mwt	Molecular weight
NCBI	National Center for Biotechnology Information
NF- κB	Nuclear factor-κB
NK cells	Natural killer cells
NTCP	Na(+)/taurocholate co-transporting polypeptide
OSPCA	5-oxo-1-(4-sulphophenyl)-2-pyrazoline-3-carboxylic acid
PAPS	3′-phosphoadenosine 5′-phosphosulfate
PBB	Polybrominated biphenyls
PBC	Primary biliary cholangitis
PBS	Phosphate buffered saline
PCB	Polychlorinated biphenyls
PCR	Polymerase chain reaction
PDC	Pyruvate dehydrogenase complex
PEI	Polyehtyleneimine
PFIC	Progressive familial intrahepatic cholestasis
rER	rat oestrogen receptor
RNA	Ribonucleic acid
RNS	Reactive nitrogen species
ROS	Reactive oxygen species
rRNA	Ribosomal ribonucleic acid
RT-PCR	Reverse transcriptase polymerase chain reaction
SA	Sulfanilic acid
SA-NAc	Sulfanilic acid N-acetate
SCAP	1-(4-sulfophenyl)-3-carboxy-4-amino-5-pyrazolone
SEC	Sinusoidal endothelial cells
SERD	Selective oestrogen receptor degrader
SERM	Selective oestrogen receptor modulator
SP-1	Specificity protein-1
SPH	4-sulfophenylhydrazine
SULT	Sulfotransferase
T	Tartrazine

TBS	Tris-buffered saline
TF	Transcription factor
tg	Transgenic
TNFα	Tumor necrosis factor alpha
wt	Wild type

Chapter 1. Introduction

The development of novel medicines and materials for products has significantly contributed to the presence of synthetic chemicals within the environment. There is increasing concern regarding the adverse effects that these xenobiotics may cause in wildlife and humans. Extensive research has shown that many of these chemicals have the potential to disrupt the endocrine system which may lead to the development of endocrine-related diseases (e.g., reproductive disorders, metabolic disorders and cancer (Schug *et al.*, 2011)). A large proportion of chemicals were found to have oestrogenic properties thus potentially targeting normal oestrogen signalling. Oestrogenic chemicals are contained in many consumer products and our diet. In order to reduce the health risk that oestrogenic chemicals may pose, it is critical to develop a better understanding of the effects of these chemicals. Given the hepatic toxic effects that high systemic levels of oestrogens can have, work in this thesis focuses on examining the effects of oestrogenic chemicals on the liver.

1.1. The liver

The liver is the largest internal organ as well as the largest gland in the human body. It is of brownish-red colour and located in the right upper portion of the abdominal cavity beneath the diaphragm and to the right above the stomach (Figure 1.1). Weighing between 1300-1800 g depending on body size and gender, the liver contributes to approximately 2% of a healthy adult's total body weight. A thin layer of fibrous tissue called the Glisson's capsule, sheaths the liver and extends within to support inter- and intralobular vessels. The liver is further encased by the peritoneum, a serous membrane for protection and reduction of friction against other organs. A number of ligaments, namely the falciform, round, coronary and triangular ligaments hold the liver in place by anchoring it to the abdominal wall and diaphragm (Figure 1.2A) (Monga, 2011).

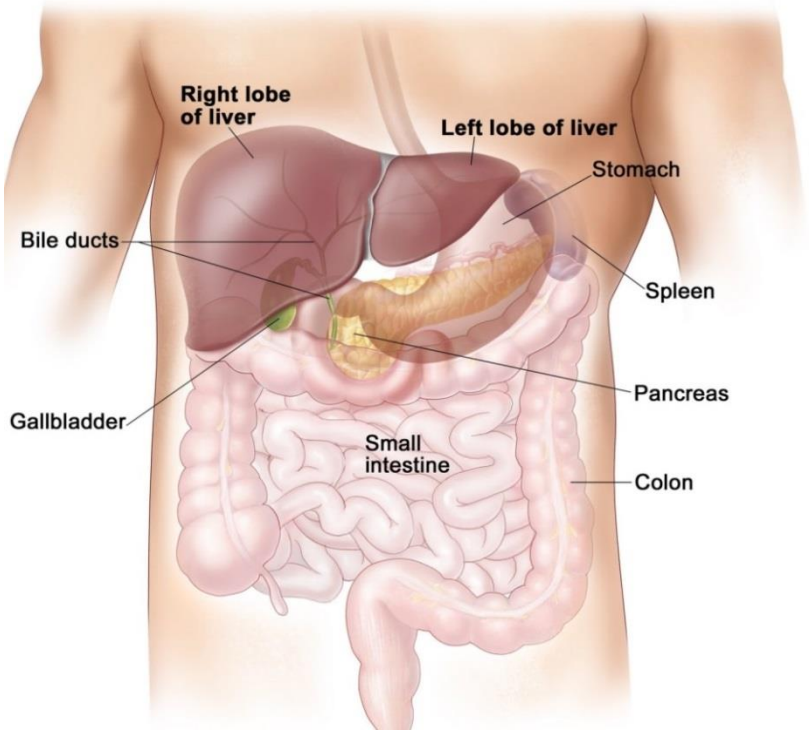

Figure 1.1 Location of the liver in the human body. Source: Herbal Health (2014).

1.1.1. Anatomy

The human liver is commonly described to consist of four primary lobes: the left, right, caudate and quadrate lobe. From an anterior view, the left lobe and the larger right lobe are separated by the falciform ligament (Figure 1.2A). The caudate and quadrate lobes are located at the posterior and inferior sides of the right lobe. A more precise way to characterise the liver's functional anatomy, however, is described by the Couinaud classification. By looking at the vascular in and out flow, this classification allows for subdivision of the liver into eight segments. Each segment is supplied by a portal vein, hepatic artery and bile duct generally known as the portal triad (or portal tract), and drained by a hepatic vein located in the periphery of each segment (Figure 1.2B).

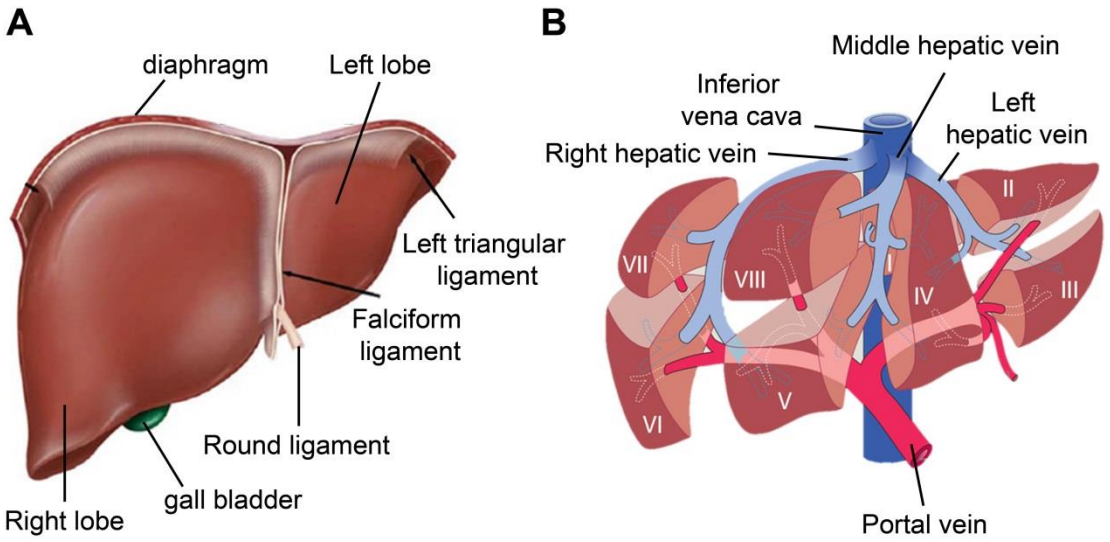

Figure 1.2 Anatomy of the human liver. A. Anterior view of the liver. The falciform ligament separates the left and right lobes of the liver. A number of other ligaments including the round and left triangular ligaments anchor the liver to the abdominal wall and diaphragm. Adapted from Brunicardi et al. (2010)**. B. Couinaud segmentation of the liver.** According to Couinaud, the liver can be divided into 8 segments. Each segment is supplied with blood by a portal vein and drained by a hepatic vein in the periphery of each segment. Hepatic veins converge to form three major hepatic veins, the right, middle and left, which empty into the inferior vena cava. Adapted from Dancygier (2009).

1.1.2. Intrahepatic vascular system

1.1.2.a Blood flow

The liver has a dual blood supply which means that it receives blood from two sources: the portal vein and the hepatic artery. Around 75% of the blood is delivered by the portal vein which carries partially oxygenated and nutrient- and toxin-rich blood collected from the intestinal system, spleen and pancreas. The hepatic artery delivers the remaining blood (~25 %) which is rich in oxygen but nutrient-poor. Mixing of the portal venous and arterial blood takes place mainly in the hepatic capillaries, termed liver sinusoids. Sinusoids possess a fenestrated endothelium which allows oxygen and nutrients to be delivered to hepatocytes, the main cell type of the liver. Liver sinusoids eventually intersect to create the central vein at the centre of the liver's functional unit, the lobule, from where the blood is drained from the liver. Central veins combine to form three major hepatic veins and the blood is emptied into the inferior vena cava which carries de-oxygenated blood to the right atrium of the heart (Kuntz and Kuntz, 2009).

1.1.2.b Biliary system

Bile produced by hepatocytes is transported to the duodenum through a complex network of bile ducts which increase in size the closer they are located to the duodenum. Bile canaliculi, formed by the apical membrane surfaces of 2-3 neighbouring hepatocytes are the smallest unit of the three-dimensional biliary system. Actin and myosin filaments in the ectoplasm of hepatocytes support the transport of canalicular bile towards an area called canals of Hering. This area is partly lined by hepatocytes and biliary epithelial cells and serves as the link between bile canaliculi and bile ductules of the biliary tree. From the canals of Hering, bile flows into pre-ductules which continue into cholangioles. Cholangioles converge to interlobular bile ducts running along the portal triad. Through a series of increasingly wider bile ducts, bile leaves the liver through the right and left hepatic ducts which eventually empty into the common bile duct (Dancygier, 2009; Kuntz and Kuntz, 2009).

1.1.2.c Lymphatics

Most of the lymph in the body is generated by the liver. Its primary site of production in the liver is the perisinusoidal space between hepatocytes and the liver sinusoids, referred to as the space of Disse. Through lymph capillaries, lymph is transported to the space of Mall, the periportal space between the connective tissue of the portal tract and adjacent hepatocytes. From here lymph flows through lymph vessels that increase in size and exit the liver though lymph nodes (Dancygier, 2009; Kuntz and Kuntz, 2009).

1.1.3. Functional units of the liver

The liver's complex architecture is subject to a distinctive vascular pattern in which a system of blood vessels and bile ducts infiltrates the parenchymal tissue. Several models for the functional unit of the liver have been proposed, mirroring the organs functional diversity. Each model describes the hepatic functional unit from a different angle, considering different aspects such as morphology, structure, microcirculation and functionality. The two most commonly used models to describe the functional hepatic unit are the liver lobule and the liver acinus.

1.1.3.a Liver lobule

The liver lobule was first defined by Kieran in 1833 and this model mainly describes the functional unit of the liver from a structural and anatomical perspective. Cross-sectioned, the lobule features a hexagon which is defined by portal triads surrounding the central vein located at the centre (Figure 1.3A). Blood enters the liver lobule through the portal vein and

hepatic artery and flows towards the central vein with oxygen and substrate levels falling. Blood may also enter adjacent lobules. Bile flows in the opposite direction towards the bile duct in the portal triad. An adult liver contains around 1.0-1.5 million lobules (Kuntz and Kuntz, 2009).

1.1.3.b Liver acinus

The liver acinus was first described by Rapport and is the preferred model for histopathologists because it assists in the description of pathological lesions (Wallace *et al.*, 2008). In contrast to the liver lobule, this concept of the hepatic functional unit is descriptive of functional and structural correlations and concentrates on the secretory and metabolic functions of the liver. In this model, blood enters the acinus via the portal vein and hepatic artery and is drained radially towards central veins located to the left and right periphery of the acinus (Figure 1.3B). The centre of the acinus comprises the terminal branches of the hepatic artery and portal vein. According to their distance from the portal triad, hepatocytes are situated along a gradient of oxygen and substrates and are therefore allocated to one of three zones. Zone 1 is closest to the portal triad and receives blood high in oxygen and substrates which decrease along Zone 2. Zone 3 is situated closest to the central vein and contains blood low in oxygen and substrates. The bile flow occurs centripetally, opposite to the direction of the blood flow (Kuntz and Kuntz, 2009).

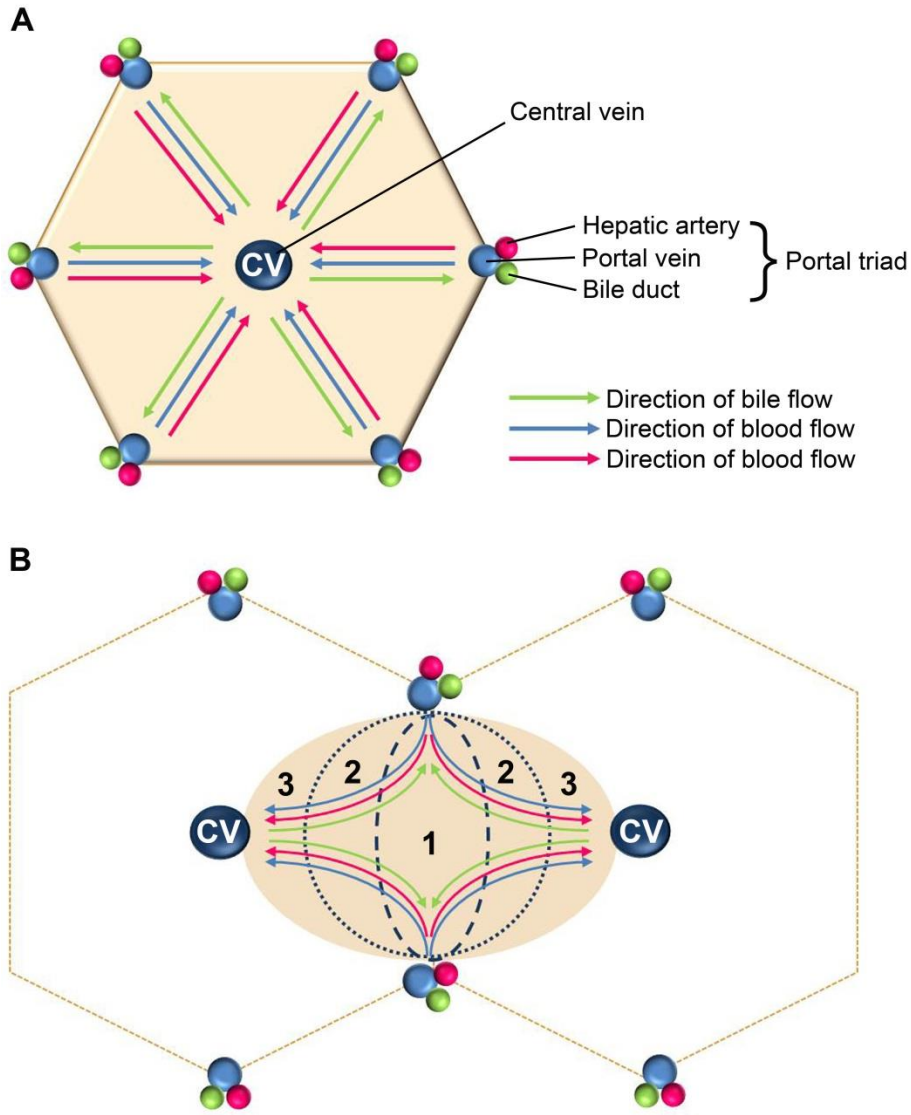

Figure 1.3 Schematic diagrams of the functional units of the liver. (A) Liver lobule. In the model of the liver lobule, blood enters the unit through the portal vein and hepatic artery which, together with the bile duct, form the portal triad. As the blood flows towards the central vein (CV), oxygen and nutrient levels decrease. Note that blood may also flow into adjacent lobules. (**B) Liver acinus.** In the liver acinus, blood delivered via the portal vein and hepatic artery is thought to remain within the acinar structure as it flows through Zone 1 to 3 towards the central veins in the periphery. A decrease in oxygen and substrate levels can be observed within the different zones with Zone 1 containing the highest and Zone 3 the lowest levels. Adapted from Wallace *et al.* (2008).

Not only do the zones correspond with oxygen and substrate supply, hepatocytes can also be divided into zones depending on their enzymatic and metabolic capacity which is referred to as metabolic heterogeneity (Kuntz and Kuntz, 2009). Based on the model example of cytochrome P450 (CYP450) gene expression, hepatocytes in the periportal region (Zone 1) express low levels of CYP450 enzymes whereas centrilobular hepatocytes surrounding the central vein (Zone 3) express high levels of CYP450. Although periportal hepatocytes are exposed to higher levels of toxins, the damage is generally detected in the centrilobular region due to the presence of high levels of metabolising CYP450 enzymes (Dancygier, 2009).

1.1.4. Microarchitecture of the liver

Within the lobular and acinar hepatic structures, hepatocytes are arranged in plates which radially extend towards the central vein. In mammals, each plate is one cell thick and comprises 15-25 hepatocytes. The plates of hepatocytes are surrounded by sinusoids which facilitate the blood flow from the portal vein and hepatic artery towards the central vein. Hepatic sinusoids are lined by fenestrated endothelial cells (see also Section 1.1.5) which direct the exchange of materials between the blood and the basolateral hepatocyte surface. The sinusoidal lumen known as the space of Disse contains extracellular matrix components which support the parenchyma and are fundamentally important for hepatocyte proliferation and regeneration. With their apical surface membranes, hepatocytes form bile canaliculi which direct the bile flow towards the bile duct (Figure 1.4) (Dancygier, 2009; Kuntz and Kuntz, 2009).

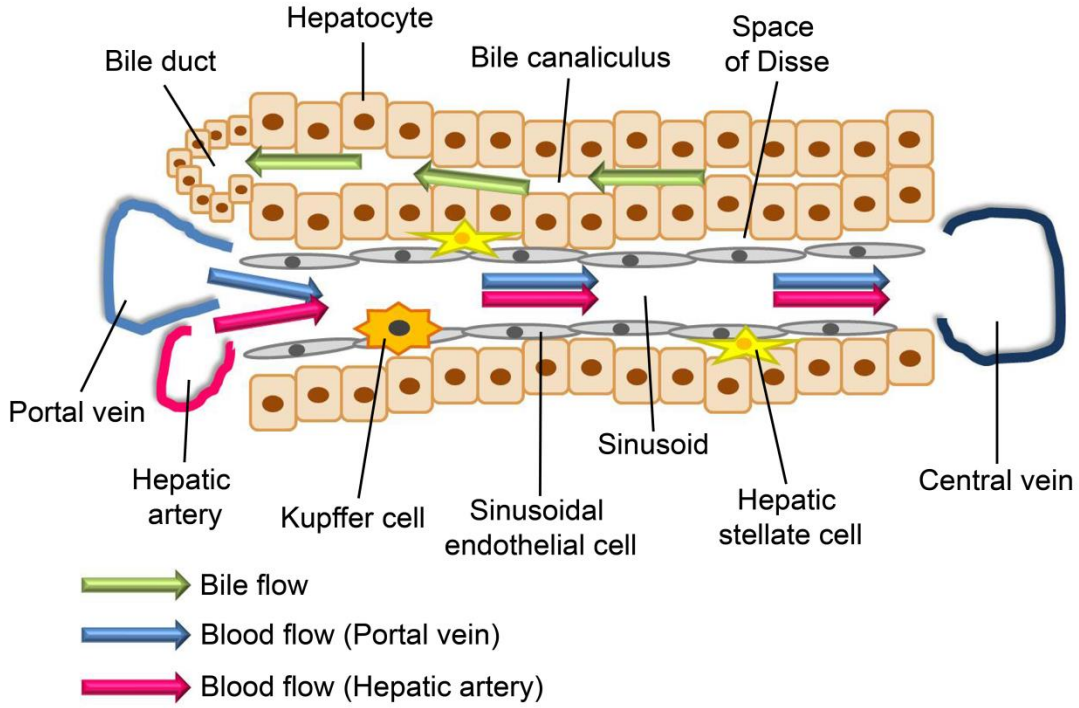

Figure 1.4 Schematic diagram of the hepatic microarchitecture. Blood supplied by the portal vein and hepatic artery mixes in the liver sinusoid through which it flows towards the efferent central vein. Sinusoids are lined by sinusoidal endothelial cells and infiltrate the liver parenchyma. Hepatocytes are arranged in plates and secrete bile into the bile canaliculus. Bile flow occurs opposite to the direction of the blood towards the bile duct.

1.1.5. Cells of the liver

The liver comprises at least 7 different cell types which can broadly be divided into parenchymal (hepatocytes) and non-parenchymal cells (all other liver cells). Non-parenchymal cells can further be subcategorised into a cell population called sinusoidal cells

which are cells associated with the liver sinusoids. These include sinusoidal endothelial cells, Kupffer cells, hepatic stellate cells and Pit cells. Biliary epithelial cells and oval cells complete the list of non-parenchymal cells. The following sections will describe the different cell types which are crucial to normal functioning of the liver (Kuntz and Kuntz, 2009; Monga, 2011).

1.1.5.a Hepatocytes

Hepatocytes are the main hepatic functional cells and account for approximately 80% of the total volume of the liver. They have many important roles including detoxification, metabolism and protein synthesis and are therefore responsible for the liver's metabolic and synthetic functions. Hepatocytes are surrounded by sinusoids and are involved in the exchange of a variety of substances present in the blood. Given their location, hepatocytes are structurally polarised with three distinct surfaces: the sinusoidal (basolateral) side which faces the sinusoids; the canalicular (apical) surface forms the bile duct network; and the lateral sides. The sinusoidal membrane of the hepatocyte accounts for around 37% of the membrane surface and contains many microvilli which extend into the space of Disse as well as into the sinusoids facilitating the bi-directional exchange of substrates and proteins (Kuntz and Kuntz, 2009). The canalicular surface makes up approximately 15% of the hepatocyte surface and faces the bile canaliculus which collects and transports bile generated by hepatocytes to the bile ducts. Neighbouring hepatocytes are linked by intercellular adhesion complexes on their lateral sides allowing for the separation of the perisinusoidal space from the bile canaliculi, therefore forming the blood-bile barrier. The expression of a large diversity of membrane-associated transport proteins on the hepatocyte surface further contributes to their secretory and absorptive functions (Kuntz and Kuntz, 2009; Monga, 2011).

1.1.5.b Sinusoidal endothelial cells

Sinusoidal endothelial cells (SECs) line the network of liver sinusoids and constitute approximately 50% of the non-parenchymal cell type. Positioned on a layer of extracellular matrix, SECs are primarily involved in the regulation of transport and exchange of fluids and material between the blood and the subjacent hepatocytes. Unlike other mammalian endothelial cells, SECs have a distinctive phenotype in that they lack a basal membrane but possess pores and fenestrae which are essential to filtering solutes from the blood and allow for solutes to pass the endothelium. To further enhance the exchange of solutes and fluids from the blood, SECs possess a number of specific receptors on their surface for incorporation and transport of material to hepatocytes (Dancygier, 2009; Monga, 2011).

1.1.5.c Hepatic stellate cells

Hepatic stellate cells (HSCs), also known as Ito cells or fat storing cells, represent around 25% of the of the non-parenchymal liver cell population. They are situated in the space of Disse, between hepatocytes and SECs (see also Figure 1.4). In the normal liver, HSC are usually in a quiescent state in which their primary functions are the storage of retinoids (Vitamin A) as esters with fatty acids (retinylesters), as well as the secretion of non-fibril extracellular matrix components. In the injured liver, HSCs are predominantly found in an activated state, induced by various inflammatory signals including reactive oxygen species (ROS), cytokines and chemokines. When they become activated, HSCs transdifferentiate into a myofibroblast-like cell and lose their ability to store retinylesters. Activated HSCs further produce a number of cytokines and secrete fibrillary components of the extracellular matrix which makes them the key contributor to the development and progression of liver fibrosis. Their ability to contract and modulate the sinusoidal blood flow is thought to further enhance the progression of hepatic fibrosis (Dancygier, 2009; Monga, 2011).

1.1.5.d Kupffer cells

Kupffer cells are the residential macrophages of the liver and account for around 20% of non-parenchymal liver cells. They migrate along the endothelium of the sinusoids and are more abundantly found in periportal regions (Kuntz and Kuntz, 2009) (see Figure 1.4). Kupffer cells make up the first line defence by responding to gut-derived bacterial and fungal components delivered via the portal vein (Monga, 2011). Once activated, Kupffer cells release a number of pro-inflammatory cytokines including tumour necrosis factor alpha (TNFα). The activation of Kupffer cells by the gut-derived bacterial component endotoxin, a lipopolysaccharide (LPS), has been extensively studied and will be further discussed in Section 1.5.3.

1.1.5.e Pit cells

Pit cells are natural killer (NK) cells specific to the liver. They are granular lymphocytes mainly found in the liver sinusoids and the space of Disse where they communicate with SECs and Kupffer cells. The primary function of Pit cells is to eliminate tumour, necrotic and foreign cells. It has also been proposed that they may destroy virally infected cells (Kuntz and Kuntz, 2009; Monga, 2011).

1.1.5.f Biliary epithelial cells

Biliary epithelial cells (BECs) or cholangiocytes line the extra- and intrahepatic bile ducts of the biliary tree and constitute 3-5% of all liver cells. Depending on their location within the biliary network, BECs display morphological and functional heterogeneity explaining why many liver diseases that directly involve bile ducts (cholangiopathies) are restricted to certain regions of the biliary tree. BECs are primarily concerned with the production and transport of bile from the liver to the gall bladder. They are responsible for the generation of the final bile composition by alkalinisation and modification of the primary bile secreted by hepatocytes. Primary cilia on their apical plasma membrane extend into the bile duct and facilitate changes in bile composition and flow. In the healthy liver, BECs arrest in G_0 phase of the cell cycle and are replicatively quiescent. Upon liver injury, however, they are able to proliferate and fill a role in the repair response which consequently may distort the structure of the bile duct network. Especially small BECs closest to the site of injury are thought to be capable of marked proliferation which incites a fibrotic response, mainly through interactions and cross-talk with other hepatic cell types (Dancygier, 2009; Monga, 2011).

1.1.5.g Oval cells

Oval cells are bi-potential hepatic progenitor cells situated in the canals of Hering, the transition zone that delivers bile from bile canaliculi formed by hepatocytes to the bile ducts of the portal triads (Dancygier, 2009). In the presence of severe liver damage or if hepatocyte proliferation is impaired, oval cells are thought to be able to differentiate into both hepatocytes and BECs, playing a crucial role in liver regeneration (Oh *et al.*, 2002; Newsome *et al.*, 2004).

1.1.6. Functions of the liver

The liver performs a vast array of metabolic and regulatory processes which are essential for an organism's health and wellbeing.

1.1.6.a Xenobiotic metabolism

One of the liver's major metabolic functions is the detoxification and clearance of xenobiotics to which the human body is exposed daily in the form of pharmaceuticals, environmental contaminants, household chemicals and dietary supplements. The general principle of drug metabolism is the conversion of a lipophilic chemical into a more water-soluble metabolite to facilitate its urinary and biliary excretion. Drug metabolism processes are carried out by drug metabolising enzymes which are most abundantly expressed in hepatocytes, making the liver

cell the centre of the detoxification process. Generally, biotransformation processes can be divided into phase I and phase II reactions. Phase I reactions are also referred to as functionalization reactions and executed by CYP450 enzymes, flavin containing monooxygenases (FMO) and alcohol and aldehyde dehydrogenases (Klaassen, 2007). Phase I enzymes catalyse oxidation, reduction, hydrolysis and hydration reactions which transform a parent compound to a more water-soluble and active metabolite by inserting a polar functional group (e.g. –OH, –COOH, –SH, $–NH_2$). Phase II reactions, also known as conjugation reactions, are executed by specific enzymes termed transferases. These enzymes conjugate active metabolites often formed in phase I with charged endogenous molecules such as activated glucuronic, sulfate, acetic or amino acids, glutathione or S-adenosyl methionine. The resulting conjugation product is more hydrophilic and more readily excreted in the urine or bile (Kuntz and Kuntz, 2009; Monga, 2011).

1.1.6.b Bilirubin metabolism

The liver is not only responsible for the elimination of xenobiotics; it also serves as a degradation and detoxification site for endogenously produced substances. An example for this is the elimination of bilirubin. Bilirubin is a breakdown product of haemoglobin and is primarily produced when ageing red blood cells are degraded in the spleen. It is a lipophilic substance and potentially toxic. Bound to serum albumin, bilirubin is transported to the liver for detoxification by hepatocytes. After separation from albumin at the sinusoidal hepatocyte membrane, free bilirubin is conjugated with glucuronic acid by specific transferases resulting in the formation of hydrophilic secondary bilirubin which is eliminated via the bile and urine (Kuntz and Kuntz, 2009).

1.1.6.c Carbohydrate metabolism

The liver plays a key role in the regulation and storage of carbohydrates and plays a significant role in the maintenance of blood glucose concentrations within a narrow range. In response to accumulation of glucose in the blood following the ingestion of carbohydrates, insulin is secreted from the pancreas promoting the uptake of glucose by hepatocytes which transform glucose molecules into glycogen for storage. During periods of fasting, blood glucose levels decrease and the liver catabolises glycogen to release glucose in response to signals such as the hormone glucagon to maintain optimal blood glucose concentrations (Kuntz and Kuntz, 2009; Monga, 2011).

1.1.6.d Protein synthesis and degradation

The liver is involved in both the synthesis and turnover of proteins and is the main site for the degradation of essential amino acids in the body. The metabolism of amino acids can result in the release of toxic ammonia which is mainly detoxified by the liver-specific urea cycle. In the urea cycle, ammonia is transformed into the less toxic urea through an array of catalytic reactions. A smaller portion of ammonia is also rendered non-toxic by the enzyme glutamine synthase which catalyses the reaction of ammonia and glutamate to glutamine. This reaction, however, only temporarily detoxifies ammonia and serves as a nontoxic ammonia transport form (Kuntz and Kuntz, 2009).

1.1.6.e Maintenance of hormonal homeostasis

Contributing to the maintenance of hormonal homeostasis, the liver plays an important role in the inactivation of steroid hormones which include androgens, oestrogens, gestagens and glucocorticoids. Glucuronidation, sulfation or hydroxylation reactions increase the hormones polarity to facilitate their excretion via the urine, intestine or skin (Kuntz and Kuntz, 2009).

1.1.6.f Lipid metabolism

The liver's functions in the metabolism of lipids include the synthesis and degradation of fatty acids as well as the maintenance of plasma lipid levels through its capacity to synthesise and secrete but also remove lipids in the form of lipoproteins from the circulation. Lipoproteins are macromolecules that consist of both lipids and proteins, essential for the transport of hydrophobic lipids in the blood. The liver also forms the majority of the body's cholesterol which is the initial substrate in steroid and bile acid biosynthesis and an important substance to form and maintain cell membranes (Kuntz and Kuntz, 2009).

1.1.6.g Bile acid metabolism

Another important function of the liver is the metabolism of bile acids. Bile acids are derived from cholesterol and are a major component of bile which facilitates the digestion and absorption of lipids in the duodenum. The synthesis of bile acid takes place exclusively in the liver and is primarily localised to centrilobular hepatocytes (Staels and Fonseca, 2009; Monga, 2011). Through a series of enzymatic reactions involving the CYP450 family of enzymes, lipophilic cholesterol is transformed into the more water soluble, primary bile acids cholic acid and chenodeoxycholic acid. To further improve their water-solubility, primary bile acids are conjugated with taurine or glycine and/or are sulfated by sulfotransferases before secretion into the bile canaliculi. Bile acids are stored in the gallbladder and are released into the

duodenum following ingestion of a meal. Enterohepatic circulation allows for 95% of bile acids to be reabsorbed from the small intestine and transported back to the liver which simultaneously serves as a feedback mechanism for bile acid synthesis (Staels and Fonseca, 2009; Monga, 2011). Alterations in bile acid homeostasis, such as through inhibition of bile acid transporters or bile acid detoxification enzymes by xenobiotics can lead to an impaired excretion and thus interruption of the bile flow through the liver, a condition known as cholestasis (Rodrigues *et al.*, 2014).

1.2. Cholestasis

Cholestasis is commonly known as a condition in which the normal bile flow through the liver is interrupted or impaired. Although a large number of possible causes exist, cholestatic conditions can generally be categorised into one of two types: an obstructive type where the bile flow is impaired by physical blockages such as gallstones or tumours; or a metabolic type, where cholestasis occurs as a result of functional defects in bile formation and secretion caused by drugs, hormones or genetic defects (Monga, 2011). As a result of an impaired bile flow, bile acids accumulate in the liver where they have toxic effects causing liver cell necrosis and apoptosis and therefore liver injury (Woolbright and Jaeschke, 2012; Woolbright *et al.*, 2015). Cholestasis also results in a build-up of bile acids in the serum which causes the common clinical symptoms typically associated with cholestatic disorders including pruritus (itchy skin) and fatigue (Kuntz and Kuntz, 2009).

There is rapidly growing interest in the role that bile acid transporters play in the development and progression of cholestasis. Hepatocytes possess a large number of sinusoidal and canalicular transport proteins involved in the uptake and excretion of bile acids. Canalicular excretion of bile salts is mediated by a range of ATP-binding cassette (ABC) transporters which are the rate-limiting step of bile formation (Trauner and Boyer, 2003; Oude Elferink *et al.*, 2006). Many cholestatic disorders have been linked to genetic defects of hepatobiliary ABC transporters such as the bile salt export pump (BSEP) or the multidrug resistance protein 3 (MDR3) (Trauner and Boyer, 2003). These hereditary mutations result in inherited progressive cholestatic liver disorders including progressive familial intrahepatic cholestasis (PFIC) (Deleuze *et al.*, 1996; Strautnieks *et al.*, 1998). Not only can cholestasis result from hereditary genetic transport protein defects, there are many other factors including drugs and hormones, such as oestrogens, that can cause acquired cholestatic disorders by directly inhibiting transport protein function or by reducing transporter protein expression (Wagner *et al.*, 2009).

1.3. Oestrogen

Oestrogens are commonly defined as the primary female sex hormones and belong to the family of steroid hormones. They are predominantly implicated in the development and regulation of the sexual reproductive system but also exert a variety of other biological functions in the immune, cardiovascular, musculoskeletal, and central nervous system (Gustafsson, 2003; Heldring *et al.*, 2007). The most potent endogenous oestrogen is 17β-oestradiol (E2) which is the major oestrogen present in pre-menopausal women. Oestrone (E1) and oestriol (E3), playing larger roles in the post-menopausal stage and during pregnancy, respectively, are metabolites of E2 and much less potent (Heldring *et al.*, 2007). Ethinyl oestradiol (EE) is a synthetic derivate of E2 and commonly used in oral contraceptive pills. The chemical structure of these oestrogens and relevant information is summarised in Table 1.1.

Name	**Structure**	**Description**
Oestrone (**E1**)	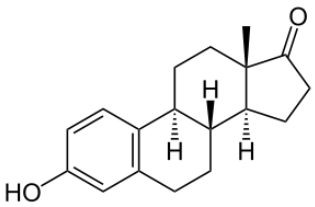	Least abundant of the three naturally occurring oestrogens. Major oestrogen found in menopausal women.
17β-oestradiol (**E2**)	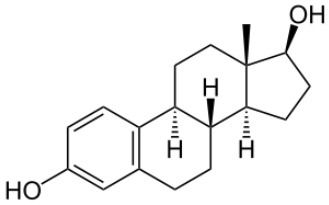	Most potent endogenous oestrogen. Most abundantly present in women but also found in men as a metabolite of testosterone.
Oestriol (**E3**)	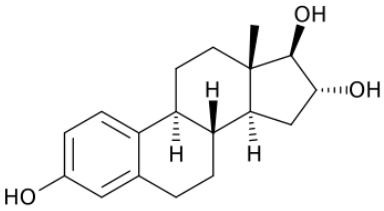	Mainly produced during pregnancy by the placenta. If not pregnant, levels in women and men are similar.
Ethinyl oestradiol (**EE**)	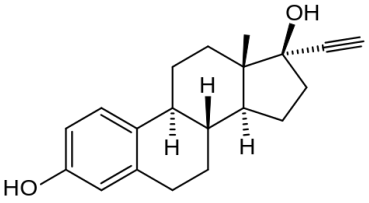	Synthetic orally bioactive derivate of E2. Present in most modern oral contraceptives.

Table 1.1 Oestrogens – chemical structure and relevant information.

1.3.1. Oestrogen synthesis and metabolism

Oestrogens are primarily synthesised in the ovaries or testes by metabolic conversion of the precursors androstenedione and testosterone (both derived from cholesterol) to E1 and E2, respectively, although extragonadal tissues such as the brain and adipose tissue produce low but significant levels of oestrogens (Mauvais-Jarvis *et al.*, 2013; Gao *et al.*, 2015). The conversion reaction is catalysed by a group of enzymes termed aromatases which belong to the cytochrome P450 superfamily (Nelson and Bulun, 2001). Oestrogen levels are tightly regulated by mechanisms which include the conversion of the most potent oestrogen E2 to the less potent E1 or E3 or by sulfation of E2 by sulfotransferases which renders E2 inactive by inhibiting its interaction with the oestrogen receptor (Cui *et al.*, 2013).

1.3.2. Oestrogen receptor

Cellular signalling of oestrogens is mediated by the oestrogen receptors (ERs), members of the nuclear receptor family of transcription factors. Two subtypes of the ER exist: the ERα (NR3A1) and the ERβ (NR3A2). For many years, the ERα was believed to be the only ER responsible for the regulation of oestrogen signalling, however, the discovery of the ERβ in 1996 altered the way in which ER signalling was understood (Green *et al.*, 1986; Greene *et al.*, 1986; Kuiper *et al.*, 1996; Mosselman *et al.*, 1996; Moore *et al.*, 1998).

ERα and ERβ are derived from distinct genes located on different chromosomes but share a high degree of sequence homology (Menasce *et al.*, 1993; Enmark *et al.*, 1997; Klinge, 2000; Heldring *et al.*, 2007; Kumar *et al.*, 2011). Both ERs consist of six functional domains, labelled A to F (see Figure 1.5). Domains A and B encode the activation function-1 (AF-1) which modulates oestrogenic transcriptional activity independent of a ligand. The central C domain contains the DNA recognition and binding region (DBD) and with 96% homology between ERα and ERβ is the most conserved domain. The hinge region can be found in the D domain and contains sequences for nuclear translocation and receptor dimerisation. The ligand-binding domain (LBD, within the E domain) encodes activation function-2 (AF-2) which regulates transcriptional activity in a ligand-dependent manner. The function of the C-terminally located F-domain was found to be involved in transcriptional activity and receptor dimerisation (Nilsson and Gustafsson, 2000; Koide *et al.*, 2007; Yang *et al.*, 2008).

The full length human ERα (hERα), regarded as the wild type form, is 595 amino acids long with an approximate size of 66 kDa (also referred to as hERα66) whereas an ERβ variant of 530 amino acids and 59 kDa is regarded as the wild type hERβ (Etienne *et al.*, 1998).

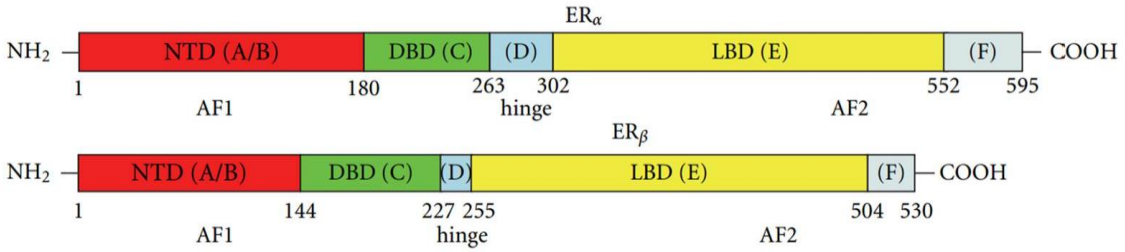

Figure 1.5 Domain organisation of the ER subtypes ERα and ERβ. Source: Kumar et al. (2011).

1.3.2.a ERs: tissue distribution and roles

ERα and ERβ exhibit both overlapping and distinctive physiological roles that are highly dependent on the tissue and cell type (Shanle and Xu, 2011). Mammalian tissues reported to contain detectable levels of ERα include the cardiovascular system, central nervous system and bones with peak levels in the male and female reproductive tracts (uterus, ovaries, vas deference), mammary glands as well as the pituitary (Couse *et al.*, 1997; Gustafsson, 2003) (see also (NURSA, 2016a)). The primary role of ERα is the regulation of sexual reproduction, as exemplified in ERα knock out mice - females are infertile and males have decreased fertility (Lubahn *et al.*, 1993). Further, ERα activation is thought to mainly exhibit proliferative effects on target tissues and cells (Helguero *et al.*, 2005).

The ERβ is commonly found in ovaries, prostate, certain brain regions, pancreas, lung and adipose tissue (Nilsson *et al.*, 2001; Mollerup *et al.*, 2002; Naaz *et al.*, 2002; Nomura *et al.*, 2002; Morales *et al.*, 2003) (see also (NURSA, 2016b)). ERβ knockout mice develop relatively normally and have normal fertility (Krege *et al.*, 1998). As opposed to ERα, ERβ signalling is commonly associated with anti-proliferative effects (Paruthiyil *et al.*, 2004; Helguero *et al.*, 2005; Warner and Gustafsson, 2010; Mancuso *et al.*, 2011).

Co-expression of the two ER subtypes has been reported for the mammary gland, bone, liver and certain regions of the brain although they may not be expressed in the same cell type (Matthews and Gustafsson, 2003). If co-expression in the same cell type occurs, ERβ has been reported to be able to antagonise ERα transcriptional activity, presumably by altering the recruitment of co-regulatory proteins or by enhancing the proteolytic degradation of ERα (Matthews and Gustafsson, 2003; Matthews *et al.*, 2006).

In the classical oestrogen signalling pathway, both ERα and ERβ are ligand-activated by oestrogenic compounds such as E2 and mediate changes in gene expression by interacting with specific DNA sequences. The mechanisms of this pathway as well as alternative oestrogen signalling pathways are described in more detail in Section 1.3.3.

1.3.3. Oestrogen signalling pathways

Several distinct oestrogen signalling pathways exist by which oestrogens and ERs regulate biological processes (Figure 1.6).

In the classical signalling pathway, ligand-dependent activation of the ER results in the formation of ER homo- or heterodimers which, dependent on the dimerisation partner, may have independent and distinct functions (Kumar and Chambon, 1988; Cowley *et al.*, 1997). ER dimers translocate and interact with specific DNA sequences termed oestrogen response elements (EREs) which are located in the regulatory regions of oestrogen-responsive genes (Tsai and O'Malley, 1994; Klinge, 2001). The ERE consensus sequence, GGTCA-nnn-TGACC, is a 5-bp palindrome which is separated by a tri-nucleotide spacer (nnn) (Klein-Hitpass *et al.*, 1986; Shu *et al.*, 2010). Following binding of the ER-ligand complex to DNA a variety of co-activators and -regulators are recruited which initiate transcriptional responses to oestrogens (Cowley *et al.*, 1997; Shibata *et al.*, 1997; Klinge, 2000).

Another oestrogen signalling pathway which results in the modulation of gene expression is the crosstalk of ERs with other transcription factors. ERs have been shown to interact with nuclear factor-κB (NF-κB), specificity protein-1 (SP-1), activator protein-1 (AP-1) and ERK-1 and may therefore regulate transcription of genes independent of EREs (Kushner *et al.*, 2000; Saville *et al.*, 2000; Shou *et al.*, 2004; DeNardo *et al.*, 2005).

Oestrogens may also act through a non-genomic pathway which is also referred to as rapid signalling. This form of signal transduction occurs within minutes following oestrogen exposure. Membrane bound ERs such as GP30 and other membrane localised proteins including MAP kinase can be activated by oestrogen or extranuclear ER variants leading to the initiation of signalling cascades (Levin, 2002; Bjornstrom and Sjoberg, 2005; Thomas and Dong, 2006; Stephen and Ellis, 2007).

ER-mediated induction of gene expression in the absence of a ligand is a fourth possible signalling mechanism. Phosphorylation of the ER induced by growth factors and as a result of downstream signalling of oestrogen independent pathways can lead to ER activation (Font de Mora and Brown, 2000; Roman-Blas *et al.*, 2009).

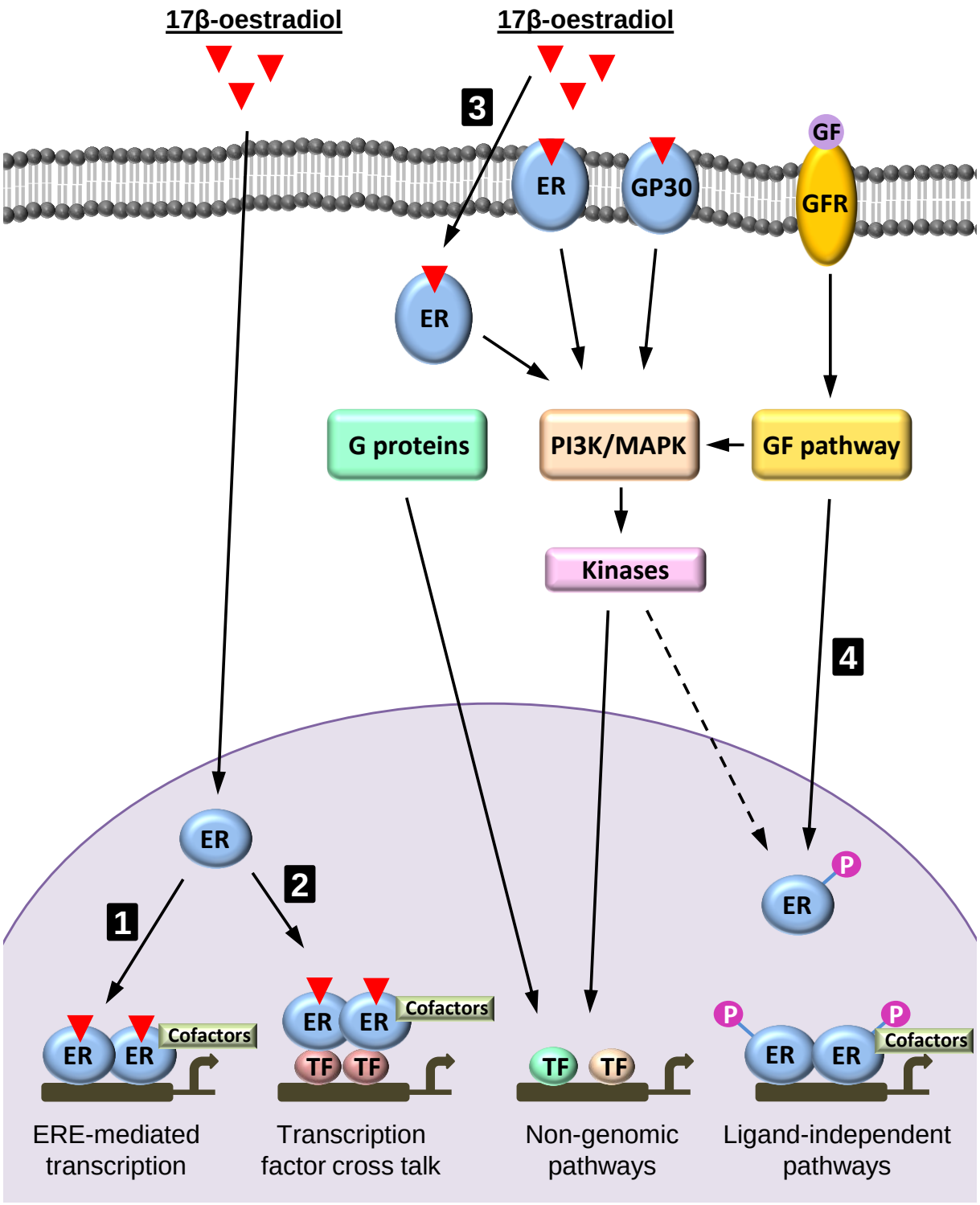

Figure 1.6 Oestrogen signalling pathways. (1) In the classical signalling pathway, ligand-dependent dimerisation of the ER leads to nuclear translocation and binding of the ER to the oestrogen response element (ERE) in the regulatory regions of oestrogen responsive genes. The recruitment of co-factors leads to the initiation of transcription of target genes. (2) Activated ER can regulate gene transcription by interacting with other transcription factors such as AP-1 and NF-κB. (3) ERs can act through a non-genomic pathway where membrane-bound or cytosolic ERs initiate rapid responses by activating the phosphatidylinositol-3/Akt (PI3K/Akt) and/or PKC/MAPK signal transduction pathways. (4) In the ligand-independent pathway, ERs can be activated as part of growth factor (e.g. IGF-1 and TGF-β) - mediated signalling by direct interaction or by MAP and PI3/Akt kinase-dependent phosphorylation. ER, oestrogen receptor; GF, growth factor; GFR, growth factor receptor; TF, transcription factor.

1.3.4. ER splice variants

Several different splice variants for both the ERα and the ERβ have been described in humans. Over 20 different hERα splice variants have been found in breast cancers, other tumours and cell lines, however, only 3 were reported to have functional activity (Poola *et al.*, 2000; Sotoca *et al.*, 2012). The two most referenced hERα splice variants are hERα36 and hERα46. hERα36 is a truncated form of wild type hERα which lacks AF-1 and AF-2 and thus has no transcriptional activity (Wang *et al.*, 2005). This variant was reported to inhibit full length hERα and hERβ transcriptional activity, however, and is capable of activating non-genomic ER pathways (Wang *et al.*, 2006). hERα36 was cloned from a human uterus cDNA library suggesting that it is a naturally occurring isoform. hERα46 was first identified in the human breast cancer cell line MCF-7 (Flouriot *et al.*, 2000) but was later found to also be expressed in primary human osteoblasts (Denger *et al.*, 2001) and endothelial cells (Figtree *et al.*, 2003; Li *et al.*, 2003). This truncated variant lacks AF-1 and has been shown to play a role in cell cycle control (Penot *et al.*, 2005). hERα46 is a functional ligand-dependent transcription factor with AF-2 and has been reported to inhibit hERα transcriptional activity (Figtree *et al.*, 2003; Sotoca *et al.*, 2012).

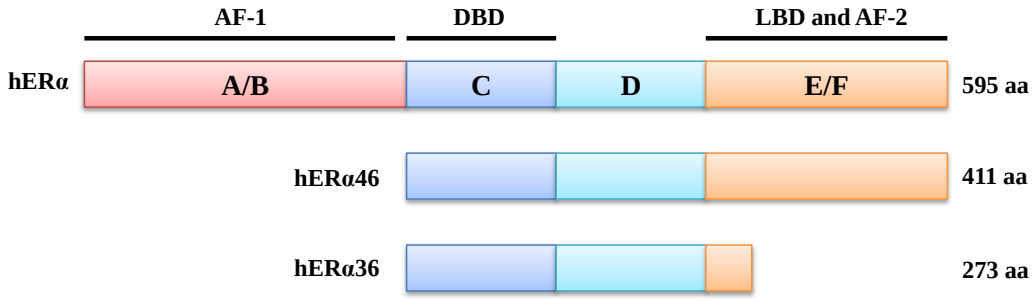

Figure 1.7 Schematic diagram of full length hERα and its splice variants hERα46 and hERα36. AF, activation function; DBD, DNA binding domain; LBD, ligand binding domain; aa, amino acid.

Although some of the hERα variants have only been found in tumours and cell lines and have not been reported to have functional activity (Flouriot *et al.*, 2000), many variants of the hERβ are expressed as functional proteins in tissues and are implicated in the modulation of oestrogen signalling, impacting the regulation of target genes (Matthews and Gustafsson, 2003; Ramsey *et al.*, 2004; Poola *et al.*, 2005; Leung *et al.*, 2006). At least 5 hERβ isoforms exist, named hERβ1-hERβ5 with hERβ1 (hERβ) referred to as the full-length wild type receptor. Most hERβ splice variants are truncated C-terminally and have been shown to form heterodimers with full length hERβ and hERα thus playing an important role in the regulation of ER transcriptional activity (Ogawa *et al.*, 1998; Inoue *et al.*, 2000; Leung *et al.*, 2006).

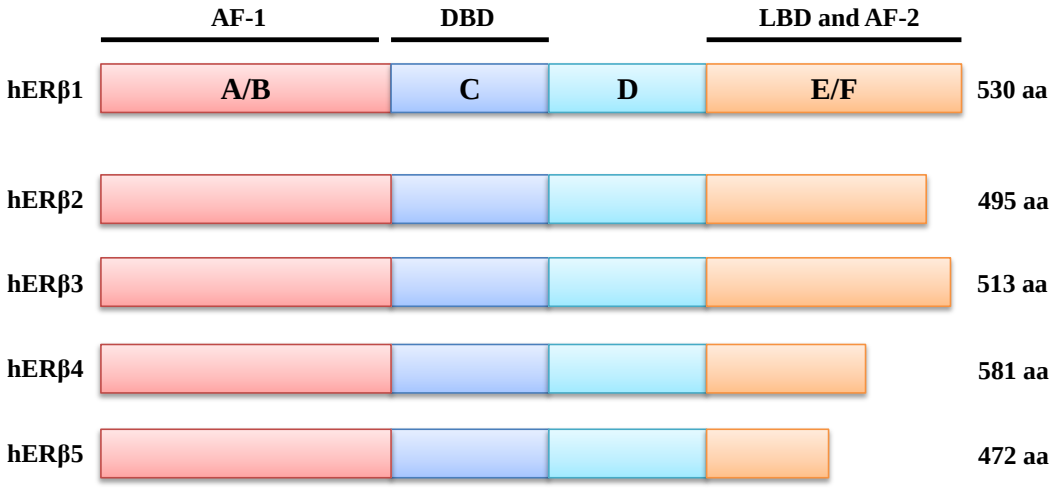

Figure 1.8 Schematic diagram of full length hERβ (hERβ1) and its splice variants hERβ2-5. AF, activation function; DBD, DNA binding domain; LBD, ligand binding domain; aa, amino acid.

Similar to ERs in humans, many different isoforms of the mouse ER (mER) α and mERβ have been identified (Couse *et al.*, 1997; Tremblay *et al.*, 1997; Lu *et al.*, 1998; Lu *et al.*, 2000; Nielsen *et al.*, 2000). Full length mERα comprises 599 amino acids (White *et al.*, 1987) whereas the full-length mERβ isoform consists of 549 amino acids (Tremblay *et al.*, 1997).

1.3.5. Other oestrogen receptors

Several other receptors through which oestrogens can mediate their effects have been identified expanding the possible mechanism by which oestrogens may affect target cells/tissues. These include other nuclear receptors such as the oestrogen related receptors (ERRs) which are insensitive to E2 but interact with some isoflavones, and the constitutive androstane receptor (CAR) in both mouse (Kawamoto *et al.*, 2000) and humans (Koh *et al.*, 2012). Membrane-bound oestrogen binding proteins such as GPER1 (also known as GP30) have been reported to mediate non-genomic oestrogen signalling by activation of kinases and modulation of intracellular calcium levels (Rainville *et al.*, 2015).

1.3.6. Modulators of oestrogen signalling

For many decades, oestrogen signalling has been a therapeutic target for the treatment of a variety of medical conditions. A large number of drugs have been developed to modulate oestrogen signalling pathways or alter levels of oestrogen signalling by modulating oestrogen metabolism or by displaying ER agonistic or antagonistic effects. ER agonists are commonly used for contraceptive purposes or in hormonal replacement therapy in post-menopausal women whereas drugs with ER antagonistic properties find, among others, use in the treatment of breast cancer (Burkman, 2003; Vogel, 2003; Ng *et al.*, 2014). For a long time,

drugs were designed to exclusively target the ERα, however, the discovery of the ERβ lead to the design of ERα and ERβ specific drugs. The distinct tissue distribution pattern of ERα and ERβ further contributes to the interest in novel oestrogenic agents for therapy and has led to the awareness of new sites for pharmacological intervention in a variety of diseases (Gustafsson, 2003).

1.3.6.a Selective oestrogen receptor modulators

Selective oestrogen receptor modulators (SERMs) are nonsteroidal compounds that bind to the ERs. SERMs can have both agonistic and antagonistic activities depending on the type of target tissue and the ER subtype they interact with. Although drugs with SERM-properties have been used for a long time, their tissue-specificity in humans has only recently been recognised which makes them a major therapeutic advance for clinical application (Riggs and Hartmann, 2003). Examples of SERMs are the drugs tamoxifen and raloxifene which are widely used as treatment for breast cancer. Tamoxifen and raloxifene are capable of binding to both the ERα and ERβ but depending on the ER they interact with, display either agonistic or antagonistic properties (Riggs and Hartmann, 2003). Their agonist-antagonist activity further depends on the tissue type in which they operate. In the mammary gland, both drugs exhibit ER antagonistic effects where they prevent oestrogen-stimulated breast cancer growth (Jordan, 2003; Barrett-Connor *et al.*, 2006). In endometrial cells, however, tamoxifen is an ER agonist and promotes endometrial cancer whereas raloxifene has neither agonistic nor antagonistic activities and is therefore considered neutral (Gottardis *et al.*, 1988; Shang and Brown, 2002; DeMichele *et al.*, 2008). The chemical structure of tamoxifen and raloxifene is shown in Table 1.2.

Although only partially understood, the mechanism of selective agonist-antagonist and tissue-specific SERM action can mostly be explained by three interactive mechanisms: 1) SERM action depends on the type of ER present in a particular target tissue, 2) the ER can have differential conformational changes on ligand binding which determines SERM function and 3) SERM action depends on the type of co-regulatory proteins expressed in the target tissue which determine ER functional activity (Riggs and Hartmann, 2003; McDonnell and Wardell, 2010). Shang and Brown (2002) have shown that in breast tissue, tamoxifen and raloxifene recruit regulatory co-repressor proteins to ER target promotors thus inhibiting ER target gene expression (Shang and Brown, 2002). In endometrial cells, however, tamoxifen leads to the recruitment of co-activators making it an ER agonist whereas raloxifene does not recruit co-activators and therefore has no effects. The interest of SERMs for use as therapeutic agents

has heightened because of their potential to display beneficial oestrogenic effects while avoiding most of its negative effects (Riggs and Hartmann, 2003).

1.3.6.b Selective oestrogen receptor degraders

Selective oestrogen receptor degraders (SERDs) represent a new class of drugs used to antagonise oestrogen signalling. As the name suggests, SERDs interact with the oestrogen receptor and facilitate ER degradation in target cells. The drug ICI182,780 (ICI; also known as Fulvestrant or Faslodex) is a SERD used for treatment of ER-positive breast cancers. ICI is capable of interacting with both the ERα and ERβ, however, similar to SERMs, has differential effects on the stability of the ER subtypes as it only induces turnover of the ERα (Peekhaus *et al.*, 2004). The chemical structure of ICI182,780 is shown in Table 1.2.

Name	Structure	Description
17β-oestradiol (E2)	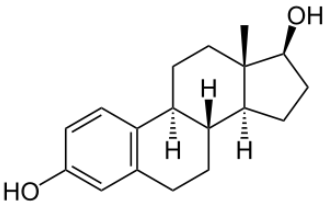	Most potent endogenous oestrogen.
Tamoxifen	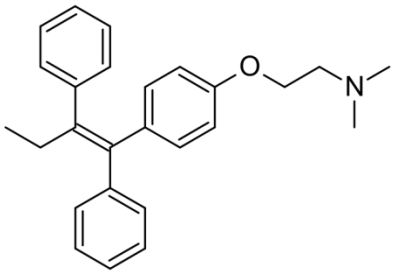	Has agonistic and antagonistic effects on ERα but mainly antagonises ERβ (Barkhem *et al.*, 1998) (Paige *et al.*, 1999). ER antagonistic effects in breast but agonist in uterus and bone (Paige *et al.*, 1999).
Raloxifene	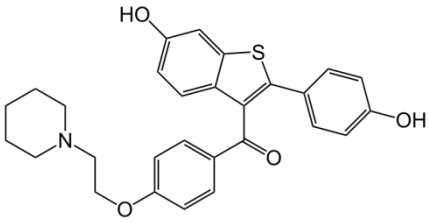	ER antagonist in breast, agonist in bone but not uterus (Black *et al.*, 1994) (Paige *et al.*, 1999).
ICI182,780	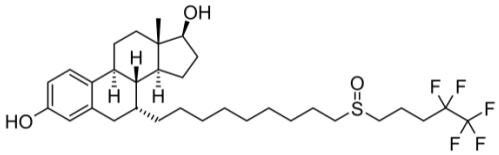	Antagonistic effects on both ERα and ERβ (Wakeling *et al.*, 1991; Paige *et al.*, 1999).

Table 1.2 Chemical structure of selected SERMs and SERDs compared to E2.

Not only can oestrogen signalling be modulated by the deliberate use of pharmaceuticals such as SERMs and SERDs, there are a large number of chemicals present in the environment, diet and consumer products that can inadvertently interfere with and alter oestrogen signalling (Diamanti-Kandarakis *et al.*, 2009). Chemicals that are capable of modifying the hormone system are referred to as endocrine disrupting chemicals (EDCs) and are elaborated upon in Section 1.3.7.

1.3.7. Endocrine disrupting chemicals

EDCs have long been recognised to pose a potential health threat due to their ability to interfere with normal hormone signalling, synthesis and metabolism which can result in disruption of the endocrine system (Diamanti-Kandarakis *et al.,* 2009). Adverse effects of exposure to EDC was first reported by Sumpter and co-workers (1994) who showed that male fish exposed to sewage waste water were subject to feminisation (Purdom *et al.,* 1994; Sumpter, 1995). Ever since, many studies have been conducted showing that EDCs adversely affect the male and female reproductive system, can lead to the development of cancer and have disruptive effects on the metabolic, neuroendocrine and cardiovascular systems (Bay *et al.*, 2006; Soto and Sonnenschein, 2010; Alonso-Magdalena *et al.*, 2011; Mattison *et al.*, 2014). The group of molecules identified as EDCs is heterogeneous and includes both synthetic and natural compounds. Synthetic chemicals with endocrine disrupting activity include industrial solvents/lubricants and their by-products such as polychlorinated biphenyls (PCBs) and dioxins, flame retardants (polybrominated biphenyls (PBB)), plastics and plasticisers (Bisphenol A (BPA) and phthalates), pesticides (methoxychlor, dichlorodiphenyltrichloroethane (DTT) and chlorpyrifos) as well as pharmaceutical agents (Legler and Brouwer, 2003; Diamanti-Kandarakis *et al.*, 2009). Natural compounds present in the diet include genistein and coumestrol (Pierre M *et al.*, 1978; Diamanti-Kandarakis *et al.*, 2009). EDCs may disrupt the endocrine system via several mechanisms involving different pathways including the oestrogenic pathway.

1.3.8. Xenooestrogens

Xenoestrogens are EDCs which are able to mimic the effects of natural oestrogens thus interfering with normal oestrogen signalling. Similar to natural oestrogens, xenoestrogens can modulate both genomic and non-genomic ER signalling pathways through direct interaction with the ERs, indirectly through other transcription factors or by interfering with normal oestrogen biosynthesis, sequestration, metabolism or excretion (Shanle and Xu, 2011).

Xenoestrogens can be found in many everyday products including foodstuffs, personal care items, food and beverage containers and household chemicals. Commonly known xenoestrogens include the natural phytoestrogen genistein and the synthetic chemical BPA which is commonly found in plastics and food containers (Kuiper *et al.*, 1998; Laws *et al.*, 2000). Although a xenoestrogen may have little oestrogenic activity or the exposure to a particular xenoestrogenic compound may be low, recent research has shown that mixtures of xenoestrogens expected to be found in the environment can have dramatic disrupting effects

on hormonal mechanisms (Vinas and Watson, 2013). In order to reduce the risks posed by compounds with oestrogenic activity, a variety of *in vitro* and *in vivo* screening assays exist designed to identify new xenoestrogens.

1.3.9. Measurement of oestrogenic activity

A number of *in vitro* and *in vivo* assays exist that are used to determine if a chemical has oestrogenic activity. *In vitro* reporter gene assays are frequently used to assess if a compound is capable of activating the ER via the classical oestrogen signalling pathway (Huang *et al.*, 2014). In reporter gene assays, activation of the ER will result in consequent expression of a reporter gene from a reporter construct that has been transfected into the test cell line. The level of reporter gene expression can consequently be measured and indicates the level of ER activation. A commonly used cell line is the human breast cancer cell line MCF-7 which expresses the ERα and is oestrogen responsive (Wiseman *et al.*, 1993). Some ER negative cell lines may also be employed which allow testing for differential activation of the ERα and ERβ through transfection of ER-expression vectors. Other *in vitro* assays able to determine if a compound has the potential to modulate ER signalling and has oestrogenic activity include cell-free receptor binding assays and cell-based translocation and proliferation assays (Huang *et al.*, 2014).

Although *in vitro* assays typically allow cost- and time-effective high-throughput analysis, there are limitations including metabolism and clearance of the test compound and tissue-specific effects that require the use of *in vivo* assays. The classical *in vivo* method by which oestrogenic (ERα) activity of a compound is measured, and often defined, is the mouse uterine bioassay. In this assay, the growth of the uterus in response to treatment with a test compound is assessed since the treatment with oestrogens results in growth of the uterus and causes uterotropic changes including an increase of depth of the uterine epithelium. Typically, prepubertal female mice, 19 days of age, are given the test compounds or the vehicle as control by intraperitoneal injection for up to 5 days followed by euthanisation and measurement of uterine relative wet weight and uterotropic changes (Rubin *et al.*, 1951; Galey *et al.*, 1993).

1.4. Oestrogens and the liver

Previous investigations have suggested that the ERα is the only ER subtype expressed in hepatocytes making the liver a hormonal target via the ERα (Ahlbory-Dieker *et al.*, 2009). In the liver, oestrogens regulate a variety of metabolic processes including the synthesis of sex

hormone binding globulin (Hammond, 2011), stimulation of anti-lipogenic metabolism and prevention of insulin resistance (Mauvais-Jarvis *et al.*, 2013).

The liver further plays a key role in controlling circulating oestrogen levels by metabolic conversion of oestrogens to inactive products (Tsuchiya *et al.*, 2005; Bondesson *et al.*, 2015; Ziegler *et al.*, 2015). Its significance is demonstrated in men with chronic liver disease who may be subject to feminisation as a result of compromised hepatic metabolism and clearance of oestrogens (Burra, 2013). Oestrogens are also known to have toxic hepatic effects and can cause alterations in bile constituents and a disruption of the bile flow and thus cholestasis.

1.4.1. Oestrogen-mediated cholestasis

Oestrogens are known to have the ability to induce intrahepatic cholestasis. This can be seen in susceptible women during pregnancy when circulating oestrogen levels are high, as a result of oral contraceptive intake and during postmenopausal replacement therapy (Vore, 1987; Lammert *et al.*, 2000). The prevalence of oestrogen-induced cholestasis varies geographically and with ethnicity. Intrahepatic cholestasis of pregnancy is the most prevalent form of oestrogen-mediated cholestasis and is most common in Chile (Reyes, 2008). In susceptible individuals, the elevations in circulating oestrogens can be sufficient to lead to hepatic failure and death in the absence of liver transplantation (Ozkan *et al.*, 2015).

Several mechanisms as to how natural/endogenous oestrogens cause cholestasis have been proposed and often involve the inhibition or repression of bile salt transport proteins. In a rat model for oestrogen-induced cholestasis, Stieger et al. (2000) reported that the oestrogen metabolite oestradiol-17beta-glucuronide inhibited the activity of the bile acid and drug transporter BSEP thus identifying an important target involved in initiating cholestasis (Stieger *et al.*, 2000). Several years later, Yamamoto et al. (2006) showed that ethinyl oestradiol (EE2) exposure resulted in the repression of a number of bile acid and cholesterol transporters including BSEP and Na(+)/taurocholate co-transporting polypeptide (NTCP) in mice. This effect was lost in ERα null mice resistant to EE2-induced cholestasis suggesting that oestrogen-mediated adverse hepatic effects in the liver are induced by interactions with the ERα (Yamamoto *et al.*, 2006). In addition, a number of studies have reported that a microtubule-independent endocytic internalisation of both Bsep and Mrp2 in response to oestradiol 17β-D-glucuronide was observed (Mottino *et al.*, 2002; Crocenzi *et al.*, 2003; Mottino *et al.*, 2005) and mediated by ERα (Barosso *et al.*, 2012) proposing another mechanism by which oestrogen exposure may cause cholestasis.

1.4.2. Xenoestrogens and cholestasis

Given the ability of oestrogens to cause cholestasis, exposure to xenoestrogens may have similar adverse hepatic effects. Recently, experimental data has shown that the food colourant tartrazine is an activator of the human ERα *in vitro* (Datta and Lundin-Schiller, 2008; Axon *et al.*, 2012) and intraperitoneal injection of tartrazine into mice resulted in a mild cholestatic liver injury (Axon, Thesis 2012). A similar cholestatic injury in mice has been observed after the exposure to E2 (Axon *et al.*, 2010).

Not only can xenoestrogens mediate their effects through interaction with the oestrogen receptors, but they may target the oestrogen pathway by altering synthesis, transport and metabolism of endogenous oestrogens. For example, research has shown that metabolites of PCBs, environmental pollutants known for their xenoestrogenic properties, are potent inhibitors of oestrogen sulfotransferases (Kester *et al.*, 2000). The sulfation of oestrogens prevents their interaction with the ERs thus rendering them inactive. Impaired oestrogen inactivation due to sulfotransferase inhibition increases their bioavailability in target tissues, such as the liver, which may explain their hepatotoxic effects (Guzelian, 1983).

Xenoestrogen exposure may also play a role in the development of the chronic cholestatic liver disease primary biliary cholangitis (PBC) which has been proposed to be triggered in part by exposure to xenobiotics (Prince *et al.*, 2001; Ala *et al.*, 2006; Jones, 2007).

1.4.3. Primary biliary cholangitis

Primary biliary cholangitis (PBC, formerly known as primary biliary cirrhosis) is a chronic cholestatic liver disease which primarily affects peri- and post-menopausal women over the age of 40. Histologically, PBC is characterised by inflammation of the portal tracts and disappearance of the intrahepatic bile ducts which eventually leads to a decreased bile flow and build-up of toxic substances in the liver, causing hepatocyte damage, cirrhosis and ultimately liver failure (Kaplan and Gershwin, 2005).

It has been established that genetic predisposition plays an important role in disease development. Relatives of affected individuals are more likely to develop PBC and it was reported that around 6% of cases occur within first-degree relatives (Gershwin *et al.*, 2005). In 2004, a twin study was conducted which has shown that in monozygotic twins, the concordance rate for PBC is 63% consolidating that genetics are involved in disease pathogenesis (Selmi *et al.*, 2004).

Although of unknown aetiology, PBC exhibits several hallmarks indicative of an autoimmune disorder. These include the observation that, similar to other autoimmune diseases, PBC predominantly affects women with a female-to-male ratio of 9:1 (Talwalkar and Lindor, 2003). In addition, anti-mitochondrial antibodies (AMAs) are present in the serum of the majority of patients. AMAs target 2-oxoacid dehydrogenase complexes (2-OADC), a family of enzymes located in the inner mitochondrial membrane and play a critical role in oxidative energy metabolism. 2-OACDs consist of three main subunits, namely branched chain ketoacid dehydrogenase (BCKD), ketoglutarate dehydrogenase (KGD) and pyruvate dehydrogenase complex (PDC). The majority of patients are found to produce AMAs directed at PDC, in particular the PDC subunit E2 (PDC-E2). Serum AMA of 50% of PBC patients with PCD-E2 specific antibodies have also been reported to be able to cross-react with epitopes of the E2 subunit of BCKD and KGD.

Whilst PBC is often considered as an autoimmune disease, several observations have been made which will question its mere autoimmune background. First, all nucleated cells contain 2-OADC, however, AMA, which are distributed throughout the body, predominantly target the liver (Kaplan and Gershwin, 2005; Selmi *et al.*, 2007). Second, AMAs are only found in 90-95% of all PBC patients indicating that they may not be solely responsible for the development of the disease (Mayo, 2008). Third, compared to other autoimmune disorders, the treatment with immunosuppressant is relatively ineffective and does not significantly improve symptoms (Mauss *et al.*, 2014). Fourth, development of PBC in individuals under the age of 25 is rare and PBC is absent in children (Gershwin *et al.*, 2000; Kaplan and Gershwin, 2005).

Although genetic predispositions seems to be a major determinant in disease development, more recent studies have implicated a role for environmental factors as potential triggers of PBC. These triggers are thought to be either of infectious (bacteria and viruses) or chemical (xenobiotics) nature. In regard to infectious agents, previous research has documented that microbes, in particular bacteria, are capable of inducing an autoimmune response by presenting peptides with similar homology to self-proteins which may lead to the production of antibodies that will react with the bacterial peptide and simultaneously targeting self-epitopes thus causing the destruction of self-tissue (Van de Water *et al.*, 2001). A number of infectious agents have been proposed to be able to trigger PBC including *Escherichia coli* (Shelley *et al.*, 1990), *Salmonella minnesota* (Stemerowicz *et al.*, 1988), *Staphylococcus aureus* (O'Farrelly and Doherty, 2007) and *Novosphingobium aromaticivorans*, the latter increasingly gaining interest as it has been shown to cause a specific antibody reaction and

faecal samples of PBC patients have been reported to contain 16s rRNA sequences specific to this bacterium (Selmi *et al.*, 2003; Kaplan, 2004).

More recently, research findings suggest that a link between the exposure to environmental xenobiotics and the development of PBC exist. In theory, xenobiotics may bind to and therefore alter self-proteins which will result in conformational changes of native protein forming an unrecognised structure capable of inducing an immune response. An autoimmune response may then in turn lead to cross-reactivity with the self-epitope sustaining the immune response and thus causing chronic autoimmunity (O'Farrelly and Doherty, 2007). In terms of PBC, it has been proposed that a xenobiotic may conjugate to the PDC subunit E2 which consequently leads to protein alterations and creation of unrecognised structures. This in turn may induce the production of antibodies against the unrecognised protein as well as the native form resulting in loss of self-tolerance to PDC-E2. In fact, research has shown that serum AMAs from PBC patients target synthetically produced xenobiotic-conjugated PDC-E2 with higher affinity than to the native form of the protein (Long *et al.*, 2001). Many of the conjugated xenobiotics were halogenated hydrocarbons which are commonly found in pesticides and detergents (Long *et al.*, 2001; Kaplan and Gershwin, 2005).

A likely role for xenobiotics as a causative agent in PBC is further supported by the demonstration that disease 'hot spots' exist. A cluster analysis of data from the UK found that PBC occurs more frequently in former industrial and coal mining areas such as in the north-east of England (Prince *et al.*, 2001). Moreover, the analysis also revealed that the risk of developing PBC was higher in urban areas than in surrounding rural areas (Prince *et al.*, 2001). Incidences of PBC have further been linked to living in close proximity to waste tip sites (Ala *et al.*, 2006) indicating that exposure to environmental xenobiotics may increase the susceptibility of genetically predisposed individuals to developing PBC. Although associations between the use of nail polish and hair dyes and PBC exist (Gershwin *et al.*, 2005) they should be interpreted with caution. PBC primarily occurs in women and therefore associations made between PBC and products predominantly used by women do not necessarily mean causation.

1.5. Gut-liver axis

The term gut-liver axis describes the close interplay that exists between the gut and the liver which together play a critical role in absorption and metabolism of nutrients and xenobiotics. Approximately 70% of the liver's blood supply, delivered via the portal vein, is derived from

the intestine which makes the liver one of the first and major organs to be exposed to gut-derived toxins, including bacteria and bacterial components (Szabo and Bala, 2010). The gut is home to billions of microorganisms and the gut epithelial barrier keeps microbiota from entering the portal circulation (Lieber, 2004). Trace amounts of bacterial components, such as the lipopolysaccharide (LPS) present in the cell wall of Gram-negative bacteria, may escape the gut and translocate to the liver where they are readily cleared by Kupffer cells and hepatocytes to maintain immune homeostasis (Szabo and Bala, 2010). Uptake and detoxification of endotoxin is critical for prevention of systemic inflammatory responses to blood-borne LPS.

An increase in endotoxin translocation from the gut may outweigh the liver's clearance capacity thus leading to the induction of transcription of a number of pro-inflammatory genes and release of cytokines. An acute inflammatory response in the liver will lead to the recruitment of immune cells such as neutrophils which, through their activity, further contribute to the development of liver damage. Elevated endotoxin translocation from the gut to the liver has been linked to a variety of liver disorders, including alcohol-induced liver disease (Han, 2002).

1.5.1. Alcohol, endotoxin and liver disease

Long term alcohol abuse is linked to the development of a variety of medical disorders including liver injury, brain injury and heart disease. Endotoxin seems to be a key factor in inducing alcohol-mediated tissue/organ damage and plays a convincing role in initiating a spectrum of liver diseases; fatty liver, alcoholic hepatitis and cirrhosis are the most prevalent types of alcohol-associated liver injury (Menon *et al.*, 2001; Mann *et al.*, 2003; Adachi and Brenner, 2006). The involvement of endotoxin in alcohol-induced liver damage became conspicuous when patients with alcoholic liver disease (ALD) showed elevated plasma endotoxin levels (endotoxemia) (Bode *et al.*, 1987; Fukui *et al.*, 1991). Since then, several studies provided the evidence that increased plasma endotoxin levels in humans is linked with ALD (Hanck *et al.*, 1998; Fujimoto *et al.*, 2000; Parlesak *et al.*, 2000).

A number of studies employing a rat model of alcoholic liver injury have highlighted the connection between alcohol, endotoxin and liver damage in a number ways. First, administering LPS on a background of ethanol feeding was found to induce fatty and necrotic changes in the liver and increased the bioactivity of a number of pro-inflammatory cytokines in the plasma (Pennington *et al.*, 1997). Second, ethanol feeding and simultaneous treatment of rats with antibiotics to eliminate bacteria residing in the gut prevented alcohol induced liver

injury by reducing plasma endotoxin levels (Adachi *et al.*, 1995). Third, animals fed with ethanol and Lactobacilli, which suppress the growth of gram negative bacteria in the gut, showed reduced endotoxin plasma levels and the absence of liver injury (Nanji *et al.*, 1994). More recent studies have also found a connection between ethanol-induced liver damage in rats and increased plasma endotoxin levels (Mathurin *et al.*, 2000; Nanji *et al.*, 2001). These findings indicate that endotoxin plays a key role in the initiation of alcohol-induced liver disease.

1.5.2. Oral ingestion of alcohol affects intestinal barrier function

The mechanisms leading to elevated plasma endotoxin levels have received significant attention. Three explanations have been proposed to account for the processes involved in alcohol-mediated endotoxemia: 1) Kupffer cells, the residential macrophages of the liver responsible for the clearance of toxins and pathogens, are dysfunctional with a decreased ability to eliminate endotoxin; 2) overgrowth of bacteria in the gut causes excessive production of endotoxins; and 3) an increased intestinal permeability due to alcohol-induced disruption of intestinal barrier function results in increased uptake of endotoxins and bacteria by the gut (Rao *et al.*, 2004).

The third explanation has received particular attention and clinical and experimental data have shown that alcohol intake results in augmented gut permeability to macromolecules. Using ^{51}CrEDTA as an indicator for gut permeability, alcoholics showed an increased intestinal permeability to this molecule (Bjarnason *et al.*, 1984). Further, assessing gastrointestinal permeability by the excretion of polyethylene glycol (PEG) 400, an increase in intestinal permeability was measured in healthy subjects after oral administration of alcohol (Robinson *et al.*, 1981). The administration of PEG with different molecular weights (M_r 400-10000) to subjects chronically abusing alcohol and healthy controls shows that especially larger molecules were increasingly excreted in the urine of alcoholics compared to healthy subjects. This suggests that alcohol increases intestinal permeability to macromolecules by impairing the intestinal barrier function.

Chronic alcohol administration to rats by gavage led to an increase of permeability of the intestinal mucosa to macromolecules such as haemoglobin (Bungert, 1973) and horseradish peroxidase (Worthington *et al.*, 1978). Furthermore, the assessment of gut permeability by the lactulose/mannitol (L/M) ratio showed that intragastric infusion of ethanol in rats increased the L/M ratio significantly (Mathurin *et al.*, 2000).

In vitro studies using a cell culture model of the intestinal epithelium (Caco-2 cell line) revealed that ethanol and especially its metabolic product acetaldehyde effectively reduced the transepithelial electrical resistance which was used as a measure of paracellular permeability. These results along with measuring the unidirectional flux of extracellular markers such as inulin and mannitol, which could increasingly pass the cell monolayer, indicate an increase in paracellular permeability (Rao, 1998; Atkinson and Rao, 2001).

The cumulative results of these studies suggest that alcohol consumption can lead to an increase in gut permeability to macromolecules including endotoxin. The effect that alcohol has on the gastrointestinal mucosa and intestinal barrier function is likely to be the first site of injury which initiates a complex cascade of cellular responses causing liver inflammation and damage.

1.5.2.a The role of acetaldehyde in disruption of intestinal epithelial tight junctions

Acetaldehyde, a metabolic product of ethanol, may be associated with the development of alcohol-related diseases (Salaspuro, 1996). In the gastrointestinal tract, ethanol is oxidised to acetaldehyde by alcohol dehydrogenases in the mucosa and especially by alcohol dehydrogenases of bacteria residing in the gut. Acetaldehyde is then further oxidised to acetate by mucosal or bacterial aldehyde dehydrogenases (Figure 1.9). Enzymatic activities of aldehyde dehydrogenases in the colon are generally lower compared to other tissues so that acetaldehyde is likely to accumulate in the colon (Salaspuro, 1996).

It has been reported that acetaldehyde impairs the epithelial barrier function by disrupting tight junctions (Atkinson and Rao, 2001; Basuroy *et al.*, 2005). Tight junctions are junctions between the apical membrane of neighbouring cells forming a barrier to the paracellular flux of water and solutes in epithelia (Fanning *et al.*, 1998). A study investigating intracolonic acetaldehyde levels in rats reported concentrations of up to 3 mM of the alcohol metabolite in the colon (Salaspuro, 1996). In Caco-2 cells, acetaldehyde concentrations of 0.1-0.6 mM were able to disrupt tight junctions and subsequently increase paracellular permeability in Caco-2 cells (Rao, 1998; Atkinson and Rao, 2001). In comparison, it seems likely that intracolonic acetaldehyde in alcoholics is able to cause endotoxemia by disrupting tight junctions.

The mechanism by which acetaldehyde loosens tight junctions and impairs epithelial barrier function is by redistribution of tight junction proteins from the intercellular junctions (Rao *et al.*, 2004). As has been shown in Caco-2 cells, this is mediated by the effects of acetaldehyde on tyrosine kinases by inhibiting protein tyrosine phosphatase activity (Atkinson and Rao,

2001). A subsequent increase in tyrosine phosphorylation of a number of proteins such as ZO-1 and beta-catenin (a protein involved in tight junctions/adherens junctions respectively) may be a key mechanism of acetaldehyde-initiated tight junction destabilisation and inhibition of protein tyrosine phosphatase activities (Atkinson and Rao, 2001). By altering intracellular signal-disruption pathways, acetaldehyde has the ability to disrupt protein complexes involved in tight junction regulation causing an increase in intestinal permeability to endotoxin. Acetaldehyde production and accumulation in the intestinal lumen may therefore result in augmented endotoxin uptake and liver damage by triggering a cascade of cellular responses.

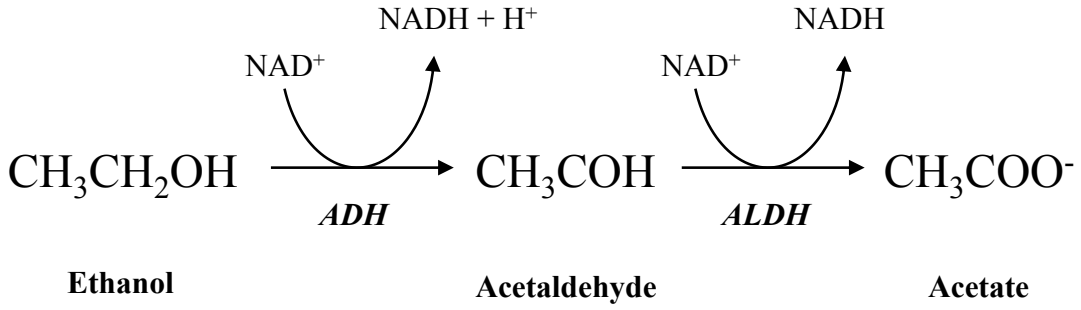

Figure 1.9 Ethanol metabolism. Ethanol is oxidised to acetaldehyde by the alcohol dehydrogenases (ADH). Acetaldehyde is then further oxidised to acetate by aldehyde dehydrogenases (ALDH).

1.5.3. Endotoxin-mediated activation of Kupffer cells

Alcohol-induced liver damage is mediated by ethanol metabolites, gut-derived endotoxin, ROS and inflammatory cytokines such as TNF-α and Interleukin (IL)-1/IL-6 (Ajakaiye *et al.*, 2011). In alcohol-mediated liver damage, ROS and pro-inflammatory cytokines are predominantly released by the liver's residential macrophages, the Kupffer cells (Figure 1.10). The phagocytotic activity of Kupffer cells plays an important role in removing antigens and other foreign substances such as intestine-derived endotoxin from the general and specifically portal circulation which is critical to prevention of hepatic injury (Toth and Thomas, 1992). Despite their disease preventing function, Kupffer cells can also contribute to the development of liver damage by releasing pro-inflammatory mediators as seen in alcohol- and endotoxin-associated injury. Their ability to induce hepatic damage has been shown by Adachi *et al.* (1994) who were able to prevent alcohol-induced liver damage by treating ethanol-exposed (by intragastric feeding) rats with gadolinium chloride ($GdCl_3$) (Adachi *et al.*, 1994). $GdCl_3$ is selectively toxic to Kupffer cells inhibiting their activity and preventing them

from functioning normally. These results provide an insight in the important and paradoxical role of Kupffer cells in the onset of early liver injury.

Other studies also support the hypothesis that Kupffer cell activation is involved in alcohol- and endotoxin-mediated liver disease in various ways. First, Kupffer cell function including phagocytosis, bactericidal activity and cytokine production is affected by ethanol (Yamada *et al.*, 1991). Second, patients chronically abusing alcohol showed elevated levels of TNF-α which is generated by monocyte-derived macrophages only; Kupffer cells represent this lineage's largest population. Third, intracellular calcium levels in Kupffer cells isolated 24 hours after intragastric administration of ethanol to rats rose significantly in response to low-dose LPS treatment (Enomoto *et al.*, 1998). Temporary Ca^{2+} influx is necessary for LPS-induced production of TNF-α (Watanabe *et al.*, 1996).

Kupffer cells once activated are responsible for the secretion of TNF-α, Interleukin (IL)-1 and IL-12 as well as ROS and RNS (Ajakaiye *et al.*, 2011). In Kupffer cells, ROS generation is catalysed by the enzyme nicotinamide adenine dinucleotide phosphate (NADPH) oxidase. The release of TNF-α and Kupffer cell mediated infiltration of neutrophils further contribute to continuous oxidative stress through the production of ROS leading to liver damage (Ajakaiye *et al.*, 2011).

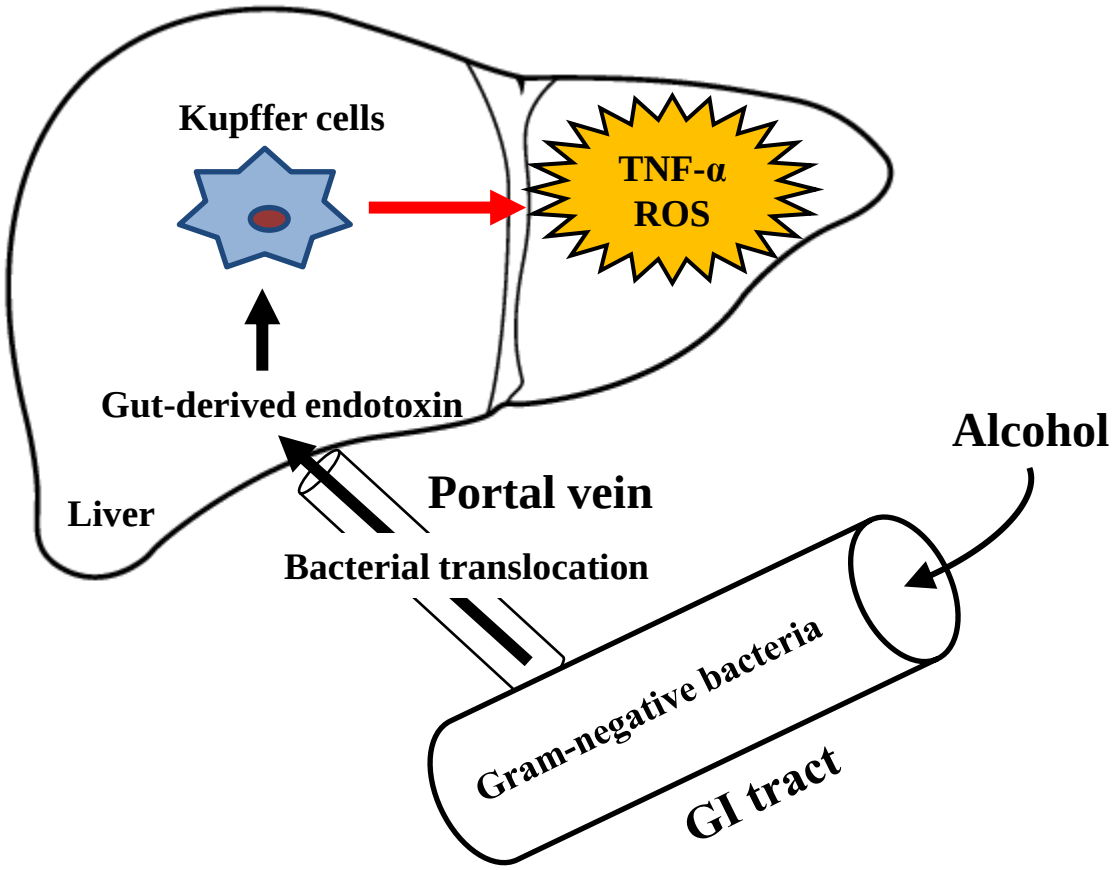

Figure 1.10 Alcohol-mediated translocation of endotoxin and subsequent Kupffer cell activation results in pro-inflammatory cytokine and ROS production causing liver injury. Chronic alcohol consumption can impair the epithelial barrier function causing gut derived endotoxin of intestinal Gram-negative bacteria to translocate to the liver via the portal vein. Endotoxin then activates Kupffer cells which subsequently release ROS and pro-inflammatory cytokines including TNF-α resulting in liver damage.

1.6. Study objectives

The main hypothesis underpinning this thesis was that exposure to xenoestrogens causes adverse hepatic effects. This hypothesis was formulated in light of the ability of oestrogens to cause cholestasis. To test this hypothesis, the three main aims of the study were:

1. Develop an *in vitro* mouse-based reporter gene assay in order to be able to examine a variety of xenobiotics for their potential to interact with the mouse ERs and to determine their suitability for use in an *in vivo* mouse model

2. Examine the potential hepatic adverse effects that xenoestrogens may have *in vivo* by employing a mouse model.

3. Determine if alcohol co-administration results in increased uptake of orally administered xenoestrogens and thus cholestatic injury.

Chapter 2. Materials and Methods

2.1. Materials

Unless otherwise stated, all materials, chemicals and reagents were purchased from Sigma-Aldrich (Poole, UK) and were of molecular or analytical grade.

2.2. Animal work

All experiments were conducted in accordance with the UK Animal (Scientific procedures) Act of 1986, with UK Home Office Guidance on the implementation of the Act and with all the applicable Codes of Practice for the care and housing of laboratory animals. Animal welfare and Ethical Review Body (Newcastle University) and UK Home Office approval were granted for all animal procedures.

2.2.1. Husbandry

All animals were housed in the Comparative Biology Centre at Newcastle University and kept in an air conditioned environment of 23°C ± 1°C with a controlled relative humidity of 47% and a 12-hour light/dark cycle. Mice were kept in saw-dust filled and filter top individually ventilated cages in groups of up to six mice per cage. The bedding was changed twice weekly and animals had access to water and food *ad libitum*.

2.2.2. C57Bl/6 wild type mice

C57Bl/6 wild type (wt) mice were sourced from Charles River (Kent, UK) and housed as described in Section 2.2.1. Mice were bred in house. Mice were at least 10 weeks old and between 25-34 g body weight at the beginning of all experiments.

2.2.3. Transgenic C57Bl/6-NF-κB-luciferase mice

Transgenic (tg) C57Bl/6-NF-κB-luciferase (NF-κB-luc) mice (bearing a transgene composed of three NF-κB sites from the Ig κlight chain promoter coupled to the gene encoding *Firefly* luciferase) were originally obtained from Dr Harald Carlsen (Oslo University, Norway). Mouse colonies were expanded in house. Animals were housed as described in Section 2.2.1. and were at least 10 weeks old and between 21-35 g body weight at the beginning of all experiments.

2.2.4. Genotyping

Mice were genotyped at an age not younger than 6 weeks using the *In Vivo* Imaging System (IVIS) as described in Section 2.2.6. Tg NF-κB-luc mice show a basal level of NF-κB-driven luciferase activity as can be seen in Figure 2.1.

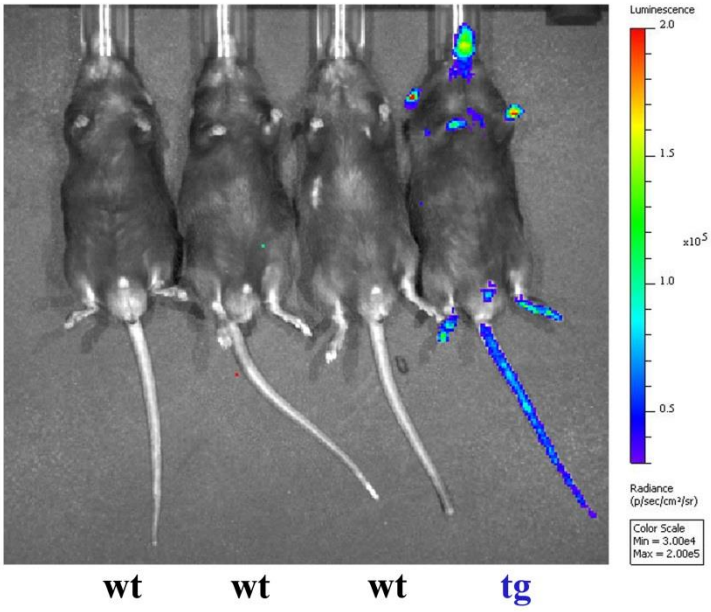

Figure 2.1 Phenotyping of mice using IVIS. Tg NF-κB-luc mice exhibit basal levels of luciferase activity following intraperitoneal (i.p.) injection of D-Luciferin. Wt, wild type; tg, transgenic.

2.2.5. In vivo studies

2.2.5.a Ethanol-mediated gut permeability pilot study

Oral alcohol exposure is believed to increase gut permeability and/or alter the gut microbiota (Kirpich *et al.*, 2012b; Szabo, 2015). A pilot study was carried out to determine the time of ethanol dosing required to see an increase in gut permeability. One male adult mouse per group was assigned to 1 of 4 groups and dosed twice daily by oral gavage for 14 days (except alpha-naphthyl isothiocyanate (ANIT)), dosed orally once at beginning of study) as outlined in Table 2.1. Dextrose treatment served as a control to account for the energy content of ethanol. ANIT is known to cause liver injury (Goldfarb *et al.*, 1962) and was therefore included as a positive control. An oral dose of 50 mg/kg bw ANIT has previously been shown to cause detectable liver injury in tg NF- κB-luc mice (Probert, Thesis 2014).

Group	Animals	Dose	Vehicle
1	1x C57BL/6 wt	Dextrose (6.32 g/kg bw)	H_2O
2	1x NF-κB-luc	Dextrose (6.32 g/kg bw)	H_2O
3	1x NF-κB-luc	Ethanol (3 g/kg bw)	H_2O
4	1x NF-κB-luc	ANIT (50 mg/kg bw)	Olive oil

Table 2.1 Pilot study dosing regimen. Dosing solutions were prepared as follows: Dextrose was dosed from a 0.33 g/ml solution in H_2O at 19 ml/kg bw. Ethanol was dosed from a 20% (v/v) ethanol solution in H_2O at 19 ml/kg bw. 100 mg of ANIT was dissolved in 8 ml of olive oil, mixed on a roller and dosed at 4 ml/kg bw. wt, wild type; bw, body weight.

On day 1, mice were imaged before and at 1 and 6 hours after the initial dose and from then on mice were imaged once on day 3, 6, 9, 12 and 14 using the IVIS as described in Section 2.2.6. On day 14 post imaging, tail vein blood was collected for serum enzyme analysis (see Section 2.2.7).

2.2.5.b Oral tartrazine study

To study the hepatic and gastrointestinal effects of oral tartrazine exposure, female adult tg NF-κB-luc mice and male C57Bl/6 wt mice were randomly assigned to 4 groups. In order to increase gut permeability, mice were pre-dosed with 3 g/kg body weight (bw) ethanol (control mice were dosed with 6.32 g/kg bw dextrose to account for the energy content of ethanol) for 2 weeks followed by dosing with 50 mg/kg bw tartrazine (+/- 3 g/kg bw ethanol) for 10 consecutive weeks. A dose of 50 mg/kg bw tartrazine was used because at this dose, tartrazine has previously been shown to induce mild cholestasis in mice following i.p. injection (Axon, Thesis 2012). Tartrazine (Sigma, cat# T0388) used in all studies had a purity of 85% or greater (which meets the EC specifications for its use as a food additive). Control mice were dosed with dextrose or ethanol alone. All dosing was carried out by oral gavage, twice daily with at least 7 hours between doses. The dosing regimen of all groups is specified in Table 2.2.

Group	Animals	Pre-dose (2 weeks)	Dose (10 weeks)
1	3x wt 3x tg	Dextrose (6.32 g/kg bw)	Dextrose (6.32 g/kg bw)
2	6x wt 3x tg	Dextrose (6.32 g/kg bw)	Tartrazine (50 mg/kg bw)
3	6x wt 4x tg	Ethanol (3 g/kg bw)	Ethanol (3 g/kg bw)
4	7x wt 4x tg	Ethanol (3 g/kg bw)	Tartrazine (50 mg/kg bw) + Ethanol (3 g/kg bw)

Table 2.2 Dosing regimen to assess *in vivo* effects of oral tartrazine exposure. Dosing solutions were prepared and dosed as follows: Dextrose was dosed from a 0.33 g/ml solution in H_2O at 19 ml/kg bw. Ethanol was dosed from a 20% (v/v) ethanol solution in H_2O at 19 ml/kg bw. For tartrazine treatments with or without ethanol, 50 mg of tartrazine was dissolved in 19 ml of ethanol or dextrose solution respectively. Tg, transgenic NF-κB-luc mice; wt, C57Bl/6 wt mice; bw, body weight.

Tg NF-κB-luc mice were imaged for inflammation before and after the pre-treatment period and then at 4, 8 and 10 weeks from the beginning of tartrazine dosing by IVIS as outlined in Section 2.2.6. After 12 weeks, tg mice were imaged and then terminated by cervical dislocation and their liver, spleen, kidney and intestinal tract removed immediately and imaged for inflammation *ex vivo*.

Wt mice were terminated on the last day of the study and their livers harvested and fixed in 10% (w/v) formalin in 1x phosphate buffered saline (PBS, 137 mM NaCl, 2.7 mM KCl, 2 mM KH_2PO_4, 8 mM Na_2HPO_4, pH 7.4) or snap frozen in liquid nitrogen and stored at -80°C. Blood was collected for serum enzyme analysis as described in Section 2.2.7. Body weights were measured once a week for the purposes of health monitoring and dosage adjustments.

2.2.5.c Hepatic effects of xenoestrogens

To investigate the hepatic effects of xenoestrogen exposure, male adult tg NF-κB-luc mice were randomly assigned to 4 groups and were dosed at 0, 24 and 48 hours by intraperitoneal (i.p.) injection (except ANIT, dosed once at beginning of study by oral gavage) as described in Table 2.3. EE was dosed at 0.5 mg/kg which has previously been shown to result in hepatic adverse effects in mice (Axon *et al*., 2010).

Group	Animals	Dose	Vehicle
1	3x NF-κB-luc	Control vehicle	10% ethanol/90% olive oil (v/v)
2	3x NF-κB-luc	EE (0.5 mg/kg bw)	10% ethanol/90% olive oil (v/v)
3	3x NF-κB-luc	Butyl paraben (50 mg/kg bw)	10% ethanol/90% olive oil (v/v)
4	1x NF-κB-luc	ANIT (50 mg/kg bw)	Olive oil

Table 2.3 Dosing regimen to investigate *in vivo* hepatic effects of xenoestrogens. Dosing solutions were prepared and dosed as follows: Vehicle was dosed at 5 ml/kg bw. Ethinyl oestradiol (EE) treatment was prepared by diluting 0.1 mg/ml in 10% ethanol/90% olive oil (v/v) and dosed at 5 ml/kg bw. Butyl paraben was dosed from a 10 mg/ml solution in 10% ethanol/90% olive oil (v/v) at 5 ml/kg bw. 100 mg of ANIT was dissolved in 8 ml of olive oil, mixed on a roller and dosed at 4 ml/kg bw.

After 72 hours, mice were imaged for inflammation by IVIS as detailed in Section 2.2.6. Mice were then terminated by cervical dislocation and their livers harvested and fixed in 10% (w/v) formalin in 1x PBS or snap frozen in liquid nitrogen and stored at -80°C. Blood was collected to measure serum enzyme activities as described in Section 2.2.7.

2.2.5.d Hepatic effects of soil sample extracts

To examine the effects that ethanol extracts prepared from soil samples collected from around a landfill site and from 3 control sites (extract preparation is described in Section 2.17) have on the liver, male tg NF-κB-luc mice were randomly assigned to 4 groups and were dosed once by i.p. injection as outlined in Table 2.4.

Group	Animals	Dose	Vehicle
1	3x NF-κB-luc	Control vehicle	10% ethanol/90% olive oil (v/v)
2	3x NF-κB-luc	EE (0.5 mg/kg bw)	10% ethanol/90% olive oil (v/v)
3	3x NF-κB-luc	Combined oestrogen-positive soil ethanol extracts* from landfill site (20 ml/kg bw)	10% ethanol/90% olive oil (v/v)
4	3x NF-κB-luc	Combined oestrogen-negative soil ethanol extracts* from landfill site (20 ml/kg bw)	10% ethanol/90% olive oil (v/v)

Table 2.4 Dosing regimen to examine the *in vivo* hepatic effects of soil sample extracts. Dosing solutions were prepared and dosed as follows: Vehicle was dosed at 20 ml/kg bw. EE treatment was prepared by diluting 0.025 mg/ml in 10% ethanol/90% olive oil (v/v) and dosed at 20 ml/kg bw. For preparation of soil sample extracts, 3.5 ml of ethanol soil extracts were dried down to 175 µl with nitrogen, diluted 1:9 (v/v) with olive oil and dosed at 20 ml/kg bw. *As determined by dual-glo luciferase reporter gene assay.

Mice were imaged for inflammation at 0, 1, 6 and 24 hours post i.p. injection using the IVIS as detailed in Section 2.2.6. Mice were then terminated by cervical dislocation and their livers harvested and fixed in 10% (w/v) formalin in 1x PBS or snap frozen in liquid nitrogen and stored at -80°C. Blood was collected to measure serum enzyme activities as described in Section 2.2.7.

2.2.6. In vivo luminescent imaging

Tg NF-κB-luc mice were imaged using the IVIS Xenogen 200 Spectrum imaging system and luminescence was quantified and analysed using the Living Image 4.0 software (Caliper Life Sciences, Hoplinton, USA).

To genotype mice, animals were anaesthetised with isoflurane prior to imaging and injected i.p. with 100 µl of 15 mg/ml D-luciferin (Synchem, Altenburg, Germany) in 1x PBS, sterile filtered. Ten minutes after injection, mice were imaged, marked with ear punches for identification and returned to their cages. For luminescent imaging as part of *in vivo* studies, mice were anaesthetised with isoflurane and their abdominal fur removed by shaving using

clippers. Mice were then injected i.p. with 200 µl of 15 mg/ml D-Luciferin in 1x PBS followed by imaging at 1, 5 and 10 minutes post injection. Following imaging, animals were returned to their cages. For imaging of organs *ex vivo*, mice were injected with 200 µl D-luciferin and euthanised 10 minutes post injection. Organs were dissected rapidly and images taken.

In order to quantify the luminescent signal from captured images, regions of interest were manually circled using the Living Image software and total flux values (photons/second) were calculated.

2.2.7. Serum enzyme assays

Serum samples were collected by tail vein bleed or by terminal bleed after autopsy. Blood was left to clot before centrifugation at 16,000 x*g* for 5 minutes. The serum was aspirated and transferred to a clean microcentrifuge tube. Serum samples were stored at -80°C until analysis for liver serum enzyme activities of alkaline phosphatase (ALP, biomarker for cholangiocyte injury (Scharschmidt *et al.*, 1983) and alanine aminotransferase (ALT, biomarker for hepatocyte injury (Sherman, 1991)). ALP serum levels were determined using a fluorimetric alkaline phosphatase assay kit (Abcam, cat# ab83371) following the manufacturer's instructions. ALP cleaves the phosphate group of the non-fluorescent 4-methylumbelliferyl phosphate disodium salt substrate which results in a fluorescent signal (Ex/Em = 360 nm / 440 nm) being emitted by the reaction product 4-methylumbelliferone (Figure 2.2). The fluorescent signal was measured using a microplate reader (Synergy HT, BioTek, Swindon, UK). Serum ALT activities were measured by the Royal Victoria Infirmary Clinical Biochemistry Department in Newcastle Upon Tyne, UK.

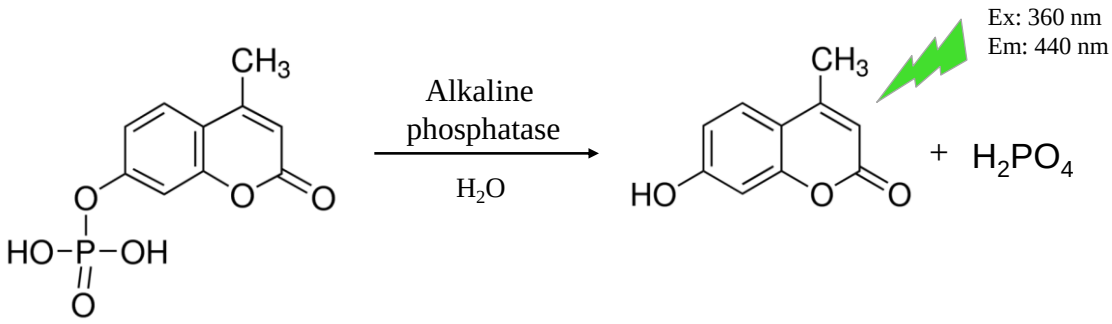

4-Methylumbelliferyl phosphate **4-Methylumbelliferone**

Figure 2.2 Alkaline phosphatase reaction.

2.3. Cell culture

2.3.1. Materials and reagents

Dulbecco's Modified Eagle's Medium (DMEM, cat# D5546), Minimum Essential Medium Eagle (MEME, cat# D2279), Ham's F12 medium (cat# 51651C), Foetal Bovine Serum (FBS, cat# F9665), glutamine, penicillin-streptomycin solution, adenine, triiodothyronine, epinephrine, ITS solution, hydrocortisone and trypsin-ethylenediaminetetraacetic acid (Trypsin-EDTA) were purchased from Sigma. Non-essential amino acids and sodium pyruvate were sourced from Gibco (Life technologies). 1x PBS was prepared from tablets (Sigma) dissolved in ultrapure laboratory grade (MilliQ) water and sterilised by autoclaving. All routine culture plastic ware was obtained from Greiner Bio-one Ltd (Stonehouse, UK).

2.3.2. Culture of adherent cell lines

Adherent cell lines were sourced and routinely cultured in 75 cm^2 cell culture flasks in appropriate complete culture medium as specified in Table 2.5. Cells were maintained at 37°C in a 5% CO_2, humidified atmosphere. Cell culture medium was changed every 2-3 days.

Cell line	Source	Species/Morphology	Culture medium
603B	Gift from Dr Yedidya Saiman (Mount Sinai School of Medicine, New York)	murine biliary epithelial	DMEM (low glucose), 10% (v/v) FBS, 2 mM glutamine, 100 U/ml penicillin, 100 µg/ml streptomycin
MCF-7	Gift from Dr Katherine Rennie (Newcastle University, UK)	human breast cancer	
HEK293	ECACC (catalogue 85120602, Porton Down, UK)	human embryonic kidney	
SH-SY5Y	Gift from Dr Peter Hanson (Newcastle University, UK)	human neuroblastoma	
AR42J-B13	Gift from Dr Karen Wallace (Aberdeen University, UK)	rat pancreatic acinar	
LTPA	ATCC (catalogue CRL-2389, Manassas, Virginia)	murine pancreatic epithelial	MEME, 10% (v/v) FBS, 2 mM glutamine, 100 U/ml penicillin, 100 µg/ml streptomycin, 1% (v/v) NEAA, 1 mM sodium pyruvate
H69	Gift from Dr Andrew Axon, Newcastle University	human biliary epithelial	DMEM:Ham's F12 (2:1), 10% (v/v) FBS, 2 mM glutamine, 100 U/ml penicillin, 100 µg/ml streptomycin, 240 ng/ml adenine, 27 ng/ml triiodothyronine, 10 µg/ml epinephrine, 1x ITS solution, 1 µM hydrocortisone

Table 2.5 Adherent cell lines, source and cell culture media. ECACC, European Collection of Cell Cultures; DMEM, Dulbecco's Modified Eagle's Medium; FBS, Foetal bovine serum; MEME, Minimum Essential Medium Eagle; NEAA, Non-Essential Amino Acids; ITS, Insulin-Transferrin-Selenium.

2.3.3. Cell passage

To maintain cell lines in an exponential growth phase, cells were passaged 2-3 times a week or upon reaching 80-100% confluency. Cells were washed with 10 ml of sterile 1x PBS before incubation with 2-3 ml (for a 75 cm^2 flask) of 1x Trypsin-EDTA diluted in 1x PBS to detach cells (typically no more than 10 minutes). Careful impact to the cell culture vessel was used to encourage detachment. The trypsin was inactivated by adding complete culture medium to the cell suspension. Cells were collected in 50 ml tubes and centrifuged at 200 x*g* for 5 minutes. The supernatant was discarded and cells were re-suspended in fresh complete culture medium. Cells were then seeded into 75 cm^2 flasks or multi-well plates for maintenance or subsequent experiments.

2.3.4. Long term cell storage

Cell stocks for all cell lines used were periodically frozen and stored in liquid nitrogen. After trypsinisation, cells of one confluent 75 cm^2 flask were pelleted and re-suspended in 2 ml freezing medium containing 90% (v/v) FBS and 10% (v/v) dimethyl sulfoxide (DMSO). One ml of cell suspension was added per sterile cryogenic storage vial and frozen at a controlled rate in a freezing container filled with isopropyl alcohol. Frozen cell stocks were then transferred to liquid nitrogen for long-term storage.

2.3.5. Revival of cell stocks

Cell stocks cryogenically stored in liquid nitrogen were thawed in a 37°C water bath. The cell suspension was carefully re-suspended and transferred to 10x its volume of pre-warmed (37°C) complete medium in a 50 ml tube. Cells were pelleted by centrifugation at 200 x*g* for 5 minutes, the supernatant was discarded and the cell pellet was re-suspended in fresh complete culture medium. The cell suspension was added to a 25 cm^2 tissue culture flask and viable cells were allowed to attach for 24 hours before the culture medium was replaced. Upon reaching confluency, cells were trypsinised, transferred to 75 cm^2 culture flasks and cultured as previously described.

2.3.6. Assessment of cell viability and number

Cell viability was measured by trypan blue exclusion assay (Strober, 2001), a dye that is able to pass the membrane of dead cells thus staining them blue. Cells that stain blue are considered as non-viable whereas cells with a clear cytoplasm are considered viable. Cell suspensions were diluted 1:1 with 0.2 % (w/v) trypan blue solution and loaded onto a disposable haemocytometer (C-Chip, Neubauer improved, Digital Bio). Total cell number and

cell viability in a known volume were determined by counting both trypan blue excluding (viable) and non-excluding (non-viable) cells.

2.3.7. Charcoal/dextran-treated FBS

FBS contains a number of steroid hormones which can affect nuclear receptor activities. It is therefore often required to deplete or 'strip' FBS of endogenous hormones for experiments investigating steroid hormone signalling. Pre-treatment of FBS with activated charcoal and dextran can be carried out to remove steroid hormones and other low molecular weight compounds from the serum (Aakvaag *et al.*, 1990).

3% (w/v) of activated charcoal and 0.03% dextran T70 were added to 24 ml MilliQ H_2O which was subsequently vortexed and incubated for 15 minutes at room temperature. The charcoal/H_2O mixture was then centrifuged at 9000 x*g* for 10 minutes and the supernatant discarded. The wash step in H_2O was repeated once more. The charcoal pellet was then re-suspended in 25 ml FBS and incubated at 4°C for 30 minutes on a rotator followed by incubation at 45°C for 30 minutes in a water bath, vigorously shaking. The charcoal/FBS was centrifuged at 3200 x*g* at 4°C for 10 minutes. The supernatant was removed to a clean tube and centrifuged again at 3200 x*g* at 4°C for 15 minutes followed by removal and transferal of the supernatant to a clean tube and a final spin at 25,000 x*g* at 4°C for 20 minutes. The FBS supernatant was aliquoted and stored at -20°C. Following addition of stripped FBS to media, the media was sterilised by filtering through a 0.22 μm filter unit.

2.4. Isolation of primary human biliary epithelial cells from human liver

Primary human biliary epithelial cells (hBECs) were isolated from surgical liver resections from the margins of tissue from patients with both benign and malignant tumours. Tissue was obtained with informed donor consent and ethical approval from the Newcastle & North Tyneside 2 Research Ethics Committee.

2.4.1. Digestion

The liver tissue was perfused with Hank's Balanced Salt Solution (HBSS) without calcium and magnesium ($HBSS^-$) (10x stock (1.38 M NaCl, 53.3 mM KCl, 56 mM glucose, 4.4 mM KH_2PO_4, 3 mM Na_2HPO_4 and 0.3 mM phenol red) made up with sterile water to 1x and further supplemented with 6 mM sterile (4-(2-hydroxyethyl)-1-piperazineethanesulfonic acid) (HEPES) and 4 mM $NaHCO_3$) to remove the remaining blood from the resected tissue. To facilitate digestion, the resected liver tissue was then perfused with $HBSS^+$ ($HBSS^-$ with the

addition of 1 mM $CaCl_2$) containing 1 mg/ml Collagenase A and 80 μg/ml DNAse I to reduce clumping. Following perfusion, the fibrous Glisson's capsule was removed and the liver was divided into pieces (around 30-40 g) which were minced (1-2 mm^2 pieces) in a sterile petri dish using a sterile scalpel. The liver tissue was then transferred to a sterilin. All following steps apply to 30-40 g of tissue. Five ml of 10 mg/ml collagenase type A and 2 ml of 2 mg/ml DNase I was added to the minced tissue and diluted with 43 ml of 1x PBS. The liver was incubated at 37°C for 30-45 minutes. After incubation, the liver tissue and collagenase mixture was sieved through a 125 μm Nybolt mesh attached to a beaker (sterile) using a plunger from a 10 ml syringe. 1x PBS was added frequently to facilitate cell passage. The tissue was mashed for 10-15 minutes until only connective tissue remained. The mesh was carefully removed from the beaker and squeezed to encourage further cell extraction. Five ml of 2 mg/ml DNase I was added to the resulting cell suspension which was made up to 400 ml with 1x PBS and then divided between 8 x 50 ml tubes. The tubes were centrifuged for 5 minutes at 600 x*g* at room temperature. The supernatant was discarded and each pellet was re-suspended in 20 ml 1x PBS. Two pellets were pooled in one 50 ml tube, made up to 50 ml with 1x PBS and centrifuged again for 5 minutes at 600 x*g*. This step was repeated until all pellets were pooled in one 50 ml tube, re-suspended in 24 ml 1x PBS.

2.4.2. Semi-purification of hBECs using density gradient

Following digestion, hBECs were semi-purified using non-toxic low viscosity and low osmolarity density gradients made from Percoll which consists of colloidal silica particles of 15-30 nm diameter (23% w/w in water) coated with polyvinylpyrrolidone (PVP) (GE Healthcare, Amersham, UK). To prepare a percoll stock solution, percoll was diluted 9:1 (v/v) with 10x PBS. The percoll stock solution was then used to generate a 33% (v/v) and a 77% (v/v) percoll solution by dilution with 1x PBS. Gradients were prepared in 15 ml centrifuge tubes by underlying 3 ml of 33% percoll with 3 ml of 77% percoll. Next, 3 ml of the liver cell suspension were carefully layered onto each Percoll gradient. The tubes were centrifuged at 670 x*g* for 30 minutes at 80% acceleration and 0% deceleration at room temperature. Centrifugation results in the appearance of 2 rings, the top ring containing hepatic stellate cells (HSCs) and the bottom ring comprises the hBECs (Figure 2.3).

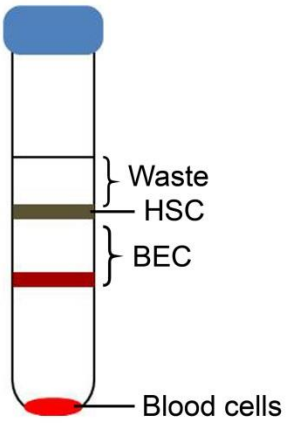

Figure 2.3 Semi-purification of hBECs by percoll density gradient centrifugation. HSC, hepatic stellate cells; BEC, biliary epithelial cells.

The bottom ring and the overlying aqueous layer containing primarily hBECs were carefully extracted using a Pasteur pipette and transferred to 50 ml tubes. To wash the extracted hBECs, three volumes of 1x PBS were added and cells were centrifuged at 600 x*g* for 5 minutes. The supernatant was discarded and the pellet re-suspended in 9 ml of cold 0.1% (w/v) bovine serum albumin (BSA) in 1x PBS. The mixture was transferred to a 15 ml centrifuge tube.

2.4.3. Anti-HEA-125 immuno-magnetic affinity purification of hBECs

After semi-purification by density gradient, hBECs were purified by immuno-magnetic cell separation using HEA-125 Dynabeads (Thermofisher, UK). These Dynabeads are superparamagnetic polymer beads coated with the monoclonal antibody HEA-125 specific for the epithelial cell surface antigen epithelial cell adhesion molecule (EpCAM) (Shan, 2011) which allow for hBECs to be separated using a magnet (Figure 2.4).

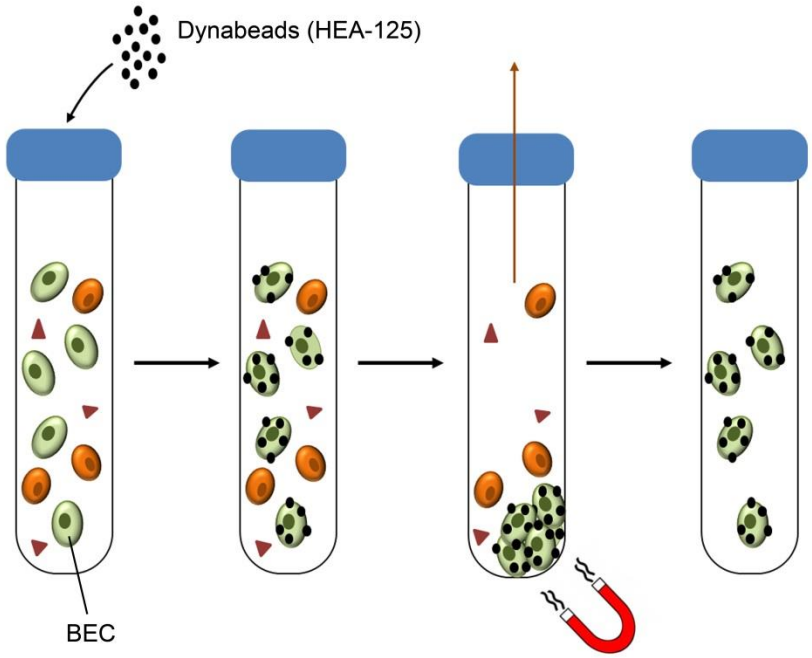

Figure 2.4 Immuno-magnetic separation of hBECs.

Following adequate mixing on a roller, 50-100 µl of Dynabeads were transferred to a 1.5 ml microcentrifuge tube and 1 ml of cold 0.1% BSA in 1x PBS was added. The tube was placed on the magnet (Dynamag, Life technologies) for 1 minute. The supernatant was carefully removed with a pipette and 1 ml of 0.1% BSA in 1x PBS was added. The tube was removed from the magnet and Dynabeads were resuspended and added to the semi-purified hBEC suspension. The suspension was incubated on a roller at 4°C for 30 minutes. The tube was then placed on the magnet for 5 minutes before carefully removing the supernatant with a Pasteur pipette. Ten ml of 0.1% BSA in 1x PBS was added to the tube, the tube was removed from the magnet and hBECs bound to Dynabeads were resuspended. The tube was placed back on the magnet for 2 minutes following careful removal of the supernatant. The last wash step was repeated once more to ensure removal of non-binding cells. Human BECs bound to Dynabeads were resuspended in 10 ml of pre-warmed BEC medium (see Section 2.4.4) and transferred to a 25 cm^2 tissue culture flask.

2.4.4. Culture of hBECs

Isolated primary hBECs were grown in 1:1 DMEM:Hams F12 medium supplemented with 10 % (v/v) FBS, 2 mM glutamine, 100 U/ml penicillin, 100 µg/ml streptomycin, 10 ng/ml epidermal growth factor (EGF), 0.248 IU/ml Insulin, 2 µg/ml hydrocortisone, 10 ng/ml cholera toxin, 2 nM tri-iodo-L-thyronine and 5 ng/ml hepatocyte growth factor (HGF). Cells were grown in 25 cm^2 culture flasks or 6-well plates in conditions described in 2.3.2. Cell culture medium was changed every 1-2 days.

2.5. Isolation of primary mouse biliary epithelial cells from mouse livers

Primary mouse biliary epithelial cells (mBECs) were isolated from livers of female and male C57Bl/6 wt mice and tg NF-κB-luc mice. Mice were terminated by cervical dislocation and their livers dissected.

2.5.1. Digestion

Livers were cut into small pieces in a sterile petri dish and up to six livers were pooled in a 50 ml tube containing 25 ml $HBSS^+$ supplemented with 1 mg/ml collagenase type A (made up as a stock of 10 mg/ml) and 80 μg/ml DNAse I (from a 2 mg/ml stock). The livers were incubated at 37°C for 30-45 minutes until digested. After incubation, the liver tissue and collagenase mixture was poured onto a Nybolt mesh attached to a beaker (sterile) and sieved into the beaker using a plunger from a 2 ml syringe. $HBSS^+$ was added frequently to facilitate cell passage. The mash was carefully removed from the beaker and 0.5 ml of 2 mg/ml DNase I was added to the resulting cell suspension which was made up to 100 ml with $HBSS^+$ and then divided between 2 x 50 ml tubes. The tubes were centrifuged for 5 minutes at 600 x*g* at room temperature. The supernatant was discarded and each pellet was re-suspended in 20 ml $HBSS^+$. The pellets were pooled in a 50 ml tube, filled up to 50 ml with $HBSS^+$ and centrifuged again for 5 minutes at 600 x*g*. The pellet was washed one more time with $HBSS^+$. The final pellet was resuspended in 12 ml $HBSS^+$.

2.5.2. Semi-purification and culture

Next, mBECs were semi-purified by Percoll density gradient as described in Section 2.4.2 with the following changes: after the wash step with PBS, the supernatant was discarded and the pellet re-suspended in BECs growth medium as specified in Section 2.4.4. Anti-HEA125 affinity purification was not carried out since the antibody did not crossreact with its mouse orthologue and did not improve the yield or purity.

Mouse BECs were seeded into a 25 cm^2 tissue culture flask, 6-well plates or 4-chamber microscope slides (BD Falcon) as required and maintained as described in Section 2.3.2.

2.6. Cell transfections

2.6.1. Transfection using Effectene reagent

Effectene transfection reagent (Qiagen, Manchester, UK) was used to routinely transfect 603B and LTPA cells according to the manufacturer's instructions. On the day before transfection,

cells were seeded into 24-well tissue culture plates in 0.5 ml of growth medium and allowed to reach 60-70% confluency. Typically for one well of a 24-well plate, 250 ng of total plasmid DNA was mixed with 20 µl EC buffer before the addition of 1.5 µl enhancer. Following 5 minutes incubation at room temperature, 1.6 µl effectene reagent was added to the transfection mix, vortexed and incubated at room temperature for 15 minutes. The transfection mix was made up to 150 µl with complete culture medium and added to the cells in a drop-wise manner. Cells were incubated for 24 hours under normal culture conditions. For transfection of cells seeded into smaller/larger multi-well plates, volumes of transfection reagents and DNA amounts were scaled down/up according to the surface area of the well.

2.6.2. Transfections using polyethyleneimine

MCF-7 and HEK293 cells were routinely transfected using polyethyleneimine (PEI). A 1 mg/ml PEI working solution was prepared by dissolving PEI in MilliQ H_2O. The solution was neutralised to pH7 with NaOH, filter sterilised (0.22 µm) and aliquoted for longer term storage at -20°C. Once thawed, the working stock was stored at 4°C for up to 6 months. To transfect cells, a transfection mix was prepared by adding 7 µg of total plasmid DNA and 21 µl PEI working solution to 1 ml of serum-free DMEM. The mix was vortexed and incubated at room temperature for 20 minutes before drop-wise addition to ~70% confluent cells. Typically for one well of a 24-well plate, 30 µl of the transfection mix was added. Cells were incubated for 24 hours under standard culture conditions before the experimental procedure continued. The volume of transfection mix to add to the cells was scaled up/down according to the surface area of the wells that cells were grown in.

2.6.3. Transfections using Lipofectamine 2000 reagent

B-13 cells were transfected using Lipofectamine 2000 (Invitrogen) according to the manufacturer's instructions. Cells were seeded into 24-well tissue culture plates in 0.5 ml of medium 24 hours before transfection to grow to around 70% confluence. Typically for transfection in one well of a 24-well plate, 500 ng of total plasmid DNA and 1.1 µl of Lipofectamine 2000 reagent were used. The appropriate amount of plasmid DNA and Lipofectamine 2000 were added to serum free medium in separate vials and incubated for 5 minutes at room temperature. Vials were then combined, gently mixed by tapping and incubated at room temperature for 20 minutes before 50 µl of transfection mix were added drop-wise to each well of a 24-well plate. Transfected cells were incubated for 24 hours under standard conditions before the culture medium was changed and the experimental procedure continued.

2.6.4. Assessment of transfection efficiency

For the assessment of transfection efficiency, a green fluorescent protein (GFP) control plasmid (peGFP-N1, Clonetech) was included for all transfection methods as described above. GFP expression was visualised 24-48 hours after transfection by fluorescent microscopy (see Figure 2.5). GFP-positive cells were counted and expressed as a percentage of the total cell number of cells per field of view, the average transfection efficiency of 3 fields per view was calculated.

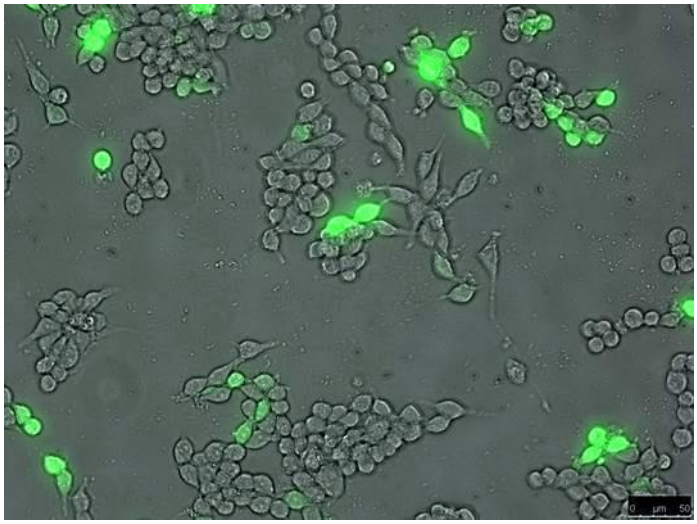

Figure 2.5 peGFP-N1 transfected AR42J-B13 cells. Merged bright field and FITC image of AR42J-B13 cells transfected with the peGFP-N1 plasmid.

2.7. Dual-glo luciferase reporter gene assay

A dual luciferase reporter system was used to assess ER transcriptional activity. This system is designed to decrease experimental variability between replicates which can occur due to unequal cell numbers and transfection rates. Cells were co-transfected with two different plasmids resulting in the expression of two different reporter enzymes, Firefly (*Photinus phyralis*) and Renilla (*Renilla reniformis*, sea pansy) luciferase, within a single system. In these experiments, Firefly luciferase is normally regulated by response elements in conjuction with a minimal promotor whereas the Renilla luciferase is under the control of a constitutively active promoter. The dual-glo assay system (Promega, Southampton, UK) measures both Firefly and Renilla luciferase activities in the same sample. The addition of luciferin, the substrate for Firefly luciferase, permits the measurement of Firefly luciferase activity. The reaction is then quenched by the addition of the Stop and Glo solution which inhibits Firefly luciferase and at the same time provides the substrate for and initiates Renilla luciferase

activity (Figure 2.6). Both reactions produce a luminescent signal as readout for luciferase activity which can be read using a luminometer.

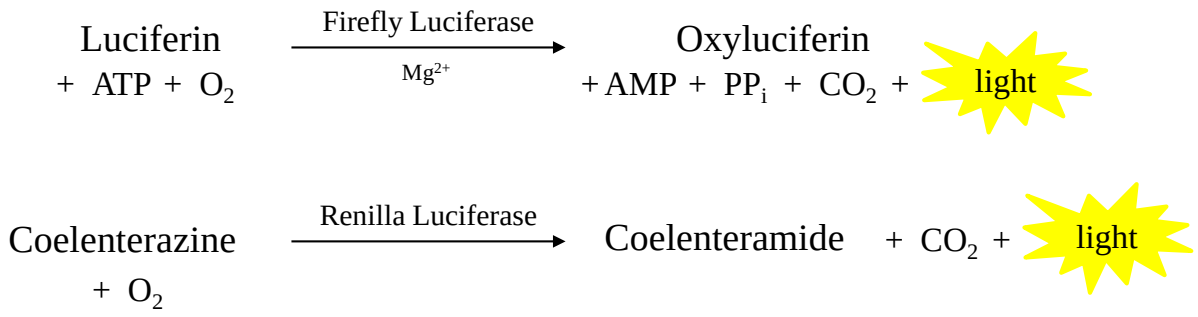

Figure 2.6 Bioluminescent Firefly and Renilla luciferase reactions.

Cells in 24-well plates were transfected with a reporter construct (either the $(ERE)_3$-pGL3promotor construct or the 3XERE TATA luc construct, for vector maps see Sections 2.8.1 and 2.8.2) and the control construct RL-TK as outlined in Section 2.6 at a ratio of not less than 6:1 followed by incubation for 24 hours and treatments as indicated for another 24 hours. On the day of the dual-glo luciferase assay, the culture medium was removed and cells were washed with sterile 1x PBS. Cells were then lysed with 150 µl of NETN buffer (100 mM NaCl, 20 mM Tris-Cl (pH 8.0), 0.5 mM EDTA, 0.5 % (v/v) Nonidet P-40 (NP-40)) per well of a 24-well plate for 15 minutes at room temperature on an orbital shaker before 50 µl of the lysate was transferred to a well of a white 96-well microplate. An equal volume of luciferase buffer (prepared following the manufacturer's instructions) was added to the cell lysate which was then incubated for 10 minutes at room temperature before the measurement of the luminescent signal produced by Firefly luciferase using a microplate reader (Synergy HT, BioTek, Swindon, UK). The luciferase activity was subsequently inhibited by adding 50 µl of pre-diluted Stop and Glo reagent per well and the luminescent signal produced by active Renilla luciferase was measured. After subtraction of background luminescence (from non-transfected cells), expression of Firefly luciferase was normalised to the expression of Renilla luciferase by dividing the Firefly value by the Renilla measurement. All measurements were further normalised to the control group (vehicle control) or to a group as indicated and values constituted as a fold change in normalised luciferase activity in response to different treatments.

2.8. Plasmid DNA constructs and cloning

2.8.1. $(ERE)_3$-pGL3promotor construct

The $(ERE)_3$-pGL3promotor plasmid is a luciferase reporter construct that allows to quantitatively measure the regulation of oestrogen-dependent gene expression *in vitro* (Axon *et al.*, 2012). It consists of three repeats of the consensus oestrogen response element (ERE) with a three base pair (ATT) spacer (GGTCA ATT TGACC) located upstream of the reporter gene coding for Firefly luciferase. Activation of the ER and consequent binding to the ERE will result in the expression of the Firelfy luciferase reporter gene which can subsequently be measured by dual-glo reporter gene assay (see Section 2.7).

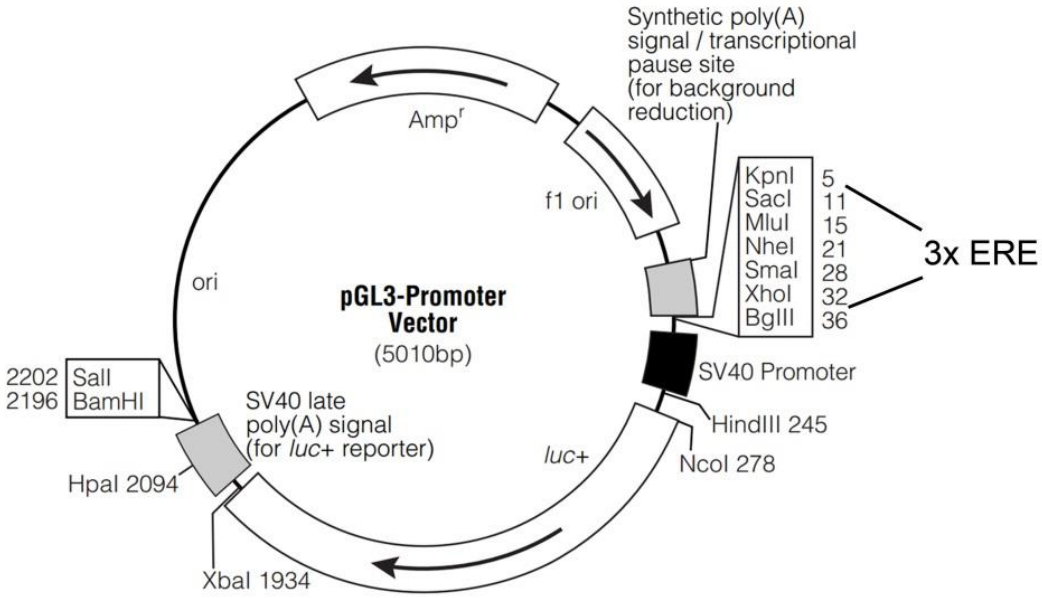

Figure 2.7 $(ERE)_3$-pGL3promotor vector map. Adapted from Promega (2016a).

2.8.2. 3XERE TATA luc construct

The 3XERE TATA luc plasmid (5757 bp) was a gift from Dr. Donald McDonnell (Addgene plasmid #11354 (Hall and McDonnell, 1999)) and similar to the $(ERE)_3$-pGL3promotor construct, it provides a basis to measure the regulation of oestrogen-dependent gene expression *in vitro*. The 3XERE TATA luc plasmid differs from the $(ERE)_3$-pGL3promotor construct in that it has a different vector backbone (pGL2-TATA-Inr) and it comprises three copies of the vitellogenin ERE (GGTCA CAG TGACC) situated upstream of the *Firefly* luciferase reporter gene.

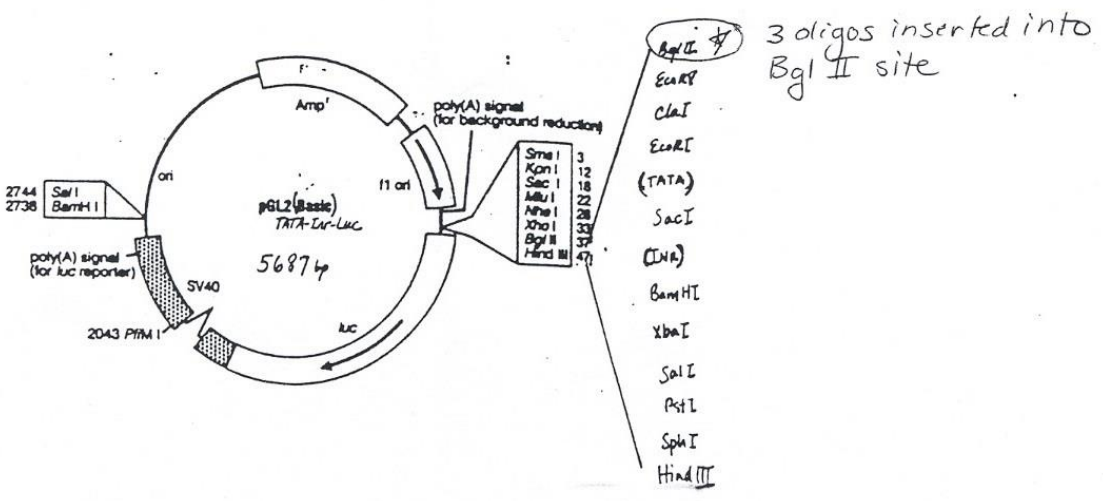

Figure 2.8 3XERE TATA luc vector map. Addgene (plasmid #11354).

2.8.3. RL-TK construct

The RL-TK construct (Promega, cat# E2241) was used as an internal control reporter and was co-transfected into cells along with the experimental ERE luciferase reporter constructs described in Sections 2.8.1 and 2.8.2. The RL-TK plasmid encodes the Renilla luciferase (RL) gene which is under the control of a constitutively active minimal promotor from the housekeeping gene thymidine kinase (TK). Constitutive expression of Renilla luciferase (i.e. independent of nuclear receptor regulation) allows for experimental data to be normalised, a process which is required to account for experimental variations such as cell number and transfection efficiency between treatment groups.

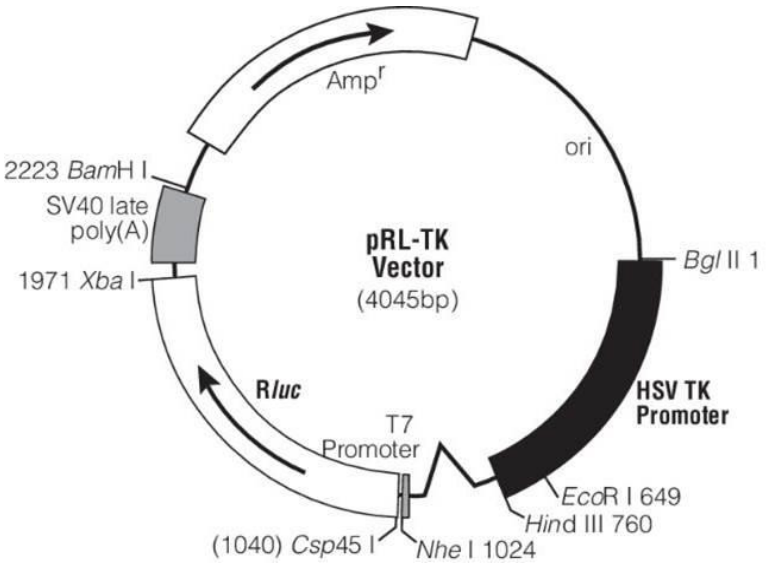

Figure 2.9 RL-TK vector map. Catalogue #E2241. Source: Promega (2016b).

2.8.4. pcDNA3.1 vector

The pcDNA3.1 vector (5428 bp) is designed for high level constitutive protein expression in a range of mammalian cell lines. It contains a CMV promotor and a multiple cloning site containing a large number of common restriction sites which allow a gene of interest to be inserted.

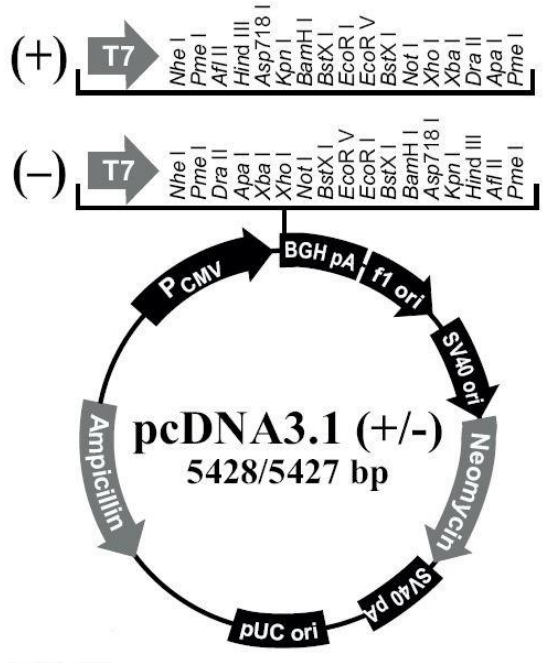

Figure 2.10 pcDNA3.1 vector map. Source: Xenbase (2016).

2.8.5. Ligation of a gene of interest into a pCR-Blunt or pcDNA3.1 vector

After amplification of a gene of interest by Polymerase Chain Reaction (PCR, see Section 2.10), gel extracted (see Section 2.8.11) blunt-end PCR products were ligated into the pCR-Blunt vector using the Zero Blunt PCR Cloning Kit (Life technologies) according to the manufacturer's instructions. The ligation reaction was typically set up as specified in Table 2.6. The ligation reaction was incubated at 16°C for 4 hours before transformation into *E.coli* cells (Section 2.8.6).

Reagent	**Volume**
pCR-Blunt vector	1 µl (25 ng)
PCR product (blunt-end)	5 µl
5X T4 DNA ligase buffer	2 µl
Sterile H_2O	1 µl
T4 DNA ligase	1 µl

Table 2.6 Set up of ligation reaction using the Zero Blunt PCR Cloning Kit.

For ligation of a specific gene into the destination vector pcDNA3.1, the linearised vector was first treated with Antarctic Phosphatase (New England Biolabs, Hitchin, UK) which removes 5' phosphates to prevent recircularization. Generally, 3.3 µl of 10x reaction buffer and 1 µl of phosphatase were added to 30 µl of vector DNA. The reaction was incubated at 37°C for 15 minutes followed by heat-inactivation of the enzyme at 70°C for 5 minutes.

Two ligation reactions were then set up with molar vector:insert ratios of 1:3 and 1:6. The following equation was used to calculate the amount of insert needed for 100 ng of pcDNA3.1 destination vector:

$$insert\ [ng] = \frac{100\ ng\ vector\ x\ size\ of\ insert\ (kb)}{size\ of\ vector\ (kb)}\ x\ molar\ ratio\ of\ \frac{insert}{vector}$$

The appropriate amounts of phosphatase-treated vector and insert were then set up in a ligation reaction as outlined in Table 2.7. Before addition of T4 DNA ligase (Promega), the ligation mix was incubated at 65°C for 5 minutes and then cooled down on ice. T4 DNA ligase was added and the ligation mixture was incubated at room temperature for 3 hours or at

16°C overnight before transformation of the ligation product into *E.coli* bacterial cells (see Section 2.8.6).

Reagent	Amount/Volume
pcDNA3.1 plasmid	100 ng
Insert (gene of interest)	to be calculated
10X T4 DNA ligase buffer	1 µl
Sterile H_2O	Make up to 9 µl
T4 DNA ligase	1 µl

Table 2.7 Set up of ligation reaction to clone a gene of interest into the mammalian expression vector pcDNA3.1.

2.8.6. Transformation of competent E. coli cells

To propagate plasmid DNA, chemically competent TOP10 *E. coli* cells (Life technologies) were transformed with the plasmid or ligation product of interest. The bacterial cells were stored at -80°C and thawed on ice before use. In order to transform cells, 50-100 ng of plasmid DNA was added to one vial of *E. coli* cells which were gently mixed by tapping and incubated on ice for 30 minutes. To facilitate cellular uptake of DNA, *E. coli* cells were heat-shocked in a 42°C water bath for 30 seconds followed by incubation on ice for at least 2 minutes. Two hundred and fifty microlitres of pre-warmed S.O.C. medium (2% (w/v) tryptone, 0.5% (w/v) yeast extract, 10 mM NaCl, 2.5 mM KCl, 10 mM $MgCl_2$, 10 mM $MgSO_4$, and 20 mM glucose) was added to each vial of bacterial cells which were then incubated for 1 hour at 37°C in an orbital rotating incubator set to 225 rpm. The cells were spread on LB agar plates (Luria Broth: 10 g NaCl, 10 g tryptone, 5 g yeast extract + 15 g agar in 1L MilliQ H_2O) containing the appropriate selective antibiotic (Ampicillin: 100 µg/ml, Kanamycin: 50 µg/ml) in order to select clones. The plates were incubated upside-down at 37°C overnight. On the next day, several colonies were picked and each colony was grown in mini cultures (5 ml of LB (10 g NaCl, 10 g Tryptone, 5 g yeast extract in 1L MilliQ H_2O) containing the appropriate selective antibiotic marker) at 37°C overnight, shaking at 225 rpm, for the purpose of making glycerol stocks for storage or to purify plasmid DNA by miniprep.

2.8.7. Storage of transformed bacterial cultures

To safely store transformed bacterial clones long-term, glycerol stocks were prepared. Bacterial overnight mini cultures were mixed with sterile glycerol at a ratio of 1:1 before storage at -80°C. Whenever required, glycerol stocks were used to produce more plasmid

DNA by streaking out 10 µl of the stock onto a LB agar plate containing the appropriate selective antibiotic followed by incubation at 37°C overnight. A mini culture was then prepared from a single colony as previously described and plasmid DNA was purified by mini- or maxiprep.

2.8.8. Plasmid DNA miniprep

For low-scale plasmid DNA purification from transformed *E. coli* cells, minipreps were performed according to the manufacturer's instructions (Qiagen). Generally, 5 ml of overnight mini culture were pelleted at 3200 x*g* for 15 minutes at 4°C. Following plasmid extraction according to the manufacturer's protocol, plasmid DNA was re-suspended in 50 µl nuclease-free H_2O (Qiagen) and stored at -20°C.

2.8.9. Plasmid DNA maxiprep

Maxipreps (Qiagen) were performed when large amounts of plasmid DNA were required. Typically, 1 ml of overnight mini culture was added to 200 ml of LB containing the appropriate selective marker on the day before plasmid extraction and grown overnight at 37°C, shaking at 225 rpm. Bacterial cells were then pelleted at 3200 x*g* for 30 minutes at 4°C. Plasmid DNA from transformed *E. coli* cells was extracted as per protocol supplied by the manufacturer. The resulting plasmid DNA pellet was re-suspended in 500-750 µl nuclease-free H_2O and stored at -20°C. DNA concentration was determined as described in Section 2.9.3.

2.8.10. Restriction digest

Following isolation by mini- or maxiprep, plasmid DNA was analysed for correct assembly by digest with restriction endonucleases, enzymes which cut DNA at a particular place dependent on the sequence. Restriction digests were essentially carried out as per the manufacturer's protocol (New England Biolabs). Typically, restriction digests were prepared to contain 2 µl of 10x reaction buffer (depending on type of enzyme used), 2 µl of plasmid DNA as obtained after mini- or maxiprep, 1 µl of restriction enzyme and made up to 20 µl with nuclease-free H_2O. Reactions were incubated at 37°C for 3-4 hours. Following incubation, DNA loading buffer was added to the samples and DNA fragments were separated by agarose gel electrophoresis as described in Section 2.10.4.

2.8.11. Purification of DNA from agarose gel

Following restriction digest and agarose gel separation (see Section 2.10.4) DNA fragments and vector backbones were isolated from agarose gels using the QIAquick gel extraction kit (Qiagen) according to the manufacturer's instructions. In brief, DNA was visualised with UV light in a gel documentation system (G:BOX, Syngene) and the desired fragment was excised using a sterile scalpel. The gel containing the DNA fragment was weighed and transferred to a microcentrifuge tube followed by extraction of DNA as per supplied protocol. DNA was essentially eluted with 30 µl of nuclease-free H_2O and quantified as outlined in Section 2.9.3.

2.8.12. DNA sequencing

When required, plasmid DNA was sequenced by DNAseq (Dundee, UK) with sequence specific primers. DNA sequencer chromatogram data was analysed using the publically available software Finch TV (Geospiza, Inc.).

2.9. Isolation and quantification of RNA

2.9.1. RNA purification using Trizol

Trizol (Invitrogen, Paisley, UK) was used to isolate RNA from cultured cells or whole tissue. For isolation of RNA from adherent cells, growth medium was removed, cells were washed twice with sterile 1x PBS and 1 ml of Trizol was added to 1 well of a 6-well plate. Cells were incubated in Trizol for 3 minutes at room temperature before mixing by pipetting and transfer to a 1.5 ml microcentrifuge tube. For isolation of RNA from tissue, 1 ml of Trizol was added to tissue not exceeding 10% of the volume of Trizol. Tissue samples were manually homogenised and debris were spun down at 1500 x*g* for 4 minutes using a table-top centrifuge. The supernatant was then transferred to a clean 1.5 ml tube. The following steps apply to both cell and tissue samples. 0.2 ml of chloroform was added to the cells/tissue in Trizol and tubes were mixed for 15 seconds by vigorously shaking and incubated at room temperature for 5 minutes. Tubes were then centrifuged at 16,000 x*g* for 15 minutes at 4°C. The upper aqueous layer which contains the RNA was transferred to a clean 1.5 ml tube. 0.5 ml ice-cold isopropanol were added, the tube was inverted once and incubated on ice for 10 minutes. The tube was then centrifuged at 16,000 x*g* for 10 minutes at 4°C. The supernatant was discarded and 0.5 ml of ice-cold 70% ethanol was added to wash the pelleted RNA. The tube was again centrifuged at 16,000 x*g* for 10 minutes at 4°C. The supernatant was removed and the pellet was air-dried for 5-10 minutes before it was re-suspended in 10-20 µl RNase free H_2O (Qiagen). RNA samples were stored at -20°C or -80°C for long term storage.

2.9.2. DNAse treatment

To remove any potentially contaminating genomic DNA from RNA samples, isolated RNA was treated with RQ1 RNase-free DNase (Promega). To an RNA sample of 10 µl, 1 µl (0.1 x the volume of the RNA sample) of both RQ1 RNase-free DNase and 10x DNase buffer were added and incubated at 37°C for 30 minutes. The DNase was then inhibited by adding 0.1 x the volume of RNA sample of DNase stop solution followed by incubation at 65°C for 10 minutes.

2.9.3. Quantification of RNA and DNA concentration and integrity

RNA and DNA concentration and purity within a sample were determined by measuring their absorbance at 260 nm and 280 nm using a NanoDrop 2000 spectrophotometer (Thermo Scientific, Loughborough, UK). Nuclease-free H_2O was used as a blank. An A260/A280 (Absorbance at 260nm and 280nm) ratio between 1.8 and 2.0 generally suggests a pure nucleic acid sample whereas deviant values indicate sample contamination such as with proteins or phenol. RNA samples were then diluted to 200 ng/µl with nuclease-free H_2O and stored at -20°C.

2.10. Reverse Transcription Polymerase Chain Reaction (RT PCR)

2.10.1. cDNA synthesis by reverse transcription

Moloney murine leukaemia virus (MMLV) reverse transcriptase is a RNA dependent polymerase used for first strand cDNA synthesis. Four microlitres of a to 200 ng/µl diluted RNA sample (800 ng RNA) were mixed with 1 µl of random primers (50 ng/µl, Promega) and incubated at 90°C for 3 minutes. Samples were then placed on ice. A reverse transcription master mix containing (per reaction) 4 µl of 5x RT buffer, 8 µl H_2O, 2 µl of 10 mM dNTP's and 1 µl of MMLV was prepared on ice and added to each RNA sample (total volume of 20 µl). The reaction mix was incubated at 42°C for 50 minutes to generate cDNA and samples were stored at -20°C.

2.10.2. Primer design

Forward and reverse primer pairs to amplify specific DNA sequences by PCR were designed using Primer BLAST, a publically available tool on the National Center for Biotechnology Information (NCBI) website (www.ncbi.nlm.nih.gov). Primers were designed to have a length of around 20 nucleotides with a GC content of approximately 60% and melting temperatures

(Tm) close to 60°C. The annealing temperature for each primer set was optimised by starting at 5°C below the calculated Tm. All primers were custom synthesised from Sigma.

2.10.3. Polymerase Chain Reaction (PCR)

PCR is a technique that allows accurate and rapid amplification of specific DNA sequences by using thermostable DNA polymerases in a thermal cycling process. As demonstrated in Figure 2.11, double stranded DNA is initially denatured at high temperatures (>90°C) before annealing of short 5'-3' DNA oligonucleotides (primers) to complementary DNA sequences upstream and downstream of a target region that is to be amplified (amplicon). DNA polymerases then elongate single stranded DNA molecules from 5'-3'. Over several cycles, the target sequence will in principle be amplified exponentially creating large amounts of the amplicon which can be separated and visualised by agarose gel electrophoresis (see Section 2.10.4).

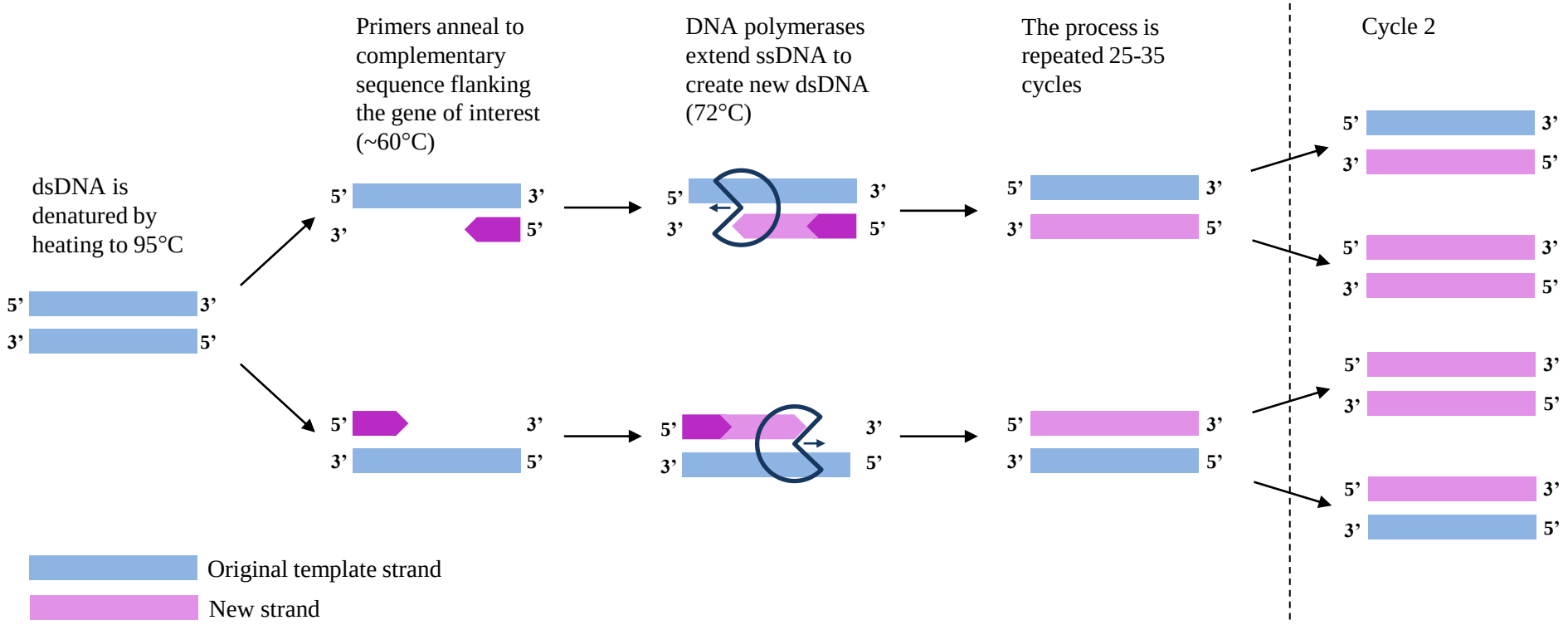

Figure 2.11 The PCR cycle. dsDNA = double stranded DNA, ssDNA = single stranded DNA.

Taq polymerase, derived from the thermophile bacterium *Thermus aquaticus*, is generally used in PCR for amplification of short DNA fragments. The Taq polymerase, however, has a comparatively high error rate as it lacks 3'-5' exonuclease proofreading activity (Lundberg *et al.*, 1991). For applications that require a greater accuracy (e.g. cloning) Phusion High Fidelity polymerase which possesses exonuclease activity was used.

Routine semi-quantitative PCR was carried out using 2x Go-Taq green master mix (contains Taq DNA polymerase, 1.6 mM dNTPs, 3mM $MgCl_2$ and reaction buffer, Promega). The 2x Phusion High-Fidelity PCR Master Mix with HF Buffer (40 units/ml Phusion polymerase, 1.6 mM dNTPs, 4 mM $MgCl_2$, HF reaction buffer, New England Biolabs) was used for cloning work. PCR reactions with the above mentioned DNA polymerases were set up as outlined in Table 2.8.

Taq polymerase		**Phusion polymerase**	
Reagents	**Volume**	**Reagents**	**Volume**
2x Master Mix	10 µl	2x Master Mix	25 µl
Fwd primer (10 µM)	1.5 µl	Fwd primer (10 µM)	3.75 µl
Rev primer (10 µM)	1.5 µl	Rev primer (10 µM)	3.75 µl
cDNA	1 µl	cDNA	4 µl
Nuclease-free H_2O	to 20 µl	Nuclease-free H_2O	to 50 µl

Table 2.8 PCR reactions using Taq or Phusion polymerase. Fwd, forward; Rev, reverse.

A bench top thermocycler (Px2, Thermo Scientific) was used to perform the PCR reactions with optimised cycle parameters and annealing temperatures for each set of primers (detailed in Table 2.10). A typical program for both Taq and Phusion polymerases is shown in Table 2.9.

Step	Taq Polymerase		Phusion Polymerase		Cycles
	Temp (°C)	Time	Temp (°C)	Time	
Denaturation	90	2 min	98	30 s	1
Denaturation	90	50 s	98	10 s	
Annealing	x	1 min	x	30 s	30
Elongation	72	1 min/kb	72	30 s/kb	
Final Elongation	72	10 min	72	10 min	1
Hold	4	∞	4	∞	1

Table 2.9 Typical PCR protocol for Taq and Phusion polymerases.

2.10.4. Agarose gel electrophoresis

PCR amplified DNA was separated for identification using agarose gel electrophoresis. This method allows nucleic acids to be identified by their length since a DNA fragment migrates inversely proportional towards the positive pole of an electrical field across a polymerised agarose gel. A DNA ladder was run alongside for comparison of the DNA fragments with fragments of known size. DNA is visualised by the addition of ethidium bromide to the agarose gel. Ethidium bromide forms a fluorescent complex with nucleic acids which can be visualised under UV light (Lepecq and Paoletti, 1967).

Depending on the size of the target DNA fragment, the percentage of agarose in the gel was chosen to be between 1-2%. Agarose gels were made by adding the required mass of agarose powder (w/v) to 1x tris-acetate-EDTA (TAE) buffer (40 mM tris, 20 mM acetic acid, 1 mM EDTA). The solution was heated to 180°C on a hot-plate and left to boil until the agarose was completely melted and degassed. Once the mixture cooled down to approximately 60°C, 1 µl ethidium bromide per 100 ml melted agarose was added and gently swirled to mix. The gel was cast and a comb was used to form sample wells. The gel was left to set for 1 hour and then placed into an electrophoresis chamber were it was covered with 1x TAE. The PCR samples were mixed with 5x loading dye where appropriate and loaded onto the gel alongside a 2-log DNA ladder (0.1-10 kb, New England Biolabs). Gels were run at 80V until desired migration was reached and PCR products were then visualised under UV light (G:BOX, Syngene).

Oligo ID	5'-3' sequence	Annealing [°C]	Comments
hERαUS hERαDS	CAGTCTATGGGTTGGGGCTC CTGGAACCCATGACCGGAAA	57	Will amplify all 4 human ERα transcript variants (NM_000125; NM_001122740; NM_001122741; NM_001122742) cDNA sequences of 423 bp
hERβUS hERβDS	GGAGTCTGGTCGTGTGAAGG TGTACCAACTCCTTGTCGGC	57	Will amplify 6 human ERβ transcript variants (NM_001437; NM_001040275; NM_001214902; NM_001214903; NM_001271876; NM_001271877) cDNA sequence of 440 bp
humanCK19 F humanCK19 R	GCCACTACTACACGACCATCC CAAACTTGGTTCGGAAGTCAT	57	Will amplify human cytokeratin 19 (NM_002276.4) cDNA sequence of 126 bp
hCYP2E1US hCYP2E1DS	GTTCTTTGCGGGGACAGAGA GAGGGTGATGAACCGCTGAA	59	Will amplify human cytochrome P450, family 2, subfamily E, polypeptide 1 (NM_000773.3) cDNA sequence of 202 bp
rmhGAPDHUS rmhGAPDHDS	TGACATCAAGAAGGTGGTGAAG TCTTACTCCTTGGAGGCCATGT	55	Will amplify rat (NM_017008), human (NM_002046) or mouse (NM_008084) glyceraldehyde 3 phosphate dehydrogenase cDNA sequence of 243 bp
mERαUS mERαDS	AAGGGCAGTCACAATGAACC GCCAGGTCATTCTCCACATT	59	Will amplify mouse ERα (NM_007956) cDNA sequence of 155 bp
mERβUS mERβDS	GGGTGAAGGAGCTACTGCTG GTGTCAGCTTCCGGCTACTC	59	Will amplify mouse ERβ transcript variants 1 and 2 (NM_207707 and NM_010157) cDNA sequence of 576 bp and 522 bp respectively
mCK19US mCK19DS	GTACGCATTGGGTCAGGGGGT TAGGGCGCGCACCTTGTCCAA	55	Will amplify mouse cytokeratin 19 (NM_008471.2) cDNA sequence of 246 bp
mERβUScloning mERβDScloning	TCCGCCTTAAGCCTGGCCGTCACTG TCCGCCTTAAGCCTGGCCGTCACTG	65	Will amplify mouse ERβ transcript variants 1 and 2 (NM_207707 and NM_010157) cDNA sequence of 1744 bp and 1690 bp respectively

Oligo ID	5'-3' sequence	Annealing [°C]	Comments
mERaCloningDSHindIII_1 mERaCloningUSEcoRI	CCTGGAAGCTTTCAGATCGTGTTGGGG CGCCGAATTCCACTTACCATGACCATG	72	Will amplify mouse ERα transcript variants 1, 2 and 3 (NM_007956.5, NM_001302531.1, NM_001302532.1) cDNA sequence of 1829 bp (2-step PCR)
mVimentinUS mVimentinDS	GTGGCTCCGGCACATCGAGC GCGTCGGCCAGCGAGAAGTC	56	Will amplify mouse vimentin (NM_011701.4) cDNA sequence of 226 bp
mCYP2E1US mCYP2E1DS	GTGTTCCGAGGATATGTCATC AAAGCAGAAACAGTTCCATGC	56	Will amplify mouse CYP2E1 (NM_021282.2) cDNA sequence of 223 bp

Table 2.10 DNA oligonucleotide sequences used in RT-PCR.

2.11. Isolation and quantification of protein

2.11.1. Protein isolation from cell lines

The culture medium was aspirated and cells were washed twice with sterile 1x PBS. Whole cell protein extracts were obtained by scraping cells directly into 1x LDS sample buffer (lithium dodecyl sulfate, diluted from 4x stock, Invitrogen) containing 5% 2-mercaptoethanol. Samples were boiled at 95°C for 5 minutes and the protein concentration was determined using the Bradford assay (Section 2.11.3).

2.11.2. Protein isolation from tissue

Tissue samples (snap frozen in liquid nitrogen and stored at -80°C) were manually homogenized in ice-cold RIPA buffer (150 mM NaCl, 1% (w/v) NP-40, 0.5% (w/v) sodium deoxycholate, 0.1% (w/v) SDS, 50 mM Tris, pH 8.0) on ice in a 1.5 ml centrifuge tube (~300 µl RIPA buffer per 15 mg tissue). The samples were incubated by inverting for 2 hours at 4°C. Tissue debris were then spun down at 13,500 x*g* for 20 minutes at 4°C. The supernatant was transferred to a clean tube and the protein concentration was determined by Bradford assay (Section 2.11.3).

2.11.3. Determination of protein concentration by Bradford assay

Total protein concentration was determined by Bradford assay (Bradford, 1976). Bovine serum albumin (BSA, Thermo Scientific) was used to make standards of known protein concentration, ranging from 0 µg/ml to 2000 µg/ml diluted in MilliQ H_2O (final volume: 20 µl). Unknown protein samples were diluted 1:20 with MilliQ H_2O prior to analysis. Five µl of each standard and diluted unknown sample were pipetted into wells of a flat-bottom 96-well plate in triplicates. Two hundred and fifty microlitres of coomassie protein assay reagent (Thermo Scientific) was added to each well which was then incubated at room temperature for 10 minutes. The absorbance of each sample at 595 nm was measured using a microplate reader (BioTek Synergy). A standard curve was produced from the absorbance of the BSA standard concentration samples and the equation for the line of best fit was rearranged to quantify the protein concentration of the unknown samples (Figure 2.12).

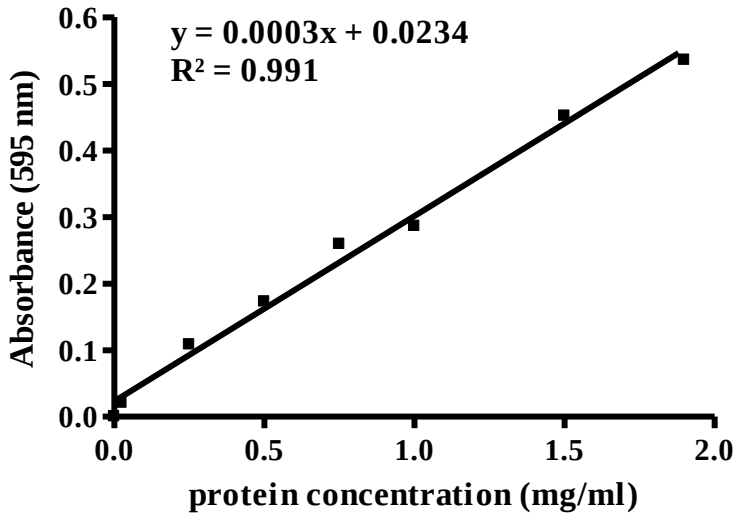

Figure 2.12 BSA protein standard curve as part of the Bradford assay.

2.12. SDS-PAGE and Western Blotting

2.12.1. SDS-PAGE

Sodium dodecyl sulfate-polyacrylamide gel electrophoresis (SDS-PAGE) is a commonly used method to separate proteins according to their molecular weight. As required, complete denaturisation and lineralisation of proteins is achieved by heating the samples in the presence of SDS (or LDS) and a reducing agent such as 2-mercaptoethanol. The negatively charged SDS binds to proteins and when loaded onto a polyacrylamide gel, allows proteins to migrate towards the positive electrode within an electric field resulting in their size-dependent separation. Pre-cast 4-12% Bis-Tris polyacrylamide gels (Novex by Life Technologies) were secured in an electrophoresis tank and submerged with 1x running buffer (20x stock from NuPAGE, Novex by Life Technologies, made up to 1x with MilliQ H_2O) before protein samples were loaded onto the gel.

2.12.2. Preparation of protein samples for SDS-PAGE

Protein samples were diluted to 2 mg/ml with 4x LDS sample buffer (Life technologies). 2-mercaptoethanol (Sigma) was used as reducing agent and was added to a final concentration of 5% (v/v). DNA was sheared by sonication of protein samples for 15-20 seconds. Where necessary, DNA was further eliminated by incubation of protein samples with Benzonase endonuclease (Millipore, Consett, UK). Before loading on a gel, proteins were denatured by heating to 95°C for 5 minutes. Twenty micrograms of protein were then added to each sample well and the gel was run at 160V until the sample front reached the end of the gel. Following

this, the gel was removed from its cassette and proteins were transferred to a nitrocellulose membrane for immunodetection.

2.12.3. Western blotting

The transfer of proteins from a polyacrylamide gel to a nitrocellulose membrane is known as Western Blot. The iBlot device (Invitrogen) was used to perform a semi-dry electrotransfer. Proteins on the membrane were then stained with Ponceau S (Sigma) to check if the transfer was successful. At this point, membranes were appropriately cut and labelled before they were de-stained in 2 x 10 minute washes with TBST (Tris buffered saline (50 mM Tris-Cl, pH7.6; 150 mM NaCl) including 0.02% (v/v) Tween-20).

2.12.4. Immunodetection

After the transfer, nitrocellulose membranes were blocked in blocking buffer (5% dried skimmed milk (w/v) in TBST) for 1 hour at room temperature. Membranes were then incubated with specific primary antibodies (Table 2.11) diluted in blocking buffer overnight at room temperature. Excess antibody was removed by washing the membranes with TBST twice for 10 minutes. Membranes were then incubated with the appropriate HRP-conjugated secondary antibody in blocking buffer for 45 minutes at room temperature followed by several washes with TBST for at least 1 hour. The protein of interest was visualised by chemiluminescent detection. ECL prime reagent (GE healthcare) was applied to the membranes, incubated for 30 seconds and signals from the secondary antibody (Table 2.11) were then detected in a gel documentation system (G:BOX, Syngene; software: GeneSnap from Syngene).

Antigen	Mwt (kDa)	Dilution	Comments and Source
Primary antibodies			
ERα	68	1/500 WB 1/250 ICC	Rabbit polyclonal to oestrogen receptor alpha (Santa Cruz, sc-7207)
ERα	68	1/100 ICC 1/250 WB	Mouse monoclonal [33] to Estrogen Receptor alpha - ChIP Grade (Abcam, ab2746)
ERβ	59	1/1000 WB	Rabbit polyclonal to oestrogen receptor beta (ab3576)
ERβ	59	1/250 ICC	Rabbit polyclonal to Estrogen Receptor beta (Santa Cruz, sc8974)
ERβ	59	1/100 ICC	Mouse monoclonal [14C8] to Estrogen Receptor beta (Ab288)
GAPDH	37	1/5000 WB	Rabbit monoclonal to GAPDH (Cell Signaling, 2118S) – loading control
CK19	44	1/500 ICC	Rabbit polyclonal to Cytokeratin 19 (Abcam, ab84632)
Vimentin	54	1/100 ICC	Rabbit monoclonal [EPR3776] to Vimentin – (Abcam, ab92547) – cytoskeleton marker
CYP2E1	54	1/1000 WB	Rabbit polyclonal to Cytochrome P450 2E1 (Abcam, ab28146)
Seconday antibodies			
Anti-rabbit-Alexa Fluor 647 (2°)	n/a	1/500 ICC	Goat anti-rabbit, Alexa Fluor 647 conjugated (Cell Signaling, 4414S)
Anti-rabbit-Alexa Fluor 488 (2°)	n/a	1/500 ICC	Goat anti-rabbit, Alexa Fluor 488 conjugated (Cell Signaling, 4412S)
Anti-rabbit-FITC (2°)	n/a	1/80 ICC	Goat anti-Rabbit, FITC conjugated (Sigma, F0382)

Antigen	Mwt (kDa)	Dilution	Comments and Source
Anti-mouse-Alexa Fluor 488 (2°)	n/a	1/500 ICC	Goat anti-mouse, Alexa Fluor 488 conjugated (Cell Signaling, 4408S)
Anti-mouse-HRP (2°)	n/a	1/2000 - 1/5000 WB	Anti-mouse IgG, horseradish peroxidase-linked (Cell Signaling, 7076S)
Anti-rabbit-HRP (2°)	n/a	1/2000 - 1/5000 WB	Anti-rabbit IgG, horseradish peroxidase-linked (Cell Signaling, 7074S)

Table 2.11 Specifications and source of primary and secondary antibodies. ICC, Immunocytochemistry; WB, Western Blot.

2.13. Histology

2.13.1. Tissue preparation

2.13.1.a Paraffin sections

Tissue samples were fixed in 10% formalin in 1x PBS for 24-48 hours depending on tissue type and thickness and then transferred to 70% ethanol until processing. Following a standard protocol as used by the histology laboratory (Newcastle University), fixed tissue samples were processed and embedded in paraffin wax before being sectioned (typically 4 μm) and mounted onto super frost microscope slides. Tissue sections were then de-waxed in xylene for 10 minutes and rehydrated by sequential 3-minute-washes in ethanol of decreasing concentration (100% → 95% → 90% → 70%) and then placed into tap water.

2.13.1.b Frozen sections

Tissue samples were snap-frozen in liquid nitrogen and stored at -80°C until processing. For cutting, frozen tissue samples were mounted in OCT (Optimal cutting temperature) medium (Thermo Scientific) and then sectioned (typically 10 μm) in a microtome-cryostat. Frozen sections were air-dried onto microscope slides for 2 hours at room temperature before being stored at -20°C until further processing.

2.13.2. Haematoxylin and eosin (H&E) staining

H&E staining is a common staining technique used for routine examinations of tissue histology. This staining procedure results in nuclei to appear blue (haematoxylin staining) and the cytoplasm stains pink (eosin staining). Tissue sections were de-waxed in xylene and rehydrated through a serious of ethanol washes as described in Section 2.13.1.a. Tissue sections were then stained with haematoxylin for 1 minute, washed with running tap water for 2 minutes and then placed in bluing solution (Scott's tap water (20 g $NaHCO_3$ and 3.5 g $MgSO_4$ in 1L dH_2O) for 30 seconds. For eosin counterstaining, tissue sections were immersed in eosin for 30 seconds and then thoroughly washed with running tap water before being dehydrated through a series of ethanol washes of different concentration (50% → 70% → 90% → 95% → 100%). Slides were then placed in Xylene for 10 minutes and mounted in DepexTM mountant (Sigma).

2.13.3. Oil Red O staining

Oil Red O staining is used for the detection of fat and neutral lipids in frozen tissue sections (Mehlem *et al.*, 2013). The histological mechanism behind this staining method is that the dye Oil Red O is more soluble in the lipid than in the dye solvents resulting in bright red staining of lipids.

Frozen sections cut at 10 µm were fixed in 10% formalin in 1x PBS for 15 minutes followed by rinsing with running tap water for 5 minutes. Sections were transferred to 60% isopropanol for 5 minutes and then stained with freshly prepared Oil Red O working solution (for the Oil Red O working solution, 0.5% (w/v) Oil Red O stock stain in isopropanol was diluted 3:2 with distilled H_2O, allowed to stand for 10 minutes and filtered into an airtight container) for 15 minutes at room temperature. Sections were then washed with 60% isopropanol for 5 minutes before being counterstained with Mayer's haematoxylin for 1 minute and incubation in Scott's tap water for 10 seconds. Sections were rinsed with distilled H_2O for 5 minutes and then mounted in aqueous mountant and left to dry for 24 hours. The end result is that lipids in frozen tissue sections appear red and nuclei appear blue.

2.14. Immunocytochemistry

Adherent cells were washed with 1x PBS and then fixed with 4% formaldehyde in 1x PBS for 10 minutes at room temperature. Following fixation, the fixative solution was removed and cells were washed with 1x PBS three times for 10 minutes and then permeabilised with 0.2% Triton in 1x PBS for 15 minutes at room temperature. Non-specific protein binding was blocked by incubation with the blocking buffer (PBS-T (1x PBS + 0.02% Tween 20) containing 5% of the species serum in which the secondary antibody was raised (if available)) for 20 minutes at room temperature. Cells were then incubated with the primary antibody diluted in blocking buffer at 4°C overnight. If cells were stained with two primary antibodies against two different antigens at the same time (double staining), primary antibodies that were raised in different species (e.g., rabbit and mouse) were used. The next day cells were washed three times with PBS-T for 10 minutes each and then incubated with the appropriate secondary antibody(s) diluted in blocking buffer for 45 minutes in the dark at room temperature. Following three washes with PBS-T for 10 minutes cell nuclei were stained with DAPI (6 µg/ml in 1x PBS), a fluorescent dye that binds to AT rich regions of double stranded DNA and, when bound, has an emission maximum of 461 nm (blue). Cells were then

thoroughly washed with 1x PBS and mounted with a glass coverslip using a water-based mounting medium before being left to dry at 4°C overnight.

2.15. Preparation of S9 fractions

S9 fractions prepared from an organ, most commonly the liver, contain microsomes, which contain the CYP450 enzymes, as well as the cytosolic fraction which contains several other enzymes including the majority of transferases. S9 fractions as a result are often used to study the metabolism of xenobiotics and drugs.

S9 fractions were prepared from mouse liver tissue. C57Bl/6 mice were terminated by cervical dislocation and their liver's dissected. To reduce blood contamination, livers were roughly chopped in a petri dish containing ice-cold 1x PBS using a scalpel. Chopped liver tissue was then transferred to approximately five volumes of ice-cold TKMS buffer (50 mM Tris; 25 mM KCl, 5 mM $MgCl_2$, 250 mM sucrose – pH 7.5). Mouse liver tissue was then disrupted in TKMS buffer using a potter homogeniser with tissue kept on ice throughout disruption. The homogenate was filtered through a tea strainer into centrifuge tubes and centrifuged at 12,000 x*g* for 20 minutes at 4°C to pellet the nuclear and mitochondrial/lysosomal fraction. The fatty top layer was removed from the supernatant (supernatant is the S9 fraction) and the S9 fraction was transferred to clean centrifuge tubes and centrifuged again at 12,000 x*g* for 20 minutes at 4°C. The supernatant was carefully transferred to a clean tube and then aliquoted, snap frozen in liquid nitrogen and stored at -80°C. The protein concentration of the S9 fraction was determined by Bradford assay (see Section 2.11.3).

2.16. Sulfotransferase [^{35}S]-PAPS radiometric activity assay

Sulfotransferases (SULTs) are cytosolic phase II metabolizing enzymes that play a major role in the clearance of endogenous and exogenous compounds including hormones, drugs and xenobiotics (Paul *et al.*, 2012). SULTs catalyse the transfer of a sulfo group from a donor molecule, often 3′-phosphoadenosine 5′-phosphosulfate (PAPS), to the compound to be metabolised to inactivate it or making it more water soluble and therefore less biologically active. SULT activity can be assessed by measuring the transfer of radiolabelled sulfo group [^{35}S] from [^{35}S]-PAPS to a particular substrate (Figure 2.13). S9 fractions isolated from mouse liver were used as the source of cytosolic SULTs (for preparation of S9 fraction see Section 2.15).

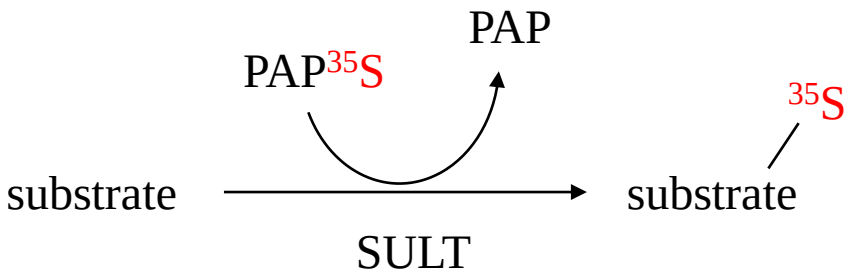

Figure 2.13 Transfer of a radiolabelled sulfo group from [^{35}S]-PAPS to a substrate catalysed by SULT enzymes.

S9 fraction (1 mg/ml), substrates (from 100x concentrated stocks) and, where applicable, SULT inhibitors (from 100 x concentrated stocks) where combined in a 0.6 ml tube on ice and made up to 100 µl with sample buffer (5 mM KH_2PO_4 (pH 6.5), 10 mM dithiothreitol (DTT), made fresh on day of assay). Fifty microlitre of reaction cocktail (25 µl 50 mM KH_2PO_4 (pH 6.5) + 25 µl of 5 mM MgCl2 containing 24 mM DTT and 1.28 µM [^{35}S]-PAPS (PerkinElmer, Seer Green, UK) were then added to each tube followed by incubation for 30 minutes at 37°C. To stop the reaction, 100 µl of stop mixture (1:1 (v/v) of 0.1 M barium hydroxide and 0.1 M barium acetate) was added to each tube. Unreacted [^{35}S]-PAPS was precipitated by adding 50 µl of 0.1M $ZnSO_4$, the tubes were then vortexed and centrifuged at 16,000 x*g* for 3 minutes at room temperature. Following centrifugation, 50 µl of 0.1 M barium hydroxide was added to each tube, tubes were vortexed, and 50 µl of 0.1 M $ZnSO_4$ were added to each tube. The precipitate was spun down by centrifugation at 16,000 x*g* for 10 minutes at room temperature. Twenty microlitres of the supernatant was transferred to a microplate and 200 µl scintillation cocktail (Optiphase HiSafe 3, PerkinElmer) was then added. [^{35}S] product radioactivity was determined in a scintillation counter (MicroBeta® TriLux, PerkinElmer).

2.17. Generation of aqueous, alcohol and organic extracts from soil

Surface soil samples (0-5 cm in depth) from around the boundary of a functioning waste site situated within a sub- or peri-urban area as well as three soil samples from rural, suburban and urban control sites were collected and aqueous, alcohol and organic extracts were generated by Dr Martin Cooke (School of Civil Engineering and Geosciences, Newcastle University). To produce aqueous and alcohol extracts, 250 g of soil (freed from stones, roots and vegetable matter) were mixed with 300 ml of methanol followed by sonication for 10 minutes. A further 100 ml of methanol were then added and sonicated again for 10 minutes. The methanol mix was filtered (25 µm), divided into 3 vials and evaporated using nitrogen. Following

evaporation, the remnants were re-dissolved in 10 ml phosphate buffer (aqueos extract) or ethanol (alcohol extract). Organic extracts were generated following the same extraction protocol but instead of methanol, chloroform was used. The remnants after nitrogen evaporation were dissolved in 10 ml chloroform. For application in cell-culture based assays, 200 µl of the chloroform extract were left to evaporat overnight in a fume cabinet and re-dissolved in the same volume of DMSO.

2.18. Statistical Analysis

Statistical analysis was performed using SPSS21 (IBM) or Excel and statistical significance was considered when $p<0.05$. To test for statistical significance of more than one treatment group versus a control group, such as in dose-response experiments, a one-way ANOVA with Dunnett's post-hoc test was performed. For multiple comparisons of 3 or more samples, a one-way ANOVA was used and Bonferroni post-hoc tests were performed to control for Type I error rate. In cases where multiple t-tests (two-tailed) were performed, such as when the effects of antagonist versus a certain treatment were examined, p-values were corrected for Type I errors using Holm-Bonferroni post-hoc tests.

Chapter 3. Development of a mouse-based *in vitro* screening system to assess transcriptional oestrogenic activity

Many everyday products contain chemicals that are able to disrupt normal hormone signalling potentially causing serious health conditions (Diamanti-Kandarakis *et al.*, 2009). Of particular concern are unwanted interactions of endocrine disrupting chemicals (EDCs) with the oestrogen receptors (ERs) which, due to the receptors involvement in a vast range of biological processes, may account for a spectrum of adverse effects in wildlife and humans including reproductive, neuroendocrinological and metabolic disorders as well as cancer (Ascenzi *et al.*, 2006; Soto and Sonnenschein, 2010; Yoon *et al.*, 2014).

Although a number of different oestrogen-signalling pathways exist, many EDCs may affect ER signalling by directly targeting the ERs. Such direct-acting chemicals include food and cosmetic additives, plasticisers, pharmaceuticals and pesticides (Rogers *et al.*, 2013). *In vitro* screening assays are often employed to identify potential EDCs that bind to the ERs. In particular, cell-based trans-activation reporter gene assays which can distinguish between agonistic and antagonistic effects are commonly used (Huang *et al.*, 2014).

In order to examine the potential adverse effects that ER-targeting EDCs may have *in vivo* in mice, a mouse-based *in vitro* screening assay was required to test a range of chemicals for activation of the mouse ERs (mERs). This chapter describes the development of a reliable mouse-based trans-activation reporter gene assay that will allow for xenobiotics to be tested for oestrogenic activity in mice. Since the primary focus of this thesis is to examine the effects that oestrogenic chemicals may have in the liver, and given that oestrogens may target the liver via the ERα which is primarily expressed in hepatocytes (Ahlbory-Dieker *et al.*, 2009; Uebi *et al.*, 2015), this cell type would have been the preferred option for screening the oestrogenicity of chemicals. Since hepatocytes are non-proliferative *in vitro*, however, transfection efficiencies are low. To develop an *in vitro* assay that will generate high signal to noise readouts and allow for semi-high throughput screening of a relatively large set of samples, the use of hepatocytes was not a realistic option. Therefore, cells with a ductal hepatopancreatobiliary phenotype were employed. Biliary epithelial cells (BECs) have been reported to not express the ER in healthy liver, however, expression of both ER subtypes ERα and ERβ was observed in BECs of patients with PBC (Alvaro *et al.*, 2004). Since oestrogens, and therefore potentially xenoestrogens are known to be cholestatic, ER expression and signalling in cholangiocytes may play an important role in the development and/or

progression of cholestatic liver conditions. The use of hepatopancreatobiliary cells was as a result considered to be an appropriate alternative to hepatocytes.

3.1. Analysis for mER expression in the mouse ductal cell lines 603B and LTPA

On account of limitations of the number of primary BECs that could be isolated from mouse liver, the mouse BEC cell line 603B as well as the mouse ductal pancreatic cell line LTPA were employed. Although LTPA cells are not derived from the liver, biliary and pancreatic ducts have the same developmental origin and are physiologically linked (Probert *et al.*, 2015).

603B and LTPA cells were examined for expression of the two mER isoforms α and β by RT-PCR, Western Blot and immunocytochemical staining. Figure 3.1A shows that mERα mRNA was detected in 603B (see lane 2) but not in LTPA cells (lane 3) and that neither cell line expressed mERβ mRNA. Murine uterus, liver and ovary tissues were included as positive controls for the mERα (uterus, liver and ovary) and the mERβ (ovary). Western Blot analysis showed that mERα and mERβ proteins were not detectable in either cell line (Figure 3.1B) which was confirmed by immunocytochemical staining (Figure 3.2). HEK293 cells which are widely used as an expression tool for recombinant proteins due to their high transfection rate and protein production (Thomas and Smart, 2005), are ER negative (see Figure 3.8) and were transiently transfected with a pcDNA3.1 expression vector coding for the mERα (pcDNA3.1-mERα) or mERβ transcript variant 1 (pcDNA3.1-mERβv1) for use as a positive control for the mERs as part of the immunostaining. Figure 3.2 shows nuclear localisation of the recombinant mER proteins in HEK293 cells.

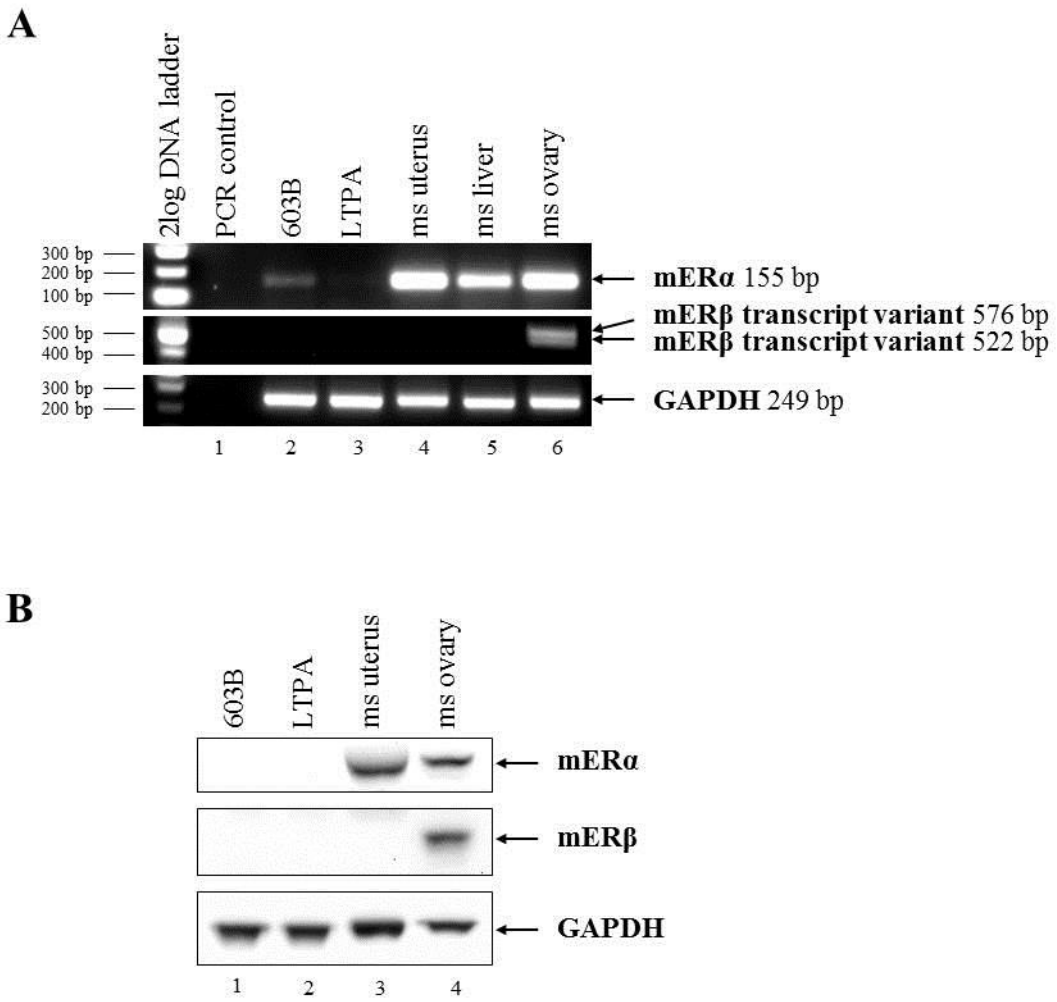

Figure 3.1 Analysis for the expression of mERs in 603B and LTPA cells by RT-PCR and Western Blot. (A) RT-PCR analysis for mERα and mERβ mRNA expression in 603B and LTPA cells and the indicated murine tissues. RNA was isolated from 603B and LTPA cells as well as murine tissue followed by RT-PCR (30 PCR cycles) using primers specific for the mERα and mERβ. GAPDH was used as a loading control. PCR products were separated by agarose electrophoresis and visualised by UV transillumination. **(B)** Western Blot analysis for mERα and mERβ protein expression in 603B and LTPA cells. Total protein was isolated from 603B, LTPA cells and murine tissue following separation by gel electrophoresis and visualisation (20 μg total protein/lane). Data are typical of three independent experiments.

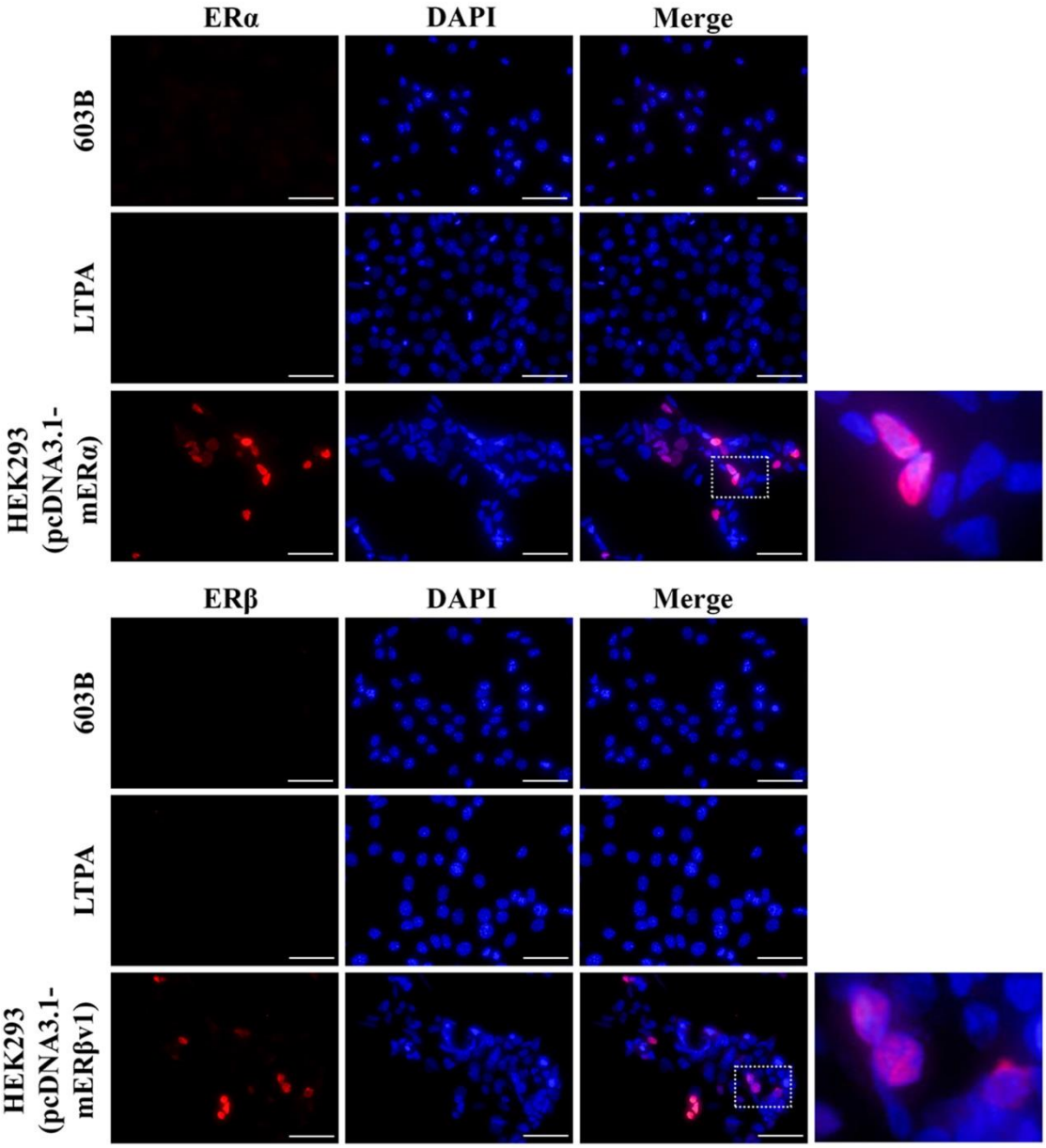

Figure 3.2 Analysis for the expression of mERs in 603B and LTPA cells by immunocytochemistry. Immunocytochemical staining for mERα and mERβ expression in 603B and LTPA cells. HEK293 cells transfected with an expression vector coding for either the mERα or mERβv1 were included as a positive control. Scale bars: 50 μm. Data are typical of two independent experiments.

3.2. Construction of the mERα and mERβ transcript variant 1 and variant 2 expression constructs

Since the mER proteins were undetectable in 603B and LTPA cells, their expression, however, required to develop an *in vitro* screening system to test for mouse ER activation, mERα and mERβ cDNA sequences were cloned from murine tissue and ligated into an mammalian expression vector in order to ectopically express the mouse ERs in the mouse ductal 603B and LTPA cell lines.

3.2.1. Cloning of the mERα and two mERβ transcript variants from murine tissue

The mERα cDNA sequence was amplified from RNA isolated from mouse uterine tissue with specific cloning primers designed to yield *EcoRI* and *HindIII* restriction sites upstream and downstream of the mERα open reading frame for subsequent ligation into an expression vector (for primer sequences see Table 2.10). Separation of the PCR reaction by agarose gel electrophoresis following amplification of mERα cDNA resulted in a single band of the approximate size predicted to be 1829 bp (Figure 3.3A).

Two mERβ cDNA sequences were amplified from RNA extracted from mouse ovaries with specific primers containing *EcoRI* and *AflII* restriction sites. PCR amplification using these primers was predicted to result in PCR products of 1744 bp (full length mERβ transcript variant 1 (mERβv1), NM_207707.1) and 1690 bp (mERβ transcript variant 2 (mERβv2), NM_010157.3, lacking an in-frame exon in the coding region, creating a protein lacking amino acids 383 – 400 present in variant 1). Amplification by PCR resulted in a single detectable band of PCR products migrating at a size of around 1.7 kb, likely containing the PCR amplification products of both mERβ variants due to their similar size (Figure 3.3B). PCR bands from both mERα and mERβ amplification reactions were purified from the gel for subsequent ligation.

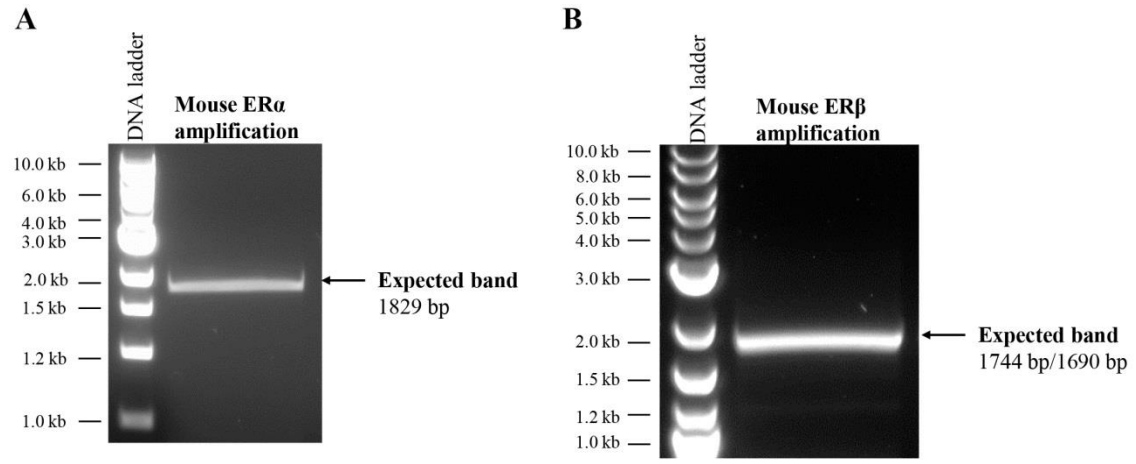

Figure 3.3 Amplification of mERα and mERβ cDNA sequences by RT-PCR. (A) Amplification of the mERα cDNA from RNA isolated from mouse uterine tissue (30 cycles) using cloning specific primers followed by agarose gel electrophoresis and visualisation by transillumination. **(B)** Amplification of the mERβv1 and mERβv2 cDNAs from RNA isolated from mouse ovaries (35 cycles) using cloning specific primers followed by agarose gel electrophoresis and visualisation by transillumination.

3.2.2. Ligation of the mERα, mERβv1 and mERβv2 cDNAs into a pCR-Blunt vector

Gel purified mERα and mERβ cDNAs were first ligated into a pCR-Blunt vector using the Zero Blunt PCR cloning kit which offers an easy method for high-efficiency (>80%) cloning of blunt-end PCR products. Recombinant pCR-mER constructs were transformed into *E.coli* bacterial cells and numerous clones were screened by restriction digest with the appropriate restriction enzymes for recombinant vectors containing the correct insert. To check for insertion of the mERα cDNA, recombinant plasmids were digested with *EcoRI* and *HindIII* restriction enzymes. Figure 3.4A shows that clones 1-6 contained an insert with the approximate predicted size of 1829 bp, the size of the mERα insert.

To check for insertion of the mERβv1 and mERβv2 cDNAs, recombinant plasmids were digested with *EcoRI*. Figure 3.4B shows that clones 1 and 4 contained an insert with the size of the mERβv1 (1744 bp, see lane 2 and 5) whereas clones 2, 5, 6 and 8 contained an insert with the size of the mERβv2 (1690 bp, lane 3, 6, 7 and 9), the latter migrating slightly further due to its smaller size compared to the mERβv1 insert.

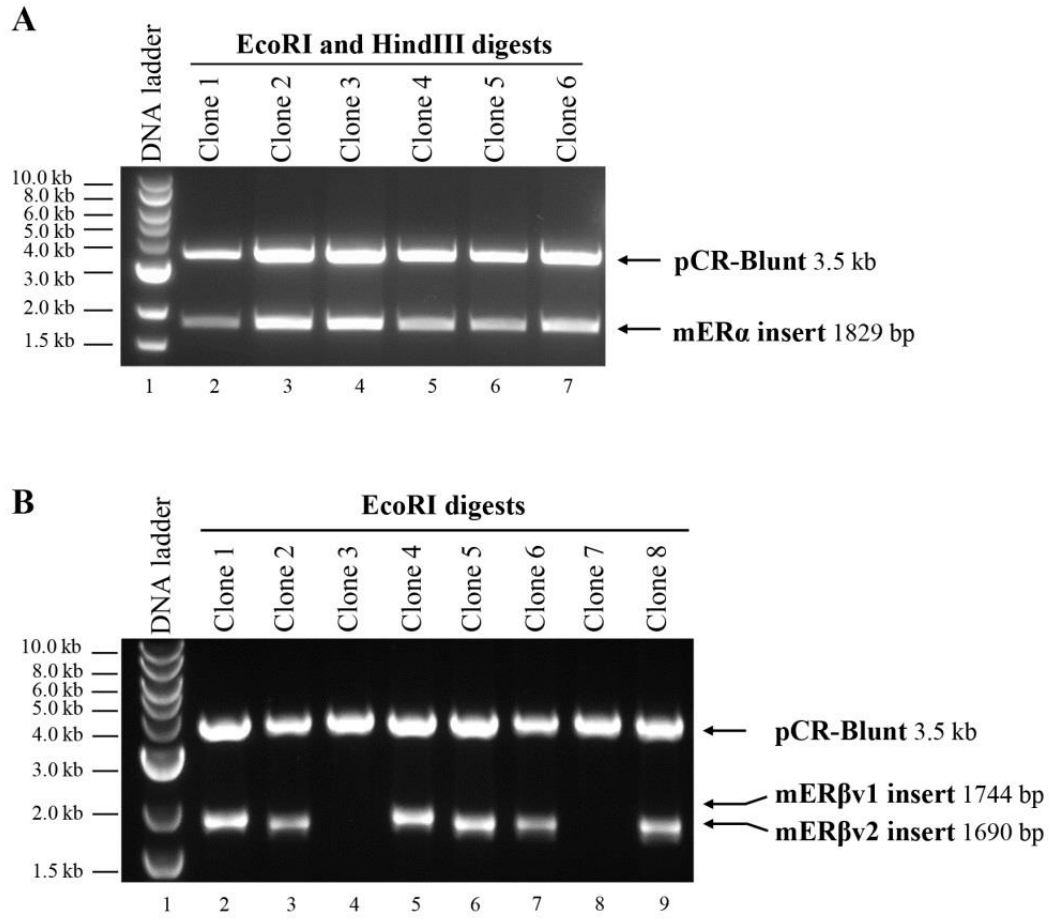

Figure 3.4 Restriction digest of recombinant pCR-Blunt constructs to test for presence of the cloned mER inserts. (A) *EcoRI* and *HindIII* double restriction digest to screen for correctly assembled recombinant pCR-Blunt vectors with the mERα insert. **(B)** *EcoRI* restriction digest to screen for correctly assembled recombinant pCR-Blunt vectors containing the mERβv1 or mERβv2 insert. Digested plasmid DNA was separated by agarose gel electrophoresis and visualised by transillumination.

All clones with an insert of the correct size were analysed by DNA sequencing to verify that the inserts were the expected mER cDNA sequences and to ensure that the sequences did not contain any mutations following PCR amplification. DNA sequencing results verified that all clones analysed contained either the mERα (NM_007956.5), mERβv1 (NM_207707.1) or mERβv2 (NM_010157.3) cDNAs with no mutations. A a result, clone 1 and 2 for the mERα, clone 1 and 4 for the mERβv1 and clone 2 and 5 for the mERβv2 were chosen to be used for the next cloning step.

3.2.3. Preparation of the mER inserts and the pcDNA3.1 destination vector for ligation

Following verification that the recombinant pCR-vectors contained the cDNAs for the mERα, mERβv1 or mERβv2, the mouse ER cDNA inserts were excised on a large scale from the respective pCR-Blunt vector from clones as indicated with *EcoRI* and *HindIII* restriction enzymes for the mERα (see Figure 3.5A) and *EcoRI* and *AflII* restriction enzymes for the

mERβv1 and mERβv2 (Figure 3.5B). The pcDNA3.1 vector (for vector map see Figure 2.10 in Chapter 2) used as the destination vector originally contained a c/EBPβ cDNA sequence which was excised with the same combination of restriction enzymes (*EcoRI* + *HindIII* or *EcoRI* + *AflII*) obtaining linearisation of the destination vector with 'sticky ends' for ligation of the mER inserts. The restricted mER inserts as well as the linearised pcDNA3.1 vector were gel purified for ligation.

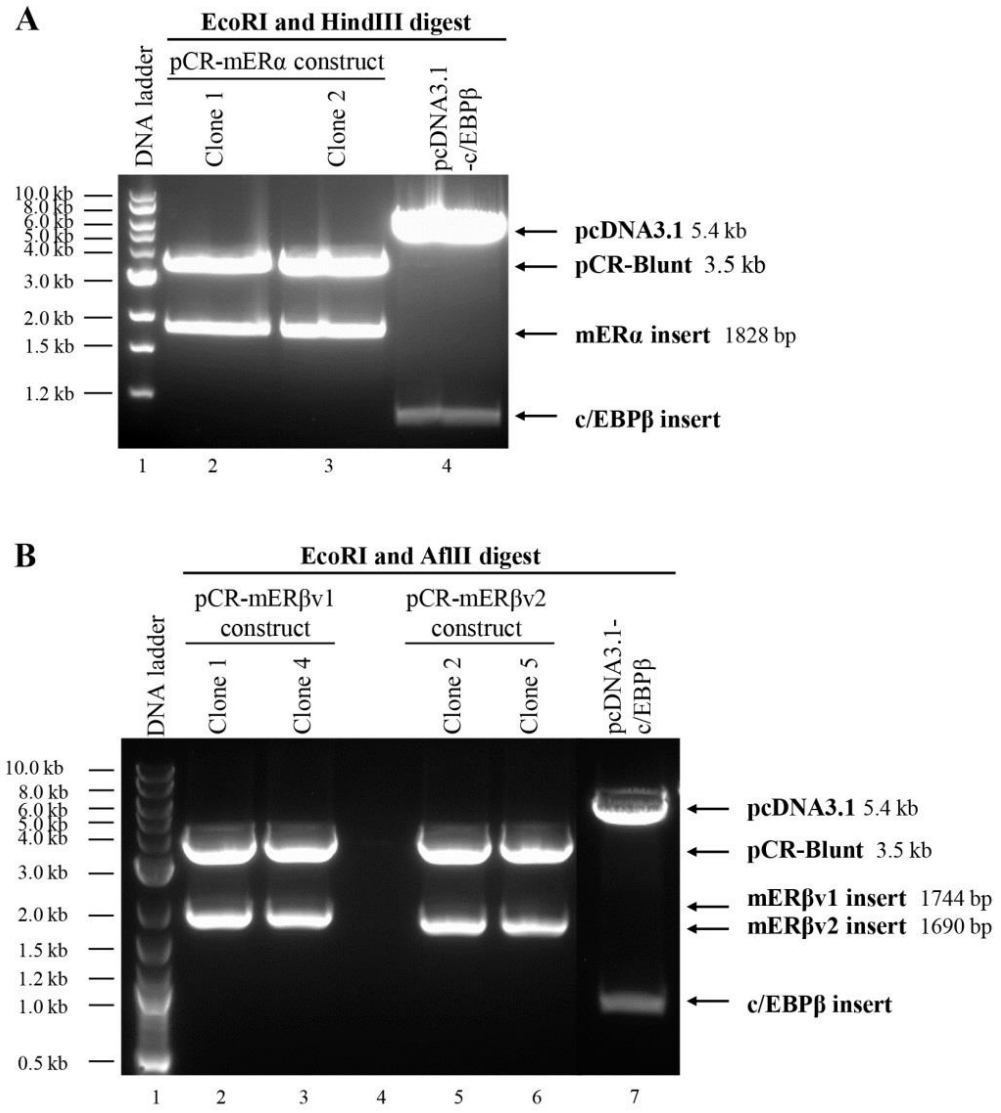

Figure 3.5 Excision of the mER inserts from recombinant pCR-Blunt vectors and linearisation of the destination vector by restriction digest. (A) Large scale *EcoRI* and *HindIII* restriction digest of the recombinant pCR-Blunt construct containing the mERα insert (pCR-mERα) from clone 1 and 2 and linearisation of the destination vector pcDNA3.1. **(B)** Large scale *EcoRI* and *AflII* restriction digest of the recombinant pCR-Blunt construct containing the mERβv1 (pCR-mERβv1, clone 1 and 4), or mERβv2 insert (pCR-mERβv2, clone 2 and 5) and linearisation of the destination vector pcDNA3.1. Digested plasmid DNA was separated by agarose gel electrophoresis and visualised by transillumination.

3.2.4. Sub-cloning of the mERα, mERβv1 and mERβv2 cDNAs into the destination vector pcDNA3.1

Gel purified mER inserts and the linearised destination vector pcDNA3.1 were combined in a ligation reaction followed by transformation into *E.coli* bacterial cells. Several clones were screened for correctly constructed recombinant plasmids by restriction digest with the appropriate restriction enzymes. Figure 3.6A shows that all clones screened contained an insert of the size of the mERα (1829 bp). Clones 3-8 in Figure 3.6B contained an insert the size of the mERβv1 (1744 bp) and clones 1-4 in Figure 3.6C contained and insert the size of the mERβv2 (1690 bp).

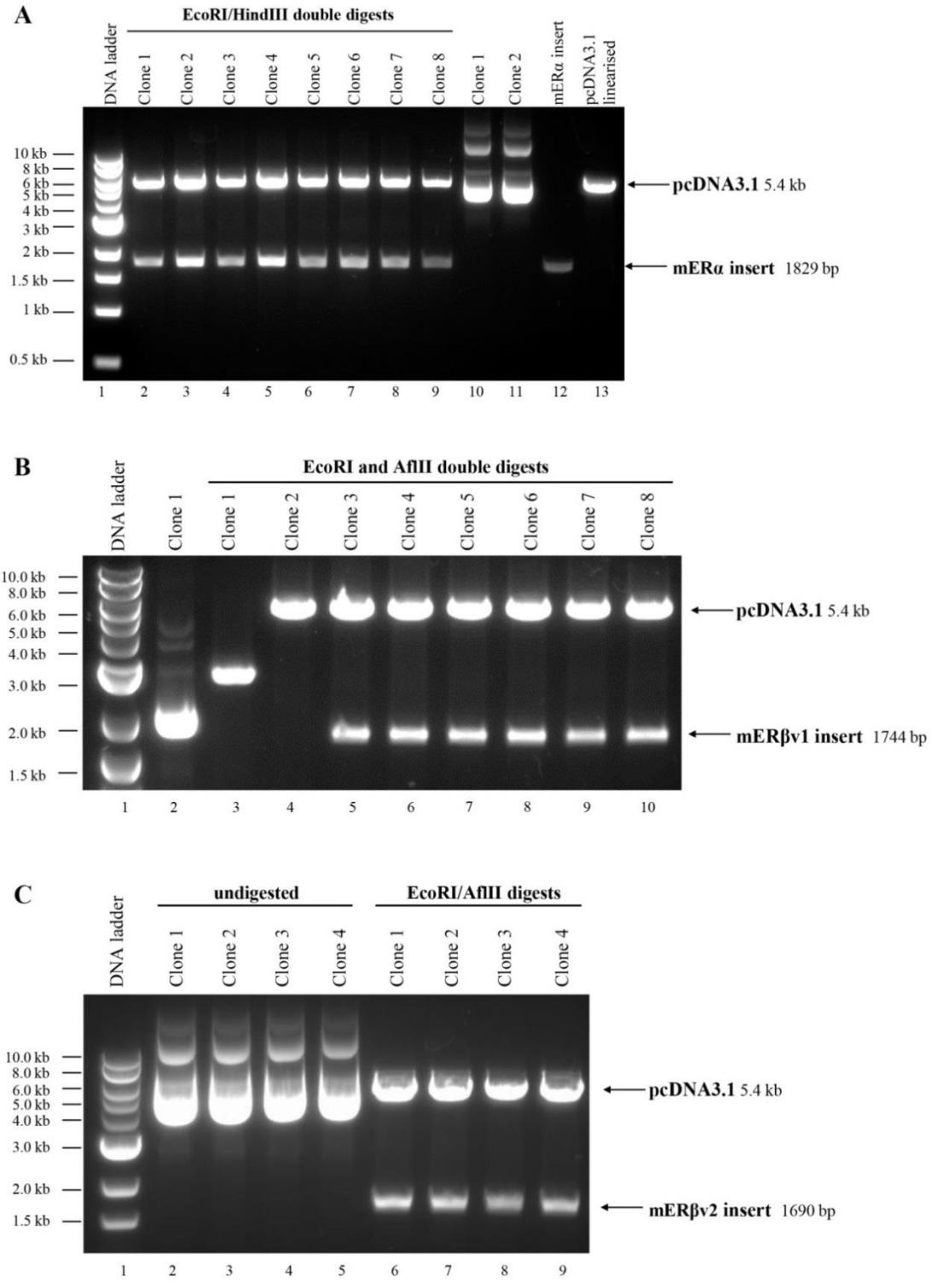

Figure 3.6 Restriction digests of recombinant mER-pcDNA3.1 plasmids to test for presence of the mER inserts. (A) *EcoRI* and *HindIII* double restriction digest to screen for correctly assembled recombinant pcDNA3.1 construct with mERα insert**. (B)** *EcoRI* and *AflII* double restriction digest to screen for correctly assembled recombinant pcDNA3.1 construct with mERβv1 insert. **(C)** *EcoRI* and *AflII* double restriction digest to screen for correctly assembled recombinant pcDNA3.1 constructs with mERβv2 insert. Digested plasmid DNA was separated by agarose gel electrophoresis and visualised by transillumination.

To verify that the excised inserts were the expected mER cDNA sequences, recombinant pcDNA3.1-mER plasmids were analysed by DNA sequencing. Sequencing results confirmed

that all analysed clones contained the cDNA sequences for the mERα, mERβv1 or mERβv2 and were correctly assembled (see Appendix A-C). Accordingly, clone 4 and 6 containing the mERα cDNA, clone 5 containing the mERβv1 cDNA and clone 1 containing the mERβv2 cDNA were chosen to be tested for their functionality.

3.3. Testing for correct functioning of the newly generated pcDNA3.1-mER expression constructs

3.3.1. Determining transfection efficiency in the mouse ductal cell lines using a variety of transfection methods

Following cloning, the newly generated pcDNA3.1-mER expression constructs were tested for correct functioning. In order to decide on the cell line to do the testing in, the transfection efficiency in 603B and LTPA cells was determined using a number of transfection reagents and a plasmid encoding the green fluorescent protein (GFP, peGFP-N1). 603B and LTPA cells transfected with the GFP-plasmid using polyethylenimine (PEI) show low levels of transfection after 24 and 48 hours, regardless of the amount of PEI added to the cells (Figure 3.7A). In LTPA cells, changes in cell morphology after 48 hours were observed indicating that PEI exhibits cytotoxic effects in these cells. The average transfection efficiency using PEI calculated from 3 fields per view was found to be less than 0.7% for 603B and less than 1.4% for LTPA cells.

Cells transfected using Effectene (Qiagen) show higher transfection rates after 48 hours compared to PEI with calculated transfection efficiencies of 8.67% for 603B transfected with a DNA:Effectene ratio of 1:10 and 3.3 % for LTPA cells using a ratio of 1:50 (Figure 3.7B).

Transfection of 603B and LTPA cells with the peGFP-N1 using the calcium phosphate transfection method resulted in an average transfection efficiency of less than 1% for both cell lines (Figure 3.7C).

Since 603B showed the highest transfection efficiency when the transfection reagent Effectene with a DNA:Effectene ratio of 1:10 was used, this cell line was employed to test the cloned mouse ER-pcDNA3.1 constructs for correct functioning.

A

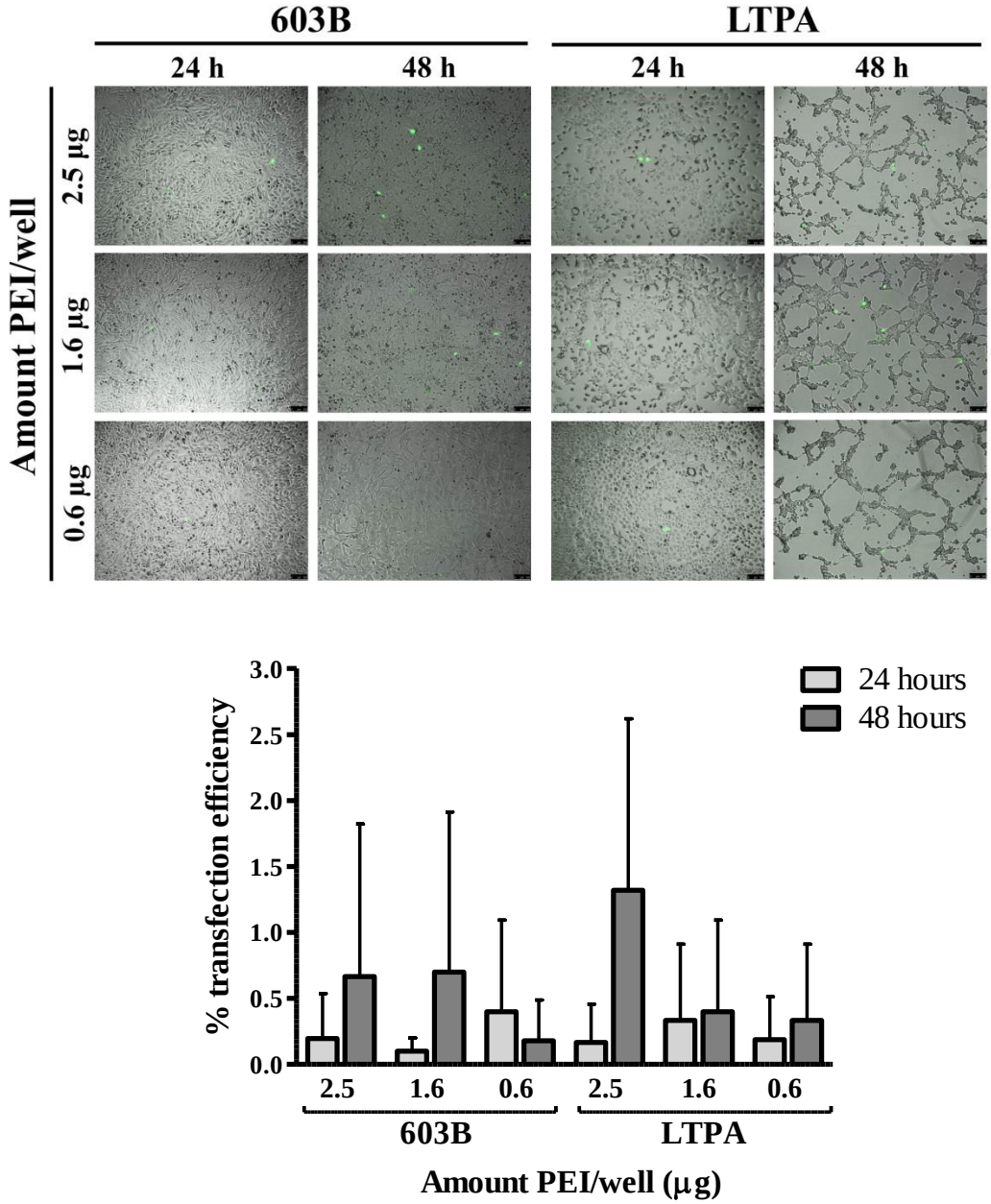

Figure 3.7 Determining transfection efficiencies in 603B and LTPA cells. Merged light and fluorescent microscope images and transfection efficiencies of 603B and LTPA cells transfected with the peGFP-N1 plasmid encoding the green fluorescent protein (GFP) using different transfection reagents. **(A)** Transfections using polyethylenimine (PEI). Different amounts of PEI (2.5, 1.6 and 0.6 µg) were added to cells in 6-well plates to determine the best working condition. Cells were imaged for GFP expression at 24 and 48 hours following transfection. Transfection efficiency was determined by expressing the number of GFP-positive cells as percentage of the number of total cells per field of view. Data are the average transfection efficiency calculated from 3 fields per view and SD, typical of two separate experiments. Scale bar: 100 µm.

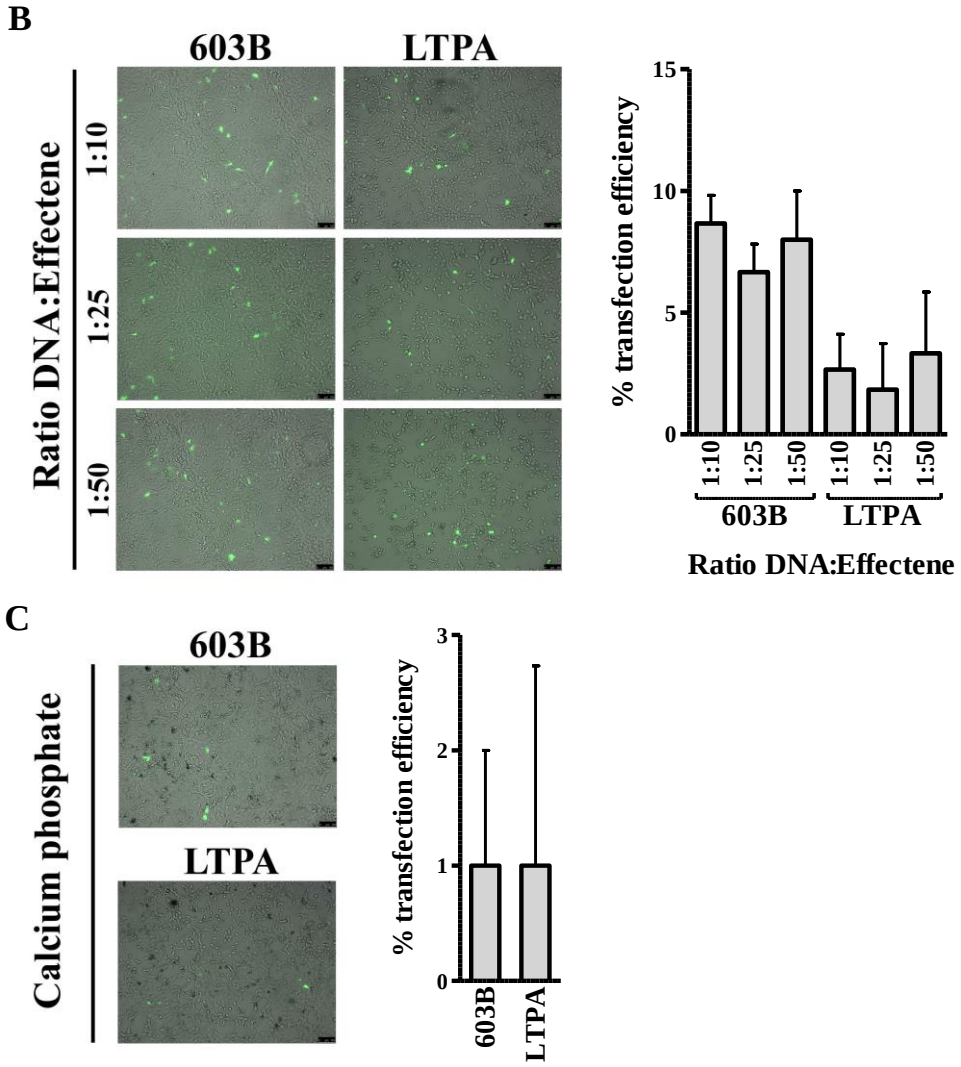

Figure 1.7 contd. Determining transfection efficiencies in 603B and LTPA cells. (B) Transfections using Effectene reagent with different DNA:Effectene ratios as indicated. Cells were examined for GFP expressing at 48 hours following transfection. **(C)** Transfections using the calcium phosphate transfection method.

3.3.2. Testing the cloned pcDNA3.1- mERβ expression constructs for correct functioning

3.3.2.a The mERβv1 and mERβv2 proteins are ectopically expressed

Initially, the constructs coding for the mERβ proteins were tested for correct functioning. To test whether these constructs produce proteins, 603B and HEK293 cells were transiently transfected with purified pcDNA3.1 plasmid DNA containing the insert for either the mERβv1 (isolated from clone 5) or mERβv2 (isolated from clone 1) cDNA and expression of the recombinant proteins was examined by Western Blot and immunocytochemical staining.

Proteins of the predicted size were generated in HEK293 cells transfected with the mERβv1 or mERβv2 expression constructs (lane 7 and 8) and low but detectable protein expression was observed in 603B cells (lane 3 and 4 in overexposed panel) (Figure 3.8A). Mouse ERβ protein was undetectable in controls transfected with an empty pcDNA3.1 expression construct (lane 2 and 6) and in non-transfected cells (lane 1 and 5).

Immunocytochemical staining confirms that the mERβv1 and mERβv2 proteins were ectopically expressed and localised in the nucleus of HEK293 and at a lower level in 603B cells transiently transfected with the corresponding pcDNA3.1- mERβ expression constructs. Mouse ERβ protein was not detected in control cells transfected with an empty pcDNA3.1 expression construct (Figure 3.8B).

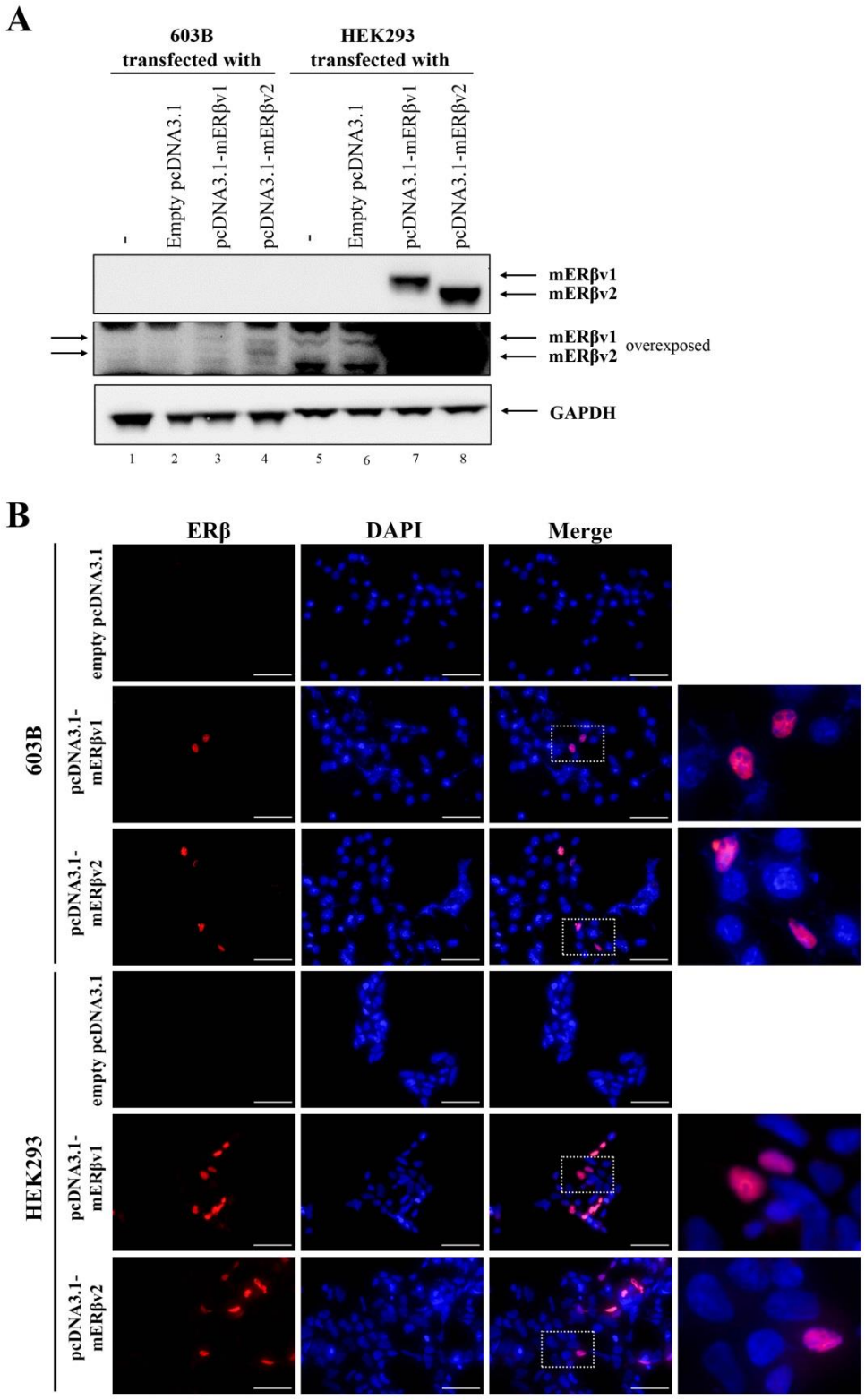

Figure 3.8 Analysis for ectopical expression of the mERβ proteins. (A) Western Blot for the expression of the mERβ proteins in 603B and HEK293 cells transiently transfected with the expression construct coding for either the mERβv1 or mERβv2 cDNA sequences or empty vector as control (20 µg total protein/lane). Theoretical molecular weights: mERβv1, 63.23 kDa; mERβv2, 61.21 kDa. **(B)** Immunocytochemical staining for the expression of the mERβ proteins in 603B and HEK293 cells transiently transfected with the expression construct encoding either the mouse mERβv1 or mERβv2 cDNA sequence or empty vector as control. Scale bar: 50 µm. Data are typical of three independent experiments.

3.3.2.b 603B cells transfected with the mERβv1 and mERβv2 pcDNA3.1 expression construct respond to oestrogen

Following confirmation that the mERβ proteins were ectopically expressed in cells transfected with the pcDNA3.1-mERβ constructs, recombinant mERβ proteins were tested for functional activity by reporter gene assay. 603B cells were transiently transfected with the pcDNA3.1 expression construct coding for either the mERβv1 or mERβv2, the $(ERE)_3$-pGL3promotor reporter construct and the control RL-TK plasmid before treatment with 10 nM E2 or 0.1% (v/v) DMSO vehicle in the absence and presence of the ER antagonist ICI182,780 for 24 hours followed by dual-glo luciferase assay. Control cells were co-transfected with an expression construct coding for a different protein not involved in oestrogen signalling, here c/EBPβ, or an empty expression construct. Vehicle-treated 603B cells expressing recombinant mERβv1 trans-activated the luciferase reporter gene in the absence of ICI182,780, a response that was significantly further induced following treatment with 10 nM E2 (Figure 3.9). Co-treatment with 100 nM of the ER antagonist ICI182,780 significantly reduced luciferase reporter gene expression in mERβv1-expressing cells treated with E2 in the absence of ICI182,780 confirming that the increase in luciferase reporter gene expression in response to E2 is mediated by the mERβv1. ICI182,780 also significantly reduced luciferase reporter gene expression over cells treated with the vehicle alone suggesting that the mERβv1 is able to trans-activate the ERE-reporter gene construct in the absence of an exogenous ligand such as E2, potentially because of oestrogens present in complete cell culture media.

In 603B cells expressing recombinant mERβv2, a small significant increase in luciferase activity by 1.52 fold following exposure to 10 nM E2 was observed over vehicle treated cells (Figure 3.9). Recombinant mERβv2-expressing 603B cells which were treated with the vehicle alone, however, exhibited high levels of basal luciferase activity compared to pcDNA3.1-mERβv1 transfected vehicle-treated cells. Co-treatment of mERβv2-expressing cells with 100 nM ICI182,780 significantly reduced luciferase reporter gene activity over vehicle and E2 treated cells to similar levels seen in mERβv1-expressing cells. These findings suggest that recombinant mERβv2 trans-activates the $(ERE)_3$-pGL3promotor reporter construct in the absence of a ligand, either because it exhibits near complete constitutive activity or because the protein is activated by oestrogens present in the culture medium.

603B cells transfected with an empty form of the pcDNA3.1 expression construct or a pcDNA3.1 vector coding for c/EBPβ did not trans-active the luciferase reporter gene in response to 0.1% (v/v) DMSO vehicle or 10 nM E2 nor did co-treatment with 100 nM

ICI182,780 reduce luciferase reporter gene expression over vehicle and E2 treated cells in the absence of ICI182,780 (Figure 3.9). This confirms that trans-activation of the luciferase reporter gene as seen in cells expressing the mERβv1 and mERβv2 proteins is a result of active ERβ proteins expression and also shows that no squelching effects are taking place.

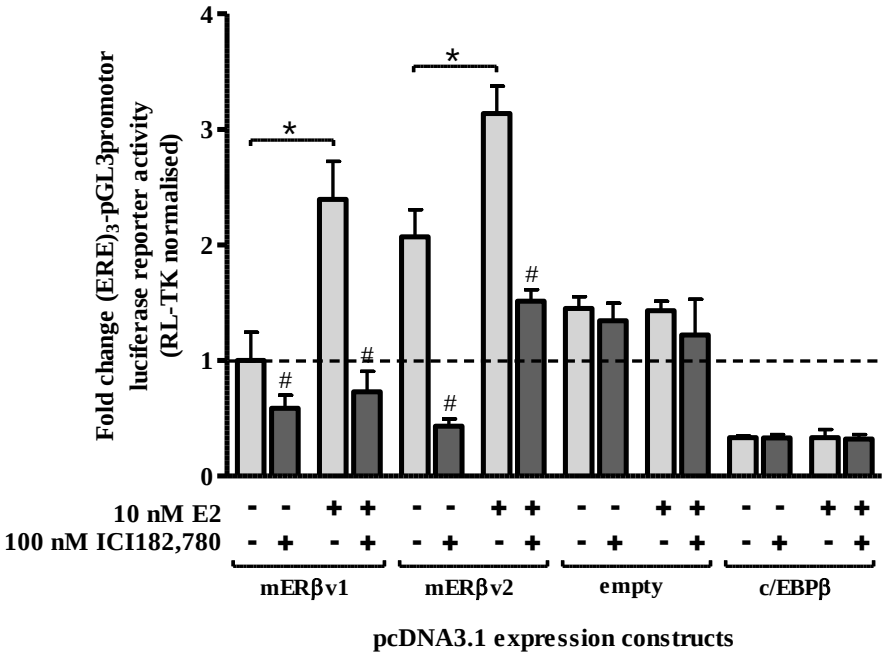

Figure 3.9 Testing the mERβ expression constructs for functional activity. Luciferase reporter gene ($(ERE)_3$-pGL3promotor) assay in 603B cells co-transfected with expression constructs coding for the mERβ proteins or control constructs as indicated. Cells were treated with 0.1% (v/v) DMSO vehicle or 10 nM E2 (± ICI182,780) for 24 hours followed by dual-luciferase assay. Mean and SD of n=3, typical of 3 separate experiments. Data are expressed in fold change versus mERβv1-transfected cells treated with DMSO vehicle. *Significantly different ($p<0.05$) over the equivalent expression vector transfected cells treated with DMSO vehicle; #Significantly different versus equivalent treatments in the absence of ICI182,780 (compound only)-treated cells using Student's t-test (two-tailed) with Holm-Bonferroni post-hoc modifications.

3.3.2.c Recombinant mERβv1 – but not mERβv2 – trans-activates the $(ERE)_3$-pGL3promotor reporter construct in a dose-dependent manner

To further test if the mERβv1 or mERβv2 proteins trans-activate the luciferase reporter construct in a dose-dependent manner, cells were treated with a range of E2 concentrations starting at 10 pM and increasing serially by a factor of 10 to a maximum of 10 μM for 24 hours followed by dual-glo luciferase assay. Figure 3.10 demonstrates that activation of the mERβv1 – but not the mERβv2 – is concentration dependent with the mERβv1 responding to E2 at a concentration as low as 1 nM. A statistically significant increase in luciferase activity in mERβv2-expressing cells was observed at 10 nM and 10 μM. Despite this, the fold induction was very low and therefore it is likely not biologically significant.

603B cells transfected with an empty expression construct did not respond to E2 at any tested concentration.

Overall, these results suggest that the cloned pcDNA3.1-mERβv1 construct generates functional protein capable of trans-activating the $(ERE)_3$-pGL3promotor reporter construct and that 603B cells produce co-factors that allow for mERβ responsiveness. Although recombinant mERβv2 did not trans-activate the $(ERE)_3$-pGL3promotor reporter construct in a dose-dependent manner, high basal levels of luciferase activities compared to mERβv1-expressing cells were observed suggesting that the pcDNA3.1-mERβv2 construct produces functionally active protein, likely to possess nearly complete constitutive activity or being almost fully activated by oestrogenic compounds present in cell culture media.

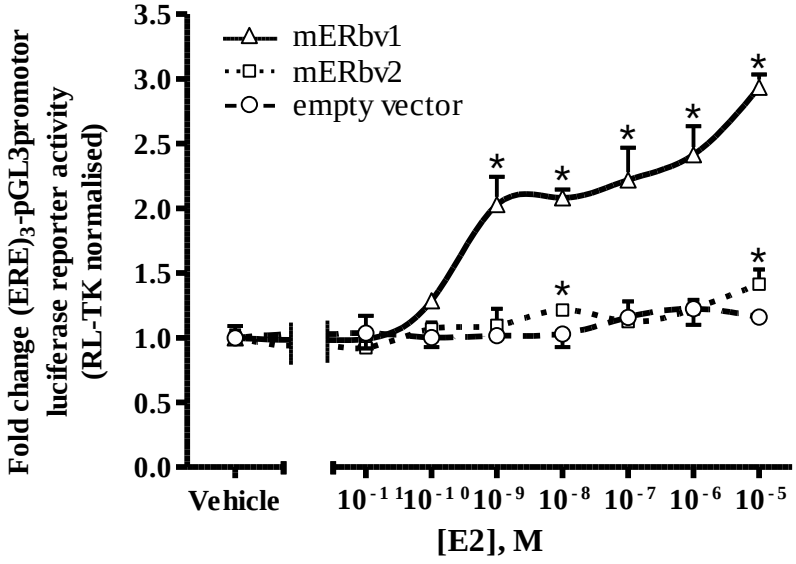

Figure 3.10 E2 activates the mERβv1 – but not the mERβv2 – in a dose-dependent manner. Luciferase reporter gene ($(ERE)_3$-pGL3promotor) assay in 603B cells co-transfected with expression constructs coding for the mERβv1, mERβv2 or an empty control vector. Cells were treated with increasing concentrations of E2 (vehicle: 0.1% (v/v) DMSO) for 24 hours followed by dual-luciferase assay. Mean and SD of n=3, typical of 3 separate experiments. Data are expressed in fold change versus the equivalent expression vector transfected DMSO vehicle-treated cells. *Significantly different ($p<0.05$) over the equivalent expression vector transfected cells treated with DMSO vehicle using One-way ANOVA with Dunnett's post-hoc modifications.

3.3.2.d Recombinant mERβv1 and mERβv2 proteins are not activated by background oestrogenic chemicals in culture media

Complete cell culture media generally contain a number of oestrogenic compounds which can result in high background levels of some nuclear receptor activities. Compounds reported to have oestrogenic activity include phenol red, a pH indicator present in most culture media

(Berthois *et al.*, 1986). Furthermore, a number of steroid hormones are naturally present in the culture media supplement foetal bovine serum (FBS). They vary from one batch to another and may influence ER activities *in vitro*.

Since 603B cells transfected with the pcDNA3.1-mERβv1 and pcDNA3.1-mERβv2 expression construct trans-activated the $(ERE)_3$-pGL3promotor reporter construct in the absence of E2, it was examined whether recombinant mERβv1 and mERβv2 proteins are activated by oestrogenic compounds or steroid hormones present in the cell culture medium.

Testing for E2-induced activation of the mERβv1 and mERβv2 proteins was carried out in 603B cells incubated in phenol red-free (phenol red (-)) or phenol red-containing (phenol red (+)) medium supplemented with 10% (v/v) FBS treated with activated charcoal/dextran (referred to as 'stripped' FBS) which removes endogenous steroid hormones and other low molecular weight compounds from the serum, and compared to cells grown in medium with non-stripped FBS (referred to as 'normal' medium). Figure 3.11A demonstrates that treatment of cells expressing the mERβv1 with 100 nM ICI182,780 similarly decreased luciferase reporter gene activity over vehicle treated cells in normal medium as well as in phenol red (+) and phenol red (-) media supplemented with stripped FBS suggesting that the mERβv1 is capable of trans-activating the $(ERE)_3$-pGL3promotor reporter construct independent of oestrogenic compounds in the medium. Furthermore, there was little difference in the fold change of E2-induced increase in reporter gene activity between cells grown in normal medium and phenol red (+) medium with stripped FBS. Recombinant mERβv1-expressing cells grown in phenol red (-) medium containing stripped FBS show a slightly greater E2-induced increase in luciferase reporter gene activity which, however, was not significantly different compared to the E2-mediated response of cells in normal medium and phenol red (+) medium with stripped FBS. Co-treatment with 100 nM ICI182,780 significantly reduced luciferase reporter gene activity over E2-treated cells within all media.

In 603B expressing recombinant mERβv2, treatment with 100 nM ICI182,780 significantly decreased luciferase reporter gene activity over vehicle treated cells in the absence of E2 in normal as well as in phenol red (+) and phenol red (-) medium containing stripped FBS indicating that recombinant mERβv2 protein trans-activates the $(ERE)_3$-pGL3promotor reporter construct independent of a ligand (Figure 3.11B). Treatment with 10 nM E2 similarly resulted in a low significant increase in reporter gene expression over vehicle treated cells across all media which, however, was not significantly decreased by co-treatment with 100 nM ICI182,780.

Since results have shown that recombinant mERβv1 and mERβv2 proteins trans-activated the $(ERE)_3$-pGL3promotor reporter construct in the absence of an exogenously added ligand in normal as well as medium containing stripped FBS, it is unlikely that the mERβ proteins are activated by background oestrogenic chemicals and steroid hormones present in normal culture media. This suggests that recombinant mERβv1 exhibits partial, and mERβv2 almost complete constitutive activities *in vitro* in this assay. Since stripping of FBS made little difference compared to results obtained from cells grown in medium containing non-stripped FBS, normal medium was used for all following experiments.

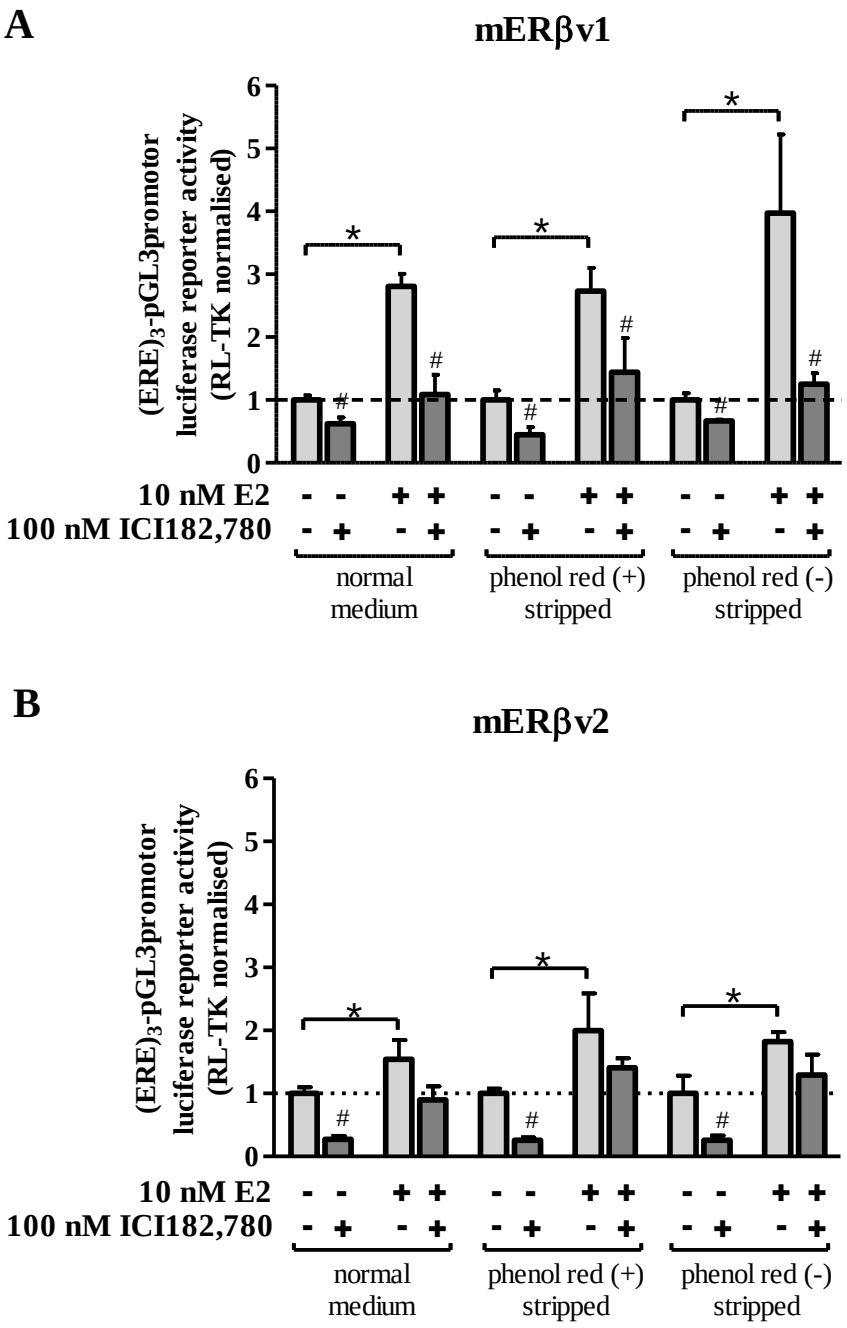

Figure 3.11 Recombinant mERβ proteins are not activated by background oestrogenic chemicals in cell culture media. Luciferase reporter gene ($(ERE)_3$-pGL3promotor) assay in 603B cells co-transfected with expression constructs coding for **(A)** the mERβv1 or **(B)** mERβv2. Cells were grown in normal medium, in medium supplemented with stripped FBS (phenol red (+) stripped) or in phenol red-free medium containing stripped FBS (phenol red (-) stripped) for 24 hours prior to transfection. Cells were then pre-treated with 100 nM ICI182,780 or 0.1% (v/v) DMSO vehicle as indicated for 6 hours followed by treatment with 10 nM E2 or 0.1% (v/v) DMSO vehicle (+/- 100 nM ICI182,780) for 24 hours. Mean and SD of n=3. Data are expressed in fold change versus DMSO vehicle-treated cells grown in the respective medium. *Significantly different ($p<0.05$) over DMSO vehicle-treated cells grown in the equivalent medium; #Significantly different versus equivalent treatments in the absence of ICI182,780 using Student's t-test (two-tailed) with Holm-Bonferroni post-hoc modifications.

3.3.2.e The mERβv2 is nearly completely constitutively active

In order to verify that the mERβv2 is almost completely constitutively active, and to find a way to test for activation of this mERβ variant, 603B cells transfected with the expression construct encoding the mERβv2, the $(ERE)_3$-pGL3promotor reporter and the RL-TK vector were pre-treated with 100 nM ICI182,780 (or 0.1% (v/v) DMSO) vehicle for 7 hours to de-activate the mERβv2 protein. Following removal of ICI182,780 and several washes with 1x PBS to reduce the levels of antagonist, cells were treated with increasing concentration of E2 (10 pM – 1 µM) with or without 100 nM ICI182,780. Figure 3.12 demonstrates that following de-activation of the mERβv2 with ICI182,780, E2 treatment resulted in a dose-dependent increase in luciferase activity both in cells treated with E2 + ICI182,780 as well as in cells treated with E2 in the absence of ICI182,780. Cells that were pre-treated with ICI182,780 and then treated with E2 in the absence of the ER antagonist, showed a significant response over vehicle treated cells at a lower E2 concentration (100 pM) compared to cells that were pre-treated with ICI182,780 and then treated with E2 + 100 nM ICI182,780, which showed a significant response to E2 at a concentration of 10 nM (Figure 3.12).

Overall these results confirm that recombinant mERβv2 protein is constitutively active and that de-activating the mERβv2 with ICI182,780 followed by washing out and treatment with a compound of interest represents a more sensitive way to test for activation of this protein compared to pre-treating cells with ICI182,780 followed by treatment with a compound of interest in the presence of ICI182,780. This is likely because in the presence of ICI182,780, E2 has to competitively displace the ER antagonist from the mERβv2, which leads to reduced sensitivity of the assay.

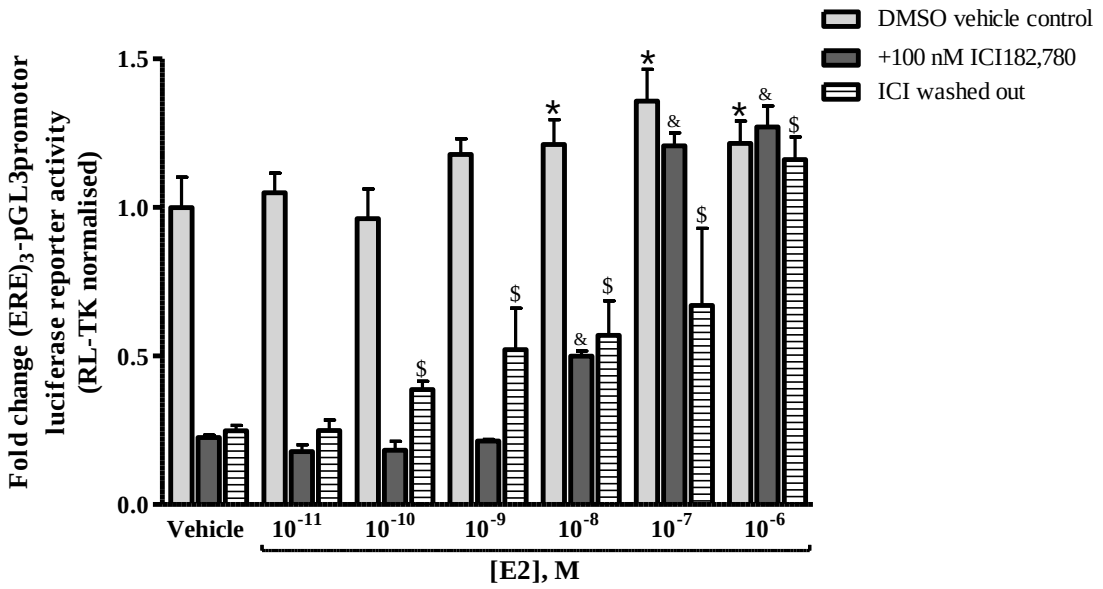

Figure 3.12 Testing for constitutive activity of the mERβv2 protein. Luciferase reporter gene ($(ERE)_3$-pGL3promotor) assay in 603B cells co-transfected with expression constructs coding for the mERβv2. Cells were pre-treated with 100 nM ICI182,780 or 0.1% (v/v) DMSO vehicle for 7 hours followed by several washes with 1x PBS to remove ICI182,780 from the cells. Cells were then treated with a range of E2 concentration ± ICI182,780 for 24 hours (light grey = pre-treated with DMSO vehicle, then treatment with E2; dark grey = pre-treated with 100 nM ICI, then treatment with E2 + 100 nM ICI; shaded = pre-treated with 100 nM ICI, several wash steps with PBS to remove antagonist, then treatment with E2 only). Mean and SD of n=3, typical of 3 separate experiments. Data are expressed in fold change versus DMSO vehicle-treated cells in the absence of ICI182,780. $^{*,\&,\$}$Significantly different ($p<0.05$) over DMSO vehicle-treated cells in the respective group using One-way ANOVA with Dunnett's post-hoc modifications.

3.3.3. Testing the cloned pcDNA3.1-mERα expression construct for correct functioning

3.3.3.a Recombinant mERα protein is expressed in 603B cells

The construct coding for the mERα was tested for correct functioning. To test whether the generated construct produces protein, 603B and HEK293 cells were transiently transfected with pcDNA3.1 plasmid DNA containing the insert for the mERα cDNA purified from clone 4 and clone 6 followed by analysis for expression of the recombinant mERα protein by Western Blot.

Figure 3.13 shows that proteins of the predicted size were generated in HEK293 cells transfected with the pcDNA3.1-mERα expression construct purified from clone 4 and 6 (see lane 7 and 8). Low but detectable mERα expression was observed in 603B cells transfected with the pcDNA3.1-mERα expression construct (lane 3 and 4) but also in cells transfected with an empty pcDNA3.1 construct (lane 2). This suggests that mERα protein may be endogenously expressed in 603B cells or that transfection induced the expression of mERα or a protein of similar size. The mERα was not detectable in HEK293 cells transfected with an

empty pcDNA3.1 expression construct (lane 6) or in non-transfected HEK293 and 603B cells (lane 1 and 5). The human breast cancer cell line MCF-7 as well as mouse uterine and liver tissue, known to express high levels of the ERα, were included as controls.

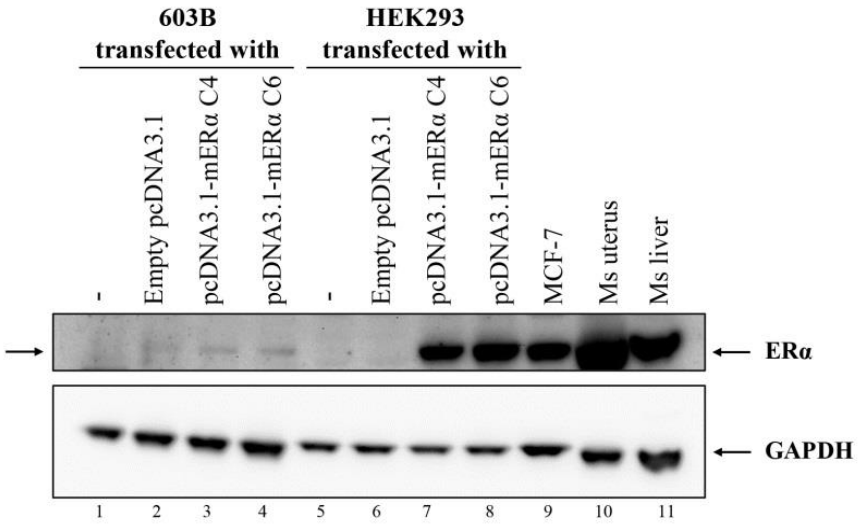

Figure 3.13 Analysis for ectopical expression of the mERα protein. Western Blot for the expression of the mERα protein in 603B and HEK293 cells transiently transfected with the expression construct coding for either the mERα from clone 4 (C4) or clone 6 (C6) or empty vector as control (20 µg total protein/lane). Theoretical molecular weight of ERα: 67 kDa.

3.3.3.b 603B cells transfected with the pcDNA3.1-mERα construct do not significantly respond to E2

Following confirmation that the mERα protein is ectopically expressed in 603B cells, recombinant mERα protein was tested for functional activity by reporter gene assay. Figure 3.14 shows that transfected 603B cells expressing the mERα from either clone 4 (C4) or clone 6 (C6) did not significantly respond to treatment with 10 nM E2. Although the combined treatment of E2 + 100 nM ICI182,780 reduced luciferase activity over E2-only treated cell from both clone 4 and 6, the decrease was not significant. Although cells transfected with an empty expression construct were shown to express the mERα/a protein of similar size by Western blot (see Figure 3.13), they show lower levels of basal luciferase activity compared to cells transfected with the pcDNA3.1-mERα expression constructs (Figure 3.14). This suggests that potentially endogenously expressed mERα is not functional and that recombinant mERα is partially able to trans-activate the $(ERE)_3$-pGL3promotor reporter construct when compared to cells transfected with an empty construct.

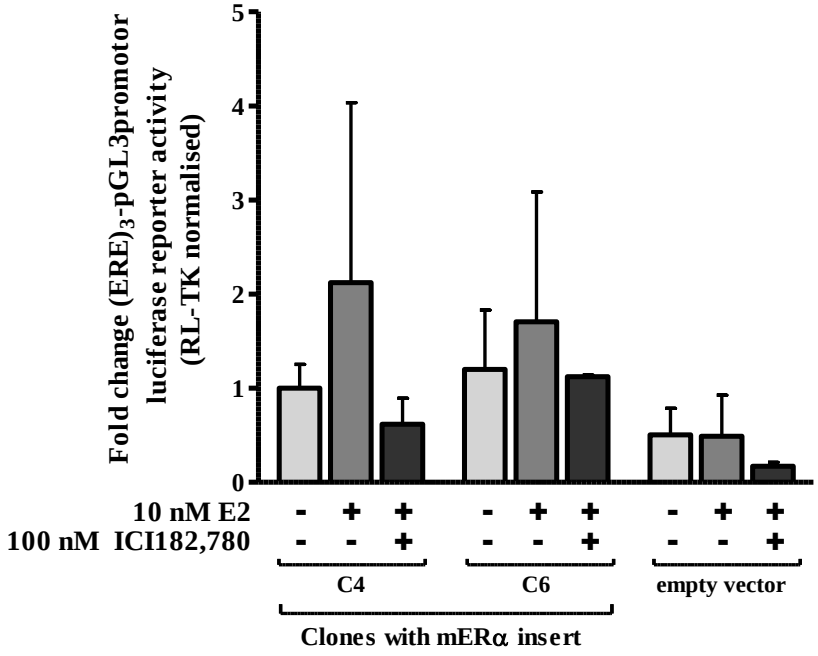

Figure 3.14 Testing of recombinant mERα protein for functional activity. $(ERE)_3$-pGL3promotor luciferase reporter gene assay in 603B cells co-transfected with the expression constructs isolated from clone 4 (C4) or 6 (C6) coding for the mERα protein or an empty vector. Cells were treated with vehicle or 10 nM E2 (± 100 nM ICI182,780) for 24 hours followed by dual-luciferase assay. Mean and SD of n=3, typical of 3 separate experiments. Data are expressed in fold change versus mERα C4-transfected cells treated with DMSO vehicle. Data was tested for statistical significance using Student's t-test (two-tailed) with Holm-Bonferroni post-hoc modifications.

3.3.3.c Testing different cell lines for mERα responsiveness

Cell line-dependent differences in availability and functionality of co-activators and adaptor proteins required for ERα-mediated transcription of the reporter gene in response to oestrogens have been described (Klinge, 2000). To determine whether the lack of a significant response in 603B cells transfected with the mERα expression construct following exposure to E2 is due to the absence of co-factors necessary for ERα responsiveness, several other cell lines were transfected with the pcDNA3.1-mERα construct purified from clone 6 and examined for their ability to trans-activate the $(ERE)_3$-pGL3promotor reporter construct compared to 603B cells. Cell lines tested were the mouse ductal LTPA cell line, the rat pancreatic acinar cell line AR42J-B13 (B13) as well as HEK293 cells, the latter because they have been shown to express high levels of recombinant mERα protein (see Figure 3.13). All cell lines were treated with 0.1% (v/v) DMSO vehicle and 10 nM E2 as well as with a range of oestrogens including the natural, less potent oestrogens oestrone (E1, 10 μM) and oestriol (E3, 10 μM), the synthetic oestrogen ethinyl estradiol (EE, 10 nM) and the known xenoestrogens butyl paraben (BP, 10 μM) and genistein (10 μM) with or without co-treatment with 100 nM ICI182,780.

Figure 3.15A demonstrates that recombinant mERα-expressing 603B cells show a significant increase in luciferase reporter gene activity in response to E1, butyl paraben and genistein compared to DMSO vehicle treated cells. The increase following exposure to butyl paraben and genistein – but not E1 - was reduced by co-treatment with 100 nM ICI182,780. ICI182,780 also reduced luciferase activity in DMSO vehicle treated cells compared to vehicle treated cells in the absence of ICI182,780 suggesting that recombinant mERα is partially active. E2, E3 and EE exposure did not result in a significant increase in reporter gene expression over DMSO vehicle treated cells. 603B cells transfected with an empty expression construct showed low basal luciferase activity compared to cells expressing the mERα with butyl paraben and genistein treatments causing an increase in luciferase activity over empty vector-DMSO vehicle treated cells. This increase in luciferase activity was not inhibited by co-treatment with ICI 182,780 suggesting that these compounds are able to trans-activate the $(ERE)_3$-pGL3promotor reporter construct independent of the mERα.

A significant increase in luciferase reporter gene activity in response to treatment with E2, E1, butyl paraben and genistein was observed in LTPA cells transfected with the pcDNA3.1-mERα construct. With the exception of E1, this increase was reduced by co-treatment with ICI182,780 (Figure 3.15B). Co-treatment with ICI182,780 also did not reduce luciferase activity over cells treated with E3 in the absence of the ER antagonist. E1 and E3 are less potent than E2 and thus were used at a higher concentration. At a concentration of 10 µM, however, it is likely E1 and E3 competitively displaced ICI182,780 from the mERα. This may account for why the ER antagonist did not reduce luciferase activity when co-treated with E1 and E3. LTPA cells transfected with an empty expression vector show low basal luciferase activity compared to cell transfected with the mERα expression construct and do not significantly respond to treatment with the indicated (xeno)oestrogens.

In the ER negative B13 cell line, treatment of recombinant mERα-expressing cells with E1 caused a significant increase in luciferase activity which was reduced by co-treatment with 100 nM ICI182,780 (Figure 3.15C). Treatment with the other indicated (xeno)oestrogens did not induce a significant response. Cells transfected with an empty expression construct show very low levels of basal luciferase activity compared to cells transfected with the mERα expression construct and treatment with oestrogens did not lead to an increase in luciferase activity.

In HEK293 cells, cells transfected with the mERα expression construct show a significant increase in luciferase reporter gene activity following the treatment with E1 and butyl paraben,

the latter which was decreased by co-treatment with ICI182,780 (Figure 3.15D). Mouse ERα-expressing HEK293 cells did not respond to E2 or any of the other indicated xeno(oestrogens). Control cells transfected with an empty construct show low levels of basal luciferase activity over mERα expressing cells and did not respond to treatment with (xeno)oestrogens.

These data suggest that in general all of the cell lines employed possess co-factors required for mERα responsiveness since cells co-transfected with the expression construct coding for the mERα show higher basal luciferase activities compared to cells transfected with an empty construct. A mERα-mediated significant increase in luciferase reporter gene activity in response to treatment with E2 over DMSO vehicle treated cells, however, was only observed in LTPA cells, although the fold induction (1.32) was small (Figure 3.15B). These findings indicate that the mERα is functionally active and that LTPA cells possess co-factors required for E2-induced trans-activtion of the $(ERE)_3$-pGL3promotor reporter construct.

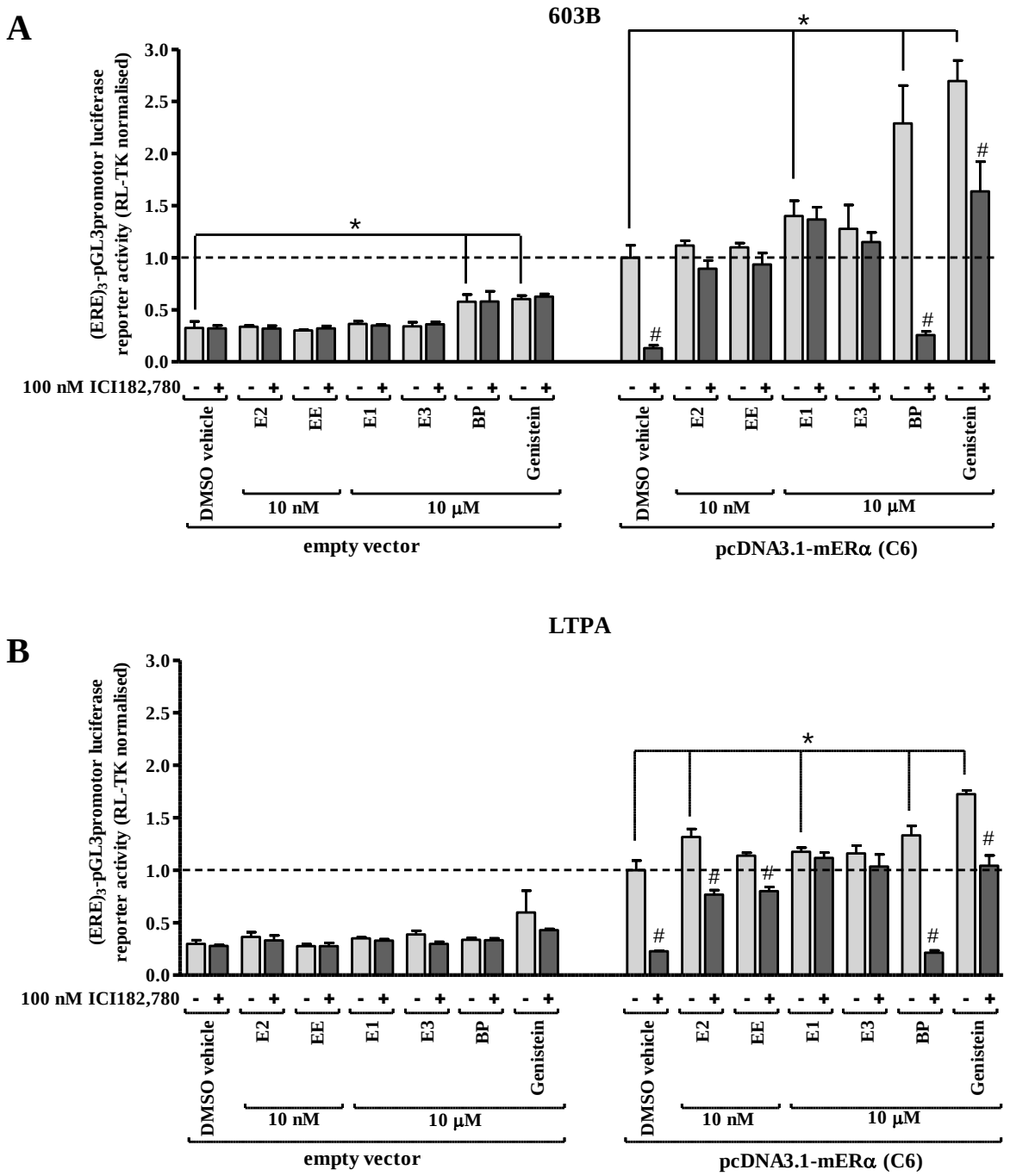

Figure 3.15 Examining different cell lines for mERα responsivness. ($(ERE)_3$-pGL3promotor luciferase reporter gene assay in **(A)** 603B **(B)** LTPA cells co-transfected with the pcDNA3.1 expression construct encoding the mERα (pcDNA3.1-mERα (C6)) or an empty expression construct (empty vector) followed by treatment with a range of natural, synthetic and xeno-oestrogens as indicated (+/- ICI182,780) for 24 hours before dual-luciferase assay. Mean and SD of n=3, typical of two separate experiments. Data are expressed in fold change versus pcDNA3.1-mERα(C6)-transfected cells treated with DMSO vehicle in the absence of ICI182,780. *Significantly different ($p<0.05$) over equivalent expression construct DMSO vehicle-treated cells in the absence of ICI182,780 using One-way ANOVA with Dunnett's post-hoc modifications. #Significantly different ($p<0.05$) versus equivalent treatments in the absence of ICI182,780 using the Student's t-test (two-tailed) with Holm-Bonferroni post-hoc modifications. BP, butyl paraben.

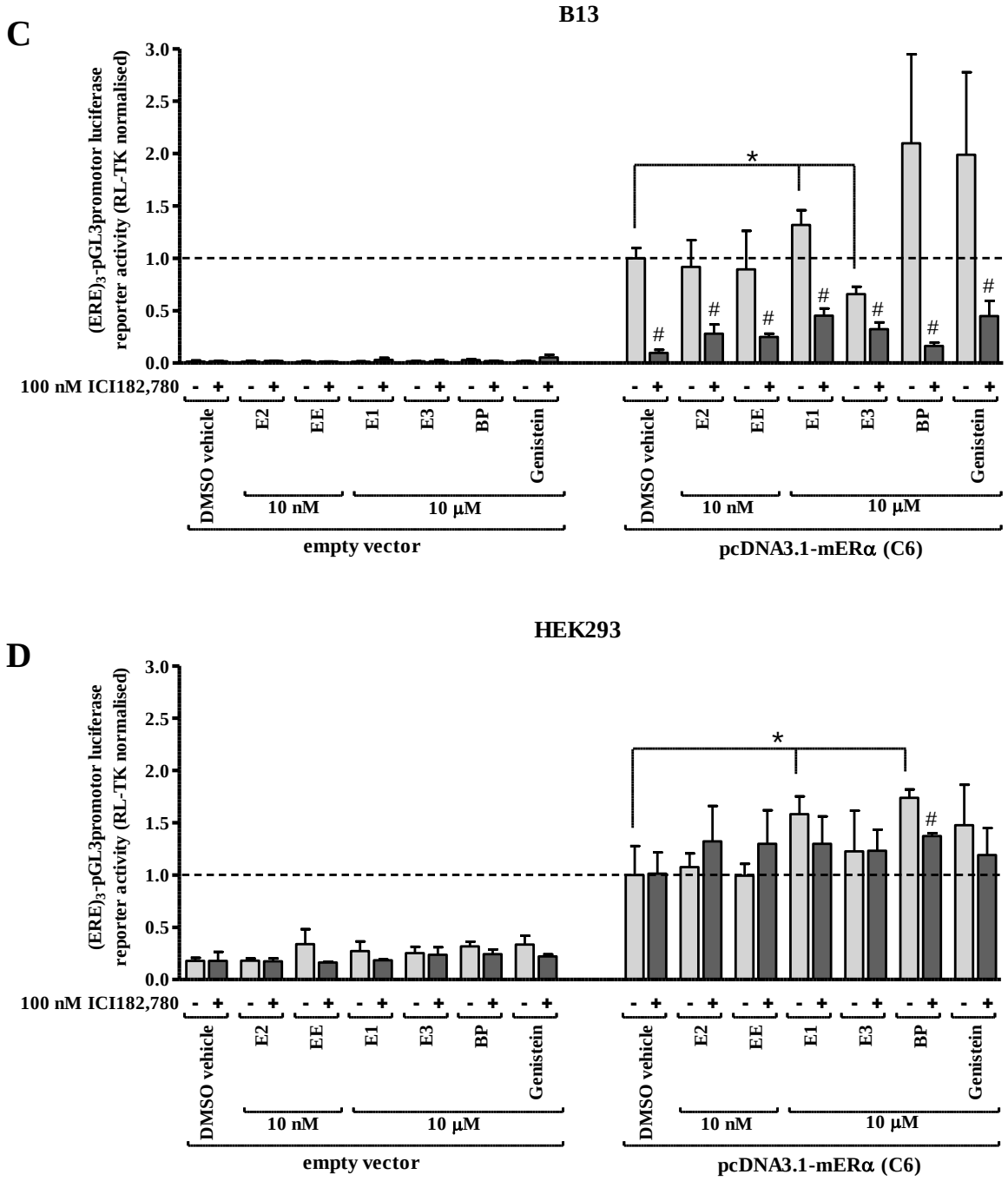

Figure 3.15 contd. Examining different cell lines for mERα responsivness. ($(ERE)_3$-pGL3promotor luciferase reporter gene assay in **(C)** B13 and **(D)** HEK293 cells co-transfected with the pcDNA3.1 expression construct encoding the mERα (pcDNA3.1-mERα (C6)) or an empty expression construct (empty vector) followed by treatment with a range of natural, synthetic and xeno-oestrogens as indicated (+/- ICI182,780) for 24 hours before dual-luciferase assay.

3.3.3.d Co-transfecting mERα-expressing LTPA cells with the 3XERE TATA luc reporter gene construct increases their response to E2

Since 603B cells did not respond to treatment with E2 and the response of mERα-expressing LTPA cells to E2 was small, it was examined whether this response could be improved by

using a different ERE reporter gene construct. The construct 3XERE TATA luc was employed as it has previously been shown to respond to mERα activation (La Sala et al., 2010). Compared to the $(ERE)_3$-pGL3promotor construct, the ERE of the 3XERE TATA luc construct contains a different nucleotide spacer sequence as demonstrated in Figure 3.16. Spacer sequences have been shown to determine transcriptional responses (Shu et al., 2010).

5' - GGTCA **ATT** TGACC - 3' **$(ERE)_3$-pGL3promotor**

5' - GGTCA **CAG** TGACC - 3' **3XERE TATA luc**

Figure 3.16 ERE of the $(ERE)_3$-pGL3promotor and 3XERE TATA luc reporter constructs.

To test and compare the 3XERE TATA luc reporter construct to the previously used $(ERE)_3$-pGL3promotor reporter construct, LTPA and 603B cells were transfected with either the 3XERE TATA luc or the $(ERE)_3$-pGL3promotor construct, the expression construct coding for the mERα or an empty construct, and the RL-TK control vector before treatment with 0.1% (v/v) DMSO vehicle or 10 nM E2 (± 100 nM ICI182,780) for 24 hours and dual-luciferase assay.

Figure 3.17A demonstrates that mERα-expressing 603B cells co-transfected with the $(ERE)_3$-pGL3promotor reporter construct do not significantly respond to treatment with E2 over DMSO vehicle treated cells. Similarly, in 603B cells co-transfected with the 3XERE TATA luc construct, treatment with E2 did not result in a significant increase in luciferase reporter gene expression over vehicle treated cells (Figure 3.17B). As seen with both reporter constructs, ICI182,780 significantly reduced luciferase reporter gene activity over DMSO vehicle treated cells suggesting that the mERα is capable of trans-activating both reporter constructs in 603B cells in the absence of a ligand. ICI182,780 also reduced luciferase reporter gene activity over E2 treated cells. Control 603B cells transfected with an empty expression construct show lower levels of basal luciferase activity in both $(ERE)_3$-pGL3promotor (Figure 3.17A) and 3XERE TATA luc (Figure 3.17B) co-transfected cells confirming that the increase in luciferase reporter gene expression as seen in cells transfected with the mERα-pcDNA3.1 construct is mediated by the mERα.

In LTPA cells, co-transfection of the mERα-pcDNA3.1 construct with the $(ERE)_3$-pGL3promotor construct resulted in a significant increase in luciferase reporter gene activity in response to treatment with E2 (Figure 3.17C). This response was further increased when the $(ERE)_3$-pGL3promotor construct was replaced by the 3XERE TATA luc construct (Figure

3.17D). ICI182,780 significantly reduced luciferase reporter gene activity over DMSO vehicle treated cells in both $(ERE)_3$-pGL3promotor and 3XERE TATA luc reporter construct co-transfected cells suggesting that the mERα is capable of trans-activating both reporter constructs in LTPA cells in the absence of a ligand. ICI182,780 also reduced luciferase reporter gene activity over E2 treated cells confirming that the E2-induced increase in luciferase reporter gene activity is mediated by the mERα. LTPA control cells co-transfected with an empty expression construct and the $(ERE)_3$-pGL3promotor reporter construct show an increase in luciferase reporter gene expression in response to E2 which, however, was not decreased by co-treatment with ICI182,780 (Figure 3.17C). LTPA cells co-transfected with an empty expression construct and the 3XERE TATA luc reporter construct show very low levels of basal luciferase activities and do not respond to treatment with E2 (Figure 3.17D).

Considered together, these data suggest that recombinant mERα is functionally active in LTPA, but not in 603B cells. The greatest mERα-mediated response following exposure to E2 can be seen in LTPA cells when co-transfected with the 3XERE TATA luc reporter construct. Therefore, LTPA cells in combination with the 3XERE TATA luc construct were used to test for activation of the mERα *in vitro*.

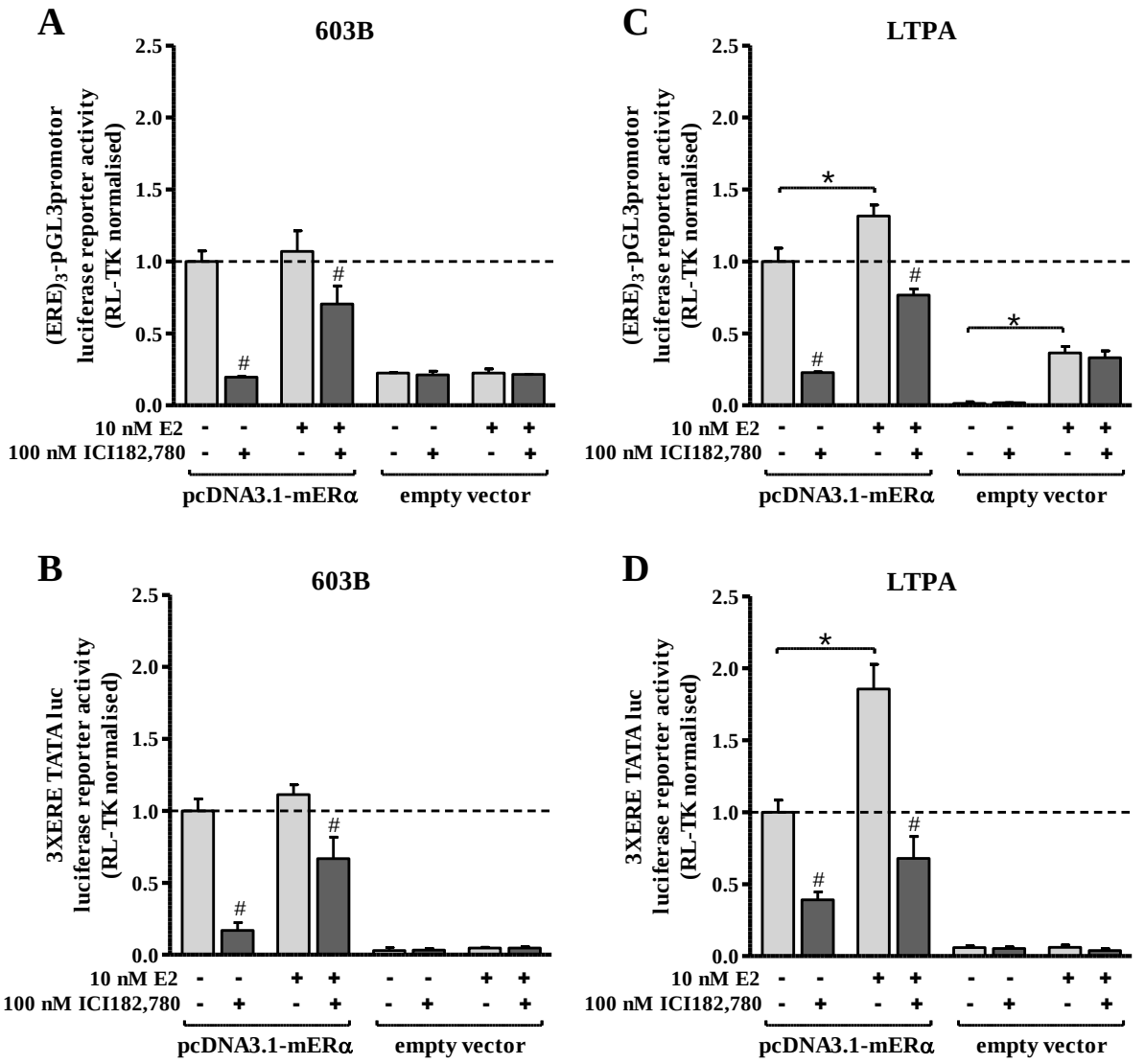

Figure 3.17 Examining the response of the $(ERE)_3$-pGL3promotor reporter construct and the 3XERE TATA construct to mERα activation in 603B and LTPA cells. 603B cells were co-transfected with the expression construct encoding the mERα or an empty construct and with **(A)** the $(ERE)_3$-pGL3promotor reporter construct or **(B)** the 3XERE TATA luc reporter construct before treatment with DMSO vehicle or 10 nM E2 (+/- 100 nM ICI182,780) for 24 hours and dual-luciferase assay. LTPA cells were co-transfected with the expression construct encoding the mERα or an empty construct and with **(C)** the $(ERE)_3$-pGL3promotor reporter construct or **(D)** the 3XERE TATA luc reporter construct before treatment with DMSO vehicle or 10 nM E2 (+/- 100 nM ICI182,780) for 24 hours and dual-luciferase assay. Mean and SD of n=3, typical of 2 separate experiments. Data are expressed in fold change versus pcDNA3.1-mERα -transfected cells treated with DMSO vehicle in the absence of ICI182,780. * Significantly different ($p<0.05$) over equivalent epression construct DMSO vehicle-treated cells in the absence of ICI182,780. #Significantly different versus equivalent treatments in the absence of ICI182,780 using the Student's t-test (two-tailed) with Holm-Bonferroni post-hoc modifications.

3.3.3.e The mERα is ectopically expressed in LTPA cells

To verify that the mERα construct produces protein in LTPA cells, LTPA cells were transiently transfected with purified pcDNA3.1 plasmid DNA containing the mERα cDNA insert and expression of recombinant protein was examined by Western Blot and immunocytochemical staining.

Figure 3.18A demonstrates that a protein of the predicted size was generated in HEK293 cells (lane 6) and low but detectable protein expression was observed in LTPA cells (lane 3). Positive controls MCF7 and mouse uterus show high levels of ERα expression. ERα protein was undetectable in LTPA and HEK293 controls transfected with an empty pcDNA3.1 expression construct (lane 2 and 5) an in non-transfected cells (lane 1 and 4).

Immunocytochemical staining confirms that the mERα is ectopically expressed in HEK293 and on a lower level in LTPA cells transiently transfected with the pcDNA3.1-mERα expression constructs, exhibiting nuclear localisation. Mouse ERα protein was not detected in LTPA and HEK293 control cells transfected with an empty pcDNA3.1 construct (Figure 3.18B).

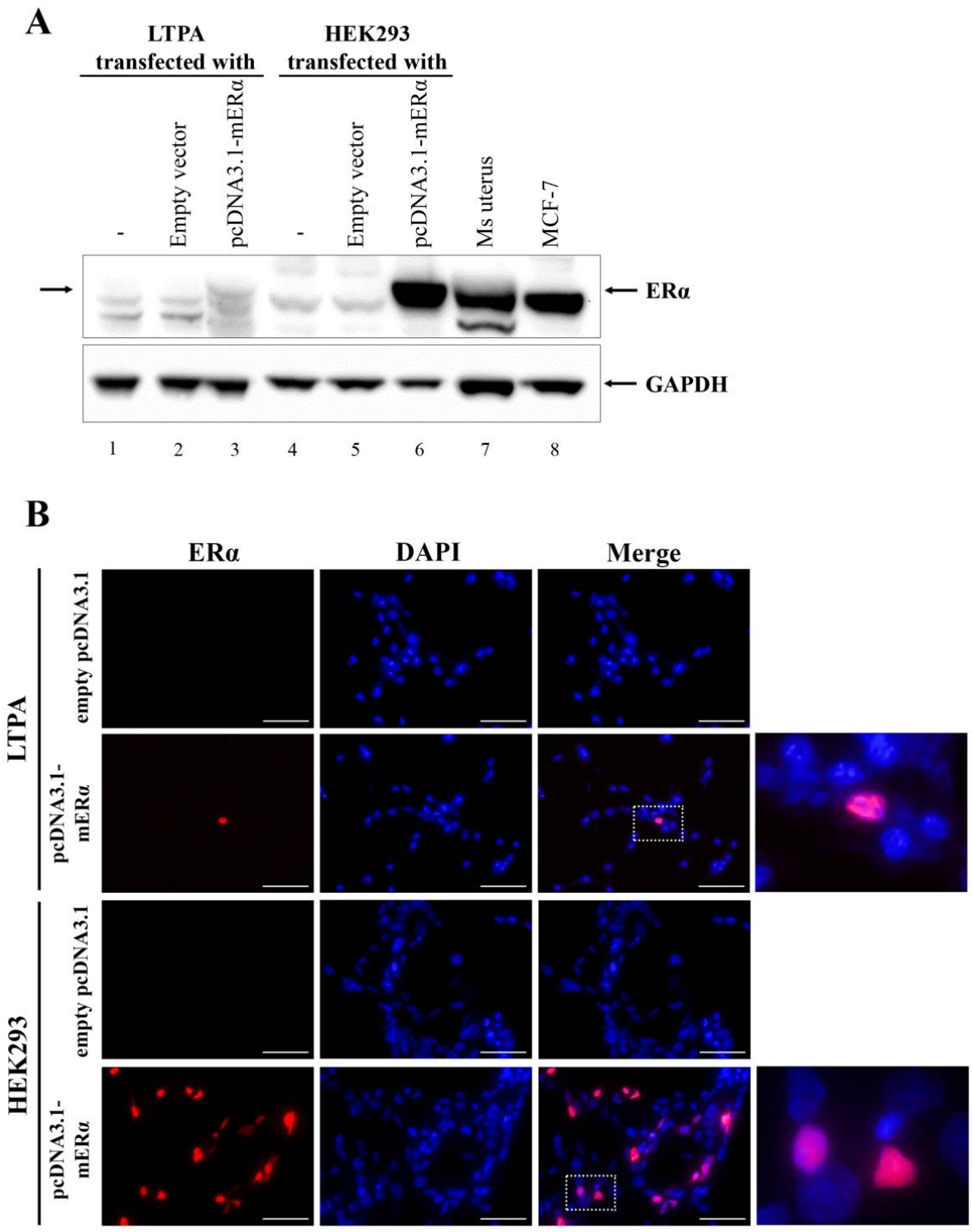

Figure 3.18 Analysis for ectopical expression of the mERα protein in LTPA cells. (A) Western Blot for the expression of the mERα protein in LTPA and HEK293 control cells transiently transfected with the expression construct coding for the mERα cDNA sequence or empty vector as control (20 µg total protein/lane). Theoretical molecular weights: mERα, 67 kDa; GAPDH, 39 kDa **(B)** Immunocytochemical staining for the expression of the mERα protein in LTPA and HEK293 control cells transiently transfected with the expression construct encoding the mERα cDNA sequence or empty vector as control. Scale bar: 50 µm.

3.3.3.f Confirmation of correct functioning of recombinant mERα protein in LTPA cells when co-transfected with the 3XERE TATA luc construct

To verify the results that the mERα construct in combination with the 3XERE TATA luc reporter construct functions correctly, LTPA cells were transfected with the pcDNA3.1 expression construct coding for the mERα, an empty expression construct or a construct coding for the c/EBPβ for the purpose of investigating squelching effects and their response to E2 was examined. Figure 3.19 shows that the mERα was activated by 10 nM E2. Cells transfected with an empty expression construct or the construct coding for the c/EBPβ gene show a reduced level of basal luciferase activity compared to cells transfected with the pcDNA3.1-mERα expression construct and they do not respond to 10 nM E2 treatment.

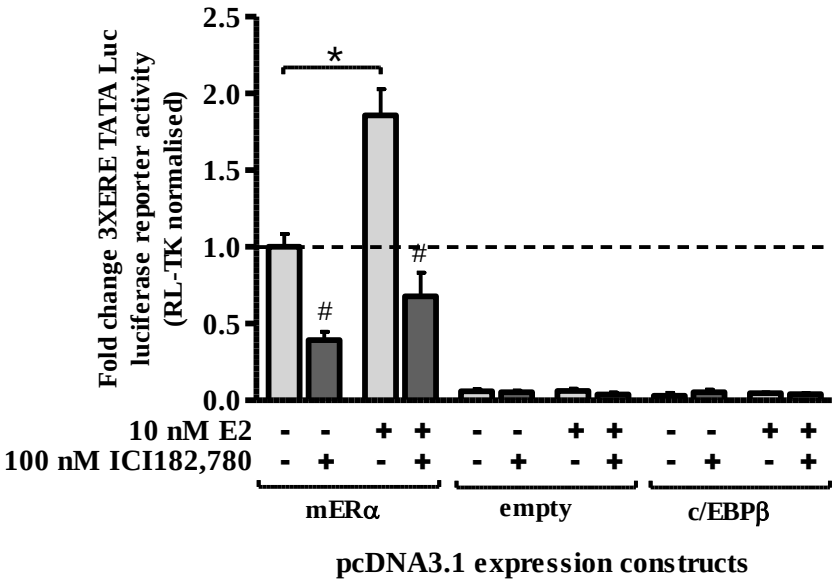

Figure 3.19 Testing the mERα expression construct for functional activity in LTPA cells. Luciferase reporter gene (3XERE TATA luc) assay in LTPA cells co-transfected with expression constructs coding for the mERα or control constructs as indicated. Cells were treated with 0.1% DMSO vehicle or 10 nM E2 (± ICI182,780) for 24 hours followed by dual-luciferase assay. Mean and SD of n=3, typical of 3 separate experiments. Data are expressed in fold change versus mERα-transfected cells treated with DMSO vehicle. *Significantly different ($p<0.05$) over the equivalent expression vector transfected cells treated with DMSO vehicle; #Significantly different versus equivalent treatments in the absence of ICI182,780 using Student's t-test (two-tailed) with Holm-Bonferroni post-hoc modifications.

3.3.3.g Recombinant mERα trans-activates the 3XERE TATA luc reporter construct in a dose-dependent manner

Dose-dependent activation of the mERα by E2 was investigated. LTPA cells expressing recombinant mERα in combination with the 3XERE TATA luc construct were treated with increasing concentrations of E2 (10 pM – 10 μM). Figure 3.20 demonstrates that the mERα

was activated in a dose-dependent manner, whereas control cells transfected with an empty expression construct did not respond to E2 at any concentration.

These results suggest that recombinant mERα protein in combination with the 3XERE TATA luc construct functions correctly and therefore, this system was used for all further experiments testing for mERα activation.

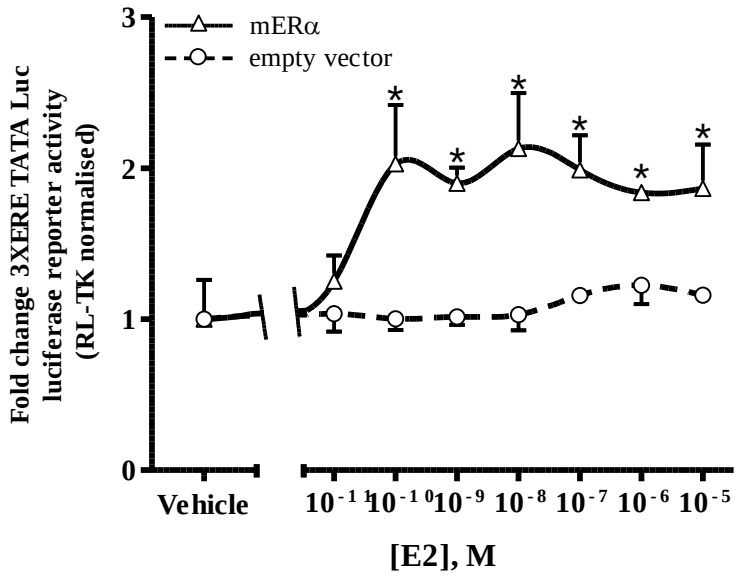

Figure 3.20 E2 activates the mERα in a dose-dependent manner. Luciferase reporter gene (3XERE TATA luc) assay in LTPA cells co-transfected with the pcDNA3.1 expression constructs coding for the mERα or an empty control construct. Cells were treated with increasing concentrations of E2 (vehicle: 0.1% DMSO) for 24 hours followed by dual-luciferase assay. Mean and SD of n=3, typical of 3 separate experiments. Data are expressed in fold change versus the equivalent expression vector transfected DMSO vehicle-treated cells. *Significantly different ($p<0.05$) over the equivalent expression vector transfected cells treated with DMSO vehicle using One-way ANOVA with Dunnett's post-hoc modifications.

3.4. Discussion

Data in this chapter has demonstrated that a mouse-based *in vitro* trans-activation reporter gene assay capable of examining transcriptional activities of recombinant mERα, mERβv1 and the mERβv2 proteins was successfully developed.

Although a number of *in vitro* assays exist that allow for chemicals to be tested for interaction with the ER and modulation of ER signalling, cell-based reporter gene trans-activation assays are commonly employed as they allow for both agonistic and antagonistic activities of xenobiotics to be detected. Cell-based reporter gene assays require the use of a cell line expressing the ER, either endogenously or recombinantly transfected.

Since data in this chapter has shown that the mouse cell lines 603B and LTPA do not express detectable levels of the ERs (Figure 3.1, Figure 3.2), the mERα, mERβv1 and mERβv2 cDNAs were cloned for ectopical expression of the ER proteins in these cell lines. Recombinant mERα, mERβv1 and mERβv2 protein expression in LTPA (mERα, Figure 3.18) and 603B (mERβ, Figure 3.8) cells was low compared to transfected control HEK293 cells, likely because data have shown that 603B and LTPA cells have low transfection efficiencies when using Effectene transfection reagent which, however, resulted in highest transfection efficiencies among all transfection methods tested (Figure 3.7).

Testing for functional activity of the generated pcDNA3.1-mER expression constructs has shown that 603B cells transfected with the construct coding for the mERβv1 trans-activated the $(ERE)_3$-pGL3promotor in the absence of E2, suggesting that the mERβv1 is partially constitutively active (Figure 3.9). Treatment with E2, however, further significantly induced luciferase reporter gene expression over vehicle treated cells confirming that recombinant mERβv1 is functionally active and that 603B cells possess co-factors required for mERβv1 responsiveness. 603B cells expressing recombinant mERβv2 appeared to almost fully trans-activate the $(ERE)_3$-pGL3promotor reporter construct in the absence of E2 and treatment with ICI182,780 reduced luciferase reporter gene activity over vehicle treated cells to levels similar as seen in mERβv1-expressing cells treated with the ER antagonist. E2 exposure further activated recombinant mERβv2 over vehicle treated cells although the fold induction was small (Figure 3.9). These data suggest that recombinant mERβv2 protein is nearly completely constitutively active *in vitro*.

Complete cell culture media generally contain a number of oestrogenic compounds and steroid hormones which could account for activation of the mERβ proteins under normal culture conditions. Culture of recombinant mERβv1 and mERβv2 expressing cells in media

supplemented with stripped serum, however, resulted in similar reporter gene activities as seen in cells grown in 'normal' medium (Figure 3.11) suggesting that background oestrogenic chemicals are not likely to be responsible for the observed constitutive activities of the mERβ proteins.

Further investigations into whether recombinant mERβv2 is constitutively active have shown that following de-activation with ICI182,780, the mERβv2 protein is activated by E2 in a dose-dependent manner (Figure 3.12). In mERβv2-expressing cells that were, following de-activation, treated with a range of E2 concentration in the presence of 100 nM ICI182,780, a significant increase in reporter gene activity was observed at a E2 concentration of 10 nM. ICI182,780 is a competitive antagonist and these data indicate that at 10 nM, E2 competitively displaces ICI182,780 from the mERβv2. In comparison, mERβv2-expressing cells that were, following pre-treatment with ICI182780, treated with E2 in the absence of the ER antagonist show a significant response to E2 at a much lower concentration (100 pM), likely because E2 does not have to compete with ICI182,780 for binding and activation of the mERβv2. All in all these data confirm that the mERβv2 protein is near complete constitutively active *in vitro* in this assay and that activation of the protein by oestrogenic compounds can be examined by first de-activating the mERβv2 with ICI182,780 followed by treatment with the compound of interest.

A reason as to why the mERβv1 protein exhibits partial and the mERβv2 nearly complete constitutive activity in this assay may be because they are activated in response to growth factor signalling. Interactions between oestrogens and growth factors play important roles in cell proliferation and tumour growth in oestrogen-mediated cancers in the mammary gland and uterus (Hayashi et al., 2003). It has been reported that in ovariectomized mice actions of oestrogens can be mimicked by epidermal growth factor (EGF) (Nelson et al., 1991; Ignar-Trowbridge et al., 1992), an effect abolished in ERα knock-out mice (Curtis et al., 1996). Several studies employing ERE-containing reporter gene constructs have confirmed that growth factors can exert their actions through the ER. These studies have described reporter gene activities in the absence of oestrogen in a number of cell lines which were mediated by growth factors such as EGF (Ignar-Trowbridge et al., 1993; Bunone et al., 1996; El-Tanani and Green, 1997)), transforming growth factor alpha (TGF-α) (Ignar-Trowbridge et al., 1996) insulin-like growth factor-1 (IGF-1) (Ma et al., 1994; Newton et al., 1994) and several others (Ishida et al., 2010). Growth factor-dependent activation of the ERs is largely mediated by direct phosphorylation carried out by a number of growth factor receptor tyrosine kinases

leading to stimulation of the ligand-independent transcriptional potential of the ERs (Smith, 1998; Ali and Coombes, 2002).

To explain the differences in transcriptional activity between the mERβv1 and the mERβv2, their structural properties were compared. According to the National Centre for Biotechnology Information (NCBI), the mERβv2 lacks an in-frame exon in the coding region creating a protein lacking 18 amino acids (383 – 400) in the ligand binding domain compared to mERβv1. This deletion may affect the type and affinity of ligands capable of binding to the mERβv2 which is likely to account for the differences in transcriptional activity observed between the two mERβ isoforms. Constitutive activity of the mERβv2 has not been reported elsewhere. Interestingly, in the literature the mERβv2 is commonly described to contain an 18 amino acid insertion in the ligand binding domain (Lu et al., 1998; Lu et al., 2000; Zhao et al., 2005) which is opposite to the information given on NCBI which states that the mERβv2 contains an 18 amino acid deletion. Protein sequence alignments of the mERβv1 and mERβv2 with the human ERβ wild type (hERβ) (Appendix D) show that there is greater sequence homology between the mERβv2 and the hERβ than there is between the mERβv1 and the hERβ. Indeed, the mERβv1 contains a 18 amino acid insertion compared to the hERβ indicating that the mERβv1 as referred to on NCBI is regarded as the mERβ isoform 2 (ERβ2) in the literature whereas the mERβv2 on NCBI is considered to be the mouse ERβ wild type or ERβ isoform 1 (ERβ1). Information regarding the mouse ER proteins as seen on NCBI and the data found in the literature is summarised in Table 3.1.

GENE	NCBI ref mRNA	NCBI ref protein	Our nomenclature	Human orthologue	Comments
Esr1	NM_007956.5 Transcript Variant: This variant (1) encodes the longer isoform (1). Variants 1, 2 and 3 encode the same protein.	NP_031982.1 Estrogen receptor isoform 1 [Mus musculus] – from transcript variant 1	mERα	hERα	First mER to be identified and cloned (White *et al.*, 1987). Orthologue identified in rat (Koike *et al.*, 1987) and human (Green *et al.*, 1986; Greene *et al.*, 1986).
Esr2	NM_207707.1 Transcript Variant: This variant (1) encodes the longer isoform (1).	NP_997590.1 Estrogen receptor beta isoform 1 [Mus musculus]	mERβv1		Identified to contain 54 nucleotides inserted in frame between exon 5 and 6 compared to "wild type" mER (or "ERβ1"), no equivalent of this transcript was detected in any of the four human tissues analysed (Lu *et al.*, 1998). Orthologue identified in rat - termed ERβ2 - bound estradiol with a lower affinity (Kd 5.1 nM) than either ERα (0.19 nM) or "ERβ1" (0.14 nM) and activated transcription in response to estradiol but at a 1000-fold greater estradiol concentration than for "ERβ1" (Chu and Fuller, 1997; Petersen *et al.*, 1998). Recombinant mERβ2 protein had markedly reduced ligand binding (KD=17.7 +/- 4.7 nM) compared with "mERb1" (KD=0.56 +/- 0.19 nM). Using a 'novel raloxifene responsive' gene reporter system estradiol and LY117018 activated both mERα and "mERβ1" on this promoter was identical, and this protein was only slightly less than that observed (Lu *et al.*, 2000). The binding affinity of estradiol was 14-fold higher for "mERβ1" than for "mERβ2". In contrast, raloxifene was dramatically (8-fold) "mERβ2" selective. "mERβ2" showed significantly decreased estradiol-induced maximal transcriptional activity as compared to "mER*β*1" (Zhao *et al.*, 2005).
Esr2	NM_010157.3 Transcript Variant: This variant (2) lacks an in-frame exon (54 nucleotides) in the coding region, compared to variant 1.	NP_034287.3 Estrogen receptor beta isoform 2. This isoform lacks an internal segment (18 aa), compared to isoform 1.	mERβv2	hERβ	Originally discovered "wild type" mERβ, protein that shares, respectively, 97% and 60% identity with the DNA- and ligand-binding domains of mERα (Tremblay *et al.*, 1997). Orthologue detected in rat, termed "ERβ1" following detection of other ERβ variants (Kuiper *et al.*, 1996; Petersen *et al.*, 1998). Orthologue detected in human (Mosselman *et al.*, 1996).

Table 3.1 Summary of available data for the mER proteins.

Testing of the cloned pcDNA3.1-mERα expression construct for functional activity has shown that the greatest fold change in luciferase activity following E2 exposure over vehicle treated cells was observed in the mouse ductal LTPA cell line when co-transfected with the 3XERE TATA luc reporter construct (Figure 3.17). A possible explanation for why a mERα-mediated significant increase in luciferase activity following E2 exposure was observed in LTPA – but not in 603B or in any of the other tested cell lines could be due to differences in availability and functionality of co-activators and adaptor proteins required for ERα-mediated transcription of the reporter gene in response to E2. In a review paper, Klinge *et al.* (2001) have listed natural ERE sequences from 38 oestrogen-responsive genes along with their ER binding affinities and transcriptional activation in different cell lines. These data show that cell line-dependent differences in the amount of transcriptional activation from the same ERE exist suggesting that cell specific factors such as the quantity and type of co-activators available are involved in determining ER transcriptional activation (Klinge, 2001).

Although an increase in luciferase reporter gene activity in mERα-expressing cells in response to E2 was only observed in LTPA cells, other tested cell lines have shown an increase in reporter gene activity in response to treatment with other oestrogenic compounds. For example, E1, butyl paraben and genistein but not E2 significantly induced luciferase reporter gene expression in 603B cells (Figure 3.15A). A response following exposure to E1 and butyl paraben – but not E2 – was also observed in HEK293 cells (Figure 3.15D). Binding of a ligand to the ER induces specific conformational changes which are ligand-specific. Depending on ER conformation, a different set of cofactor proteins required for transcriptional induction is recruited to interact with the ER and the transcription machinery determining ER transcriptional responses (Yi *et al.*, 2002).

Not only does the type of ligand determine ER-mediated transcriptional responses, but also the ERE sequence found in promotor regions of oestrogen responsive genes. Mouse ERα-expressing LTPA cells co-transfected with the $(ERE)_3$-pGL3promotor reporter construct showed a significant increase in luciferase activity following treatment with E2 (Figure 3.17C), however, this response was further enhanced by replacing the $(ERE)_3$-pGL3promotor with the 3XERE TATA luc construct (Figure 3.17D). Both the $(ERE)_3$-pGL3promotor and the 3XERE TATA luc reporter constructs contain three copies of the minimal consensus ERE palindrome 5'-GGTCAnnnTGACC-3' (n = any nucleotide). The reporter constructs, however, differ in their tri-nucleotide spacer sequence and immediate ERE flanking nucleotides. The 3XERE TATA luc reporter construct contains three copies of the vitellogenin ERE with the sequence 5'-GGTCA CAG TGACC-3' whereas the sequence for the $(ERE)_3$-pGL3promotor

construct is 5'-GGTCA ATT TGACC-3'. Shu et al. (2010) have reported that EREs with a tri-nucleotide spacer sequence of C(A/T)G are enriched within the genome and gel shift as well as reporter gene assays have shown that ERα binding affinity to EREs is highest for the spacer sequence C(A/T)G with stronger E2-stimulated transcriptional responses compared to other tri-nucleotide spacers. ER-ERE binding affinity is not only determined by the spacer sequence but also by the immediate ERE flanking nucleotides. ERα binds with highest affinity to the Xenopus vitellogenin A2 ERE compared to other natural EREs (Klinge, 2001). The xenopus vitellogenin A2 gene has a 19 bp palindromic ERE with 14 of the directly 5' flanking nucleotides being either A or T (70% AT rich) (Walker *et al.*, 1984). DNA enriched with A and T nucleotides is reported to be more readily deformed which is believed to be required for facilitation of interaction between the transcription machinery located at different sites (Kerppola and Curran, 1991). The 14 5'-flanking nucleotides of the 3xERE TATA luc reporter construct contain 70% A/T nucleotides (5'-TGATATCAGATCTA-3'). In comparison, 5' flanking nucleotides of the $(ERE)_3$-pGL3promotor construct contain less than 30% A or T nucleotides (5'-GGTACCGAGCTCGG-3'). These differences between the reporter constructs could explain why an enhanced transcriptional activity is seen in LTPA cells co-transfected with the 3XERE TATA luc reporter construct compared to cells co-transfected with the $(ERE)_3$-pGL3promotor construct. The expression of recombinant mERα protein (Figure 3.18) and E2-mediated dose-dependent activation of the mERα in LTPA cells has been shown (Figure 3.20) confirming that the pcDNA3.1- mERα expression construct creates functional protein.

Overall, data in this chapter demonstrate that a mouse-based *in vitro* trans-activation reporter gene assay to test for activation or inhibition of the mERα, mERβv1 and mERβv2 proteins has been successfully developed. Using this assay, a variety of compounds can be tested for oestrogenic activity in mice. As a result this assay will assist in determining which ER-targeting chemicals can be used to examine the potential adverse effects that oestrogenic chemicals may have *in vivo* in mice.

Chapter 4. Oral tartrazine exposure causes hepatic and gastrointestinal inflammation *in vivo* independent of the ER

A number of xenoestrogens are found in our diet and these chemicals can both be natural (e.g., isoflavones (Kuiper *et al.*, 1998)) or man-made (e.g., bisphenol A (Laws *et al.*, 2000)). A platform of human-based reporter gene *in vitro* assays exist enabling chemicals to be rapidly screened for potential oestrogenic activity in humans. Using these assays, the food additive tartrazine has previously been shown to have xenoestrogenic properties since it activated the human ERα *in vitro* (Datta and Lundin-Schiller, 2008; Axon *et al.*, 2012).

Tartrazine (E102, also known as FD & C Yellow No. 5) is a synthetic yellow azo dye commonly found in a variety of food items and pharmaceuticals. As stated by the European Food Safety Agency (EFSA), the food dye consists of 3-carboxy-5-hydroxy-1-(4'-sulphophenyl)-4-(4'-sulphophenylazo)pyrazole trisodium salt with sodium chloride and/or sodium sulfate as the principal uncoloured components. The purity is at least 85% of total colouring matter with the remaining 15% being sodium chloride/sulfate, water insoluble matter, subsidiary colouring matters and other organic contaminants such as 5-oxo-1-(4-sulphophenyl)-2-pyrazoline-3-carboxylic acid (OSPCA) (EFSA, 2009).

The food colourant has a history of causing intolerance reactions in a small fraction of the exposed population estimated to be 0.12% (Elhkim *et al.*, 2007). Reported intolerance reactions to tartrazine often comprise of urticaria and bronchoconstriction and have been stated to occur more likely in individuals with aspirin-intolerance (Freedman, 1977; Weber *et al.*, 1979; Rajan *et al.*, 2014). Tartrazine is also thought to cause hyperactivity in children (Schab and Trinh, 2004).

The safety of tartrazine was first assessed in 1966 by the Joint FAO/WHO Expert Committee on Food Additives (JECFA) specifying an Acceptable Daily Intake (ADI) of 0-7.5 mg/kg body weight/day (JECFA, 1966). Although the publication of new studies lead to the re-assessment of tartrazine safety by the EU Scientific Committee for Food (SCF) in 1975 and 1984, the Nordic Council of Ministers in 2002 and most recently, by the European Food Safety Authority (EFSA) in 2009, the previously established ADI of 7.5 mg/kg body weight/day remained (EFSA, 2009).

Although limited data regarding the metabolism of tartrazine is available, the food dye when administered orally is understood to be mainly metabolised by the intestinal microflora to

sulfanilic acid (SA) (which may further be subject to N-acetylation (SA-NAc)) and, via 1-(4-sulfophenyl)-3-carboxy-4-amino-5-pyrazolone (SCAP), to sulfophenylhydrazine (SPH) (see Figure 4.1). These metabolites are predominantly excreted in the urine and only a minor proportion (<5%) of intact tartrazine is absorbed (Jones *et al.*, 1964; Roxon *et al.*, 1967; Ryan *et al.*, 1969a; Ryan *et al.*, 1969b). I.p. injection of 2.4 mg/kg bw of 14C-tartrazine was found to result in excretion of unchanged tartrazine since 64-96% of the dose was recovered intact in the urine within 24 hours in rats and rabbits and no other metabolites were detected. I.p. administration of higher doses led to urinary detection of free and conjugated sulfanilic acid (Jones *et al.*, 1964).

Since oestrogens (and therefore potentially xenoestrogens) are cholestatic, it was hypothesised that tartrazine is an activator of the mouse ER and that, if significant absorption occurs, oral tartrazine administration will result in cholestasis in mice.

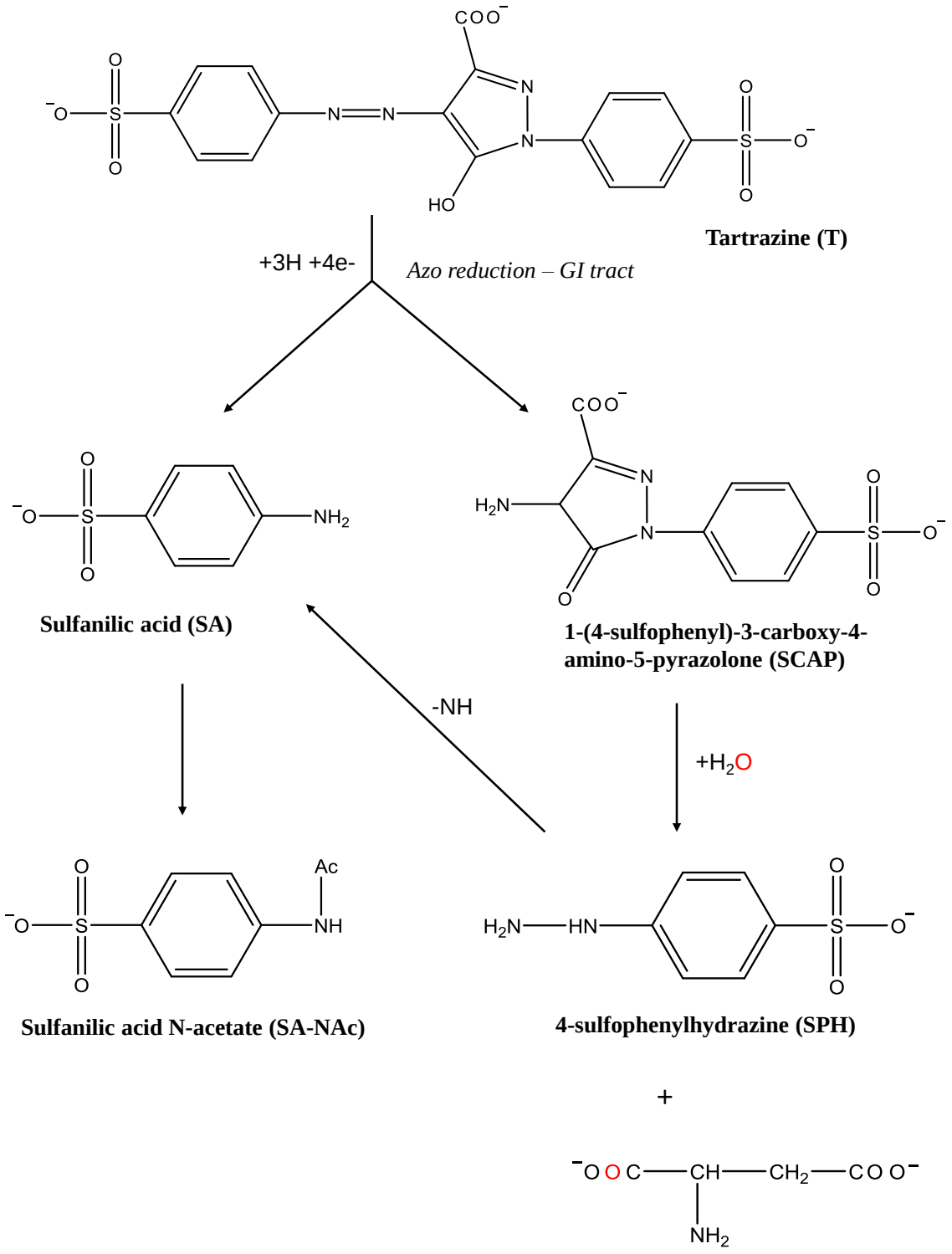

Figure 4.1 Tartrazine metabolism. Tartrazine is metabolised by intestinal microorganisms to sulfanilic acid (SA) and, via 1-(4-sulfophenyl)-3-carboxy-4-amino-5-pyrazolone (SCAP), to 4-sulfophenylhydrazine (SPH). Sulfanilic acid may further be N-acetylated (SA-NAc).

4.1. *In vitro* screening of tartrazine, its major gut-derived metabolites and a contaminant for mouse ER transcriptional oestrogenic activity

To test the hypothesis that tartrazine is an activator of the mouse ERs, the food dye, its major gut-derived metabolites and a contaminant were examined for oestrogenic activity using the mouse-based reporter gene assay developed in Chapter 3.

4.1.1. Tartrazine, metabolites and a contaminant are not activators of the mouse ERs

4.1.1.a Tartrazine, metabolites and a contaminant are not activators of the mERα

To determine if tartrazine, its gut derived metabolites and a contaminant are activators of the mERα, LTPA cells were transiently transfected with the pcDNA3.1 expression construct coding for the mERα, the 3XERE TATA luc reporter construct and the RL-TK control construct followed by treatment with E2 or tartrazine, metabolites and the contaminant starting at a concentration of 100 pM and increasing serially by a factor of 10 to a maximum of 100 µM (E2: maximum of 10 µM) and dual-luciferase assay.

Figure 4.2 demonstrates that E2 activated the mERα in a dose-dependent manner with a significant increase in reporter gene expression detectable at concentrations as low as 100 pM. There was no evidence for trans-activation of the reporter construct following exposure to tartrazine (T) or its main gut-derived metabolites sulfanilic acid (SA), 4-sulfophenylhydrazine (SPH) and 1-(4-sulfophenyl)-3-carboxy-4-amino-5-pyrazolone (SCAP) as well as the contaminant 5-oxo-1-(4-sulfophenyl)-2-pyrazoline-3-carcoxylic acid (OSPCA) at concentrations up to 100 µM. The metabolite sulfanilic acid N-acetate (SA-NAc) induced a statistically significant small increase in reporter gene activity at 100 pM, 100 nM and 1 µM which, however, was not dose-dependent and therefore likely not biologically significant. These data suggest that tartrazine, its metabolites and a contaminant are not activators of the mERα.

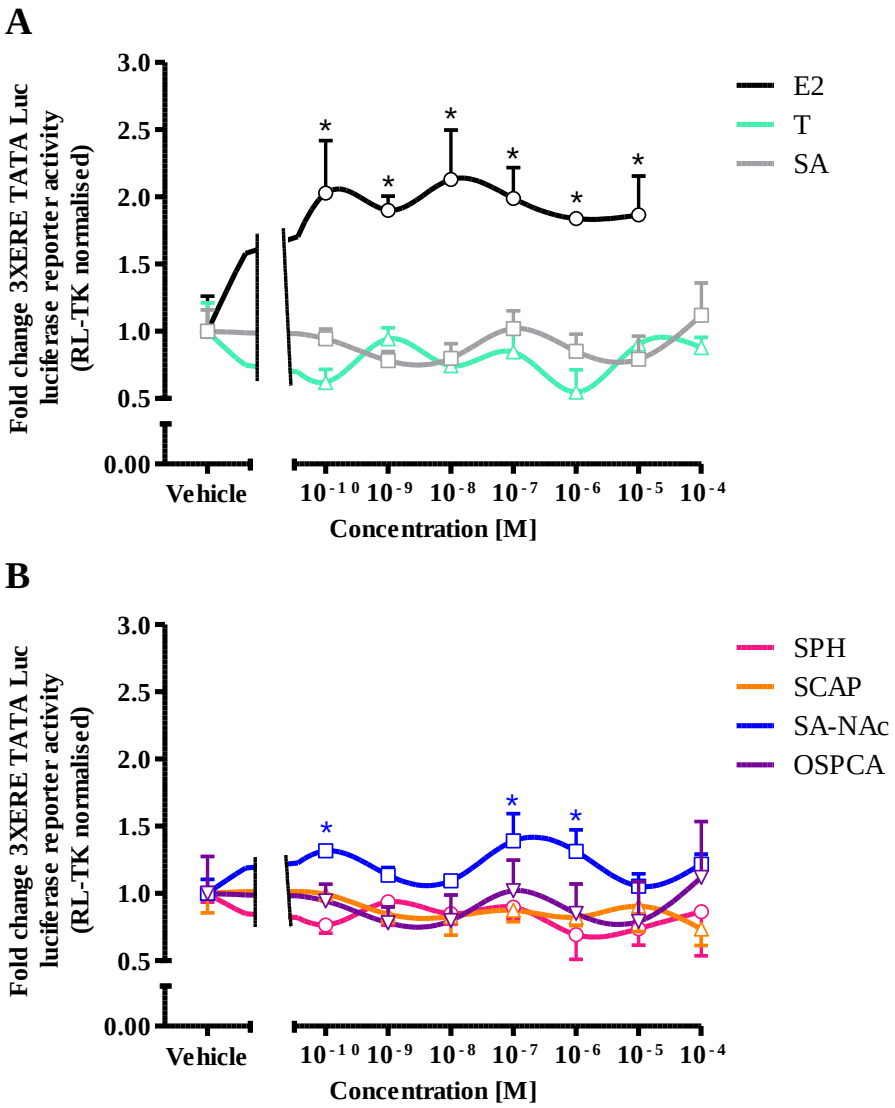

Figure 4.2 Tartrazine, its gut-derived metabolites and a contaminant are not activators of the mERα. Luciferase reporter gene assay in LTPA cells transiently transfected with the pcDNA3.1 expression constructs coding for the mERα, the 3XERE TATA luc reporter construct and the RL-TK control vector for 24 hours before treatment with increasing concentrations of (**A**) E2, tartrazine and the gut-derived tartrazine metabolites sulfanilic acid (SA), (**B**) 4-sulfophenylhydrazine (SPH), 1-(4-sulfophenyl)-3-carboxy-4-amino-5-pyrazolone (SCAP), sulfanilic acid N-acetate (SA-NAc) as well as the tartrazine contaminant 5-oxo-1-(4-sulfophenyl)-2-pyrazoline-3-carcoxylic acid (OSPCA) for 24 hours and dual-luciferase assay. Mean and SD of n=3, typical of two separate experiments. Data are expressed in fold change versus vehicle-treated cells (vehicle: 0.1% (v/v) DMSO (E2; tartrazine) or 0.1% (v/v) 1x PBS (SA; SPH; SCAP; SA-NAc; OSPCA)). *Significantly different ($p<0.05$) over cells treated with DMSO or 1x PBS vehicle using One-way ANOVA with Dunnett's post-hoc modifications.

4.1.1.b Tartrazine, metabolites and a contaminant are not activators of the mERβ

Since tartrazine and its metaboliotes did not activate the mERα, it was investigated whether these compounds are activators of the mERβ proteins. Activation of the mERβv1 was examined first. 603B cells were transiently transfected with the pcDNA3.1 expression construct coding for the mERβv1, the $(ERE)_3$-pGL3promotor reporter construct and the RL-TK control construct followed by treatment with E2, tartrazine, its metabolites and a contaminant at concentrations ranging from 100 pM to 100 µM (E2: maximum of 10 µM) and dual-luciferase assay.

Figure 4.3 shows that E2 activated recombinant mERβv1 in a dose-dependent manner at concentrations as low as 1 nM whereas treatment with tartrazine, its gut-derived metabolites SA, SPH, SCAP, SA-NAc and the contaminant OSPCA did not result in dose-dependent trans-activation of the reporter construct at concentrations up to 100 µM. These data indicate that these compounds are not activators of the mERβv1.

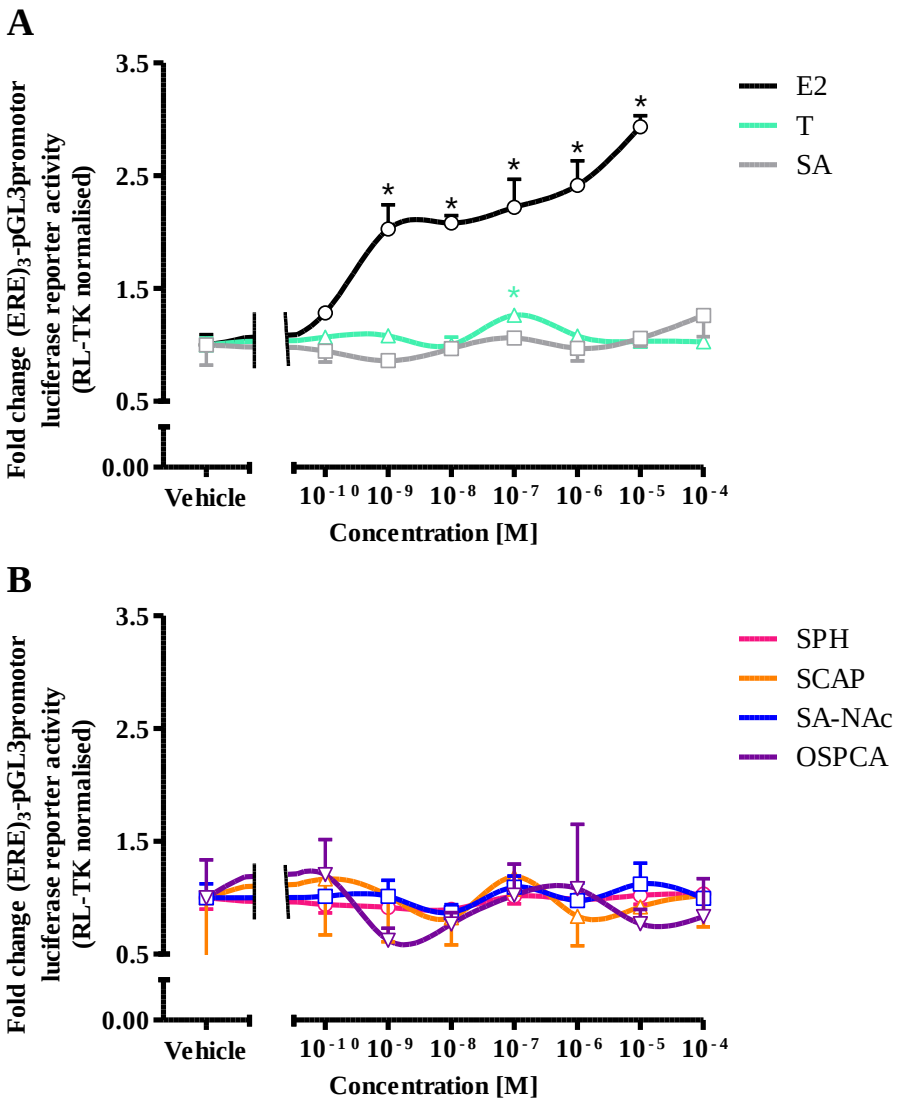

Figure 4.3 Tartrazine, its gut-derived metabolites and a contaminant are not activators of the mERβv1. Luciferase reporter gene assay in 603B cells transiently transfected with the pcDNA3.1 expression constructs coding for the mERβv1, the $(ERE)_3$-pGL3promotor reporter construct and the RL-TK control vector for 24 hours before treatment with increasing concentrations of (**A**) E2, tartrazine and the gut-derived tartrazine metabolites sulfanilic acid (SA) and (**B**), 4-sulfophenylhydrazine (SPH), 1-(4-sulfophenyl)-3-carboxy-4-amino-5-pyrazolone (SCAP), sulfanilic acid N-acetate (SA-NAc) as well as the tartrazine contaminant 5-oxo-1-(4-sulfophenyl)-2-pyrazoline-3-carcoxylic acid (OSPCA) for 24 hours and dual-luciferase assay. Mean and SD of n=3, typical of two separate experiments. Data are expressed in fold change versus vehicle-treated cells (vehicle: 0.1% (v/v) DMSO (E2; tartrazine) or 0.1% (v/v) 1x PBS (SA; SPH; SCAP; SA-NAc; OSPCA)). *Significantly different ($p<0.05$) over cells treated with DMSO or 1x PBS vehicle using One-way ANOVA with Dunnett's post-hoc modifications.

To examine if tartrazine, metabolites and the contaminant are activators of the mERβv2, 603B cells were transiently transfected with the pcDNA3.1-mERβv2 expression construct, the $(ERE)_3$-pGL3promotor reporter construct and the RL-TK control construct. Since data have shown that recombinant mERβv2 protein exhibits constitutive activity *in vitro* in this assay (Figure 3.12, Chapter 3), mERβv2-expressing 603B cells were pre-treated with 100 nM ICI182,780 followed by several wash steps to de-activate the mERβv2 and to render the protein susceptible to potential activation by subsequent exposure to E2 and tartrazine and its metabolites.

Figure 4.4 demonstrates that treatment with E2 resulted in a dose-dependent increase in reporter gene activity at concentrations as low as 100 pM. There was no evidence for trans-activation of the reporter construct following exposure to tartrazine and its main gut-derived metabolites SA, SPH, SCAP, and SA-NAc as well as the contaminant OSPCA at concentrations up to 100 µM suggesting that these compounds are not activators of the mERβv2.

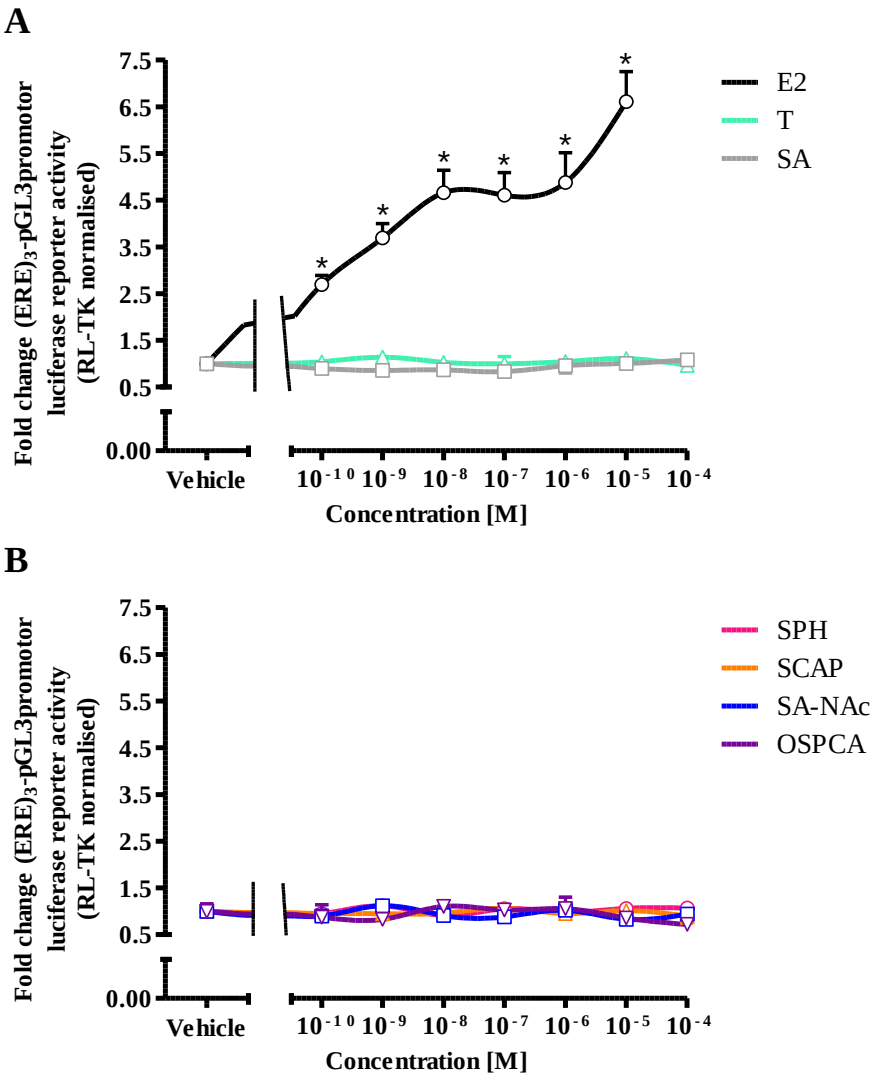

Figure 4.4 Tartrazine, its gut-derived metabolites and a contaminant are not activators of the mERβv2. Luciferase reporter gene assay in 603B cells transiently transfected with the pcDNA3.1 expression constructs coding for the mERβv2, the $(ERE)_3$-pGL3promotor reporter construct and the RL-TK control vector for 24 hours. Cells were pre-treated with 100 nM ICI182,780 for 6 hours to inactivate constitutive mERβv2 transcriptional function followed by wash-out and treatment with increasing concentrations of (**A**) E2, tartrazine and the gut-derived tartrazine metabolites sulfanilic acid (SA) and (**B**) 4-sulfophenylhydrazine (SPH), 1-(4-sulfophenyl)-3-carboxy-4-amino-5-pyrazolone (SCAP), sulfanilic acid N-acetate (SA-NAc) as well as the tartrazine contaminant 5-oxo-1-(4-sulfophenyl)-2-pyrazoline-3-carcoxylic acid (OSPCA) for 24 hours and dual-luciferase assay. Mean and SD of n=3, typical of two separate experiments. Data are expressed in fold change versus vehicle-treated cells (vehicle: 0.1% (v/v) DMSO (E2; tartrazine) or 0.1% (v/v) 1x PBS (SA; SPH; SCAP; SA-NAc; OSPCA)). *Significantly different ($p<0.05$) over cells treated with DMSO or 1x PBS vehicle using One-way ANOVA with Dunnett's post-hoc modifications.

4.1.2. Tartrazine, its metabolites and a contaminant have no antagonistic effects on mER activity

Xenoestrogens are often defined as chemicals with oestrogenic activity. ER antagonistic effects, however, can also result in disruption of natural oestrogen signalling causing adverse effects. Since tartrazine and its gut-derived metabolites did not activate the mER proteins, it was examined whether these compounds affect oestrogen signalling by exhibiting ER-antagonistic effects.

4.1.2.a Tartrazine, its metabolites and a contaminant are not antagonists of the mERα

In order to determine if tartrazine, its metabolites and a contaminant are antagonists of the mERα, LTPA cells were transiently transfected with the pcDNA3.1 expression construct coding for the mERα, the 3XERE TATA luc reporter construct and the RL-TK control construct. This was followed by pre-treatment with the vehicle control, 100 nM of the ER antagonist ICI182,780 or tartrazine and its metabolites SA, SPH, SA-NAc and SCAP as well as the contaminant OSPCA (100 nM – 100 μM, serially increasing by a factor of 10) for 6 hours. After 6 hours, cells were treated with ICI182,780, tartrazine or its metabolites at the indicated concentrations in the presence of 1 nM E2 (corresponding to the estimated half maximal effective concentration (EC_{50})) for 24 hours and *Firefly* and *Renilla* luciferase activities were determined by dual-luciferase assay.

Figure 4.5 shows that exposure to 1 nM E2 in the absence of antagonist resulted in trans-activation of the reporter construct over control vehicle treated cells which was reduced by co-treatment with 100 nM ICI182,780. Neither tartrazine, nor its metabolites or contaminant, inhibited the E2-dependent increase in reporter gene activity at concentrations up to 100 μM suggesting that these compounds are not antagonists of the mERα.

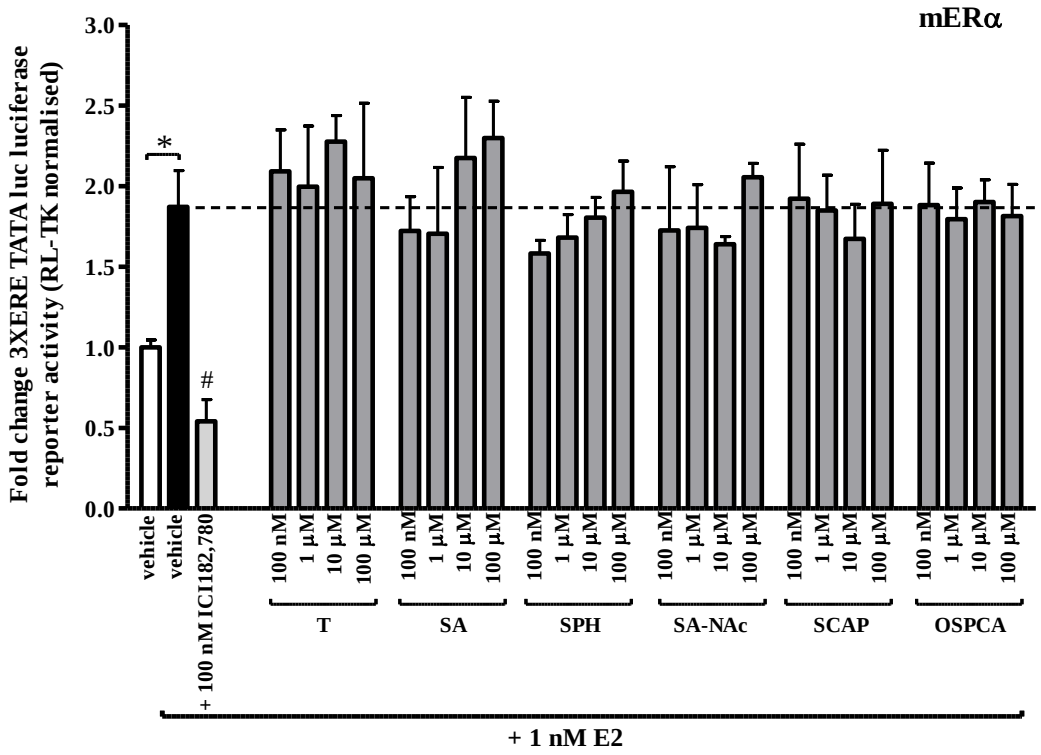

Figure 4.5 Tartrazine, its gut-derived metabolites and a contaminant are not mERα antagonists. Luciferase reporter gene assay in LTPA cells transiently transfected with the pcDNA3.1 expression constructs coding for the mERα, the 3XERE TATA luc reporter construct and the RL-TK control vector for 24 hours. Cells were pre-treated with 0.1% (v/v) control vehicle (DMSO or 1x PBS), 100 nM of the ER antagonist ICI182,780 or with tartrazine and its metabolites sulfanilic acid (SA), 4-sulfophenylhydrazine (SPH), 1-(4-sulfophenyl)-3-carboxy-4-amino-5-pyrazolone (SCAP), sulfanilic acid N-acetate (SA-NAc) as well as the tartrazine contaminant 5-oxo-1-(4-sulfophenyl)-2-pyrazoline-3-carcoxylic acid (OSPCA) (100 nM – 100 µM) as potential mERα antagonists for 6 hours. Cells were then treated with vehicle, 100 nM of ICI182,780 or with tartrazine and its metabolites (100 nM – 100 µM) in the presence of 1 nM E2 for 24 hours followed by dual-luciferase assay. Mean and SD of n=3, typical of two separate experiments. Data are expressed in fold change versus vehicle-treated cells (vehicle: 0.1% (v/v) DMSO (E2; tartrazine) or 0.1% (v/v) 1x PBS (SA; SPH; SCAP; SA-NAc; OSPCA)). *Significantly different ($p<0.05$) over cells treated with vehicle only using Student's t-test (two-tailed). #Significantly different ($p<0.05$) over cells treated with 1 nM E2 in the absence of ER antagonists using One-way ANOVA with Dunnett's post-hoc test.

4.1.2.b Tartrazine, its metabolites and a contaminant are not antagonists of the mERβv1 and mERβv2

Since tartrazine, its gut-derived metabolites and a contaminant did not exhibit mERα antagonistic effects, it was examined whether these compounds are antagonists of the mERβv1 and mERβv2 proteins. 603B cells were transfected with the pcDNA3.1 expression construct coding for the mERβv1 or mERβv2, the $(ERE)_3$-pGL3promotor reporter construct and the RL-TK control construct followed by pre-treatment with the control vehicle, 100 nM ICI182,780 or tartrazine and its metabolites SA, SPH, SA-NAc and SCAP as well as the contaminant OSPCA (100 nM – 100 µM, serially increasing by a factor of 10) for 6 hours.

Following pre-treatment, cells were treated with ICI182,780, tartrazine or its metabolites at the indicated concentrations in the presence of 1 nM E2 for 24 hours followed by dual-luciferase assay.

Figure 4.6A demonstrates that there was an E2-mediated increase in reporter gene activity in 603B cells expressing recombinant mERβv1 over control vehicle treated cells which was decreased when co-treated with 100 nM ICI182,780. Treatment with tartrazine, its gut-derived metabolites or the contaminant did not inhibit the E2-mediated increase in reporter gene expression at any tested concentration up to 100 μM suggesting that these compounds are not antagonist of the mERβv1.

In 603B cells expressing recombinant mERβv2, E2 exposure (1 nM) resulted in trans-activation of the reporter construct over control vehicle cells, a response that was inhibited by co-treatment with 100 nM ICI182,780 (Figure 4.6B). Tartrazine treatment resulted in a statistically significant decrease of E2-induced reporter gene activities at a concentration of 10 μM, however, tartrazine did not exhibit antagonistic effects on mERβv2 activity in a dose-dependent manner. There was no evidence for inhibition of E2-dependent trans-activation of reporter gene expression by the gut-derived tartrazine metabolites and the contaminant indicating that these compounds are not mERβv2 antagonists.

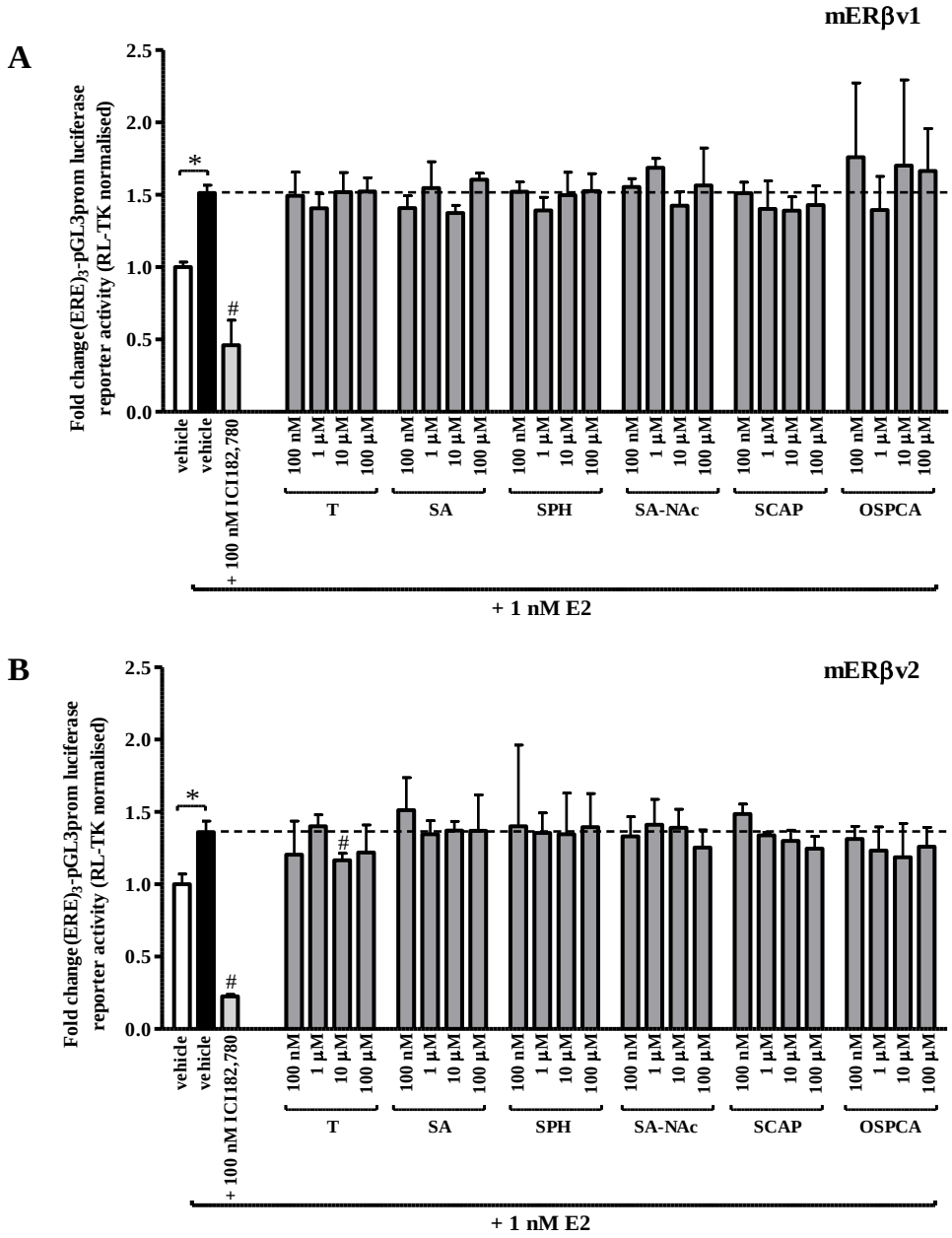

Figure 4.6 Tartrazine, its gut-derived metabolites and a contaminant are not mERβv1 and mERβv2 antagonists. Luciferase reporter gene assay in 603B cells transiently transfected with the $(ERE)_3$-pGL3promotor reporter construct and the RL-TK control vector as well as with the pcDNA3.1 expression constructs coding for (**A**) the mERβv1 or (**B**) the mERβv2. After transfection for 24 hours, cells were pre-treated with 0.1% (v/v) control vehicle (DMSO or 1x PBS), 100 nM of the ER antagonist ICI182,780 or with tartrazine and its metabolites sulfanilic acid (SA), 4-sulfophenylhydrazine (SPH), 1-(4-sulfophenyl)-3-carboxy-4-amino-5-pyrazolone (SCAP), sulfanilic acid N-acetate (SA-NAc) as well as the tartrazine contaminant 5-oxo-1-(4-sulfophenyl)-2-pyrazoline-3-carcoxylic acid (OSPCA) (100 nM – 100 µM) as potential mERα antagonists for 6 hours. Cells were then treated with vehicle, 100 nM of ICI182,780 or with tartrazine and its metabolites (100 nM – 100 µM) in the presence of 1 nM E2 for 24 hours followed by dual-luciferase assay. Mean and SD of n=3, typical of two separate experiments. Data are expressed in fold change versus vehicle-treated cells (vehicle: 0.1% (v/v) DMSO (E2; tartrazine) or 0.1% (v/v) 1x PBS (SA; SPH; SCAP; SA-NAc; OSPCA)). *Significantly different ($p<0.05$) over cells treated with vehicle only using Student's t-test (two-tailed). #Significantly different ($p<0.05$) over cells treated with 1 nM E2 in the absence of antagonists using One-way ANOVA with Dunnett's post-hoc test.

4.2. Tartrazine, its gut-derived metabolites and a contaminant of the food additive inhibit murine hepatic dopamine sulfotransferase

Previous research has shown that i.p. injection of tartrazine caused a mild cholestatic liver injury *in vivo* in mice (Axon, Thesis 2012). Since data in this chapter indicate, however, that tartrazine, its gut-derived metabolites and a contaminant are not activators of the mouse ERs, it is likely that this injury occurred independent of the ER. In order to find a possible mechanism by which tartrazine caused a cholestatic injury, and considering the chemical structure of tartrazine and its metabolites, the ability of the food dye to inhibit sulfotransferases (SULTs) was investigated.

SULTs are cytosolic enzymes which play an important role in the detoxification of various xeno- and endobiotic compounds including drugs, steroid hormones, bile salts and monoamine neurotransmitters (Weinshilboum *et al.*, 1997). The SULT-mediated transfer of a sulfo group from a donor molecule, usually 3'-phosphoadenosine 5'-phosphosulfate (PAPS) to a compound to be metabolised often makes the acceptor molecule more water soluble rendering it less biologically active and promoting its excretion (Gamage *et al.*, 2006). In terms of SULTs and cholestasis, SULT-mediated sulfation is critical for the detoxification of bile acids. If accumulation due to impaired SULT-mediated elimination occurs, bile acids may have toxic cholestatic effects in the liver (Leuschner *et al.*, 1977). In addition, SULTs mediate the inactivation process of oestrogens; sulfonated oestrogens are unable to bind to and thus activate the ERs (Song, 2001). Since oestrogens are cholestatic, impaired inactivation can lead to a build-up of 'active' oestrogen in the liver which in turn may cause cholestasis (Strott, 1996).

In order to examine if tartrazine, its gut-derived metabolites and a contaminant are inhibitors of murine hepatic SULTs, cytosolic (S9) fractions were prepared from wt C57Bl/6 mice and the ability of hepatic SULTs to transfer a radio-labelled sulfonyl group [^{35}S] from PAP[^{35}S] as sulphate donor to an acceptor substrate in the absence and presence of potential or known inhibitors was investigated. Since a number of SULT isozymes with substrate specificity exist, the experiment was performed using several different substrates as outlined in Table 4.1. These substrates have previously been reported to be subject to sulfonation by different SULT isozymes (Hernández *et al.*, 1992; Kauffman *et al.*, 1998; Dajani *et al.*, 1999; Ozawa *et al.*, 1999).

Substrate	Final concentration
2-naphthol	100 μM
p-nitrophenol (p-NP)	4 μM
Dopamine (with pargyline)	60 μM (with pargyline at 1 mM)
4-methylumbelliferone (4-MU)	10 μM
Oestrone (E1)	1 μM
Dehydroepiandrosterone (DHEA)	5 μM
Inhibitors	
Pentachlorphenol (PCP)	10 μM
Quercetin	50 μM

Table 4.1 SULT substrates and known inhibitors and their final concentration as used in the sulfotransferase [^{35}S]-PAPS radiometric activity assay.

Figure 4.7 demonstrates that the SULT inhibitors PCP and quercetin significantly inhibited SULT-mediated sulfonation of all substrates compared to the DMSO vehicle control. There was no evidence, however, for inhibition of substrate sulfonation by tartrazine, its four gut-derived metabolites SA, SA-Nac, SPH, SCAP and the contaminant OSPCA at 100 μM.

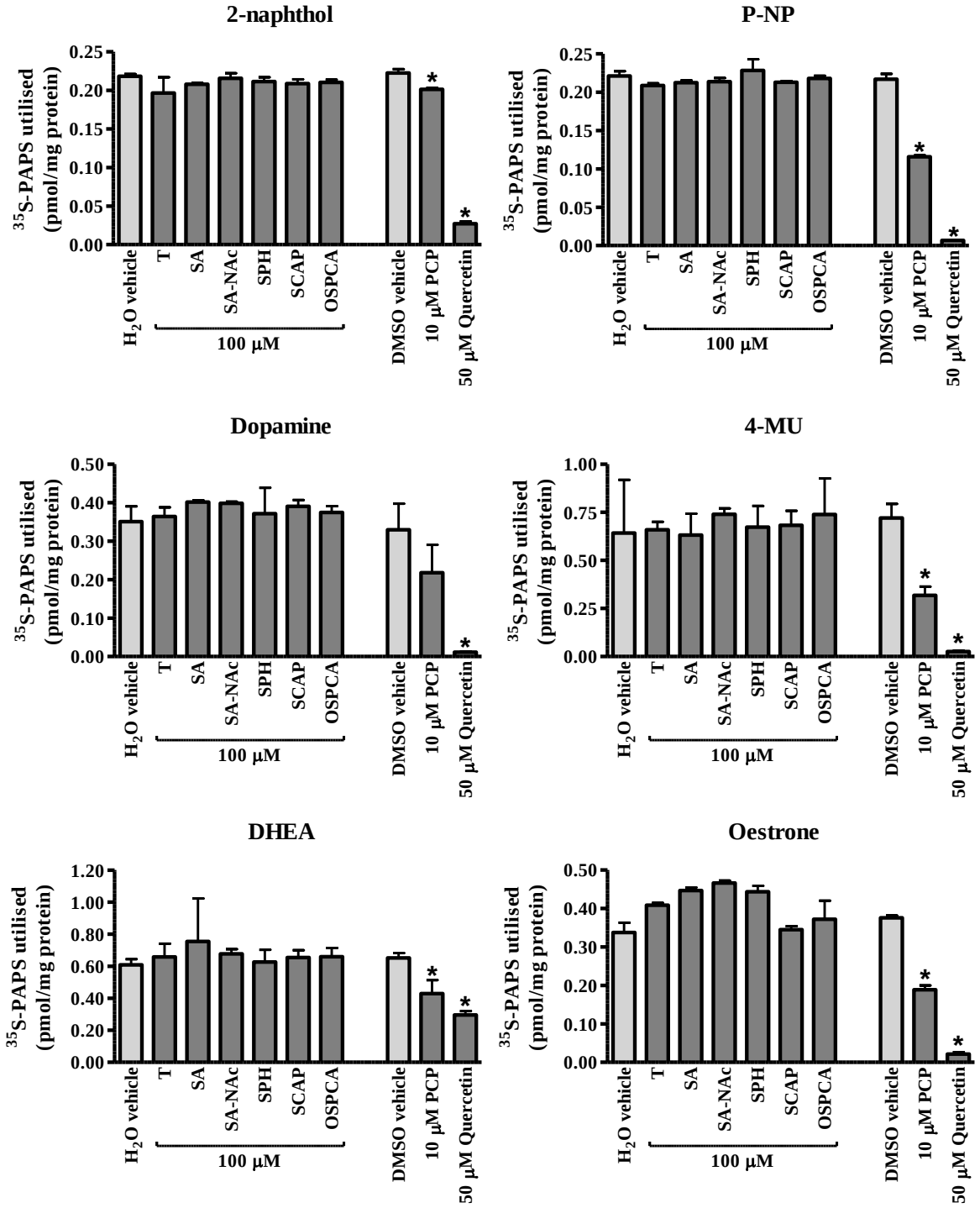

Figure 4.7 Tartrazine, its gut-derived metabolites and a contaminant are not inhibitors of murine hepatic sulfotransferases at 100 µM. Sulfotransferase [^{35}S]-PAPS radiometric activity assay in murine hepatic S9 fractions prepared from livers of wt C57Bl/6 mice. Utilisation of [^{35}S]- PAPS was determined in S9 fractions incubated with the indicated substrates alone (vehicle) or in combination with inhibitors PCP, quercertin or tartrazine, its gut derived metabolites (SA, SA-NAc, SPH, SCAP) and the contaminant OSPCA. Results were normalised to protein concentration. Data are mean and SD of n=3, typical of one experiment. *Significantly different ($p<0.05$) versus vehicle control using One-way ANOVA with Dunnett's post-hoc modifications.

Tartrazine has previously been reported to be an inhibitor of human hepatic sulfotransferases in human S9 fractions using a variety of substrates with the most potent inhibition (94 +/- 3% inhibition at 6.7μM tartrazine) observed with dopamine as substrate (Bamforth et al., 1993). Although data in this chapter has shown that tartrazine, its metabolites and a contaminant are not inhibitors of SULT-dependent dopamine sulfation at 100 μM, there is the potential that murine SULTs are less sensitive to inhibition and that higher concentrations are required for tartrazine and metabolites to see an inhibitory effect. Correspondingly, the effect of tartrazine, its metabolites and a major contaminant of the food additive on mouse hepatic S9 dopamine sulfation at higher concentrations was investigated.

Figure 4.8 shows that tartrazine, all four metabolites and the contaminant OSPCA inhibited SULT-mediated dopamine sulfation in a dose-dependent manner in hepatic S9 extracts. SCAP and OSPCA appeared to be the most potent inhibitors of murine dopamine sulfotransferases with statistically significant inhibition observed at 500 μM (Figure 4.8).

These data indicate that tartrazine, its metabolites and the contaminant inhibit murine hepatic sulfotransferases. SULT inhibition and impaired inactivation of bile acids and oestrogens may, therefore, play a role in the mechanism by which direct tartrazine exposure caused mild cholestatic liver injury.

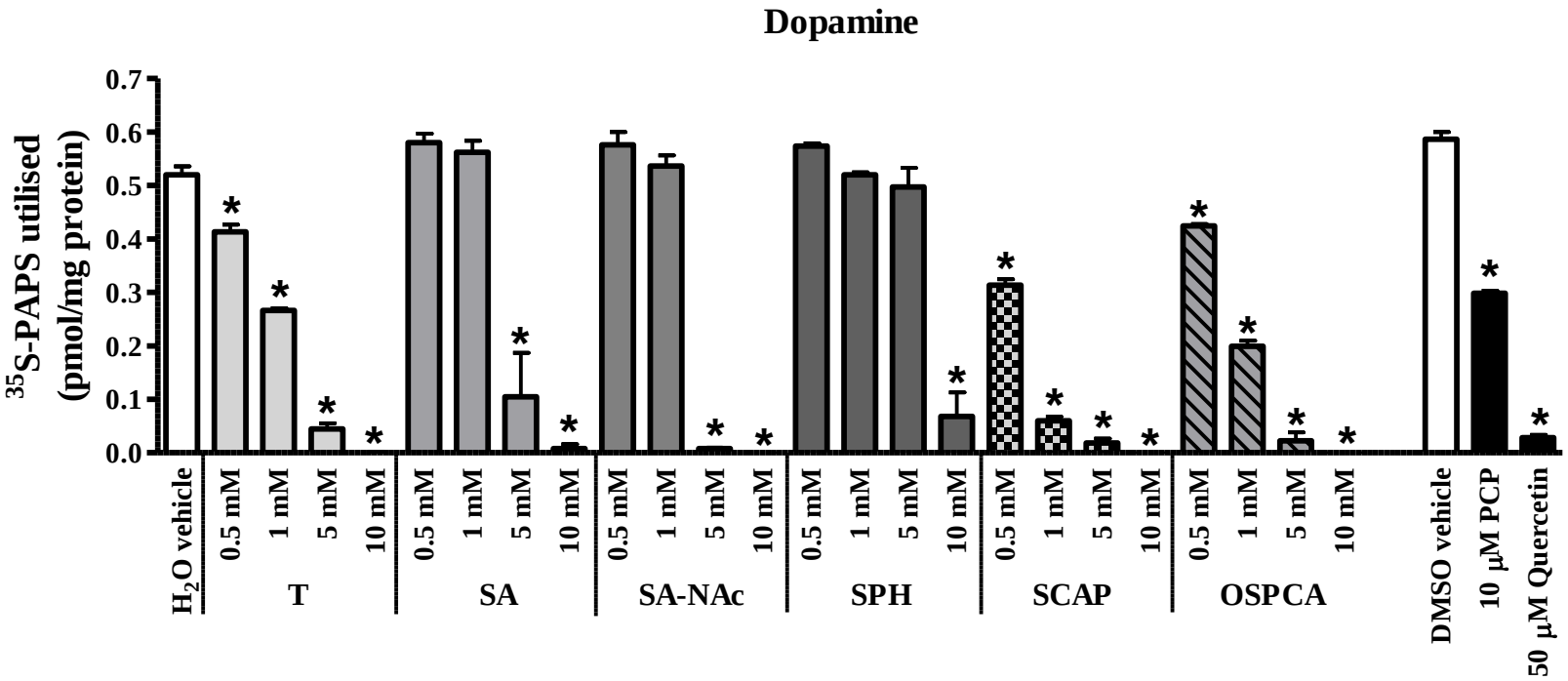

Figure 4.8 Tartrazine, its four gut-derived metabolites and the contaminant OSPCA inhibit dopamine sulfotranferase in a dose-dependent manner. Sulfotransferase [^{35}S]-PAPS radiometric activity assay in murine hepatic S9 fractions prepared from livers of wt C57Bl/6 mice. Utilisation of [^{35}S]-PAPS was determined in S9 fractions incubated with the indicated substrates alone (vehicle) or in combination with inhibitors PCP, quercertin or tartrazine, its gut derived metabolites (SA, SA-NAc, SPH, SCAP) and the contaminant OSPCA at concentrations as indicated. Results were normalised to protein concentration. Data are mean and SD of n=3, typical of one experiment. *Significantly different ($p<0.05$) versus vehicle control using One-way ANOVA with Dunnett's post-hoc modifications.

4.3. *In vivo*: Effects of orally administered tartrazine

Although i.p. injection (avoiding the need for uptake by the gut) of tartrazine caused a cholestatic injury in mice, the primary exposure of the food additive in humans is via oral administration of tartrazine-containing food items. To test its food additive relevance, it was investigated whether tartrazine causes a cholestatic liver injury *in vivo* following oral exposure. Tartrazine was therefore administered to mice by oral gavage. Due to its water solubility, absorption of unchanged tartrazine by the gut is generally low (<5%) (EFSA, 2009). Alcohol consumption, however, has been shown to cause liver injury by making the gut permeable to gram-negative bacteria residing within the gut and bacterial components such as endotoxin. We therefore hypothesised that chronic alcohol consumption could also increase the gut leakiness of orally administered compounds such as tartrazine. The combined administration of tartrazine and ethanol is also relevant since many alcoholic drinks contain tartrazine and the EFSA has listed maximum reported use levels of tartrazine in alcoholic beverages of up to 200 mg/L (EFSA, 2009).

To determine if tartrazine has adverse hepatic effects on the background of alcohol-induced hepatic injury, transgenic (tg) NF-κB-luc mice were employed. NF-κB-luc mice express luciferase under the control of three copies of an NF-κB response element allowing for NF-κB activity and thus inflammatory processes to be detected and monitored by live *in vivo* imaging (Carlsen *et al.*, 2002). Following administration of luciferin to animals, luciferase, which is expressed in cells with active NF-κB signalling, metabolises luciferin to produce light and NF-κB activity can be detected and localised within the animal using the *In Vivo* Imaging System (IVIS). NF-κB is activated in response to a variety of stimuli, including tissue injury, and as a key regulator of the immune response, plays a crucial role in tissue regeneration, inflammation and disease progression (Luedde and Schwabe, 2011). NF-κB is essentially active in all chronic liver diseases including in alcohol-induced and cholestatic liver conditions (Mandrekar and Szabo, 2009; Kosters and Karpen, 2010) and stimulates the release of pro-inflammatory (e.g. TNFα) and fibrogenic (e.g. TGFβ) cytokines which, amongst others, are produced by hepatic Kupffer cells and myofibroblasts respectively (Dooley and ten Dijke, 2012; Sunami *et al.*, 2012; Schon and Weiskirchen, 2014). NF-κB-luc mice therefore represent a valuable tool for monitoring NF-κB activity and thus inflammation and injury in the liver in response to different treatments.

4.3.1. Two weeks of alcohol pre-treatment is needed to see an increase in gut permeability

To determine how long it may take for alcohol to show an increase in gut permeability by using the detection of liver inflammation as readout, a pilot study was conducted. Mice (wt or tg NF-kB-luc mice) were assigned to four groups (1 mouse per group) and dosed as outlined in Table 4.2 for 14 days, twice daily by oral gavage (except for the hepatotoxic compound alpha-naphthyl isothiocyanate (ANIT) (Desmet *et al.*, 1968), used as a positive control for liver injury, which was dosed once at the beginning of the study). To account for the energy content of ethanol, the mouse in the control group was dosed with dextrose from an aqueous solution. Liver and abdominal inflammation was assessed at the beginning of the study and then at 3, 6, 10 and 14 days by live *in vivo* imaging and calculated using the IVIS software for integrated photon emission.

Group	Animal numbers	Treatment
Wt	1♂ C57Bl/6 wt	Dosed with 6.32 g/kg dextrose twice daily for 14 days
Dextrose	1♂ tg NF-kB-luc, calorific control	Dosed with 6.32 g/kg dextrose twice daily for 14 days
Ethanol	1♂ tg NF-kB-luc	Dosed with 3 g/kg ethanol twice daily for 14 days
ANIT	1♂ tg NF-kB-luc, positive control for liver inflammation	Dosed with 50 mg/kg ANIT once at beginning of study

Table 4.2 Gut permeability pilot study groups and dosing regimen. Ethanol was dosed at 3 g ethanol/kg body weight from a 20% ethanol solution. Dextrose was dosed at 6.32 g/kg body weight to control for the calorific content of ethanol. ANIT was dissolved in olive oil (12.5 mg/ml) and dosed at 50 mg/kg body weight. All treatments were administered by oral gavage.

Exposure to the hepatotoxin ANIT caused an increase in luminescence in the upper abdominal region (location of the liver) after 3 days with a peak signal observed on day 6 (Figure 4.9). The signal remained elevated until the end of the study (day 14) (Figure 4.9F). Although on a lower level, ethanol treatment resulted in an increase in luminescence in the upper abdominal region after 14 days compared to dextrose treatment (Figure 4.9F). An increase in luminescence following treatment with ethanol was also observed in the lower abdominal region of the mouse (corresponding to the gastrointestinal (GI) tract) (Figure 4.9G). The wild type control mouse did not show any detectable NF-κB-driven luminescent signal.

Assuming that the luminescence signal in the upper abdominal region caused by the liver toxin ANIT is localised to the liver, it may be concluded that live *in vivo* imaging in tg NF-κB-luc mice can be used to detect hepatic injury. Since an increase in luminescence was observed in the upper abdominal region following administration of ethanol for 14 days, data of this study suggest that 2 weeks of ethanol treatment induces a hepatic injury, likely due to an increase in gut permeability. These results suggest that two weeks of pre-treatment with ethanol is necessary to increase gut permeability.

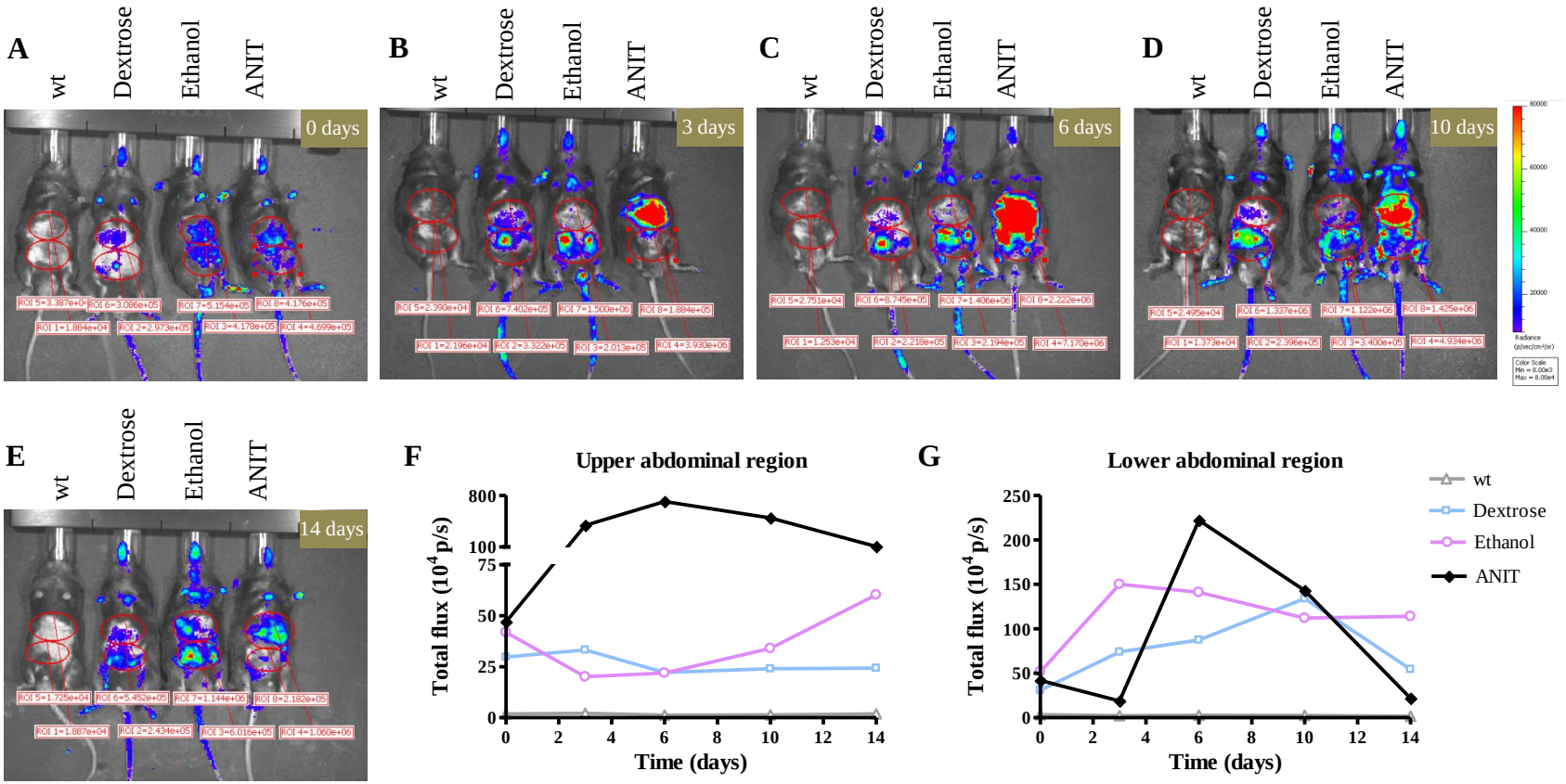

Figure 4.9 Two weeks of treatment with ethanol causes an increase in NF-κB activity in the upper abdominal (hepatic) and lower abdominal (gastrointestinal) region. Male adult C57Bl/6 wt or tg NF-κB-luc mice were dosed with dextrose or ethanol twice daily by oral gavage for 14 days or ANIT which was dosed once at beginning of study (n=1 per group). **(A-E)** IVIS images of treated mice at 0, 3, 6, 10 and 12 days, respectively. Mice were treated as indicated and imaged at different time points. For imaging, mice were anesthetised using isoflurane and injected with 200 µl of D-luciferin (15 mg/ml) intraperitoneally. Mice were imaged 10 minutes after injection with D-luciferin. **(F-G)** Quantified upper (hepatic) and lower (gastrointestinal) abdominal luminescence of treated mice.

4.3.2. Oral tartrazine exposure causes a mild inflammatory response in the liver and gastrointestinal tract which is reduced by combined alcohol exposure

To determine the toxicological relevance of the hepatic effects observed with tartrazine exposure after i.p. injection (Axon, Thesis 2012) mice were orally exposed to tartrazine at 50 mg/kg bw/day (6.6 fold of the current ADI) for 10 weeks. Female adult NF-κB-luc mice and male adult wt mice were dosed as outlined in Table 4.3. Mice were pre-treated with ethanol twice daily by oral gavage for 14 days to increase gut permeability. Control mice were pre-dosed with dextrose solution to control for the calorific content of ethanol. After pre-treatment, mice were administered tartrazine in either ethanol or dextrose solution by oral gavage twice daily for 10 consecutive weeks. Control mice received ethanol or dextrose solution alone. NF-κB-luc mice were imaged for inflammation at different time points by IVIS.

Group	Animal numbers	Treatment
Dextrose	3♀ tg NF-kB-luc 3♂ C57Bl/6 wt	Pre-treated with 6.32 g/kg bw dextrose from a 0.33 g/ml dextrose solution then dosed with dextrose solution
Tartrazine	4♀ tg NF-kB-luc 6♂ C57Bl/6 wt	Pre-treated with 6.32 g/kg bw dextrose from a 0.33 g/ml dextrose solution then dosed with 50 mg/kg bw tartrazine in dextrose solution
Ethanol	4♀ tg NF-kB-luc 6♂ C57Bl/6 wt	Pre-treated with 3 g/kg bw ethanol from a 20% ethanol solution then dosed with ethanol solution
Ethanol+Tartrazine	4♀ tg NF-kB-luc 6♂ C57Bl/6 wt	Pre-treated with 3 g/kg bw ethanol from a 20% ethanol solution then dosed with 50 mg/kg bw tartrazine in ethanol solution

All groups were pre-treated for 2 weeks and then dosed as described for 10 consecutive weeks. All dosing was carried out by oral gavage, twice daily.

Table 4.3 Oral tartrazine study treatment groups and dosing regimen. Wt, wild type; tg, transgenic; bw, body weight.

Body weights of both female tg NF-κB-luc and male wt mice were assessed weekly in order to determine if ethanol and dextrose, both having a high calorific content, have an effect on weight gain and for the purpose of monitoring the animals' health. Figure 4.10 shows that exposure to dextrose and ethanol with and without addition of tartrazine did not affect body weights in both female NF-κB-luc and male wt mice over the course of the study.

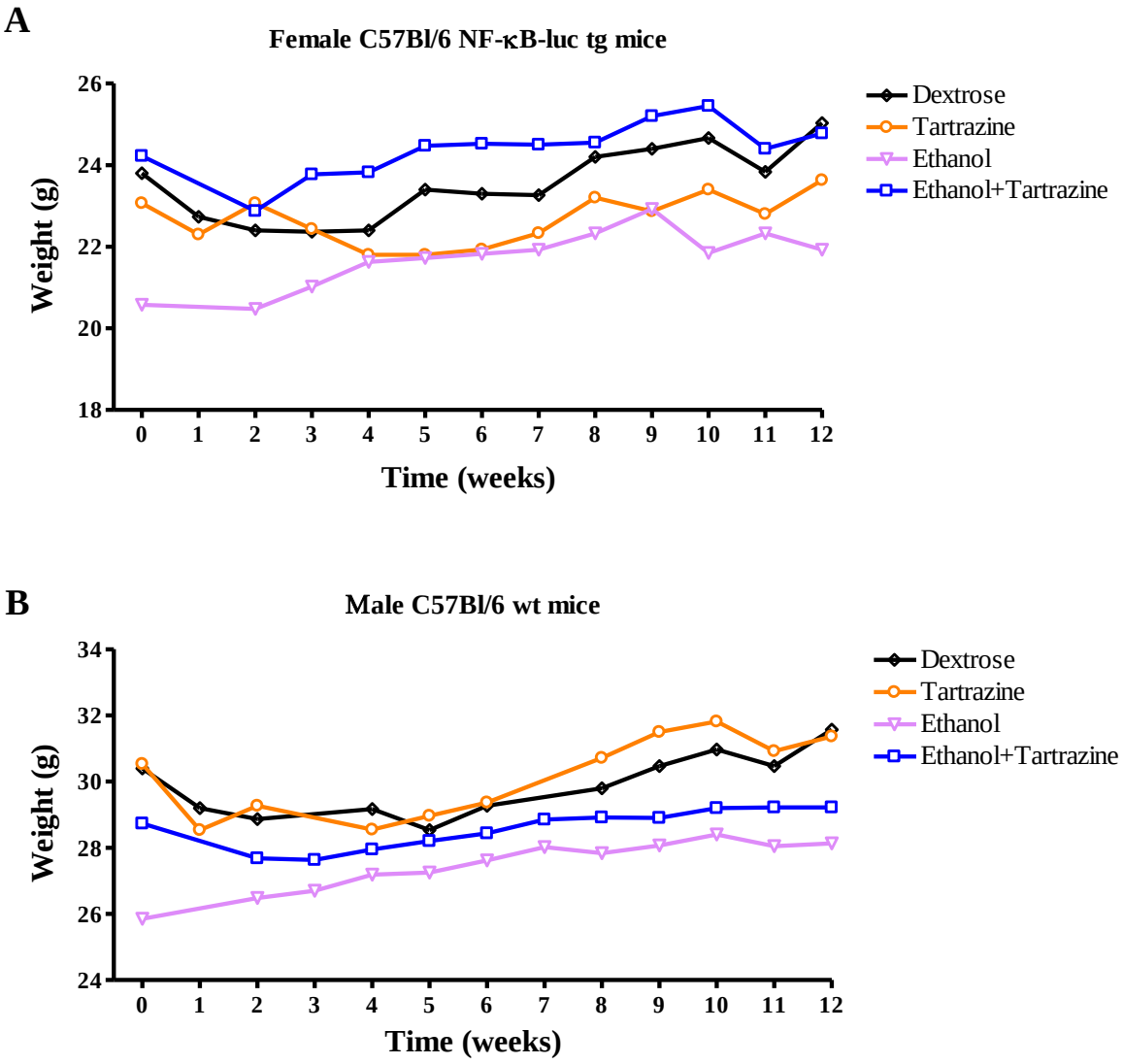

Figure 4.10 Dextrose and ethanol treatments in the absence and presence of tartrazine do not affect mouse body weights over the course of the study. Body weights of (**A**) female adult tg NF-κB-luc and (**B**) male adult C57Bl/6 wt mice following dosing with either ethanol or dextrose twice daily by oral gavage for 2 weeks (pre-treatment) and then additionally with or without tartrazine for a further 10 weeks. Mice in the control groups were dosed with ethanol or dextrose solution alone. Body weights of all animals were measured weekly. Data are the mean of the following animal numbers: Tg: dextrose, n=3; tartrazine, n=3, ethanol, n=4, ethanol+tartrazine, n=4. Wt: dextrose, n=3; tartrazine, n=6, ethanol, n=6, ethanol+tartrazine, n=6.

Treated female tg NF-κB-luc mice were imaged for inflammation *in vivo* at different time points by IVIS. IVIS imaging reveals that there was a statistically significant increase in NF-κB driven luciferase expression in the lower abdominal region (location of the gastrointestinal tract) after 10 and 12 weeks in mice exposed to tartrazine in the absence of ethanol when compared to control mice treated with dextrose solution alone (Figure 4.11C). A significant increase in luminescence in mice treated with tartrazine was also observed in the upper abdominal (hepatic) region by 12 weeks (Figure 4.11B). Exposure to ethanol did not have any apparent inflammatory effects and combined ethanol+tartrazine treatment inhibited the

increase in NF-κB driven luciferase expression associated with tartrazine only treatment in both the gastrointestinal and hepatic regions (Figure 4.11B, C).

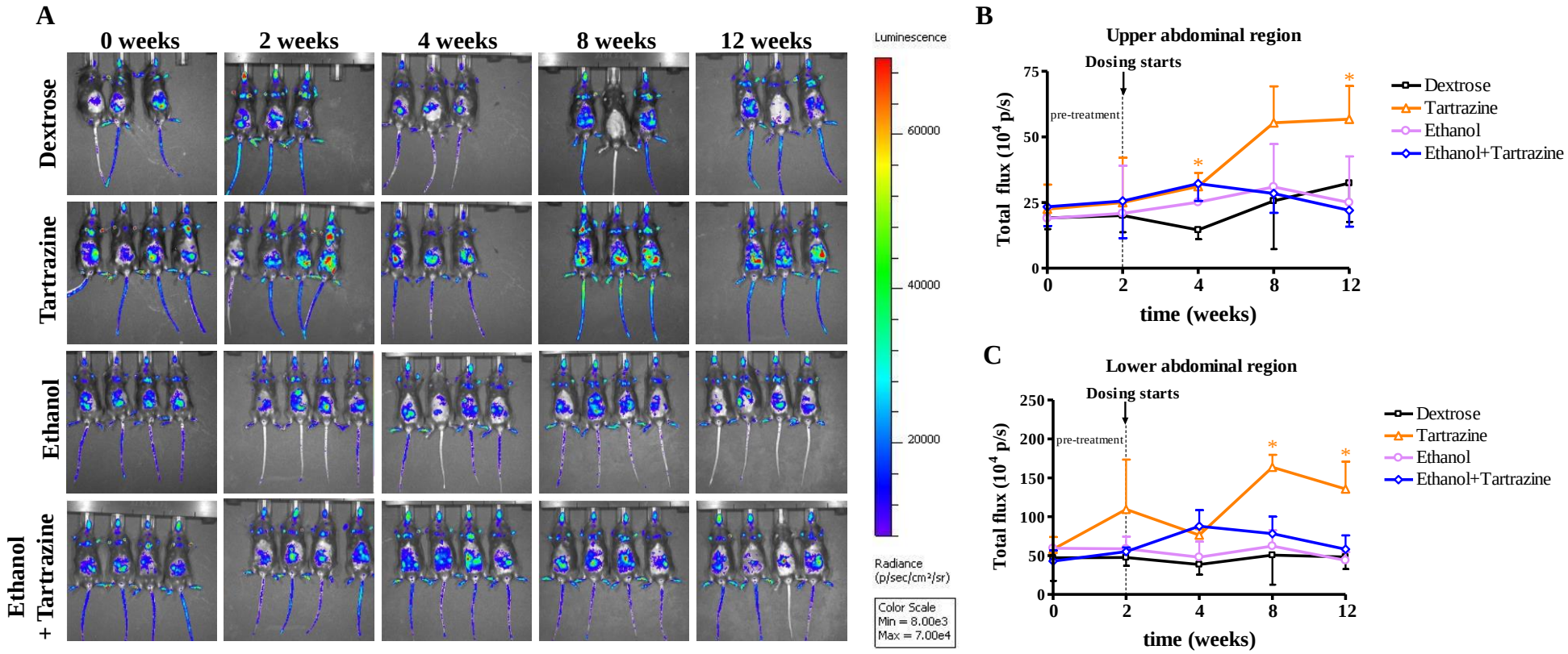

Figure 4.11 Orally administered tartrazine causes gastrointestinal and hepatic inflammation. Female adult NF-κB-luc mice were initially dosed with either ethanol or dextrose twice daily by oral gavage for 2 weeks (pre-treatment) and then additionally with or without tartrazine for a further 10 weeks. Mice in the control groups were dosed with ethanol or dextrose solution alone. **(A)** IVIS images of treated mice as indicated at different time points. For imaging, mice were anesthetised using isoflurane and injected with 200 µl of D-luciferin (15 mg/ml) intraperitoneally. Mice were imaged 10 minutes after injection with D-luciferin. **(B, C)** Quantified upper (hepatic) and lower (gastrointestinal) abdominal luminescence of treated mice at the indicated times. Data are the mean and standard deviation of the following animal numbers: dextrose, n=3; tartrazine, n=3, ethanol, n=4, ethanol+tartrazine, n=4.*Significantly different ($p<0.05$) from dextrose control vehicle treated mice at the same time point using one-way ANOVA with Bonferroni post-hoc modifications.

To confirm the source of the luminescent signal seen in the upper and lower abdominal regions in live animal imaging, individual organs (liver, kidney, spleen and GI tract) were examined *ex-vivo* by IVIS at the end of the study (Figure 4.12A). Integrated photon emission analysis of light emission profiles of the organs show a statistically significant increase in hepatic luminescence in mice treated with tartrazine compared to control mice treated with dextrose (Figure 4.12B). This increase, however, was inhibited by the combined treatment of ethanol and tartrazine. An inflammatory response was also observed in the GI tract of mice treated with tartrazine, ethanol and tartrazine+ethanol although these were not significantly different compared to dextrose treated control mice (Figure 4.12B).

A

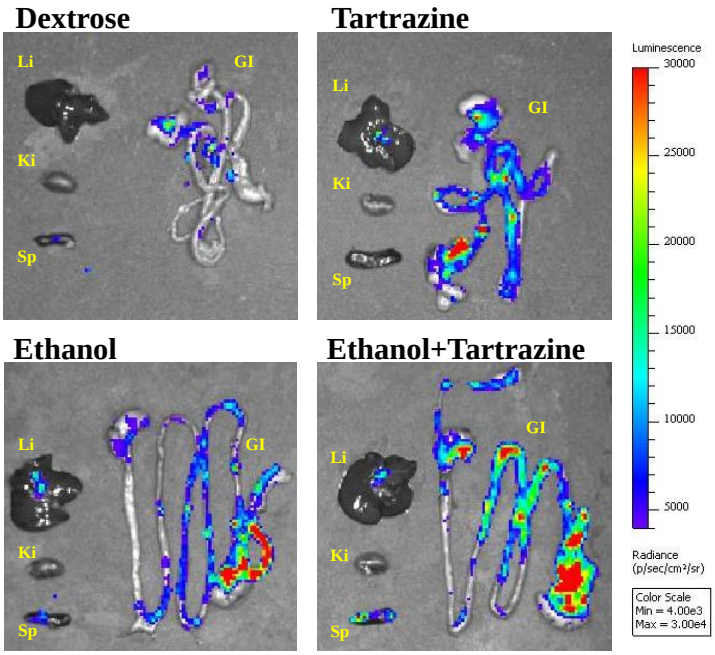

B

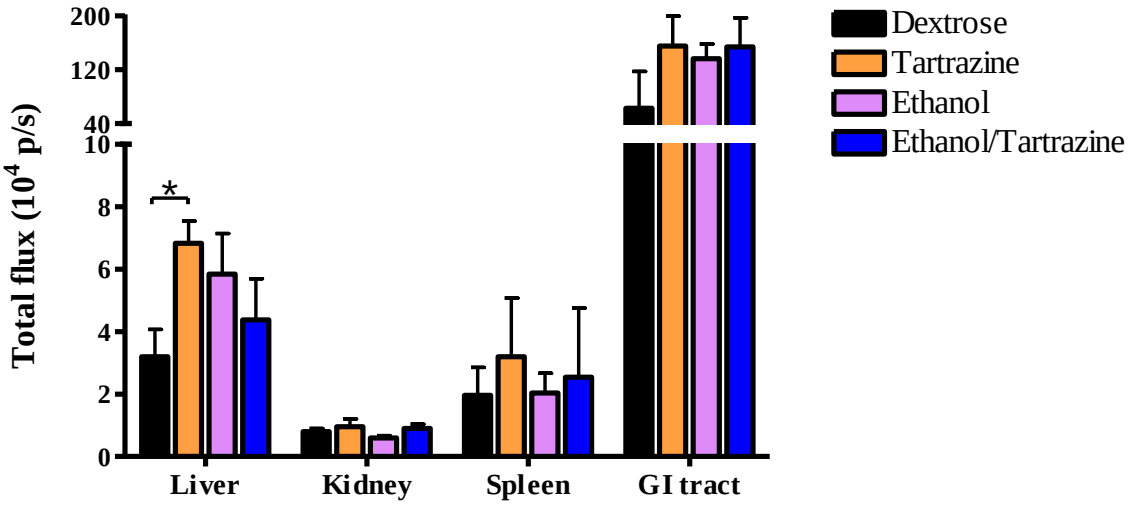

Figure 4.12 IVIS analysis of individual organs *ex-vivo*. (A) Representative *ex-vivo* IVIS images of adult female NF-κB-luc mouse organs at 12 weeks after study begin (termination of the study). For *ex-vivo* imaging of organs, mice were injected with 200 µl of D-luciferin (15 mg/ml) intraperitoneally. 10 minutes after injection with D-luciferin, mice were terminated by Schedule I method and organs dissected and imaged. **(B)** Quantified luminescence of the organs. Data are the mean and standard deviation of the following animal numbers: dextrose, n=3; tartrazine, n=3, ethanol, n=4, ethanol+tartrazine, n=4) *significantly different ($p<0.05$) from dextrose control vehicle treated mice using One-way ANOVA with Bonferroni post-hoc modifications.

A common method to assess if the liver is affected by a certain treatment is by determining the liver to body weight ratio (Bailey *et al.*, 2004). Accordingly, after 12 weeks at termination

of the study, livers from treated male adult C57Bl/6 wild type mice were dissected and weighed and the ratio of liver weight/body weight was calculated. Figure 4.13 shows that exposure to ethanol both in the absence and presence of tartrazine caused a statistically increase in liver/body weight ratio compared to dextrose treated control mice suggesting that ethanol treatment caused an enlargement of the liver. No difference between ethanol and ethanol+tartrazine treatment was observed. These data indicate that exposure to ethanol has an effect on the liver.

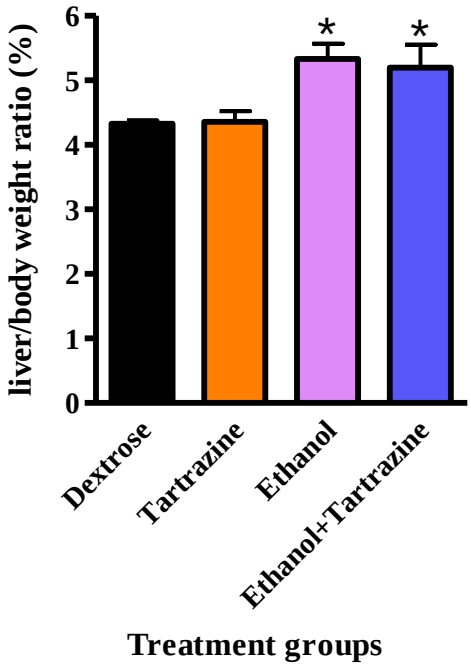

Figure 4.13 Exposure to ethanol increases the liver/body weight ratio. After 12 weeks at termination of the study, livers from treated male adult C57Bl/6 wild type mice were dissected and weighed and the liver/body weight ratio determined. Data are the mean and standard deviation of the following animal numbers: dextrose, n=3; tartrazine, n=6, ethanol, n=6, ethanol+tartrazine, n=6. *significantly different ($p<0.05$) from dextrose control vehicle treated mice using One-way ANOVA with Bonferroni post-hoc modifications.

To examine if histological changes occurred in the liver following treatment, livers from treated C57Bl/6 wild type mice were harvested at the end of the study which were then fixed, processed and sections were stained with haematoxylin and eosin (H&E). Sera of treated mice were collected at termination of the study to analyse the activity of ALP and ALT enzymes which are biomarkers for cholangiocyte and hepatocyte injury, respectively.

Since cholestatic liver disorders such as PBC are commonly asscociated with inflammatory infiltration in the periportal regions of the liver lobule (Jones, 2007), and E2 exposure has been shown to result in portal tract inflammation in mice (Axon *et al.*, 2010), portal tracts in H&E stained liver sections of treated mice were examined. Histological examination

demonstrated that no apparent histological differences in the portal tract regions could be observed between the treatment and control groups (Figure 4.14).

Analysis for ALP activities confirms that there was no evidence for cholestasis in any of the treatment groups (Figure 4.15A). Although not statistically significant, a three-fold increase in ALT activities in animals exposed to ethanol was observed over dextrose-treated control animals which was the only evidence of mild hepatocellular injury (Figure 4.15B).

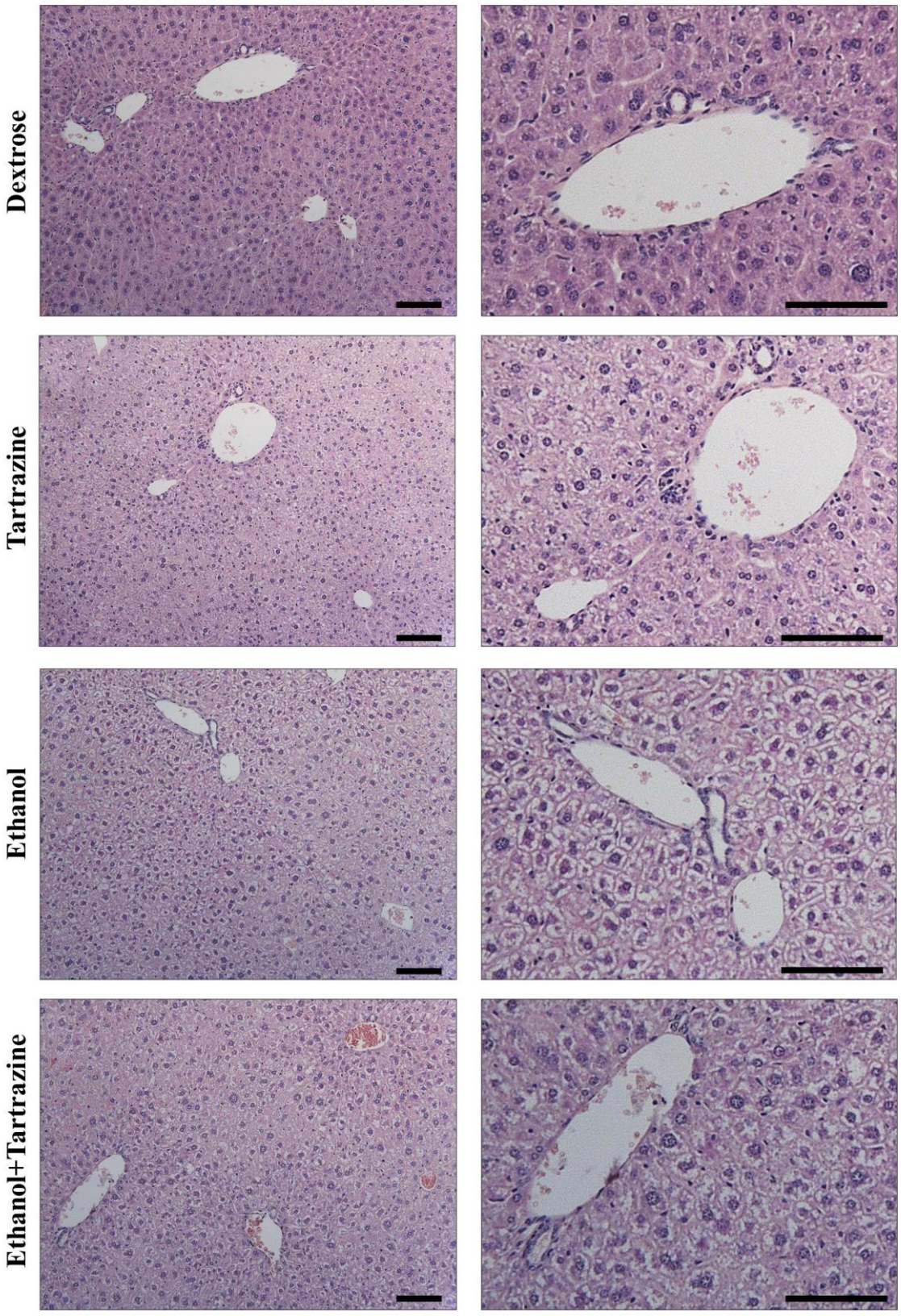

Figure 4.14 Oral tartrazine exposure does not cause any apparent hepatic histological changes. Representative H&E stained liver sections of the following animal numbers: dextrose, n=3; tartrazine, n=6, ethanol, n=6, ethanol+tartrazine, n=6. Scale bar: 100 μm. Male adult C57Bl/6 wt mice were initially dosed with either ethanol or dextrose twice daily by oral gavage for 2 weeks (pre-treatment) and then additionally with or without tartrazine for a further 10 weeks. Mice in the control groups were dosed with ethanol or dextrose solution alone.

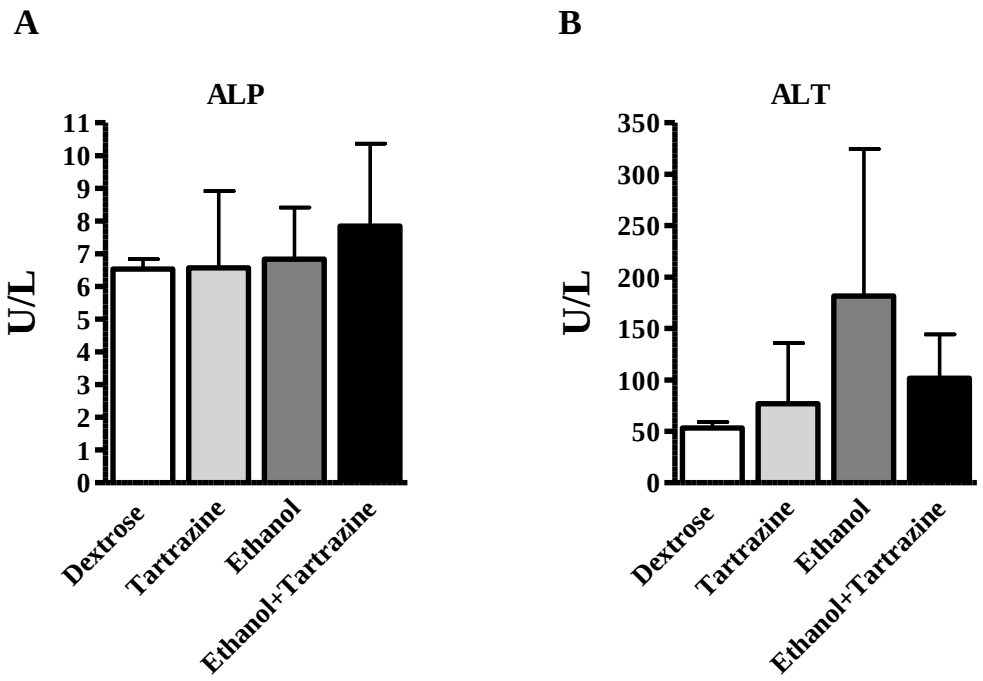

Figure 4.15 Oral tartrazine exposure does not induce clinical markers for cholestasis. (A) Serum ALP measurements at termination of the study. **(B)** Serum ALT measurements at termination of the study. Male adult C57Bl/6 wt mice were initially dosed with either ethanol or dextrose twice daily by oral gavage for 2 weeks (pre-treatment) and then additionally with or without tartrazine for a further 10 weeks. Mice in the control groups were dosed with ethanol or dextrose solution alone. Serum enzyme data are the mean and standard deviation of the following animal numbers: dextrose, n=3; tartrazine, n=6, ethanol, n=6, ethanol+tartrazine, n=6. For statistical analysis, One-way ANOVA with Bonferroni post-hoc modifications was performed.

Chronic alcohol consumption commonly leads to the development of hepatic steatosis which is often one of the first pathological changes observed in alcohol-mediated liver disease (Ji and Kaplowitz, 2003; Kang *et al.*, 2009). Since no apparent histological changes in H&E stained liver sections were observed in ethanol exposed mice compared to control mice, it was investigated whether oral ethanol treatment caused hepatic steatosis in this study. Frozen liver sections were prepared from snap-frozen liver tissue which was harvested from wt mice at termination of the study at 12 weeks. Frozen liver sections were stained with the fat-soluble dye Oil Red O which stains and visualises triglycerides and lipids in fatty tissues. Archived frozen steatotic liver tissue from an obese mouse model (gifted by Dr Fiona Oakley, Newcastle University) was similarly stained and used as positive control.

Figure 4.16 demonstrates that staining of steatotic liver tissue with Oil Red O results in the visualisation of lipids which appear bright red. No such staining was observed in livers from animals treated with dextrose and ethanol (both with and without tartrazine) indicating that oral exposure to ethanol did not result in hepatic steatosis in this study.

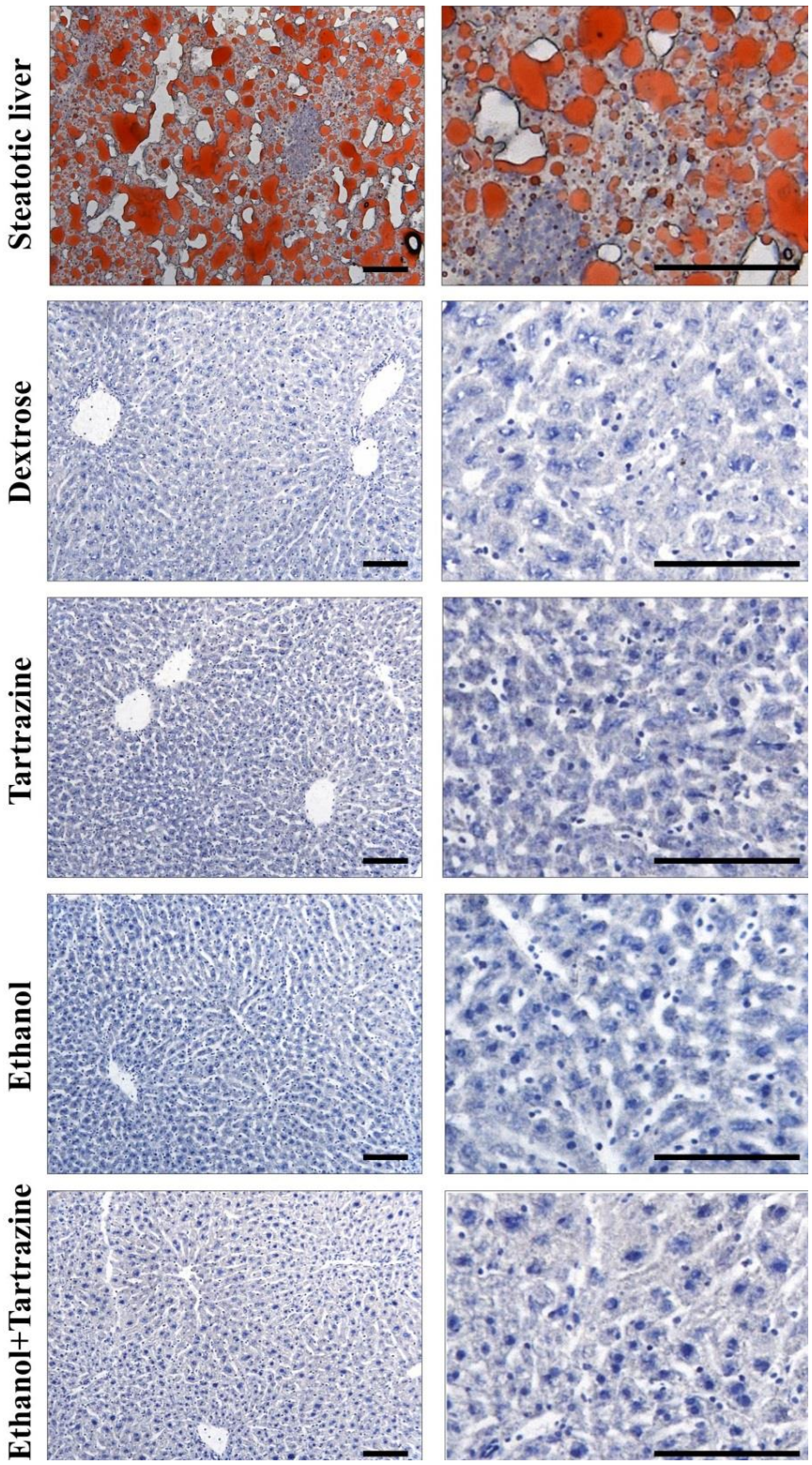

Figure 4.16 Chronic ethanol exposure does not lead to hepatic steatosis. Representative Oil Red O stained frozen liver sections of treated mice (dextrose, n=3; tartrazine, n=6, ethanol, n=6, ethanol+tartrazine, n=6). Male adult C57Bl/6 wild type mice were initially dosed with either ethanol or dextrose twice daily by oral gavage for 2 weeks (pre-treatment) and then additionally with or without tartrazine for a further 10 weeks. Mice in the control groups were dosed with ethanol or dextrose solution alone. After 12 weeks at termination of the study, liver tissue was harvested and snap-frozen in liquid N_2. Frozen tissue was sectioned (10 μm) and stained with Oil Red O and counterstained with haematoxylin. Frozen liver tissue from an obese mouse model (steatotic liver) was used as positive control. Images are representative of treatment groups. Scale bar: 100 μm.

Results from this study thus suggest that oral tartrazine exposure over the course of 10 weeks caused a mild inflammatory response in the liver and gastrointestinal tract. Such response, however, was not associated with any apparent signs of liver injury. The combined treatment of tartrazine and ethanol inhibited the increase in inflammation as seen with tartrazine treatment alone. Oral exposure to ethanol did not result in apparent hepatic injury.

4.4. Discussion

Tartrazine is a sulfonated azo dye and is often used as a colouring in a variety of food items. The food additive is known to cause intolerance reactions in susceptible individuals, even at dose-levels within the ADI (EFSA, 2009).

It has previously been reported that tartrazine is an activator of the human ERα *in vitro* (Datta and Lundin-Schiller, 2008; Axon *et al.*, 2012) and i.p. injection of tartrazine into mice resulted in mild cholestatic liver injury (Axon, Thesis 2012). Since oestrogens are cholestatic, it was hypothesised that tartrazine caused cholestasis in mice by exhibiting oestrogenic properties and by interacting with the murine ERs. Data in this chapter demonstrates that tartrazine and its gut-derived metabolites SA, SA-NAc, SPH and SCAP as well as the contaminant OSPCA did not activate or inhibited recombinant mERα, mERβv1 and mERβv2 proteins *in vitro* (Figure 4.2 – Figure 4.6). These findings suggest that tartrazine does not have oestrogenic activity in mice and that cholestatic injury in mice following direct tartrazine exposure occurred independent of the ER.

The mechanism by which oestrogens cause cholestasis is thought to either be an ERα-dependent suppression of hepatic transporter expression (Yamamoto *et al.*, 2006) and/or inhibition of hepatic bile acid transporters that leads to impaired bile acid secretion and thus cholestasis and subsequent liver toxicity (Stieger *et al.*, 2000). Since impairment of SULT-mediated sulfonation of some bile acids, which is essential for their secretion, can cause cholestasis, and tartrazine has been reported to significantly inhibit dopamine sulfotransferase in human hepatic S9 fractions (Bamforth *et al.*, 1993), the effects of tartrazine on murine hepatic sulfotransferase activities were examined. Data in this chapter shows that tartrazine, four of its gut-derived, sulfonated metabolites and a major sulfonated contaminant of the food additive inhibited dopamine sulfotransferases in a dose-dependent manner in hepatic S9 extracts at concentrations >100 μM suggesting that SULT inhibition may play a role in the mechanism by which direct tartrazine exposure caused mild cholestatic liver injury. Since tartrazine inhibited human dopamine sulfotransferase at a concentration of 6.7 μM (Bamforth *et al.*, 1993), the mouse seems to be a less sensitive model for any potential cholestatic effects of tartrazine.

Although data in this chapter suggest that tartrazine is not a mouse ER activator, findings from Axon (Thesis) (2012) suggest that if sufficient absorption occurs, intake of tartrazine may have mild adverse hepatic effects. Since tartrazine is present in food items and pharmaceuticals, and to conduct a biologically relevant study, the food additive was

administered via the oral route and hepatic as well as other organ effects were examined in mice *in vivo*. Due to low absorption of intact tartrazine by the gut, the food dye was administered in combination with ethanol which has been reported to increase gut permeability to bacteria and bacterial components residing within the gut (Enomoto *et al.*, 2001). In a pilot study to determine the duration of ethanol pre-treatment necessary to see an increase in gut permeability by the means of monitoring liver inflammation, 2 weeks of oral ethanol administration of 3 g/kg body weight twice daily (total of 6 g ethanol/kg body weight per day) resulted in an increase in NF-κB mediated luminescence in the upper and lower abdominal regions (locations of the liver and GI tract, respectively) compared to control dextrose treated mice suggesting that 2 weeks of ethanol pre-treatment is necessary to increase gut permeability (Figure 4.9).

An alcohol-mediated increase in gut permeability in mice has been reported both after acute and chronic exposure to ethanol. Lippai *et al.* have shown that an orally administered single dose of 5 g/kg body weight of ethanol from a 50% ethanol solution on 3 consecutive days caused an increase in serum endotoxin levels as indicator for increased intestinal permeability (Lippai *et al.*, 2014). Chronic alcohol feeding of a 5% (v/v) ethanol containing Lieber-DeCarli liquid diet for 5 weeks showed similar results (Lippai *et al.*, 2014). An increase in serum endotoxin levels is linked to activation of hepatic Kupffer cells which release TNFα, Interleukin (IL)-1 and IL-12 as well as ROS and RNS leading to liver inflammation and injury (Ajakaiye *et al.*, 2011). Activation of Kupffer cells by endotoxin has been reported to be mediated by the Toll-like receptor 4 (TLR4) (Uesugi *et al.*, 2001; Petrasek *et al.*, 2010). Binding of endotoxin to TLR4 further leads to activation of the NF-κB signalling pathway (Fitzgerald *et al.*, 2003; Takeda and Akira, 2004). The observed increase in NF-kB activity in the hepatic region following ethanol exposure in this chapter therefore suggests that alcohol increased gut permeability which led to endotoxin-mediated activation of NF-κB. The observation that NF-κB activity is increased in gastrointestinal region in mice treated with ethanol compared to the control group is consistent with other findings (Lippai *et al.*, 2014).

Following determination of duration of ethanol pre-treatment necessary to increase gut permeability, *in vivo* effects of oral tartrazine exposure were investigated. IVIS data has shown that oral tartrazine administration caused a mild inflammatory response in the liver and gastrointestinal tract after 10 weeks, an effect that was abolished when tartrazine was administered in combination with ethanol (Figure 4.11). *Ex-vivo* imaging of the liver and gut confirmed these findings (Figure 4.12). A possible explanation as to why combined tartrazine and ethanol exposure reduced the apparent inflammatory effect of tartrazine alone may be

because research has shown that ethanol is an inhibitor of NF-κB *in vivo*. NF-κB activation is required to result in the expression of luciferase in tg NF-κB-luc mice that were employed to monitor inflammation in this study (Pruett and Fan, 2009).

Despite evidence of an inflammatory response in the liver following tartrazine exposure, signs for cholestatic liver injury by means of hepatic histological changes and serum ALP levels were not detectable in any of the treatment groups (Figure 4.14, Figure 4.15A). A non-significant three-fold increase in serum ALT levels as well as an increase liver/body weight ratio and mild hepatic inflammation was the only evidence of mild hepatocellular injury in ethanol treated mice (Figure 4.12, Figure 4.13, Figure 4.15B). A similar fold increase in ALT activity has been reported in other studies after chronic alcohol exposure for 4-16 weeks (Yin *et al.*, 1999; Uesugi *et al.*, 2001; Ji and Kaplowitz, 2003; Kang *et al.*, 2009).

Hepatic steatosis is one of the earliest signs of alcohol-induced liver damage. In this study, mice exposed to ethanol (3 g/kg body weight) twice daily by gavage for 12 weeks did not show any signs of steatosis (Figure 4.16). This is contradictory to findings from other studies. For example, Kirpich et al. (2012a) have reported steatotic conditions detected by Oil Red O staining as early as after 3 ethanol binges (4.5 g/kg body weight) administered in 12 hour intervals (Kirpich *et al.*, 2012a). Meanwhile, Yang et al., (2014) show that steatosis occurs in mice gavaged with ethanol (4 g/kg, 30% (v/v) in saline) every 12 hours for 5 days (Yang *et al.*, 2014). In both studies, C57Bl/6 mice were employed. Mice received a greater amount of ethanol per binge, however, which is likely to result in higher blood alcohol levels determining the severity of liver damage. Although conducted in a different strain (SV129 background), Wu et al. (2012) demonstrate that steatosis can be induced in mice with ethanol binges of 3g/kg body weight following twice daily administration by gavage for 4 days (Wu *et al.*, 2012).

The most crucial factors for inducing ethanol-dependent liver injury are the quantity of alcohol consumed, the length of alcohol administration as well as the method by which alcohol is delivered to the animal. For studies requiring the use of chronic ethanol exposure, administration by oral gavage is not commonly employed. Instead, it is more common to administer alcohol by using the Lieber-deCarli ethanol feeding model which provides ethanol to mice via a nutrient competent liquid diet available to animals ad libitum (DeCarli and Lieber, 1967; Lieber and DeCarli, 1982; Lieber and DeCarli, 1989; Bertola *et al.*, 2013). Using this feeding technique, mild forms of liver injury are commonly observed in mice after 4-6 weeks as manifested by mild steatosis, inflammation and elevated serum ALT activity

(Cohen *et al.*, 2010; Mandrekar *et al.*, 2011; Nath *et al.*, 2011; Leung *et al.*, 2012; Liangpunsakul *et al.*, 2012). Intake of the Lieber-DeCarli liquid diet for longer time periods up to 12 weeks has been reported to result in pronounced steatosis but serum ALT levels were only slightly elevated (Zhong *et al.*, 2010). Using this ethanol feeding model, mice consume an avergae of 12-25 g ethanol/kg body weight/day and therefore receive at least 2-4 times the amount of ethanol per day compared to the ethanol delivery method chosen for the oral tartrazine study (Ajmo *et al.*, 2008; Hritz *et al.*, 2008; D'Souza El-Guindy *et al.*, 2010; Zhong *et al.*, 2010).

Another frequently used model to examine the effects of chronic alcohol exposure is the intragastric infusion model (Tsukamoto *et al.*, 1984; Ueno *et al.*, 2012). Using this model, mice are exposed to up to 28 g ethanol/kg body weight/day via a surgically implanted canulla which results in high blood alcohol levels and more severe forms of liver injury including steatosis, inflammation, necrosis and significanlty elevated serum ALT levels (Kono *et al.*, 2000; French, 2001; Uesugi *et al.*, 2002; Ueno *et al.*, 2012; Mathews *et al.*, 2014). Limitations of this ethanol administration method include the requirement of surgical skills, intensive medical care as well as expensive equipment. Further, this model does not account for alcohol exposure via the oral route.

Administration of alcohol by oral gavage as used in this study is mainly employed to examine the effects of acute or 'binge' ethanol exposure. Using this method, single or multiple doses of 4-6 g ethanol/kg body weight are typically administered to mice. This model has shown to cause steatosis and mild infiltration of inflammatory cells (Brandon-Warner *et al.*, 2012; Shukla *et al.*, 2013). Although administration of ethanol by oral gavage is predominantly used to mimic acute or 'binge' effects of alcohol intake, a model administering alcohol by oral gavage for chronic exposure has been successfully conducted in rats (Enomoto *et al.*, 1999). In that study, rats were dosed with 5 g/kg body weight of ethanol once a day and liver damage was assessed at different time points. The reported results demonstrated that after 2 weeks of daily single ethanol administration, mild steatosis was observed in the liver. Eight weeks of treatment caused marked steatosis, as well as mild necrosis and inflammation. It should be noted, however, that rats were simultaneously fed with a liquid diet in which 35% of the daily calorie intake were from corn oil and 47% from maltose dextrin. The presence of unsaturated fat has been reported to be necessary for the induction of liver injury and led to an increase in blood endotoxin levels and gut permeability (Kirpich *et al.*, 2012b). With regards to the oral tartrazine *in vivo* study, dosing of mice twice daily with 3 g ethanol/kg body weight is likely to result in lower alcohol blood levels compared to a single injection of 5 g/kg body

weight/day. High blood alcohol levels are critical to induce liver injury. Combined, these factors may explain why the administration of ethanol for 12 weeks did not result in any apparent hepatic injury in this study.

In conclusion, data in this chapter suggest that the cholestatic effects of tartrazine in mice are not mediated by the ER. As a result the mouse is not a good experimental model for studying the potential xenoestrogenic activity of tartrazine *in vivo.* Alcohol administration to mice by oral gavage twice daily for 12 consecutive weeks did not result in any apparent signs of liver injury. It is questionable whether ethanol treatment resulted in an increase in gut permeability, therefore, and if enough tartrazine was absorbed to cause adverse hepatic effects similar to those seen after direct exposure.

Chapter 5. An examination of the potential adverse hepatic effects of xenoestrogens present within the environment

There is increasing concern regarding man-made endocrine disrupting chemicals within the environment and the health risks these chemicals may pose. Primary biliary cholangitis (PBC), a chronic cholestatic liver disease of unknown aetiology is often considered to be an autoimmune disease because of the presence of anti-mitochondrial antibodies in many PBC patients (Kaplan and Gershwin, 2005; Bogdanos and Komorowski, 2011). Although several studies have linked genetic pre-disposition to disease development (Jones *et al.*, 1999; Parikh-Patel *et al.*, 2001; Invernizzi *et al.*, 2004; Selmi *et al.*, 2004), there is supporting evidence that PBC may in part be triggered by environmental factors. Studies of its geographic distribution have revealed that the prevalence of PBC is not random and that therefore environmental risk factors such as differences in the exposure to environmental toxins may contribute to the pathogenesis of PBC (Metcalf *et al.*, 1997; Prince *et al.*, 2001; Ala *et al.*, 2006). The involvement of man-made toxins has been demonstrated by Gershwin *et al.*, (2005) who could link PBC to the use of hair dyes and nail polish (Gershwin *et al.*, 2005). In regards to environmental risk factors, living in areas of heavy coal mining has also been implicated in the pathogenesis of PBC (Smyk *et al.*, 2010). In 2006, Ala et al. (2006) have reported that the prevalence of patients with PBC is increased in close proximity to toxic waste sites in New York City further linking PBC to the exposure to environmental toxins (Ala *et al.*, 2006). The actual chemical trigger and causative mechanisms, however, remain to be elucidated.

Given the ability of oestrogens to cause cholestasis (Ozkan *et al.*, 2015), and the link that exists between the cholestatic disorder PBC and proximity to toxic waste sites, it was hypothesised that the environment around a waste tip site contains a variety of xenoestrogens.

5.1. Extracts from soil samples around a waste site contain activators of the human ERα

To test the hypothesis that waste sites contain xenoestrogens which may have endocrine disrupting effects, thirteen soil samples were collected in close proximity to an urban waste site. Chemicals were extracted into three different solvents, namely PBS, ethanol and chloroform as described in Section 2.17. Since chloroform is not readily soluble in water, the solvent was evaporated off and soil extract residues were resuspended in the same volume of sterile DMSO to ease the use of chloroform extracts in cell culture. Separate soil samples

were also taken from three different control sites in rural areas and private gardens not in close proximity to waste sites. To test if these soil extracts contain xenoestrogens capable of activating the hER, a reporter gene assay developed by Axon et al. (2012) was employed. This assay uses the oestrogen responsive human breast cancer cell line MCF-7 which expresses the hERα. To test the functionality of the assay, MCF-7 cells were transfected with the $(ERE)_3$-pGL3promotor luciferase reporter construct and the RL-TK control vector for 24 hours followed by treatment with 10 nM E2 or 0.1% (v/v) DMSO vehicle in the absence and presence of 100 nM ICI182,780 for 24 hours and dual-luciferase assay. Figure 5.1 demonstrates that ICI182,780 reduced luciferase activity over DMSO vehicle treated cells in the absence of the ER antagonist suggesting that the hERα is partially active, likely due to oestrogenic chemicals present in cell culture media. Treatment with E2 significantly further increased luciferase activity over DMSO vehicle treated cells. This suggests that MCF-7 cells respond to treatment with oestrogen and that the assay functions correctly. The E2-mediated increase in reporter gene activity was inhibited by co-treatment with ICI182,780 indicating that the observed increase in luciferase reporter gene expression is mediated by the hERα.

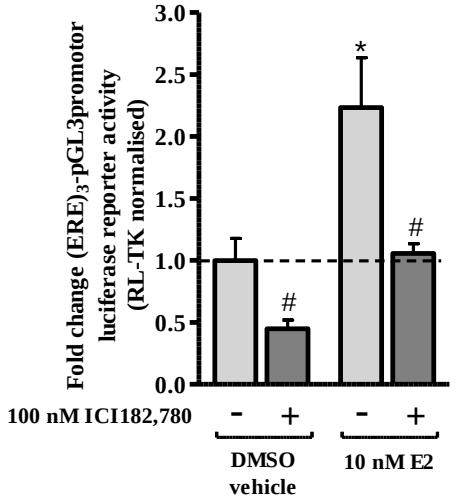

Figure 5.1 E2 activates the hERα in MCF-7 cells. Luciferase reporter gene assay in MCF-7 cells co-transfected with the $(ERE)_3$-pGL3promotor reporter construct and the RL-TK control vector. Following transfection for 24 hours, cells were pre-treated with 100 nM ICI182,780 or with DMSO vehicle (0.1% v/v) as indicated for 6 hours followed by treatment with 10 nM E2 or DMSO vehicle ± 100 nM ICI182,780 for 24 hours and dual luciferase assay. Mean and SD of n=3, typical of 3 separate experiments. Data are expressed in fold change versus DMSO vehicle-treated cells in the absence of ICI182,780. *Significantly different ($p<0.05$) versus DMSO vehicle-treated cells in the absence of ICI182,780 using Student's t-test (two-tailed). #Significantly different ($p<0.05$) versus equivalent treatments in the absence of ICI182,780 using the Student's t-test (two-tailed) with Holm-Bonferroni post-hoc modifications.

Following validation of correct functioning of the MCF-7 cell-based reporter gene assay, it was investigated whether extracts from soil samples collected from around an urban waste site

contain xenoestrogens capable of activating the hERα. MCF-7 cells were transiently transfected with the $(ERE)_3$-pGL3promotor reporter construct and the RL-TK control vector for 24 hours. This was followed by treatment with waste site and control sites PBS soil extracts, ethanol soil extracts and chloforform extracts (in DMSO) for 24 hours and dual-luciferase assay. Control cells were treated with the solvent stock used in the soil extraction procedure (1x PBS and ethanol extracts) or DMSO (chloroform extracts) (solvent stocks were labelled as 'solvent control').

Figure 5.2A shows that treatment with 0.1% (v/v) of soil extracts in 1x PBS (soil extracts were effectively diluted in medium by a factor of 1000) resulted in statistically significant increases in luciferase reporter gene activity in several sampling sites around the waste tip and to levels similar or greater than those induced by treatment with a saturating concentration of 10 nM E2. In contrast, treatment with diluted PBS soil extracts from 3 separate control sites did not result in a significant increase in reporter gene expression. Several ethanol soil extracts (Figure 5.2B) and chloroform soil extracts (in DMSO) (Figure 5.2C) in close proximity to the waste site similarly significantly induced reporter gene expression over solvent control with extracts from control sites showing little or no xenoestrogenic activity.

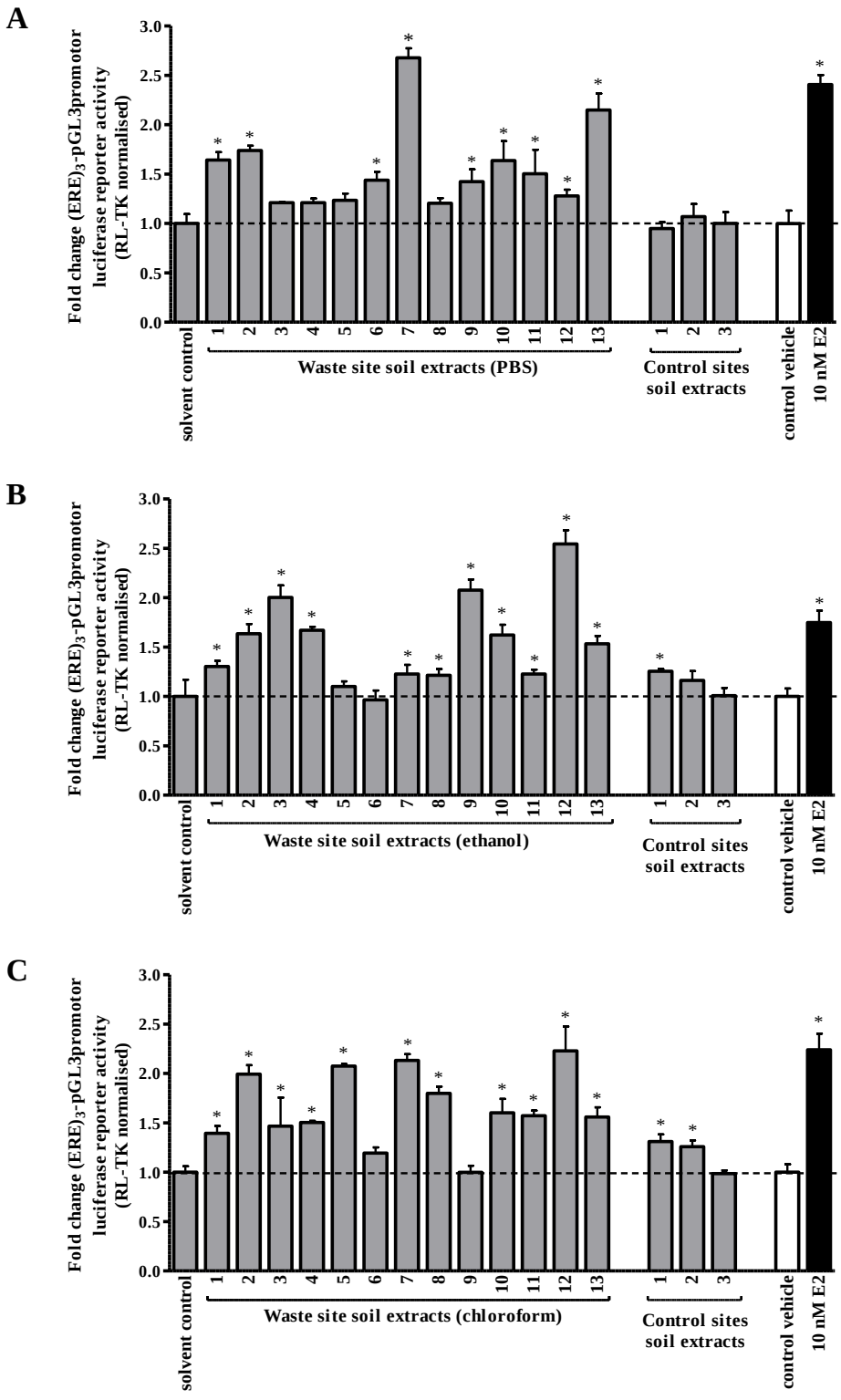

Figure 5.2 Soil sample extracts in close proximity to a waste site contain a chemical(s) that activate the hERα. $(ERE)_3$-pGL3promotor luciferase reporter gene assay in MCF-7 cells. Cells were transfected with the $(ERE)_3$-pGL3promotor reporter construct and the RL-TK control vector for 24 hours before treatment with 0.1% (v/v) of **(A)** PBS soil extracts **(B)** ethanol soil extracts or **(C)** chloroform soil extracts (in DMSO) or 10 nM E2 for 24 hours and dual luciferase assay. Data are mean and SD of n=3 from the same experiment, expressed in fold change versus solvent control-treated (same solvent as was used for the extraction process) or control vehicle-treated (0.1% v/v DMSO) cells. *Significantly different ($p<0.05$) versus solvent control-treated or control vehicle-treated cells cells using One-way ANOVA with Dunnett's post-hoc modifications.

To further investigate if waste site soil extracts activate the hERα in a dose-dependent manner, MCF-7 cells transfected with the $(ERE)_3$-pGL3promotor reporter and RL-TK construct were treated with a range of dilutions of soil sample extracts. Since waste site soil extracts in ethanol appeared to contain the highest levels of xenoestrogens with many of the ethanol soil extracts activating the hERα to levels greater than those induced by treatment with a saturating concentration of 10 nM E2, ethanol soil extracts were used for all further investigations. MCF-7 cells were treated with a range of dilutions of ethanol soil extracts from waste tip sampling sites 3 and 12 and control site 3 starting at a dilution of 1:200 (constituting a final 0.5% v/v) and serially diluted up to a dilution of 1:10,000,000 (constituting a final 0.00001% v/v). Control cells were treated with 0.5% (v/v) of ethanol solvent used for the extraction procedure (solvent control). Figure 5.3A demonstrates that waste site ethanol soil extracts 3 and 12 increased luciferase reporter gene expression in a dose-dependent manner, with a significant increase detected at a dilution as low as 1/100,000 (constituting a final 0.001% v/v) for waste site sample site 12 and 1/1000 (0.1%) for waste site sample site 3. A dose-dependent increase in reporter gene expression was not observed in cells treated with a range of dilutions from ethanol soil extract from control site 3 (Figure 5.3A). A dose-dependent increase in luciferase expression was also observed in cells treated with a range of concentrations of E2 (Figure 5.3B), however, the curve appeared flat and was not sigmoidal as seen following treatment with waste site soil extracts (Figure 5.3A). Although statistically significant at concentrations in the range from 10 pm to 10 µM, a dose-dependent increase in reporter gene expression was not observed in cells treated with a range of concentrations of EE (Figure 5.3B).

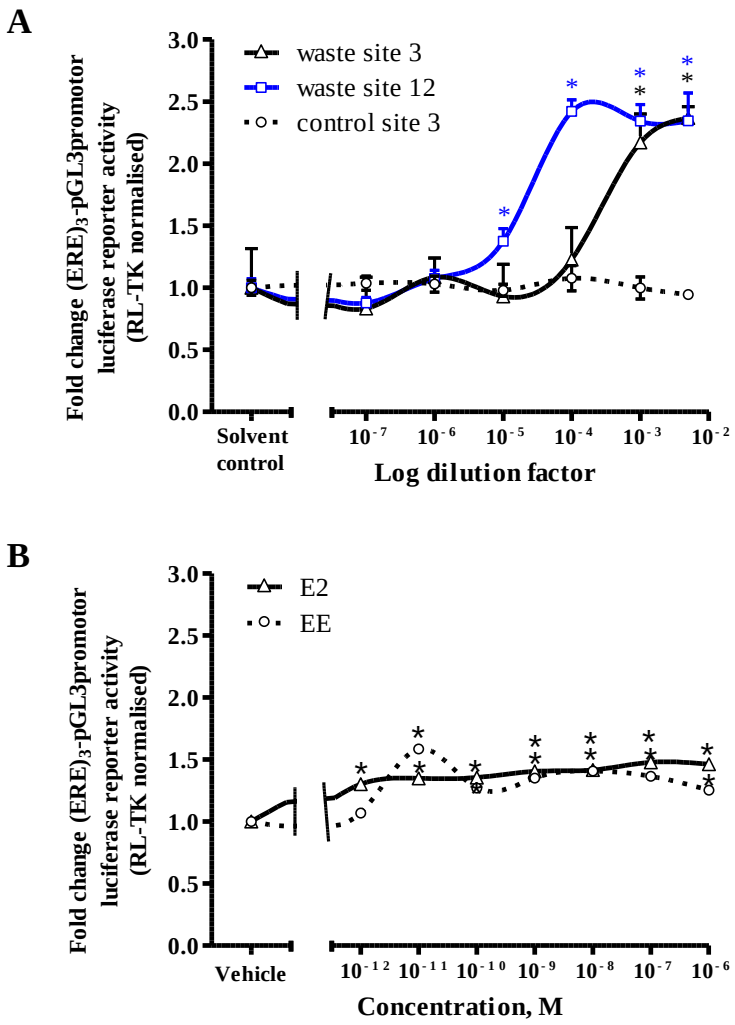

Figure 5.3 Ethanol waste site soil extracts activate the hERα in a dose-dependent manner. Concentration dependent $(ERE)_3$-pGL3promotor luciferase reporter gene assay in MCF-7 cells. Cells were transfected with the $(ERE)_3$-pGL3promotor reporter construct and the RL-TK control vector for 24 hours. (**A**) Cells were treated with the indicated dilution in medium of waste site ethanol soil extract 3 and 12 or control site soil extract 3 for 24 hours and dual-luciferase assay. Control cells (solvent control) were treated with 0.5% (v/v) of ethanol solvent used for the soil extractions. (**B**) Cells were treated with the indicated concentrations of oestradiol (E2) or ethinyl oestradiol (EE) for 24 hours and dual luciferase assay. Control cells (vehicle) were treated with 0.1% (v/v) DMSO vehicle. Data are mean and SD of n=3, typical of 3 separate experiments, expressed in fold change versus vehicle-treated cells. *Significantly different ($p<0.05$) versus DMSO vehicle-treated cells using One-way ANOVA with Dunnett's post-hoc modifications.

To confirm that the increase in luciferase reporter gene expression following treatment with soil sample extracts from around a waste site is mediated by the hERα, MCF-7 cells transiently transfected with the $(ERE)_3$-pGL3promotor reporter and RL-TK construct were treated with ethanol extracts from waste tip sites that have been shown to induce reporter gene expression (see Figure 5.2B) in the absence and presence of the ER antagonist ICI182,780. Figure 5.4 demonstrates that all ethanol waste site soil extracts screened significantly induced reporter gene expression over cells treated with ethanol solvent (solvent control) to levels

similar or greater as seen with exposure to 10 nM E2. In all cases, co-treatment with 100 nM ICI182,780 significantly reduced luciferase reporter gene expression over equivalent treatments with waste site soil extracts in the absence of ICI182,780 verifying that the observed increase following waste site soil extract exposure is mediated by the hERα.

These data indicate that extracts from soil samples collected in close proximity to an urban waste site contain a chemical/chemicals capable of activating the hERα in a human cell-based reporter gene assay.

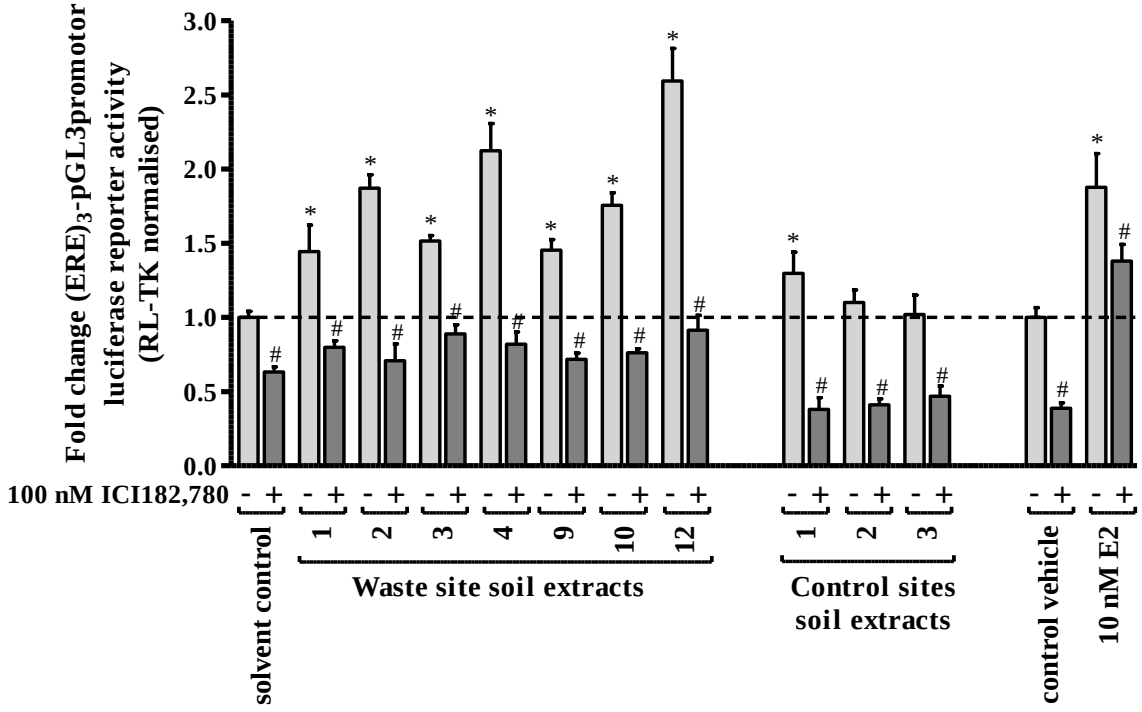

Figure 5.4 Waste site ethanol soil extract-dependent activation of the hERα is inhibited by ICI182,780. Luciferase reporter gene assay in MCF-7 cells transfected with the $(ERE)_3$-pGL3promotor reporter construct and the RL-TK control vector. Following transfection for 24 hours, cells were pre-treated with 100 nM ICI182,780 or with DMSO vehicle (0.1% v/v) as indicated for 6 hours followed by treatment with 0.1% (v/v) waste site ethanol soil extracts as indicated or 10 nM E2 in the presence and absence of 100 nM ICI182,780 for 24 hours and dual luciferase assay. Control cells were treated with 0.1% (v/v) ethanol solvent used for extraction (solvent control) or with 0.1% (v/v) DMSO vehicle (control vehicle). Data are mean and SD of n=3 from the same experiment, expressed in fold change versus solvent control-treated or control vehicle-treated cells. *Significantly different ($p<0.05$) versus solvent control-treated or control vehicle-treated cells using One-way ANOVA with Dunnett's post-hoc modifications. #Significantly different ($p<0.05$) versus equivalent treatments in the absence of ICI182,780 using Student's t-test (two-tailed) with Holm-Bonferroni post-hoc modifications.

5.2. Extracts from soil samples around a waste site activate the murine ERs

In order to investigate the potential effects of xenoestrogen exposure *in vivo*, ethanol extracts from around an urban waste tip site were examined for their potential to activate the murine ERs for use in an *in vivo* mouse model. Activation of the mERs was tested using the reporter gene assays as developed in Chapter 3.

5.2.1. Extracts from soil samples around a waste site activate the mERα

The potential of waste site soil extracts to activate the mERα was examined in LTPA cells. LTPA cells were transiently transfected with the previously constructed pcDNA3.1-mERα expression construct encoding the mERα, the 3XERE TATA luc reporter construct as well as the RL-TK control construct before treatment with 0.1% (v/v) of ethanol waste site soil extracts and ethanol control sites soil extracts in the absence and presence of 100 nM ICI182,780 for 24 hours. Control cells were treated with the ethanol solvent stock used in the soil extraction procedure (solvent control).

Figure 5.5 demonstrates that the ethanol waste site soil extracts which activated the hERα in MCF-7 cells similarly increased luciferase reporter gene expression in LTPA cells expressing recombinant mERα over solvent control treated cells to levels similar or greater as seen with a biologically saturating concentration of 10 nM E2 or 10 nM EE. This effect was inhibited by co-treatment with 100 nM ICI182,780. No such increase was observed following the treatment with soil sample ethanol extracts from the control sites.

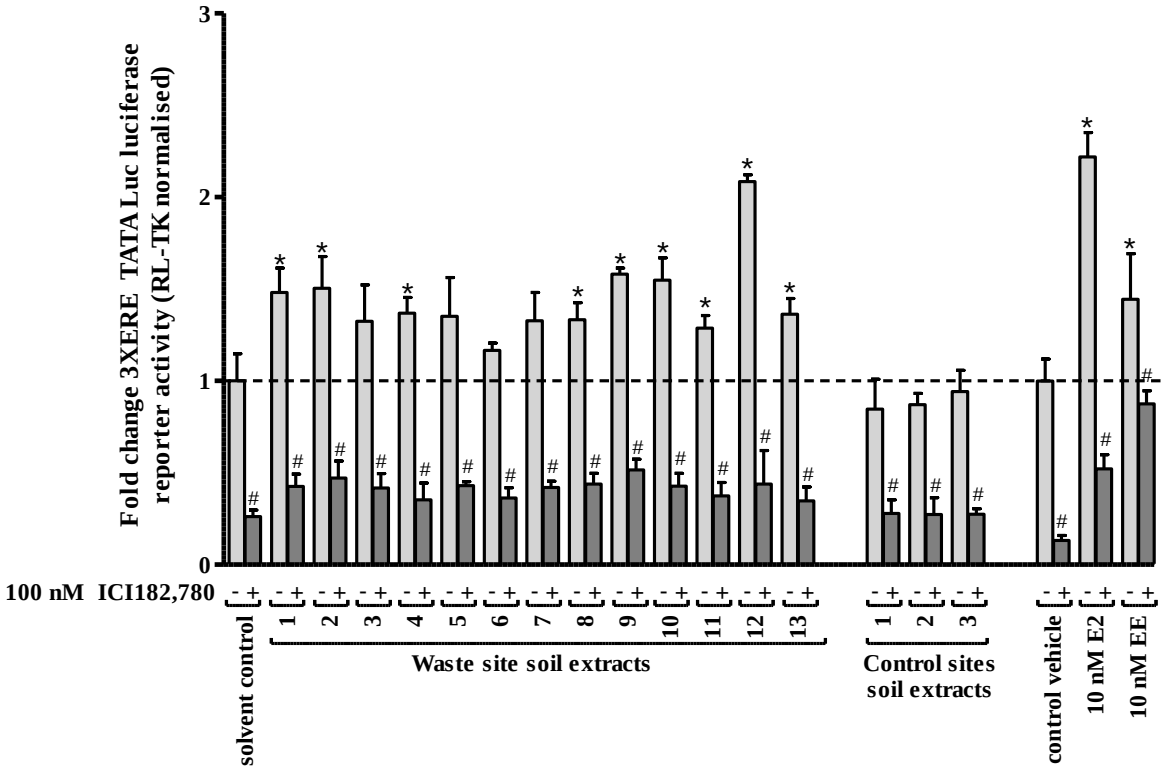

Figure 5.5. Waste site ethanol soil extracts activate recombinant mERα. Luciferase reporter gene assay (3XERE TATA luc) in LTPA cells co-transfected with the pcDNA3.1-mERα expression construct encoding the mERα. Following transfection for 24 hours, cells were pre-treated with 100 nM ICI182,780 or with DMSO vehicle (0.1% v/v) as indicated for 6 hours followed by treatment with 0.1% (v/v) waste site ethanol soil extracts, control sites ethanol soil extracts, 10 nM E2 or 10 nM EE in the presence and absence of 100 nM ICI182,780 for 24 hours and dual luciferase assay. Control cells were treated with 0.1% v/v ethanol solvent used for extraction (solvent control) or with 0.1% (v/v) DMSO vehicle (control vehicle). Data are mean and SD of n=3, typical of two separate experiments and expressed in fold change versus solvent control-treated or control vehicle-treated cells. *Significantly different ($p<0.05$) versus solvent control-treated or control vehicle-treated cells using One-way ANOVA with Dunnett's post-hoc modifications. #Significantly different ($p<0.05$) versus equivalent treatments in the absence of ICI182,780 using Student's t-test (two-tailed) with Holm-Bonferroni post-hoc modifications.

5.2.2. Extracts from soil samples around a waste site activate the mERβv1

The potential of waste site soil extracts to activate the mERβ proteins was examined in 603B cells. To test for activation of the mERβv1, 603B cells were transiently transfected with the previously constructed pcDNA3.1-mERβv1 expression construct encoding the mERβv1, the $(ERE)_3$-pGL3promotor reporter construct as well as the RL-TK control construct before treatment with 0.1% (v/v) of waste site soil extracts and control sites soil extracts in ethanol in the absence and presence of 100 nM ICI182,780 for 24 hours.

Figure 5.6 shows that almost all waste site ethanol extracts induced an increase in reporter gene expression in 603B cells expressing recombinant mERβv1 to levels similar or greater as

seen with 10 nM E2 or 10 nM EE. These increases were inhibited by co-treatment with 100 nM ICI182,780. Treatment with ethanol extracts from control sites soil samples did not result in an increase in luciferase reporter gene expression.

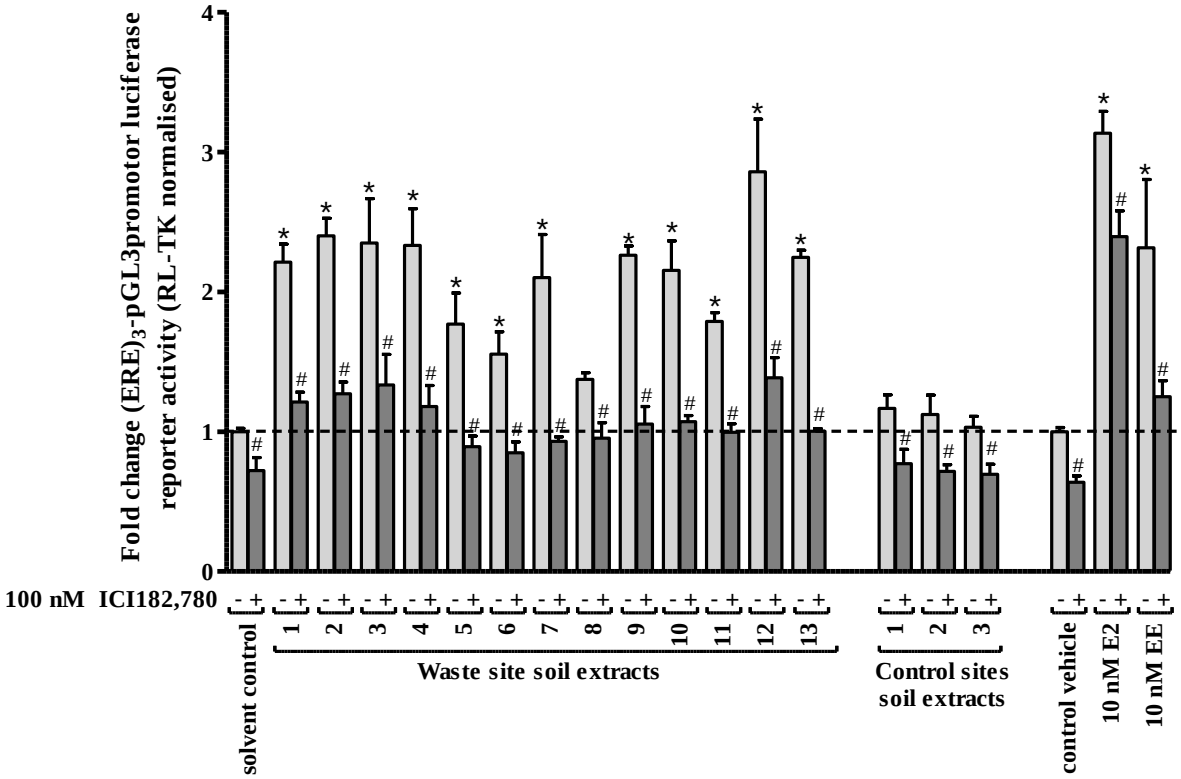

Figure 5.6 Waste site ethanol soil extracts activate recombinant mERβv1. Luciferase reporter gene assay ($(ERE)_3$-pGL3promotor) in 603B cells co-transfected with the pcDNA3.1 expression construct encoding the mERβv1. Following transfection for 24 hours, cells were pre-treated with 100 nM ICI182,780 or with DMSO vehicle (0.1% v/v) as indicated for 6 hours followed by treatment with 0.1% (v/v) waste site ethanol soil extracts, control sites ethanol soil extracts, 10 nM E2 or 10 nM EE in the presence or absence of 100 nM ICI182,780 for 24 hours and dual luciferase assay. Control cells were treated with 0.1% (v/v) ethanol solvent used for extraction (solvent control) or with 0.1% (v/v) DMSO vehicle (control vehicle). Data are mean and SD of n=3, typical of two separate experiments and expressed in fold change versus solvent control-treated or control vehicle-treated cells. *Significantly different ($p<0.05$) versus solvent control-treated or control vehicle-treated cells using One-way ANOVA with Dunnett's post-hoc modifications. #Significantly different ($p<0.05$) versus equivalent treatments in the absence of ICI182,780 using Student's t-test (two-tailed) with Holm-Bonferroni post-hoc modifications.

5.2.3. Extracts from soil samples around a waste site irreversibly activate the mERβv2

To test for activation of the mERβv2, 603B cells were transiently transfected with the previously constructed pcDNA3.1-mERβv2 expression construct encoding the mERβv2 protein, the $(ERE)_3$-pGL3promotor reporter construct as well as the RL-TK control construct. Constitutively active recombinant mERβv2 was de-activated by treatment with 100 nM ICI182,780 for 6 hours followed by several wash steps with sterile 1xPBS before treatment with 0.1% (v/v) of waste site soil extracts and control sites soil extracts in ethanol in the absence and presence of 100 nM ICI182,780 for 24 hours.

Figure 5.7 shows that several ethanol waste site soil extracts induced an increase in reporter gene activity in 603B cells expressing recombinant mERβv2 but not to the same levels as seen with exposure to 10 nM E2 or 10 nM EE. In some cases, ethanol waste site soil extracts that activated the mERβv1 also activated the mERβv2, such as soil samples 3, 4, 6, 8 and 12 (see also Figure 5.6). Other soil sample extracts such as sample 1 and 2, however, only induced luciferase reporter gene expression in cells expressing recombinant mERβv1 (Figure 5.6). Interestingly, despite effective antagonism by ICI182,780 versus E2- or EE-activation of mERβv2, the ER antagonist failed to antagonise the increase in luciferase reporter gene expression after exposure to the majority of waste site ethanol soil extracts, such as soil samples 3, 4, 9 and 12 suggesting that these irreversibly activate the mERβv2. Treatment with ethanol extracts from control sites soil samples did not show any detectable oestrogenic activity in this assay.

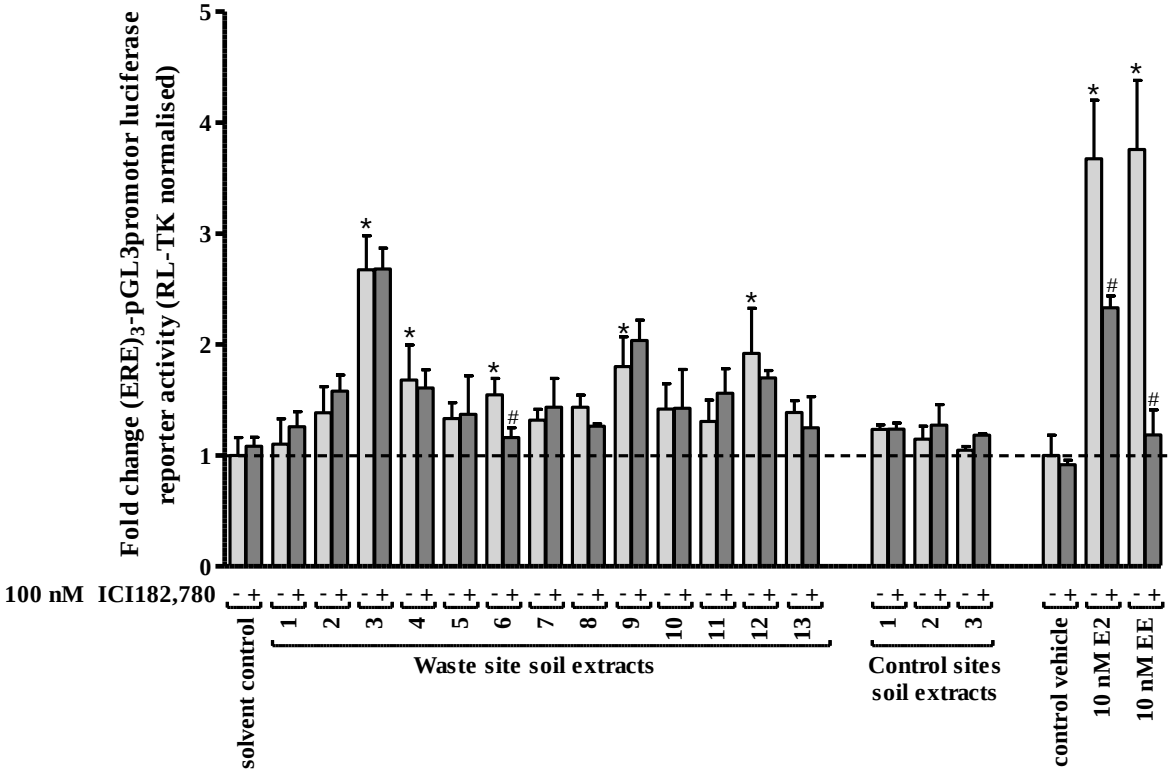

Figure 5.7 Waste site ethanol soil extracts irreversibly activate the mERβv2. Luciferase reporter gene assay ($(ERE)_3$-pGL3promotor) in 603B cells co-transfected with the pcDNA3.1 expression construct encoding the mERβv2. Following transfection for 24 hours cells were pre-treated with 100 nM ICI182,780 for 6 hours to de-activate constitutively active mERβv2 followed by several wash steps with PBS. Cells were then treated with 0.1% (v/v) waste site ethanol soil extracts, control sites ethanol soil extracts, 10 nM E2 or 10 nM EE in the presence or absence of 100 nM ICI182,780 for 24 hours and dual luciferase assay. Control cells were treated with 0.1% (v/v) ethanol solvent used for extraction (solvent control) or with 0.1% (v/v) DMSO vehicle (control vehicle). Data are mean and SD of n=3, typical of two separate experiments and expressed in fold change versus solvent control-treated or control vehicle-treated cells. *Significantly different ($p<0.05$) versus solvent control-treated or control vehicle-treated cells using One-way ANOVA with Dunnett's post-hoc modifications. #Significantly different ($p<0.05$) versus equivalent treatments in the absence of ICI182,780 using Student's t-test (two-tailed) with Holm-Bonferroni post-hoc modifications.

5.3. An acute effect of xenoestrogen exposure is an inflammatory response in the liver

Prior to investigations of potential adverse hepatic effects caused by xenoestrogens present in waste site soil extracts, it was first established whether tg NF-κB-luc mice can be employed as animal model to assess the potential adverse hepatic effects of xenoestrogens *in vivo*. Accordingly, male adult tg NF-κB-luc mice were acutely exposed to the known xenoestrogens EE and butyl paraben by single i.p. injection on 3 consecutive days, essentially as described in Table 5.1. The hepatotoxin ANIT known to cause periportal liver injury and which was used as a positive control was dosed once at the beginning of the study by oral

gavage. On day 4, whole body IVIS imaging was used to determine inflammation within the liver prior to termination of animals by cervical dislocation and collection of blood and livers.

Group	Animal numbers	Treatment
Vehicle	3♂ tg NF-kB-luc	Dosed with vehicle (90% olive oil/10% ethanol v/v)
ANIT	1♂ tg NF-kB-luc, positive control for liver inflammation	Dosed with 50 mg/kg bw ANIT once at beginning of study by oral gavage
EE	3♂ tg NF-kB-luc	Dosed with 0.5 mg/kg bw EE
Butyl paraben	3♂ tg NF-kB-luc	Dosed with 50 mg/kg bw butyl paraben
Except for ANIT, all treatments were administered by single i.p. injection at 0, 24, and 48 hours at 0.5 ml/100g bw. At 72 hours, animals were imaged by IVIS before termination by cervical dislocation and collection of blood and livers for further analysis		

Table 5.1 Dosing regimen for *in vivo* study investigating the acute effects of xenoestrogen exposure. EE and butyl paraben were dissolved in and dosed from a 90% olive oil/10% ethanol (v/v) solution. ANIT was dissolved in olive oil (12.5 mg/ml) and dosed at 50 mg/kg body weight. Tg, transgenic; bw, body weight.

Figure 5.8 shows that exposure to the hepatotoxin ANIT caused an increase in luminescence in the upper abdominal region (location of the liver). A statistically significant increase in NF-κB driven luciferase expression in the upper abdominal (hepatic) region was also observed following exposure to the synthetic oestrogen ethinyl oestradiol (EE) when compared to animals administered with vehicle alone. Exposure to the well known xenoestrogen butyl paraben did not result in a significant increase in luciferase expression in the hepatic region.

These data demonstrate that acute i.p. administration of some xenoestrogen to mice, which models a systemic exposure, leads to an inflammatory response within the liver.

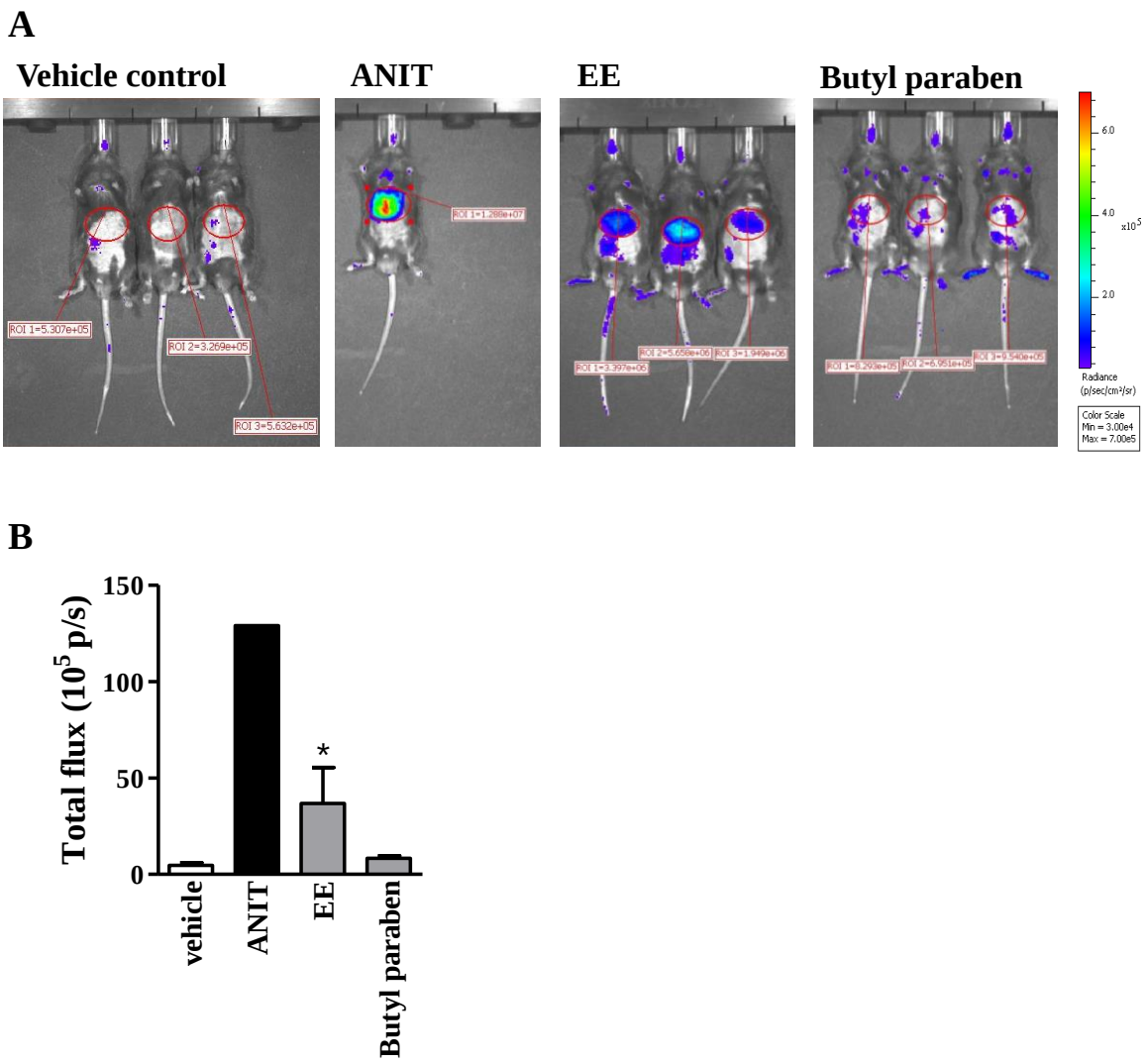

Figure 5.8 Exposure to EE causes an inflammatory response in the liver. Male adult tg NF-κB-luc mice were dosed with EE, butyl paraben or vehicle (90% olive oil/10% ethanol v/v) by i.p. injection at 0, 24 and 48 hours. The hepatotoxin ANIT was dosed once at the beginning of the study by oral gavage. (**A**) IVIS images of treated mice at 72 hours from beginning of the study. For imaging, mice were anesthetised using isoflurane and injected with 200 µl of D-luciferin (15 mg/ml) intraperitoneally. Mice were imaged 10 minutes after injection with D-luciferin. (**B**) Quantified upper (hepatic) abdominal luminescence of treated mice. IVIS data are the mean and standard deviation of the following animal numbers: vehicle: n=3; ANIT: n=1, EE: n=3; butyl paraben: n=3. *Significantly different ($p<0.05$) versus vehicle control group using One-way ANOVA with Bonferroni post-hoc modifications.

To examine if histological changes occurred in the liver following treatment, livers from treated tg NF-kB-luc mice were harvested at the end of the study which were then fixed, processed and sections were stained with haematoxylin and eosin (H&E). Sera of treated mice were collected at termination of the study to analyse the activity of serum ALP enzymes, a marker for periportal injury.

Histological examination of portal tracts demonstrated that exposure to ANIT resulted in necrotic changes and recruitment of inflammatory cells whereas no apparent histological differences in the portal tract regions could be observed in liver sections of EE, butyl paraben and vehicle control groups (Figure 5.9).

Analysis for serum ALP activities showed that ANIT markedly increased ALP activities in the serum, however, no statistical analysis could be performed since data are from n=1 (Figure 5.10). A statistically significant increase in serum ALP activities was observed in mice exposed to EE whereas butyl paraben treatment did not result in detectable differences in serum ALP activities compared to vehicle-treated animals (Figure 5.10).

Although no biologically significant histological changes were observed, overall data in this section confirm that the liver is a target for the adverse effects of xenoestrogens and that the liver imaging approach by IVIS provides a refined method for assessing the potential adverse hepatic effects of xenoestrogens.

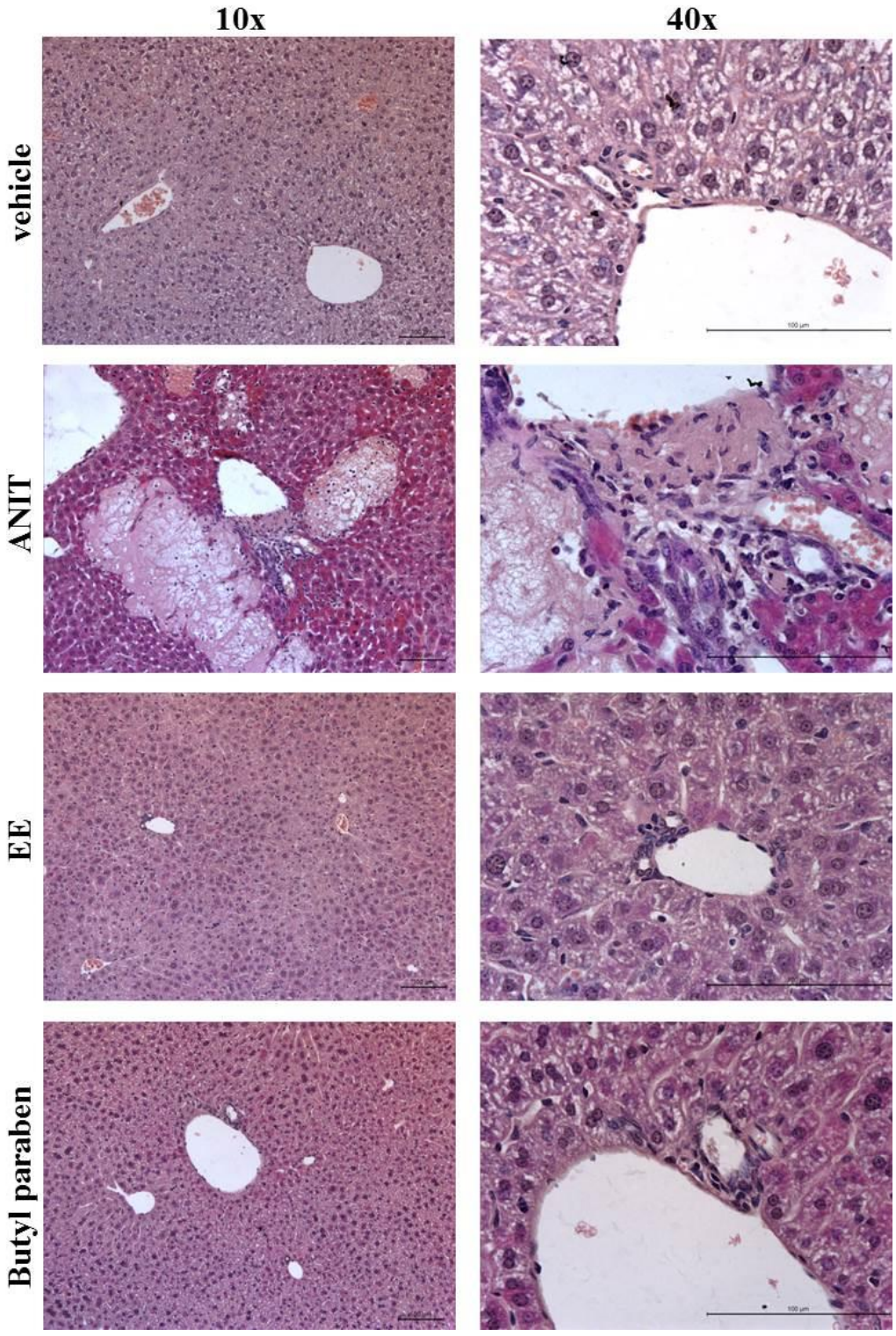

Figure 5.9 Acute exposure to EE does not cause any apparent hepatic histological changes. Representative H&E stained liver sections of treated animals (vehicle: n=3; ANIT: n=1, EE: n=3; butyl paraben: n=3). Scale bar: 100 µm. Male adult tg NF-κB-luc mice were dosed with EE, butyl paraben or vehicle (90% olive oil/10% ethanol) by i.p. injection at 0, 24 and 48 hours. The hepatotoxin ANIT was dosed once at the beginning of the study by oral gavage. At 72 hours, mice were terminated by cervical dislocation and their livers collected.

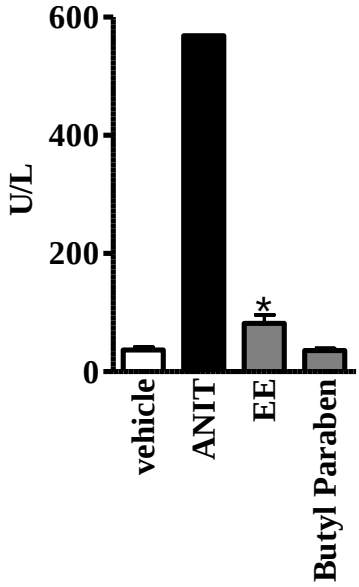

Figure 5.10 Acute exposure to EE leads to an increase in ALP serum levels. Serum ALP measurements at termination of the study. Male adult tg NF-κB-luc mice were dosed with EE, butyl paraben or vehicle (90% olive oil/10% ethanol) by i.p. injection at 0, 24 and 48 hours. The hepatotoxin ANIT was dosed once at the beginning of the study by oral gavage. At 72 hours, mice were terminated by cervical dislocation and their blood collected. Serum enzyme data are the mean and standard deviation of the following animal numbers: vehicle: n=3; ANIT: n=1, EE: n=3; butyl paraben: n=3 *Significantly different ($p<0.05$) versus vehicle control group using One-way ANOVA with Bonferroni post-hoc modifications.

5.4. *In vivo* study: an examination of adverse hepatic effects caused by oestrogen positive soil extract

As exposure to known xenoestrogens was found to have adverse hepatic effects *in vivo* in mice (Section 5.3), it was examined whether soil extracts from around an urban waste tip with oestrogenic activity also have adverse hepatic effects *in vivo*.

To calculate the amount of oestrogen positive soil extract required to potentially result in a similar hepatic effect as seen with EE, it was estimated that the concentration of xenoestrogen(s) in soil extracts is 10 µM since treatment of cells at a dilution of 1/1000 resulted in a similar increase in reporter gene expression as observed with 10 nM E2 or 10 nM EE (see Figure 5.5 and Figure 5.6). Assuming that all xenoestrogens in the soil extracts have a similar molecular weight to EE, 1 ml of soil extract would contain 2.9 µg of xenoestrogens. Exposure of animals to 500 µg/kg body weight EE (12.5 µg EE for a mouse weighing 25 g) was shown to result in a readable IVIS signal and increases in serum ALP activities. Therefore, to see a similar effect following exposure to xenoestrogens, a 25 g mouse would have to receive 4.3 ml of soil extract. Assuming, however, that injection of 500 µg/kg body weight EE lies above the top of the dose response curve and due to limited availability of soil

extracts remaining after previous analysis, it was estimated that around 1 ml of soil extract was required per mouse.

Several oestrogen positive waste site ethanol soil extracts which activated the mERs (see Section 5.2) were combined to yield a sufficient volume for injection into mice. Ethanol extracts of oestrogen negative control sites were similarly combined. Combined soil extracts were then dried down to 5% of their volume and then diluted with olive oil 1:9 (10% ethanol soil extract/90% olive oil).

5.4.1. Combined oestrogen positive ethanol soil extracts activate the mERs

Prior to examination of potential *in vivo* hepatic effects of the soil extracts, the oestrogenic potential of combined soil extracts was tested in the developed mouse-based reporter gene assays. Figure 5.11A confirms that exposure to combined oestrogen positive soil extracts resulted in a statistically significant increase in luciferase reporter gene expression in LTPA cells expressing recombinant mERα to levels greater than seen with 10 nM E2 or 10 nM EE. Treatment with combined oestrogen negative soil extracts did not result in a detectable increase. Treatment with oestrogen positive soil ethanol extracts further resulted in an increase in luciferase reporter gene activity in 603B cells expressing recombinant mERβv1 (Figure 5.11B) and mERβv2 (Figure 5.11C) to levels similar or greater as seen with 10 nM E2 or 10 nM EE with combined oestrogen negative soil ethanol extracts having no effect.

These data confirm that combined soil oestrogen positive soil extracts activated the mERα, mERβv1 and mERβv2 which indicates that they retained their oestrogenic activity in mice.

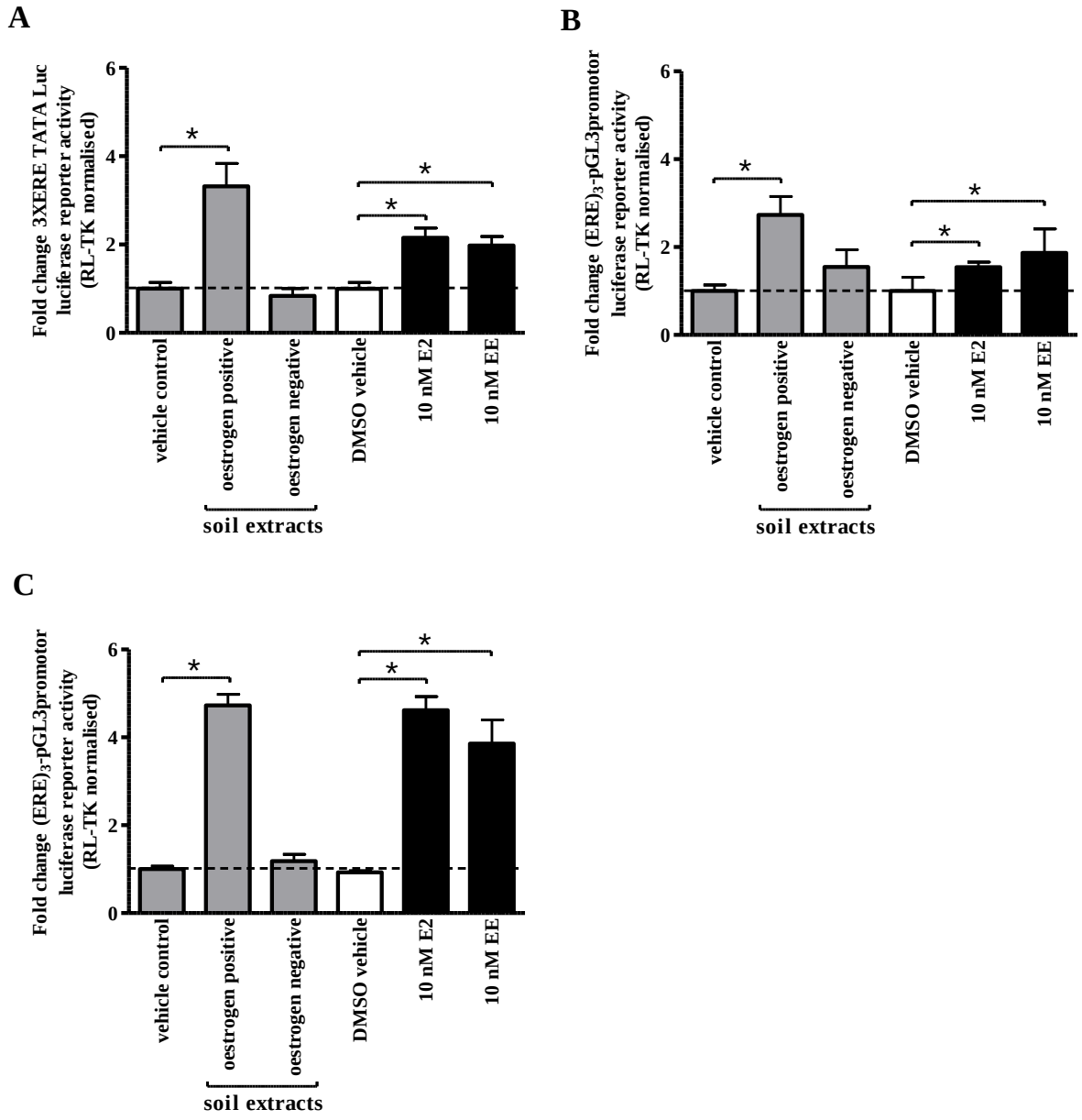

Figure 5.11 Confirmation of activation of recombinant mERα, mERβv1 and mERβv2 proteins by combined oestrogen positive waste site soil extracts. (A) Luciferase reporter gene assay (3XERE TATA luc) in LTPA cells co-transfected with the pcDNA3.1 expression construct encoding the mERα. Following transfection for 24 hours cells were treated with 0.1% (v/v) of combined oestrogen positive waste site soil extracts or combined oestrogen negative control sites soil extracts, 10 nM E2 or 10 nM EE for 24 hours and dual-luciferase assay. Control cells were treated with 0.1% (v/v) vehicle (vehicle control, 80% olive oil/20% ethanol) or with 0.1% (v/v) DMSO vehicle. (**B**) Luciferase reporter gene assay ($(ERE)_3$-pGL3promotor) in 603B cells co-transfected with the pcDNA3.1 expression construct encoding the mERβv1. Following transfection for 24 hours cells were treated as described above. (**C**) Luciferase reporter gene assay ($(ERE)_3$-pGL3promotor) in 603B cells co-transfected with the pcDNA3.1 expression construct encoding the mERβv2. Following transfection for 24 hours cells were pre-treated with 100 nM ICI182,780 for 6 hours to de-activate constitutively active mERβv2 followed by several wash steps with 1x PBS. Cells were then treated as described above. Data are mean and SD of 3 separate treatments from the same experiment, expressed in fold change versus vehicle control-treated or DMSO vehicle-treated cells. *Significantly different ($p<0.05$) versus vehicle control or DMSO vehicle-treated cells using One-way ANOVA with Dunnett's post-hoc modifications.

5.4.2. Acute exposure to oestrogen positive soil extract results in cholangiopathic injury in the absence of any hepatocellular injury

Following confirmation that combined oestrogenic waste site soil extracts activate the mERs, soil extracts were injected into mice to examine their potential to cause adverse hepatic effects.

Male adult tg NF-κB-luc mice were acutely exposed to combined oestrogen positive or combined oestrogen negative soil extracts in 10% ethanol/90% olive oil (v/v) by i.p. injection to mimic systemic exposure. Due to the volume of soil extracts available, mice could only be injected with soil extracts once. The positive control group was exposed to EE in 10% ethanol/90% olive oil (v/v) whereas animals in the vehicle control group received the vehicle (10 % ethanol/90% olive oil v/v) alone. Treatment groups and dosing regimen are outlined in Table 5.2.

Group	Animal numbers	Treatment
Vehicle	3♂ tg NF-kB-luc	Dosed with vehicle (90% olive oil/10% ethanol v/v)
EE	3♂ tg NF-kB-luc	Dosed with 0.5 mg/kg bw EE
Oestrogen negative soil extracts	3♂ tg NF-kB-luc	Dosed with combined oestrogen negative soil extracts from 3 separate control sites
Oestrogen positive soil extracts	3♂ tg NF-kB-luc	Dosed with combined oestrogen positive soil extracts from soil samples collected around an urban waste site

All treatments were administered by single i.p. injection at 2 ml/100g bw. Mice were imaged for inflammation by IVIS at 0, 1, 6 and 24 hours post injection. Following imaging, animals were terminated by cervical dislocation and their blood and liver were collected for further analysis.

Table 5.2 Dosing regimen for soil sample extracts exposure *in vivo* study. Combined oestrogen negative and oestrogen positive ethanol soil extracts were concentrated to 5% of their original volume and diluted 1:9 with olive oil (10% ethanol soil extracts/90% olive oil v/v). EE was dissolved in and dosed from a 90% olive oil/10% ethanol (v/v) solution. Tg, transgenic; bw, body weight.

Figure 5.12 demonstrates that significant increases in luminescence in the upper abdominal region (location of the liver) were undetectable in animals exposed to EE, combined oestrogen positive or combined oestrogen negative soil extracts compared to the vehicle control group at all indicated time points. It appears that at 6 hours post injection, luminescent signal and therefore NF-κB activity throughout the whole abdomen was increased in all the treatment groups as well as in animals receiving the vehicle, likely due to i.p. injection of

large volumes of dosing solutions (0.5 ml for a 25 g mouse) (Figure 5.12). IVIS images indicate that the increase in luminescent signal was decreased at 24 hours post injection (Figure 5.12). These data suggest that exposure to oestrogen positive soil extracts did not result in an apparent inflammatory response in the liver compared to vehicle treated mice and mice exposed to oestrogen negative soil extracts.

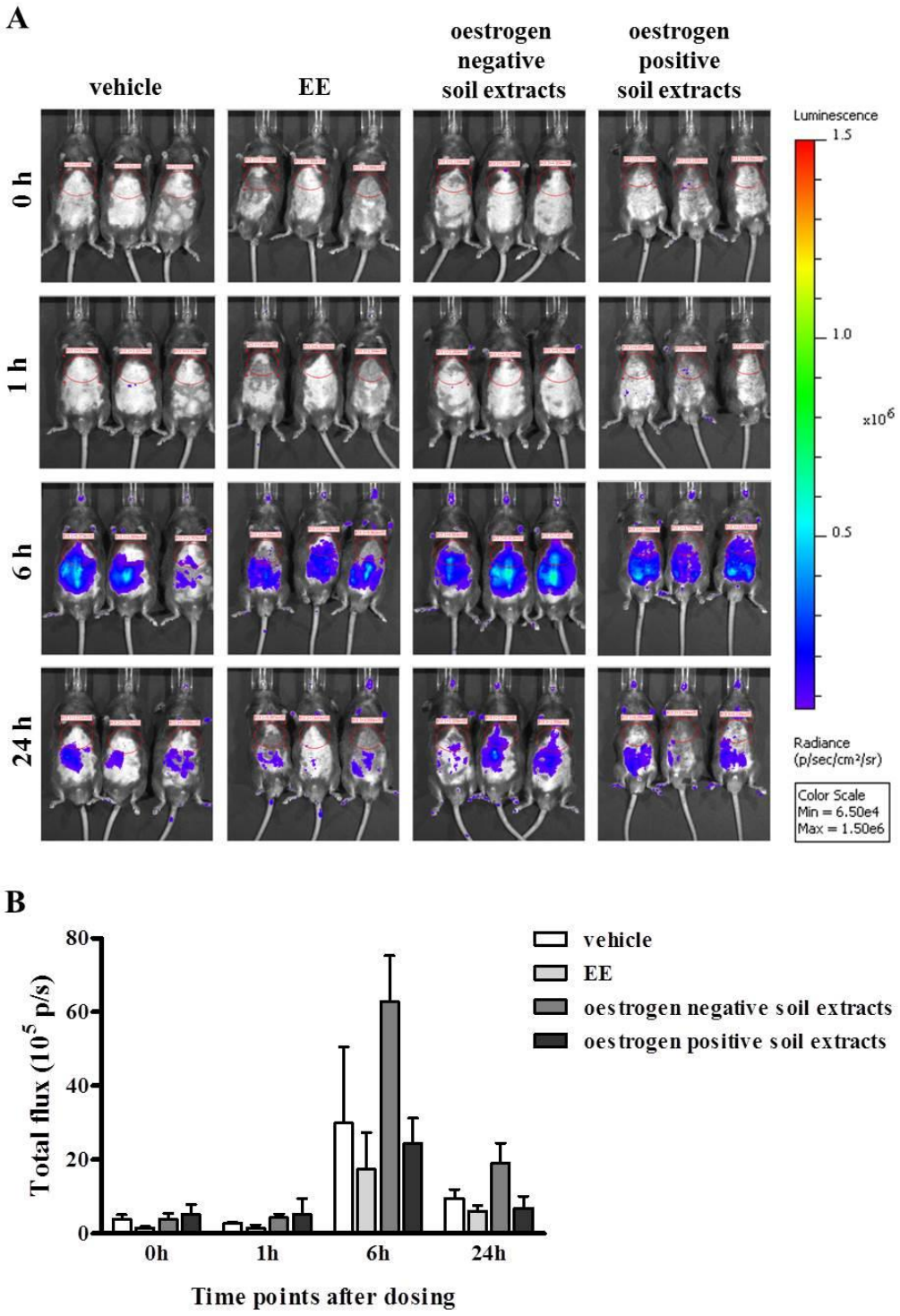

Figure 5.12 Acute exposure to combined oestrogen positive waste site soil extracts does not cause a detectable inflammatory response in the liver. Male adult tg NF-κB-luc mice were dosed with EE, combined oestrogen positive waste site soil extracts or combined oestrogen negative control sites soil extracts by single i.p. injection. Mice in the control group received vehicle (90% olive oil/10% ethanol v/v) alone. (**A**) IVIS images of treated mice at 0, 1, 6 and 24 hours post injection. For imaging, mice were anesthetised using isoflurane and injected with 200 µl of D-luciferin (15 mg/ml) intraperitoneally. Mice were imaged 10 minutes after injection with D-luciferin. (**B**) Quantified upper (hepatic) abdominal luminescence of treated mice at the indicated time points. IVIS data are the mean and standard deviation of the following animal numbers: vehicle: n=3; EE: n=3; oestrogen positive soil extracts: n=3; oestrogen negative soil extracts: n=3. For statistical analysis, One-way ANOVA with Bonferroni post hoc-modifications ($p<0.05$) was used.

To examine if histological changes occurred in the liver following treatment, livers from treated tg NF-kB-luc mice were harvested at the end of the study which were then fixed, processed and sections were stained with haematoxylin and eosin (H&E). Sera of treated mice were collected at termination of the study to analyse the activity of serum ALP enzymes.

Histological examination of portal tracts demonstrated that no apparent histological changes in the portal tract regions could be observed in liver sections of EE, oestrogen positive soil extracts and oestrogen negative soil extracts treated animals compared to the vehicle control group (Figure 5.13). In liver sections from all treatment groups, however, the presence of fat droplets (steatosis) was observed, likely due to large administration volumes of the dosing solution which contained 90% (v/v) olive oil. Despite the lack of any biologically relevant histological changes, Figure 5.14A demonstrates that exposure to the combined oestrogen positive soil extracts resulted in a significant increase in ALP activity, a marker for cholestatic injury compared to both vehicle treated mice and mice exposed to oestrogen negative soil extracts, although there was a significant decrease in ALT activity (Figure 5.14B), a marker for hepatocellular injury, compared to the vehicle control group. Exposure to EE also resulted in a small but significant increase in ALP activity compared to the vehicle control group whereas ALT activities remained unchanged. Exposure to oestrogen negative soil extracts did not result in any significant changes in serum enzyme activities.

Although no biologically relevant histological changes were observed, data in this section suggest that soil samples collected from around an urban waste site contain xenoestrogens that induce clinical chemical markers for cholestatic liver injury. Overall, these data indicate that exposure to environmental xenoestrogens in close proximity to waste sites may have adverse hepatic effects.

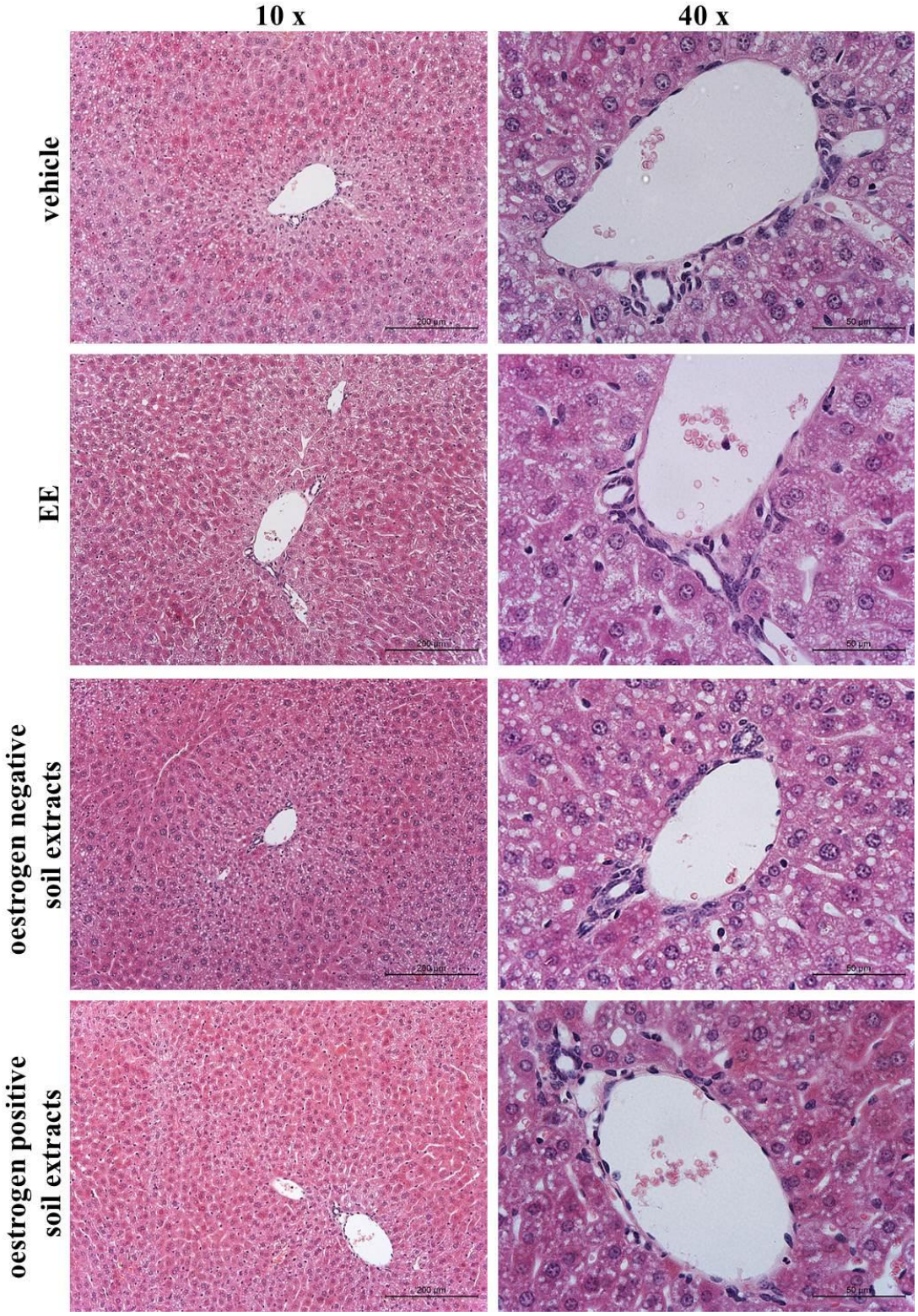

Figure 5.13 Exposure to oestrogen positive waste site soil extracts does not cause any apparent hepatic histological changes. Representative H&E stained liver sections of treated animals (vehicle: n=3; EE: n=3; oestrogen positive soil extracts: n=3; oestrogen negative soil extracts: n=3). Scale bar: 100 μm. Male adult tg NF-κB-luc mice were dosed with EE, combined oestrogen positive waste site soil extracts or combined oestrogen negative control sites soil extracts by single i.p. injection. Mice in the control group received vehicle (80% olive oil/20% ethanol) alone. At 24 hours after injection, animals were terminated by cervical dislocation and their livers collected.

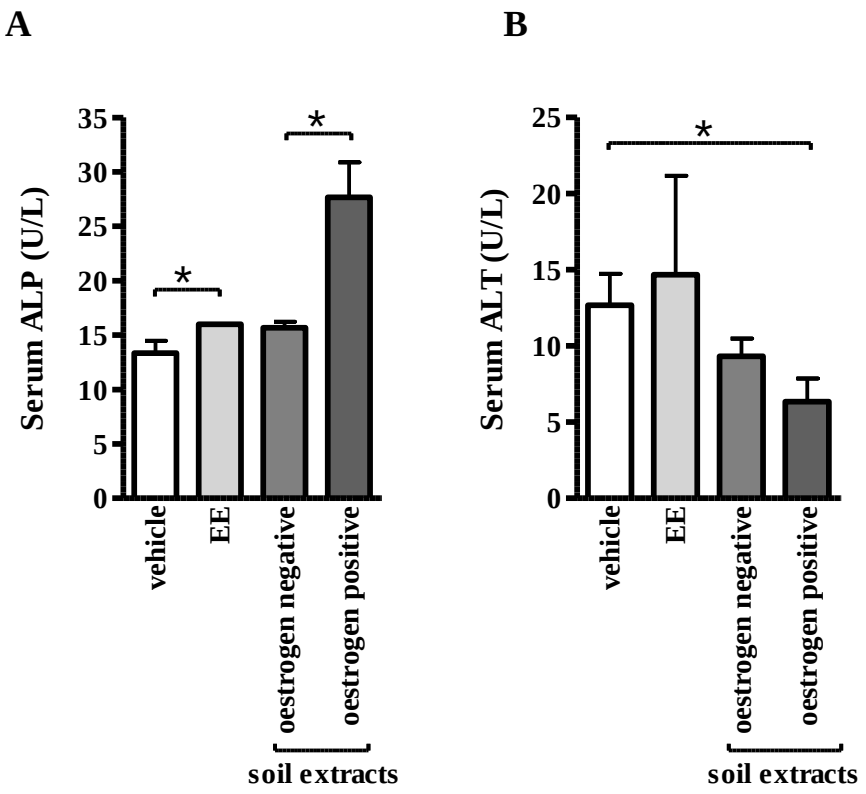

Figure 5.14 Exposure to oestrogen positive waste site soil extracts leads to an increase in ALP serum levels. (**A**) Serum ALP measurements at termination of the study. **(B)** Serum ALT measurements at termination of the study. Male adult tg NF-κB-luc mice were dosed with EE, combined oestrogen positive waste site soil extracts or combined oestrogen negative control sites soil extracts by single i.p. injection. Mice in the control group received vehicle (80% olive oil/20% ethanol) alone. At 24 hours after injection, animals were terminated by cervical dislocation and their blood collected. Serum enzyme data are the mean and standard deviation of the following animal numbers: vehicle: n=3; EE: n=3; oestrogen negative soil extracts: n=3; oestrogen positive soil extracts: n=3. *Significantly different ($p<0.05$) using One-way ANOVA with Bonferroni post-hoc modifications.

5.5. Discussion

Data in this chapter demonstrate that xenoestrogens can be extracted from and detected in soil samples. Soil extracts in close proximity to a waste site were found to contain higher levels of detectable xenoestrogens compared to those prepared from soil samples collected at control sites not expected to be contaminated with chemicals. To my knowledge, this is the first time this approach has been used to help identify potential environmental risk factors associated with adverse health effects due to endocrine disruption.

Using an ER-dependent reporter gene assay, several soil samples collected from around an urban waste site activated the hERα, an effect that was dose-dependent, suggesting that these extracts contain a chemical or a variety of chemicals with xenoestrogenic activity (Figure 5.2, Figure 5.3). In contrast, soil extracts prepared from soil sampled from three separate control sites did not activate the hERα. The observation that the waste site soil extract-induced increase in reporter gene activity is inhibited by the ER antagonist ICI182,780 further confirms that trans-activation of the reporter construct occurred via activation of the ER (Figure 5.4).

In order to test the potential endocrine disrupting effects of xenoestrogens present in waste site soil samples *in vivo*, it was decided to employ a mouse model due to the abundance of transgenic mouse lines available for potential use in follow on studies. Prior to administration of soil extracts to mice, however, it was examined if waste site soil extracts are also activators of the mERs in context of a murine cell line using previously established reporter gene assays.

Results have shown that several waste site ethanol soil extracts activated the mERα in a similar manner to the hERα and activation was inhibited by co-treatment with ICI182,780 (Figure 5.5). Control sites soil extracts did not exhibit any detectable oestrogenic activity. Similarly, several waste site ethanol soil extracts also activated the mERβv1 an effect which was antagonised by ICI182,780 (Figure 5.6). Interestingly, the majority of waste site ethanol soil extracts irreversibly activated the mERβv2 since activation of this receptor by soil-based xenoestrogens, as opposed to activation by E2 or EE, was not antagonised by ICI182,780 (Figure 5.7). Assuming that xenoestrogens bind to the mERβv2 in a similar manner as E2 and EE, this finding suggests that xenoestrogens present in waste site soil extracts may dissociate from the receptor at a significantly reduced rate. Another possible explanation is that xenoestrogens activate the mERβv2 via a different mechanism such as interacting and binding to the receptor through an alternative binding site which could prevent ICI182,780-mediated

antagonism. This suggests that soil-based xenoestrogens may have 'super-activating' characteristics with an ERβ variant.

Since waste site soil extracts activated murine ERs, the mouse was considered a good model for examining potential endocrine disruptor properties of these extract *in vivo*. The usability of transgenic NF-κB mice and the ability to detect xenoestrogen-induced hepatic adverse effects in this mouse model was explored first. Acute exposure of NF-κB mice to the known xenoestrogen EE, but not butyl paraben, caused a detectable inflammatory response in the liver and EE treatment further showed an increase in serum ALP activity, a clinical chemical marker for cholestasis (Figure 5.8, Figure 5.10). Histological changes in the portal tract regions of H&E stained liver sections, however, were not detected (Figure 5.9). An explanation for this could be that 1) the time of exposure was insufficient to cause any histological effects and 2) histological analysis was limited to the sections used which only represent a fraction of the liver's response. In contrast, IVIS imaging determines inflammation throughout the organ and might show hepatic responses to treatments not detectable in liver sections. Taken together, findings suggest that NF-κB mice represent a refined model for assessing the potential adverse hepatic effects of xenoestrogens, a model that will also allow examining inflammation at various time points without the need for animal termination.

EE is known to be able to induce cholestatic injury and is often used in *in vivo* rodent studies to induce oestrogen-mediated cholestasis (Rodriguez-Garay, 2003). Although butyl paraben did not have any adverse hepatic effects in this study, it is known to have oestrogenic activity in rodents *in vivo* (Routledge *et al.*, 1998) but the development of cholestasis as a result of butyl paraben administration has not been reported. Shah and Verma (2001) have shown that chronic butyl paraben exposure by i.p. injection caused oxidative stress in the liver of mice (Shah and Verma, 2011). Although not directly applicable to the liver, another study reported that butyl paraben inhibited dermal oestrogen sulfotransferases, enzymes which inactivate oestrogens through biotransformation reactions (Prusakiewicz *et al.*, 2007). The inhibition of hepatic sulfotransferases by butyl paraben could therefore potentially lead to elevated oestrogen levels and prolonged exposure may have cholestatic effects.

Following confirmation that NF-κB mice can be employed to detect xenoestrogen-mediated hepatic adverse effects, ethanol soil extracts that have been shown to activate the mERs *in vitro* (oestrogen positive, see Figure 5.5, Figure 5.6, Figure 5.7) were combined and concentrated to test for hepatic adverse effects in mice. Similarly, ethanol soil extracts

collected from control sites which exhibited little or no oestrogenic activity in mouse-based reporter gene assays (oestrogen negative) were pooled. The potential of combined oestrogen positive soil extracts to activate the mERs was confirmed in reporter gene assays, whereas combined soil negative extracts showed no significant oestrogenic activity (Figure 5.11).

Acute exposure (single i.p. injection) of mice to combined oestrogen positive soil extracts did not result in a detectable inflammatory response in the liver compared to the vehicle control group (Figure 5.12). There was no observation of any biologically relevant histological changes in the liver (Figure 5.13) which was expected given that 3 injections on 3 consecutive days of EE did not cause any detectable hepatic histological changes (Figure 5.9) despite a detectable inflammatory signal (Figure 5.8). A significant increase in serum ALP activities in mice exposed to combined oestrogen positive soil extracts was the only evidence for a xenoestrogen-mediated cholestatic effect (Figure 5.14A). IVIS data has shown that the luminescence signal and therefore NF-κB activity in the abdominal region was increased at 6 h post injection in all treatment groups. This is likely due to the injection of relatively large volumes of vehicle or treatment solutions (20 ml/kg body weight) which were constituted in 90% olive oil/10% ethanol (v/v). The appearance of fat depositions (steatosis) in H&E stained liver sections of all treatment groups (likely caused by olive oil) supports the observation that the injection volume was too high. It was decided, however, to inject mice with a relatively large volume in order to avoid precipitation of xenoestrogens from the olive oil/ethanol solution. The increase in NF-κB activity observed at 6 hours was reduced by 24 hours post injection in all treatment and control groups but a significant signal in mice exposed to oestrogen positive soil extracts was not detectable. Due to a limited volume of soil extracts that was available, it was only possible to expose mice to soil extracts by i.p. injection once with 3 mice per group to be able to conduct statistical analysis. Longer treatments may be necessary to detect hepatic inflammation by IVIS as observed following exposure to EE and butyl paraben which were administered by i.p. injection on 3 consecutive days.

PBC is believed to be triggered in genetically pre-disposed individuals through exposure to an environmental chemical(s)/toxin(s) or infectious agent(s). A link between the exposure to oestrogens in the form of hormonal replacement therapy and an increased risk of developing PBC exist (Gershwin *et al.*, 2005) suggesting that exposure to xenoestrogens around a waste site could, at least in part, pose an environmental risk factor for the development of PBC. Taking into consideration several factors including the amount of soil collected and the final extraction volume, it seems rather unlikely that exposure to a xenoestrogen alone could be the sole trigger for such a disease. On the basis of dose response data for the hERα and

approximation of EC_{50} values it was estimated that, at a dilution of 1/5000, waste site soil sample 3 has similar oestrogenic activity as 1 pM E2 (10^{-12} M). This suggests that the concentration of xenoestrogens in waste site sample 3 was approximately within the range of 1-10 nM E2 equivalents. The concentration of E2 equivalents in waste site soil sample 3 was therefore calculated to be in the range of 80 – 800 pmol/kg soil. If the oestrogenic activity in waste site soil sample 3 was associated solely with E2, this is equivalent to 22-220 nM E2/kg soil. In sexually mature adult women, typical serum E2 concentrations are within 200-1000 pM. Assuming a serum volume of 4L and that only serum levels of E2 are relevant, this suggests total body E2 levels of 800 – 4000 pmoles/person. If complete oral absorption occurs and the distribution, metabolism and excretion of the xenoestrogen(s) were similar to E2, an exposure to 1-10 kg soil/person to achieve low oestrogenic activity or exposure to 5-50 kg soil/person to achieve high E2 levels would be required to obtain biologically equivalent levels of E2. Human ERα dose-response data for waste site soil extract 12 has shown that this extract was more potent compared to waste site soil extract 3. Employing the above assumptions and calculations, however, exposure to 0.1-1 kg soil/person (low oestrogenic activity) or 0.5-5 kg soil/person (high oestrogenic activity) would still be required to achieve biologically relevant serum levels of E2 equivalents. Estimated concentrations of E2 equivalents present in waste site ethanol soil extracts 3 and 12 and mass of soil required for exposure to result in oestrogenic activity are summarised in Table 5.3.

	Waste site extract 3	**Waste site extract 12**
Approximate range of concentration of E2 equivalents in soil extracts	1 - 10 nM	10 – 100 nM
Approximate range of concentration of E2 equivalents per kg soil	80 – 800 pmoles	800-8000 pmoles
Range of mass of E2 equivalent per kg soil	22-220 ng	220 – 2200 ng
Mass of soil required for exposure to achieve low oestrogenic activity	1 – 10 kg	0.1 – 1 kg
Mass of soil required for exposure to achieve high oestrogenic activity	5 – 50 kg	0.5 – 5 kg

Table 5.3 Approximate concentration of E2 equivalents in waste site soil extracts 3 and 12 and mass of soil required for exposure to achieve low and high oestrogenic activity, respectively.

Taking these estimations into account, exposure to large amounts of waste site soil extracts seems to be required for xenoestrogens to cause any adverse hepatic effects through endocrine disruption. Considering that some of the soil-based xenoestrogens may have 'super-activating'

characteristics with an ERβ variant, however, these chemicals could be a component of a xenobiotic insult that triggers PBC.

Chapter 6. Investigation of ER expression in primary biliary epithelial cells

Biliary epithelial cells (BECs), which line the intrahepatic bile ducts in the liver, play an important role in disease progression of various cholestatic liver diseases collectively termed cholangiopathies. Cholangiopathies are commonly characterised by the loss of intrahepatic bile ducts and therefore also known as 'Vanishing Bile Duct Syndromes' (Desmet *et al.*, 1998). To compensate for a reduction in bile ducts, residual ducts proliferate in the early stages of the disease up to a point where the loss of ducts outweighs the proliferative potential leading to terminal ductopenia and thus cholestatic conditions (Alvaro *et al.*, 2000b; Alvaro *et al.*, 2006b).

It has been established that the proliferation of BECs is regulated by a number of factors including hormones, growth factors and neuropeptides (Alvaro *et al.*, 2000b). More recently, it was discovered that in rats, oestrogens are involved in the modulation of the proliferative response of BECs to damage *in vitro* and *in vivo* and that rat cholangiocytes express ERα and ERβ (Alvaro *et al.*, 2002). Both ER subtypes have also been reported to be expressed in BECs in several liver diseases in humans (Alvaro *et al.*, 2006a; Torrice *et al.*, 2006) including in the most frequent acquired cholangiopathy PBC (Alvaro *et al.*, 2004). In contrast, BECs in normal (healthy) liver have not been found to express any ERs (Alvaro *et al.*, 2004).

Considering the role of oestrogens in BEC proliferation in disease and the finding that, in humans, ERs are expressed in BECs in diseased liver including PBC but not in healthy liver, one may suggest that a correlation between ER expression in BECs and disease progression exists and that oestrogens may play an important role in the modulation of PBC and other liver diseases. In fact, PBC predominantly occurs in females (9:1 female/male ratio) and commonly affects women in the peri- and post-menopausal period during which oestrogen levels decrease (Alvaro *et al.*, 2006b) further highlighting a potential role for oestrogen in PBC progression.

Since oestrogens largely mediate their effect through interaction with the ERs, expression of the receptor is required in oestrogen target tissues or cells. Although a number of studies regarding ER expression in BECs have been conducted, data especially for ER expression in mouse BECs is limited. The aim of this chapter was therefore to investigate if BECs isolated from human as well as mouse liver express the ERs.

6.1. ER expression in primary hBECs

To examine the expression of hERα and hERβ in primary hBECs, cells were isolated from surgical liver resections as described in Section 2.4. Following isolations, hBECs were cultured until they were confluent enough for use in experiments.

To confirm that cells isolated from human liver tissue are BECs, and to verify that the isolated cell population is pure, cells cultured for 4 days following isolation were examined for expression of the epithelial marker CK19 and the mesenchymal cell marker vimentin, which is often used to test if cells undergo epithelial-to-mesenchymal transdifferentiation (Lamouille *et al.*, 2014), by immunocytochemistry. Figure 6.1 demonstrates that the majority of cells in the field of view stained positive for CK19 indicating that primarily hBECs were isolated. A number of cells, however, stained positive for vimentin indicating that either 1) the isolated cell population is not pure and contains cells which are of mesenchymal origin such as fibroblasts or that 2) hBECs transdifferentiate from an epithelial to a mesenchymal phenotype with time in culture.

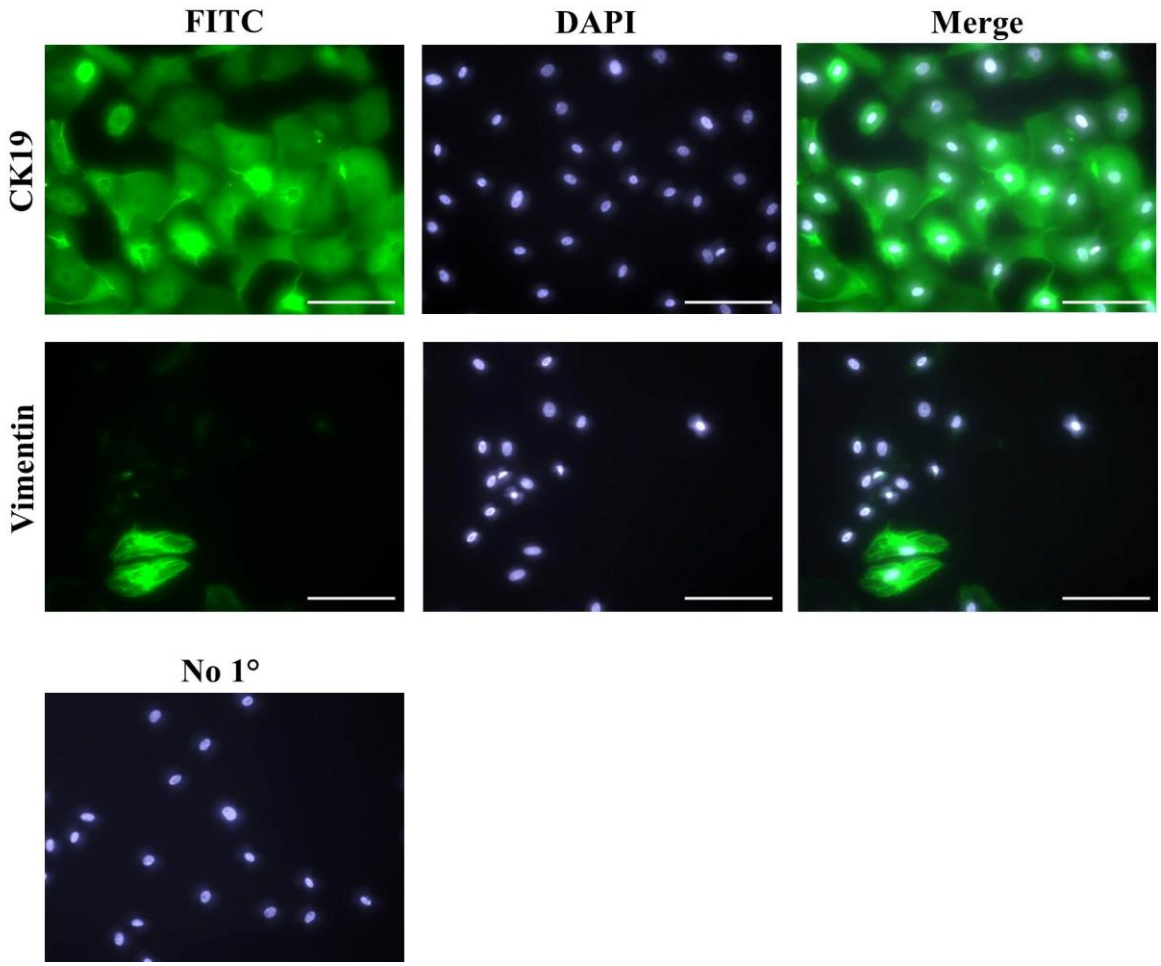

Figure 6.1 Confirmation of CK19 expression in primary hBECs. Immunocytochemical staining for the epithelial marker CK19 and the mesenchymal cell marker vimentin in hBECs isolated from human liver tissue. Following isolation, hBECs were cultured for 4 days prior to fixation, blocking and staining. No 1° control cells were incubated with the secondary antibody only. Cell nuclei were counterstained with DAPI. Scale bars: 50 μm. Data are typical of three separate experiments.

Following confirmation that isolated cells from human liver resections represent a relatively pure population of hBECs, it was examined whether hBECs express the ERs. BECs were isolated from human liver tissue and cultured for different time periods until hBECs expanded enough to be harvested for isolation of RNA and analysis for the expression of hERα and hERβ mRNA. Note that hBECs cultured for 3, 7 and 17 days are from the same liver resection whereas hBECs for all other time points were isolated from separate liver resections (see also Table 6.1).

Time in culture	Number of passages	Liver Resection #	Tissue code
0 days (1)	-	1	NHL44
0 days (2)	-	2	NHL43
3 days	-	3	NHL42
7 days	-		
17 days	-		
20 days	-	4	NHL41
24 days	-	5	No information available
30 days	1	6	No information available
41 days	1	7	No information available
43 days	1	8	No information available

Table 6.1 Details for culture time, number of passages and source of isolated primary hBECs.

Figure 6.2A shows that cells cultured for 3 days express detectable levels of hERα mRNA with reduced, but detectable levels of hERα found in cells cultured for 7 days (liver resection #3). ERα mRNA was also detected in hBECs after 24 days in culture (Figure 6.2B, liver resection #5). Human BECs cultured for other time periods (i.e. 17, 20, 30, 41 and 43 days) did not express any detectable levels of hERα mRNA. There was no evidence for the expression of hERβ mRNA in cultured hBECs isolated from any of the 8 liver resections and grown for the indicated time periods.

Cells that were harvested immediately after isolation (0 days (1) and 0 days (2)) did not show any detectable levels of hERα and hERβ mRNA (Figure 6.2A). These cells did not express detectable levels of CK19 mRNA (as opposed to hBECs that were cultured after isolation), however, suggesting that the initial number of hBECs isolated is low and that cells require time in culture to expand.

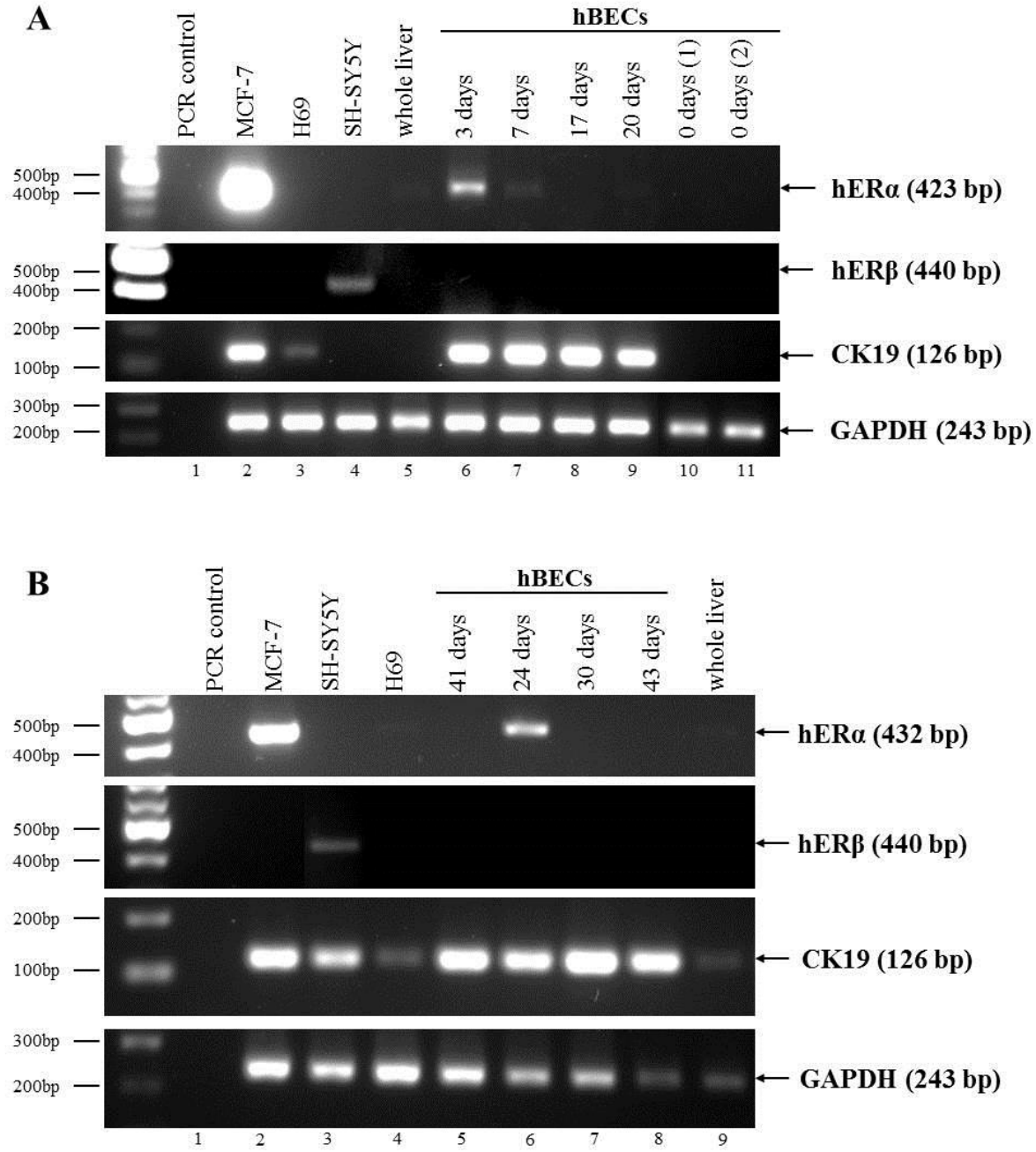

Figure 6.2 Examination for hER mRNA expression in primary hBECs. RT-PCR analysis for hERα and hERβ mRNA expression in primary hBECs that were isolated from human liver tissue and cultured for (**A**) 0-20 days or (**B**) 24-43 days as indicated. Human BECs were also analysed for CK19 expression to confirm epithelial origin. The human brest cancer cell lines MCF-7 and MDA-231, the human BEC cell line H69, the human neuroblastoma cell line SH-SY5Y as well as whole human liver were included as positive or negative controls. RNA was isolated from cells and tissue followed by RT-PCR (32 PCR cycles) using primers specific for the indicated mRNA sequences. GAPDH was used as a loading control. PCR products were separated by agarose electrophoresis and visualised by UV transillumination.

Due to generally low numbers of hBECs that can be isolated at any one time and the observation that the isolated cell population of hBECs is not pure and contains cells with a mesenchymal phenotype (either due to fibroblast contamination or epithelial-to-mesenchymal

transdifferentiation of hBECs), analysis for hER protein expression was performed by immunocytochemistry rather than Western Blot. Using immunocytochemistry to determine ER protein expression will allow examining if the hER is co-localised in cells that stain positive for CK19 for verification of potential ER expression in hBECs.

Figure 6.3 demonstrates that double staining for expression of the epithelial marker CK19 and the hERα did not show any detectable levels of hERα protein in isolated hBECs (liver resection #2) cultured for 5 days. It appears that the anti-mouse secondary antibody is, however, able to bind to Dynabeads used for immunomagnetic purification of hBECs. This results in green staining which resembles beads (see also no 1° control). Dynabeads are indicated with an arrow in expanded images of hERα staining (A and B).

Although hERα protein was undetectable in hBECs, staining for hERβ has shown that this receptor subtype was detected in some CK19 positive cells, exhibiting nuclear localisation (Figure 6.4). Arrows with a drawn-through line indicate nuclear hERβ staining whereas arrows with an interrupted line indicate staining of Dynabeads in expanded images (Figure 6.4, images A and B).

MCF-7 cells, which express the hERα and HEK293 cells which are ER negative (see Figure 3.8 and Figure 3.18) were used as controls and were similarly stained. Figure 6.5 demonstrates that hERα, but not hERβ was detectable in MCF-7 cells with hERα being localised in cell nuclei. Double staining of HEK293 cells did not show any detectable levels of hERα and hERβ (Figure 6.6).

These results indicate that although hERα mRNA was detectable in hBECs from 2 separate liver resection with culture periods of 3-7 and 24 days (#3 and #5, respectively), hERα protein was not shown to be expressed in hBECs isolated from liver resection #2 following culture for 5 days. Despite the lack of detection of hERβ mRNA in hBECs from liver resections, immunocytochemical analysis has shown that the hERβ protein can be detected in isolated, cultured hBECs.

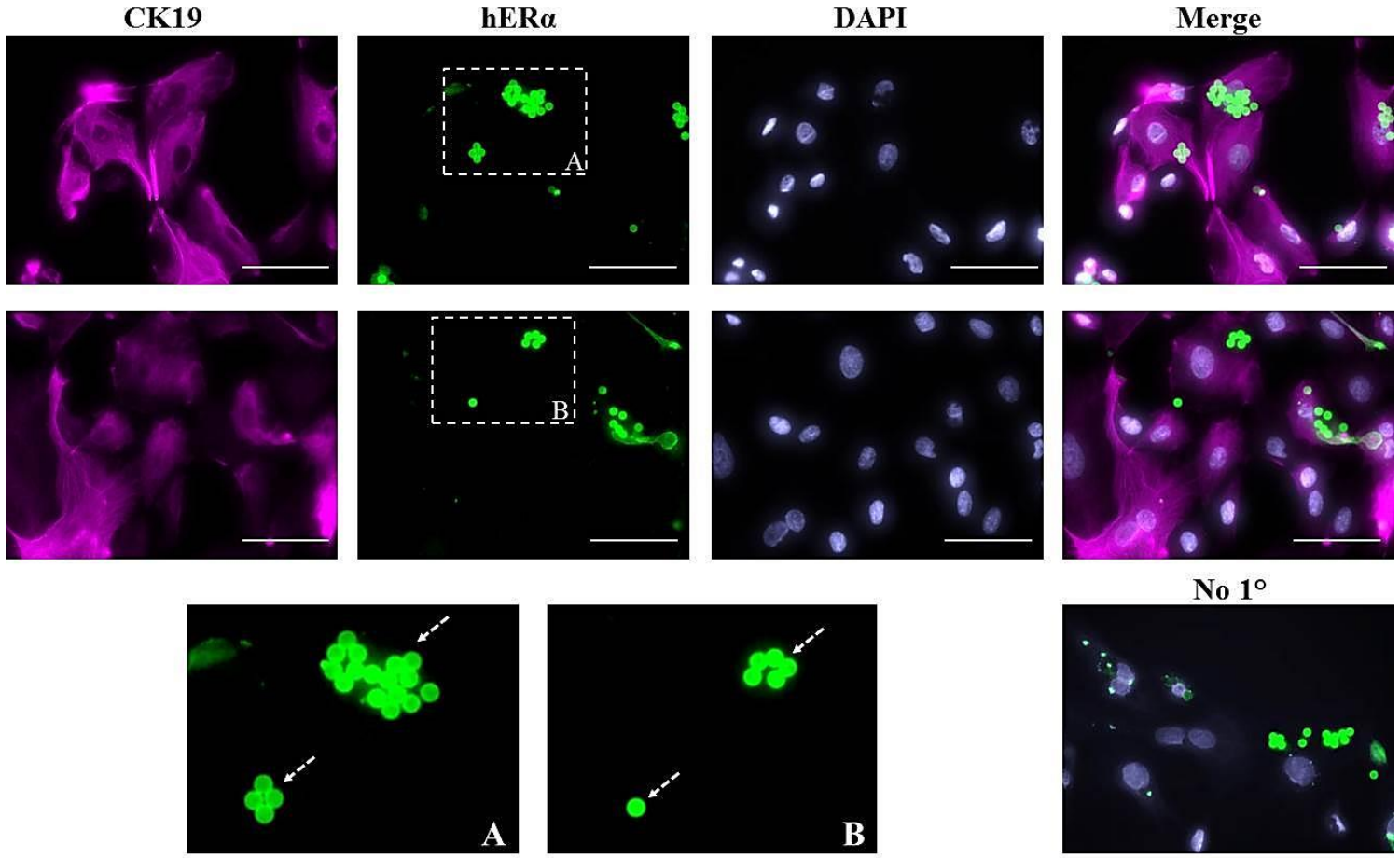

Figure 6.3 Analysis for hERα protein expression in primary hBECs. Immunocytochemical double staining for the expression of CK19 and hERα protein in primary hBECs isolated from human liver tissue. Following isolation, cells were cultured for 5 days prior to fixation, blocking and staining. No 1° control cells were incubated with the secondary antibodies only. Cell nuclei were counterstained with DAPI. Scale bars: 50 μm. Data are representative of two separate experiments.

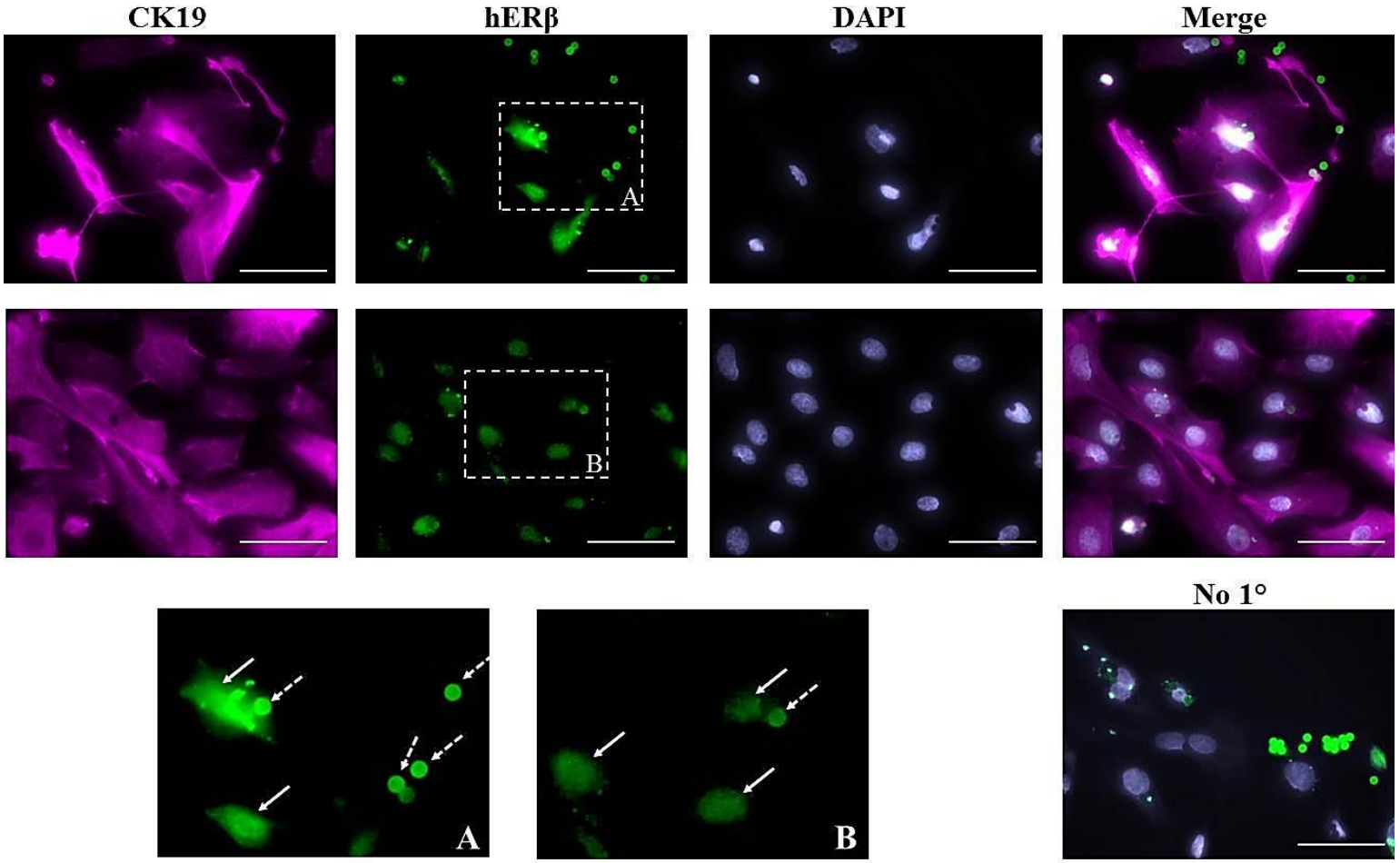

Figure 6.4 Analysis for hERβ protein expression in primary hBECs. Immunocytochemical double staining for the expression of CK19 and hERβ protein in primary hBECs isolated from human liver tissue. Following isolation, cells were cultured for 5 days prior to fixation, blocking and staining. No 1° control cells were incubated with the secondary antibodies only. Cell nuclei were counterstained with DAPI. Scale bars: 50 μm. Data are representative of two separate experiments.

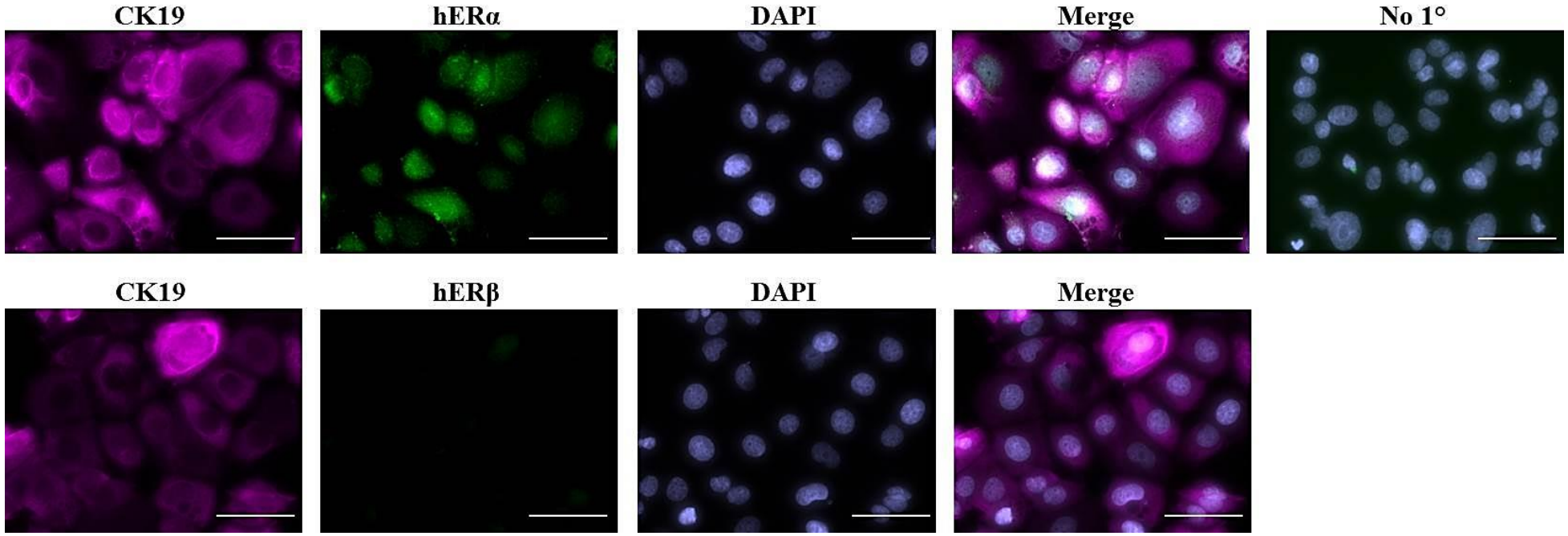

Figure 6.5 Analysis for hER protein expression in MCF-7 cells. Immunocytochemical double staining for the expression of CK19 and hERα or hERβ protein in MCF-7 cells for verification of correct antibody functioning. No 1° control cells were incubated with the secondary antibodies only. Cell nuclei were counterstained with DAPI. Scale bars: 50 μm. Data are representative of two separate experiments.

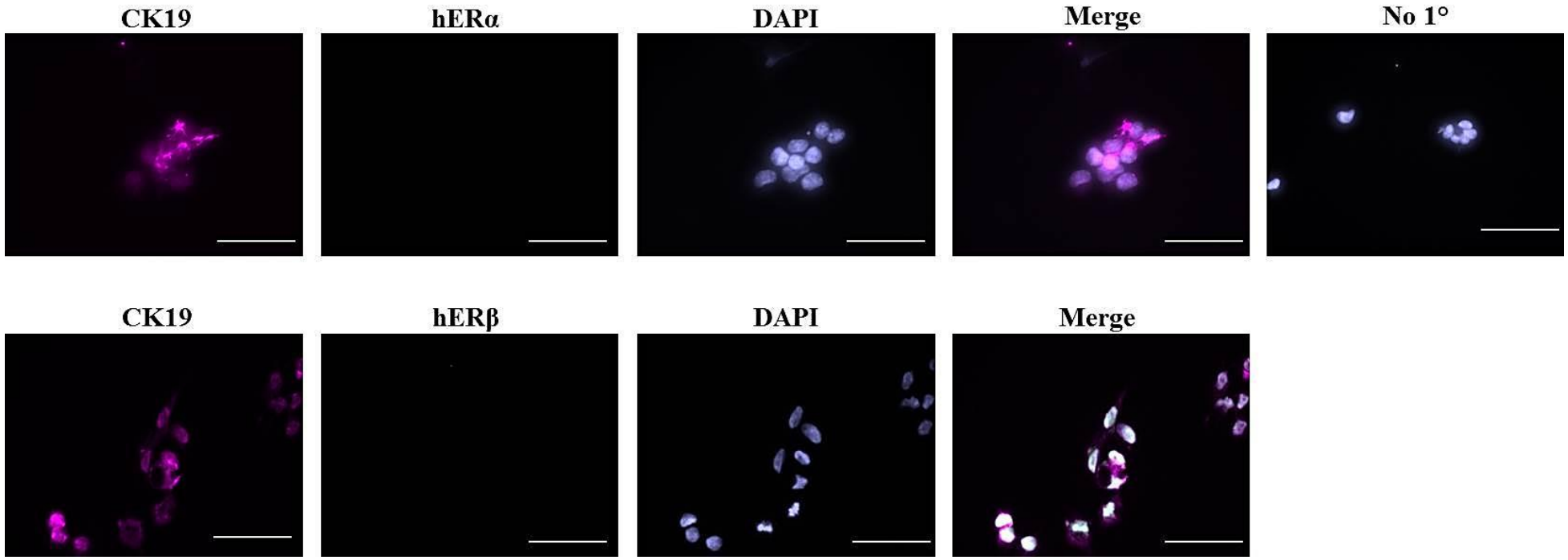

Figure 6.6 Analysis for hER protein expression in HEK293 cells. Immunocytochemical double staining for the expression of CK19 and hERα or hERβ protein in HEK293 cells for verification of correct antibody functioning. No 1° control cells were incubated with the secondary antibodies only. Cell nuclei were counterstained with DAPI. Scale bars: 50 μm. Data are representative of two separate experiments.

6.2. ER expression in primary mBECs

Although ERα and ERβ have been reported to be expressed in human and rat BECs and their expression markedly upregulated in a disease setting (Alvaro *et al.*, 2000a; Alvaro *et al.*, 2004), there is limited data in the literature regarding ER expression in mBECs.

To examine if mBECs express the mERs, primary BECs were isolated from C57Bl/6 wt mouse liver as described in Section 2.5. Since Dynabeads used for immunomagnetic purification of hBECs are specific to human, they could not be used for the isolation of mBECs. Figure 6.7 shows that isolation generated a population of cells which, after 24 hours in culture, had similar morphology and which proliferated in culture (see image taken at 48 hours).

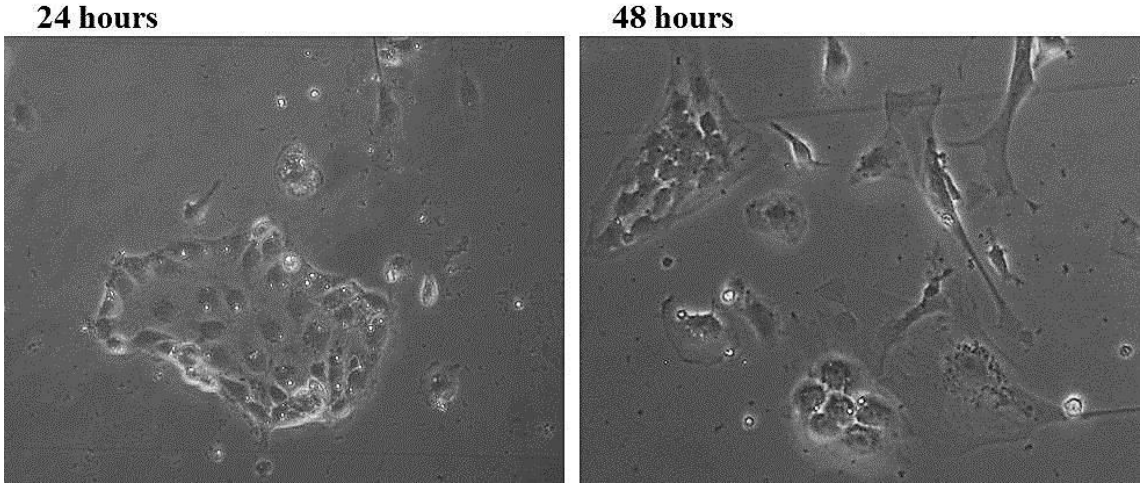

Figure 6.7 Light microscope images of primary mBECs. Images were taken 24 hours (left panel) and 48 hours (right panel) after isolation of cells from murine liver.

Immunocytochemical staining of isolated cells from mouse liver for the epithelial marker CK19 after 2 days in culture confirmed that mBECs can be isolated without immunomagnetic purification with Dynabeads (Figure 6.8). Several cells did not stain positive for CK19 indicating that isolated cells do not represent a pure population of mBECs. Counting CK19 positive cells and total cell numbers from 3 separate fields of view revealed that an average of 57% of isolated cells were mBECs.

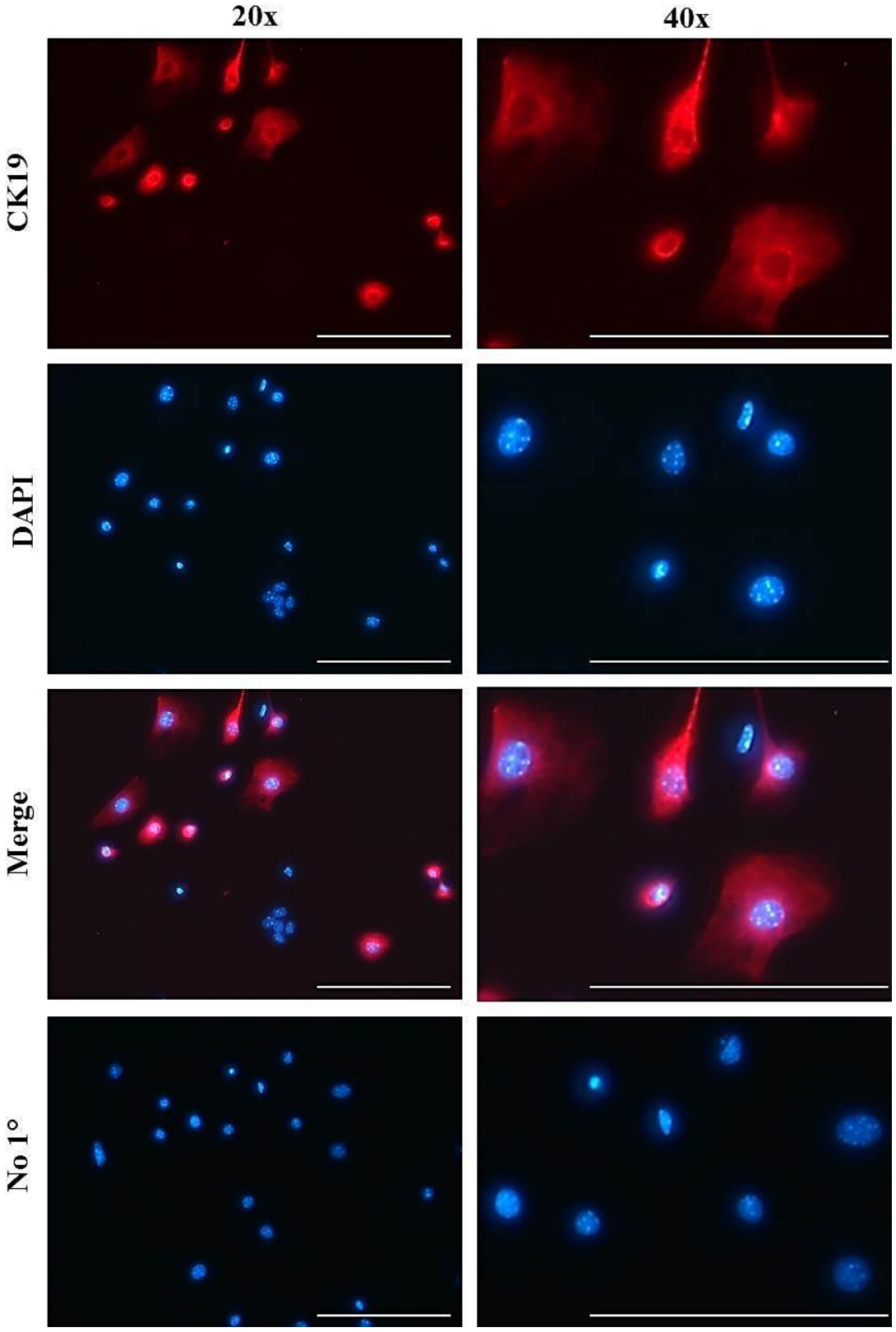

Figure 6.8 Confirmation of CK19 expression in primary mBECs. Immunocytochemical staining for the epithelial marker CK19 in mBECs isolated from mouse liver from C57Bl/6 wt mice. Following isolation, mBECs were cultured for 2 days prior to fixation, blocking and staining. No 1° control cells were incubated with the secondary antibody only. Cell nuclei were counterstained with DAPI. Scale bars: 100 μm.

Examination for mER expression by RT-PCR shows that after 6 days in culture, mERα mRNA was detectable in primary mBECs, however, there was no evidence for mERβ mRNA expression in these cells. Detectable mRNA expression of the epithelial marker CK19 confirms that the isolated cells were mBECs although the presence of vimentin positive cells suggests that during their time in culture, mBECs may have undergone epithelial-mesenchymal trans-differentiation to fibroblasts or that fibroblasts contaminated isolated mBECs and expanded in culture. The hepatocyte marker CYP2E1 was not detectable in isolated mBECs indicating that hepatocytes are not part of the isolated cell population.

Western Blot analysis showed that mERα protein was not detectable in isolated mBECs after 0 and 2 days in culture. There was evidence for the expression of mERβ protein in mBECs, however, at 0 but especially 2 days in culture suggesting that mBECs express the mERβ which may increase with time in culture. CYP2E1 protein was detectable in mBECs after 0 hours, which decreased after 2 days in culture, suggesting that hepatocytes may have been present at isolation. Since hepatocytes do not proliferate in culture and if viable, de-differentiate, they are unlikely, however, to be present in isolated cells grown in cultures. Murine uterus, liver and ovary tissues were included as positive and/or negative controls.

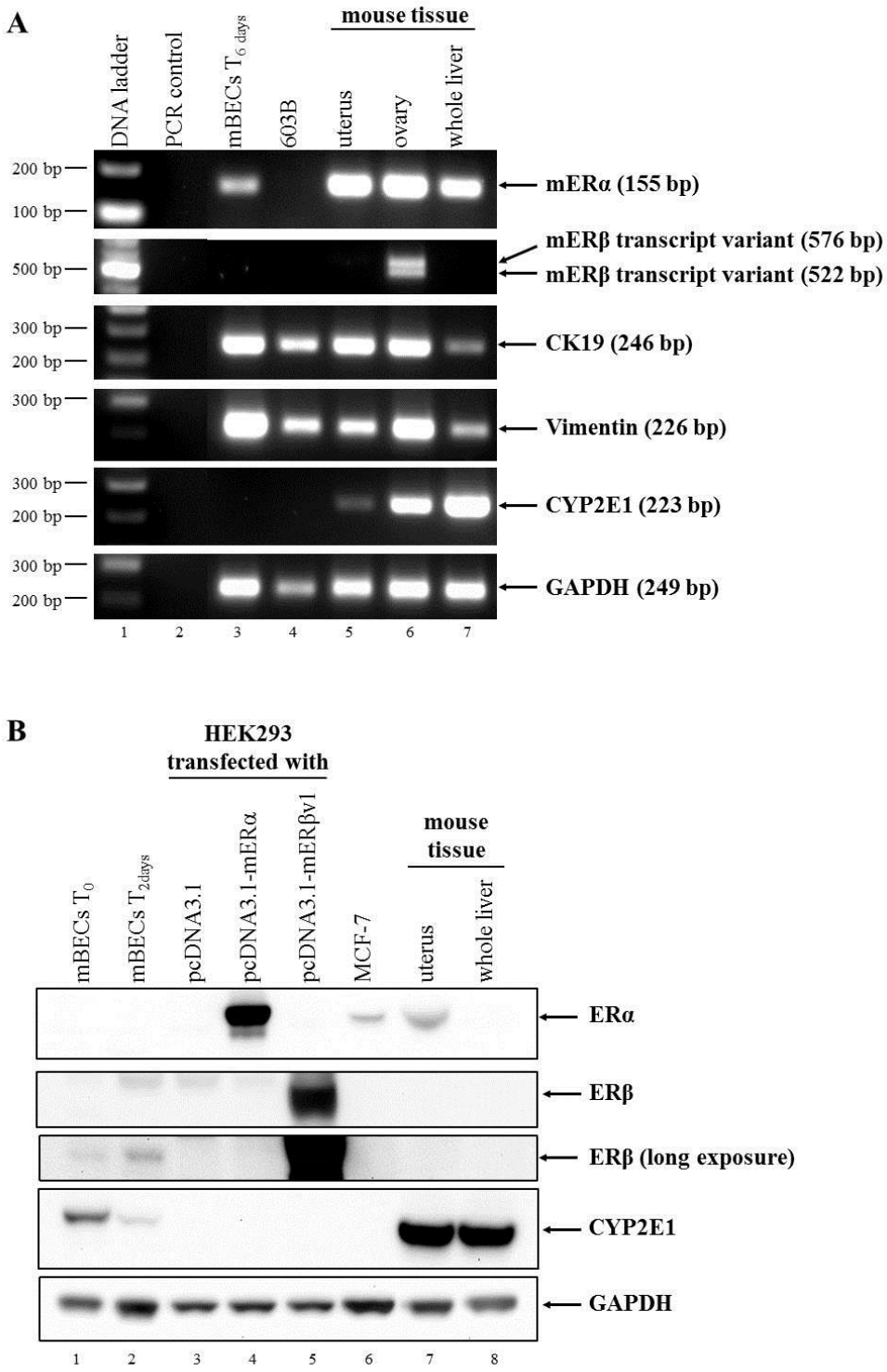

Figure 6.9 Examination for mER expression in primary mBECs by RT-PCR and Western Blot. (A) RT-PCR analysis for mouse hERα and hERβ mRNA expression in primary mBECs that were in culture for 6 days, 603B cells and the indicated murine tissues. Mouse BECs were also analysed for CK19, Vimentin and CYP2E1 mRNA expression. RNA was isolated from cells as well as murine tissue followed by RT-PCR (30 PCR cycles) using primers specific for the indicated mRNA sequences. GAPDH was used as a loading control. PCR products were separated by agarose electrophoresis and visualised by UV transillumination. **(B)** Western Blot analysis for mouse ERα and ERβ protein expression in primary mBECs that were in culture for 6 days, 603B cells and the indicated murine tissues. Total protein was isolated from cells and murine tissue following separation by gel electrophoresis and visualisation (20 μg total protein/lane).

Since RT-PCR and Western Blot analysis suggest that other cell types other than BECs may be present in the cell population, immunocytochemical double staining for the epithelial marker CK19 and the mERα or mERβ was performed to verify that the expression of the mER proteins is localised to CK19 positive cells (mBECs). Figure 6.10 demonstrates that a population of cells cultured for 1 day after isolation stained positive for CK19, however, several cells in the field of view were CK19 negative confirming that the cell population was not pure. Staining for mERα and mERβ shows that both receptor subtypes were not detectable in CK19 positive or negative cells grown in culture for 1 day.

In isolated cells that were cultured for 4 days, mERα protein was not detected in CK19 positive cells (Figure 6.11). Staining for mERβ protein demonstrates that there was evidence for mERβ protein expression in cells that also stained positive for CK19 with mERβ exhibiting nuclear localisation.

These data suggest that mBECs are unlikely to express detectable levels of the mERs in normal liver. Following time in culture which may mimic a disease setting, however, expression of mERβ protein was induced.

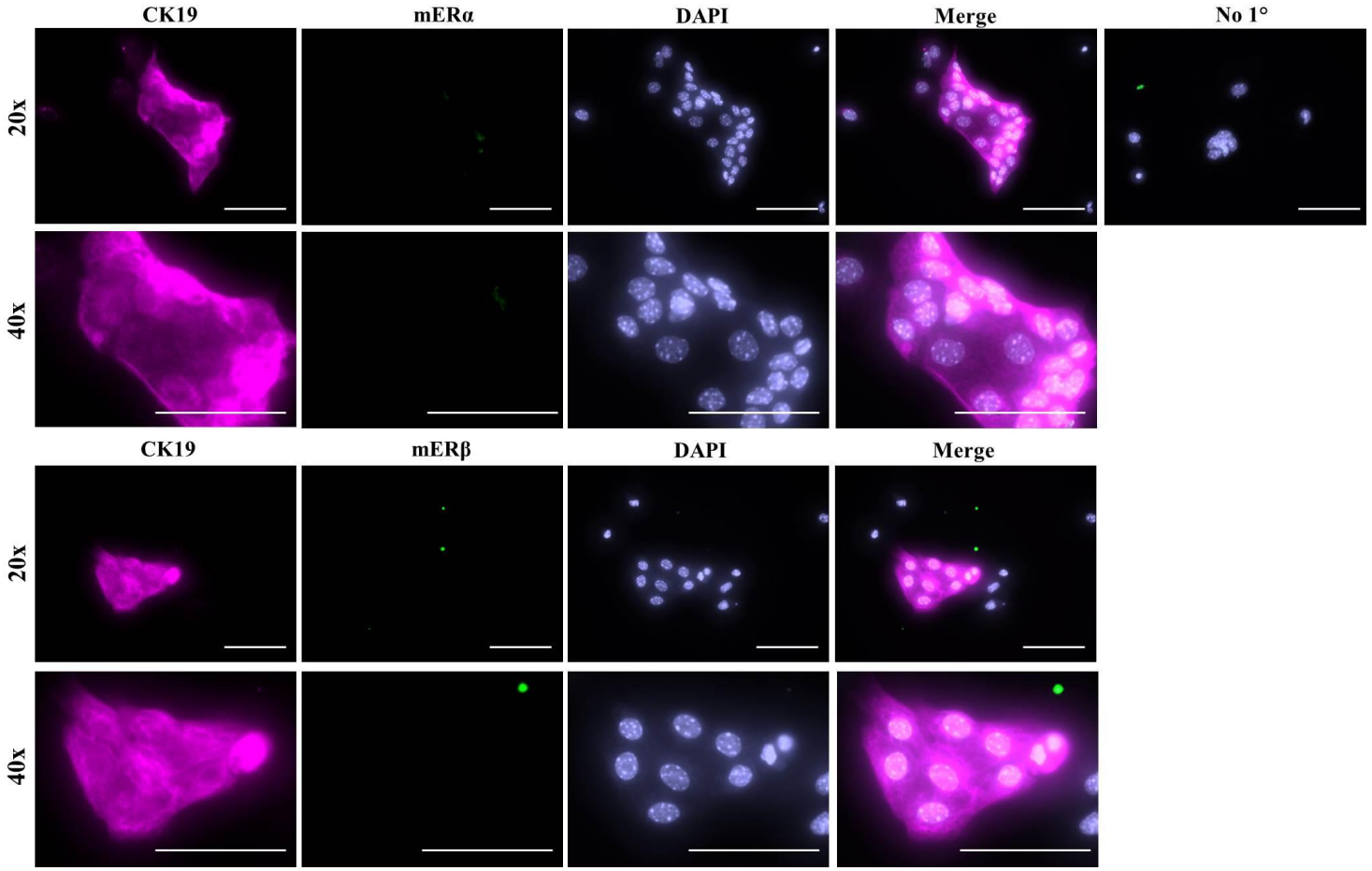

Figure 6.10 Examination for mER expression in primary mBECs (1 day) by immunocytochemistry. Immunocytochemical double staining for the expression of CK19 and mERα or mERβ protein in primary hBECs isolated from mouse livers. Following isolation, cells were cultured for 1 day as indicated prior to fixation, blocking and staining. No 1° control cells were incubated with the secondary antibodies only. Cell nuclei were counterstained with DAPI. Scale bars: 50 μm. Data are representative of two separate experiments.

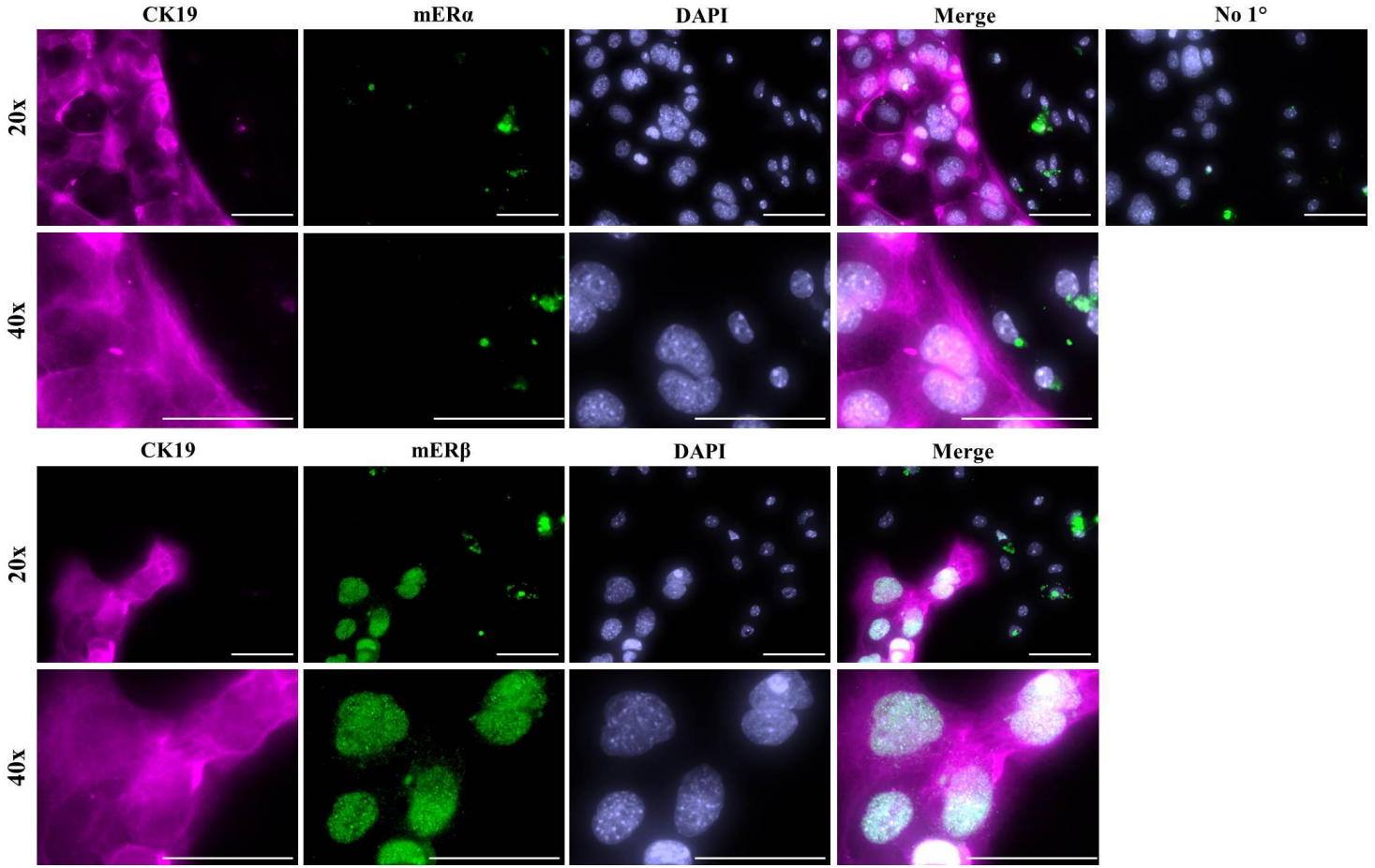

Figure 6.11 Examination for mER expression in primary mBECs (4 days) by immunocytochemistry. Immunocytochemical double staining for the expression of CK19 and mERα or mERβ protein in primary hBECs isolated from mouse livers. Following isolation, cells were cultured for 4 days as indicated prior to fixation, blocking and staining. No 1° control cells were incubated with the secondary antibodies only. Cell nuclei were counterstained with DAPI. Scale bars: 50 µm. Data are representative of two separate experiments.

6.3. Discussion

Since oestrogens have been shown to modulate the proliferative ability of hBECs in cholangiopathies, and their effects are largely mediated through interaction with the ERs, this chapter aimed to investigate if isolated human and mouse BECs express the ERs. Examination of hBECs for the expression of the hERα and hERβ has shown that hBECs hERα mRNA transcript was detected in hBECs isolated from 2 separate liver resections. The majority of hBECs isolated did not express any detectable levels of hERα mRNA (Figure 6.2). ERα protein was not found to be expressed in any of the isolated hBECs analysed by immunocytochemistry (Figure 6.3). Despite the lack of evidence for hERβ mRNA expression in all isolated hBECs (Figure 6.2), immunocytochemical staining showed that hBECs express detectable levels of hERβ protein after 5 days in culture which was localised to the nucleus (Figure 6.4). Access to patient and clinical data was not available and as a result it is unclear under which conditions (e.g. the type of liver disease or administered medication) the hERβ was expressed in isolated hBECs. Since liver resections are normally performed in patients with secondary tumours, and the tissue used was from histologically normal margins, it can be assumed that BECs were isolated from normal liver and in a healthy state.

A predominance of ERβ expression in a disease setting has been reported by several studies. Alvaro et al. (2004) have shown that expression of hERβ in hBECs from PBC patients was markedly increased (50-65%, percentage of hERβ positive BECs over the total BEC number) throughout all stages (I-IV) of the disease. The expression of hERα increased from stage I (1%) to stage III (12%) and, interestingly, in the terminal stage of the disease which is characterised by severe ductopenic conditions, hERα was found to be undetectable in hBECs (Alvaro *et al.*, 2004). Furthermore, it was reported that hERα was co-localised to hBECs which stained positive for the proliferation marker PCNA suggesting that the hERα is associated with BEC proliferation. In contrast, hERβ expression was linked to an increase in the apoptotic markers TUNEL and Fas which were detectable at high levels in disease state IV indicating that expression of hERβ may be related to apoptosis in hBECs thus leading to ductopenia. BECs from normal liver were not found to express any hERs (Alvaro *et al.*, 2004).

An increase in ERβ expression in BECs in a disease setting has also been reported in rat (Alvaro *et al.*, 2000a). Although rat BECs were shown to express low levels of rat (r) ERα and rERβ in healthy liver, rERβ expression was markedly increased in rats subject to bile duct ligation, a common model used to induce cholangiocyte injury and proliferation and thus cholangiopathic conditions (Alvaro *et al.*, 2006b). This study further showed that proliferation

of rBECs was associated with oestrogens and the rERs since treatment with the ER antagonists ICI182,780 or tamoxifen inhibited rBEC proliferation *in vivo* and *in vitro* (Alvaro *et al.*, 2000a).

In terms of ER expression in the mouse, there was little evidence for the expression of mER proteins in isolated mBECs (Figure 6.9, Figure 6.10). It appears that with time in culture, however, mBECs expressed detectable levels of mERβ protein as determined by immunocytochemical staining and Western Blot. This suggests that mERβ may be predominantly expressed in mBECs (Figure 6.9, Figure 6.11). Although limited data is available regarding mER expression in mBECs in a disease setting, Xia et al. (2012) have reported that both mERα and mERβ mRNA transcripts are expressed in mBECs and that expression of both increase in culture (Xia *et al.*, 2012). Similarly, protein and mRNA transcripts of mERα and mERβ were shown to be expressed in mBECs with mERα at least in females playing a role in the regulation of IL6 expression (Isse *et al.*, 2010). Previous work has shown that hepatocytes, but not mBECs stained positive for mERα in mouse liver sections of control animals and mERα expression was increased in hepatocytes following injury induced by bile duct ligation (Axon, Thesis 2012). ERβ was found to be expressed in mBECs but not in hepatocytes in control animals whereas bile duct ligation induced the expression of detectable levels of mERβ in hepatocytes suggesting that mERβ is upregulated in a disease setting (Axon, Thesis 2012).

Taking into account data in this chapter as well as data available in the literature, the functional role of ERβ in cholangiocytes under normal conditions is likely to be negligible since its expression is low. However, considering that ERβ protein was expressed in hBECs and mBECs with time in culture and studies reporting that ERβ is markedly upregulated in BECs in a disease setting in both human and rat, ERβ could play a role in the modulation of disease progression in cholangiopathies, such as in PBC. ERα activation is linked with proliferation and growth of target tissues and cells (Diel, 2002) whereas ERβ is largely associated with protective modulatory effects against cell proliferation (Gustafsson, 1999). Therefore, activation of the ERβ may antagonise ERα-mediated proliferative responses in BECs promoting the disappearance of bile ducts and leading to vanishing bile duct syndromes.

Chapter 7. General discussion

Numerous chemicals with potential endocrine disrupting properties are contained in many consumer products including foodstuffs, personal care products and household items. With the development of new materials for products, tools and devices aimed at improving our everyday lives, exposure to endocrine disrupting chemicals has increased and is linked to many endocrine-related diseases including reproductive disorders and cancer. Although several mechanisms exist through which EDCs may exert their adverse effects, many EDCs were found to target and modulate endogenous oestrogen activity by interfering with endogenous oestrogen signalling or by disrupting synthesis, metabolism and transport of oestrogens. A common mechanism in modulating oestrogen signalling is through interactions of oestrogenic chemicals with the ERs, often because they possess structural similarities to endogenous oestrogens. Given the cholestatic effects that high systemic levels of endogenous oestrogens can have in the liver, the overall aim of this thesis was to establish whether exposure to xenoestrogens may cause similar adverse hepatic effects.

A number of *in vitro* assays exist that allow for identification of chemicals with xenoestrogenic activity. Testing the potential adverse hepatic effects of xenoestrogens while simultaneously taking into consideration exposure routes as well as toxicokinetic and toxicodynamic effects requires the use of animal models. Since a large number of transgenic mouse models exist which can be employed to study the mechanisms behind xenoestrogen-mediated toxic effects in follow-on research, the mouse as a species was selected for work as part of this thesis.

In order to determine if chemicals are xenoestrogens in a murine context, a mouse-based *in vitro* reporter gene assay was developed. Given the focus of this thesis on the liver and the expression and role that ERα plays in hepatocytes and oestrogen-mediated cholestasis, hepatocytes were the preferred cell type for assessing the oestrogenic activity of chemicals. However, practical limitations regarding the use of hepatocytes exist. Hepatocytes do not proliferate *in vitro* and, therefore, transfection efficiencies are often low. Furthermore, the isolation of hepatocytes from mouse liver is time consuming, expensive and requires the termination of a large number of animals. Since an *in vitro* assay was required to be capable of semi-high throughput screening of a relatively large number of samples with an appropriate number of replicates, the use of mouse hepatocytes did not seem like a realistic option. Instead, the mouse pancreatohepatobiliary ductal cell lines 603B and LTPA were employed. Given the role of ERs in BECs (i.e., induction of ER expression and ER-mediated BEC

proliferation in a disease setting), these were considered as an appropriate alternative to hepatocytes.

Neither 603B, nor LTPA cells expressed detectable levels of the mER subtypes mERα and mERβ as determined by RT-PCR, Western Blot and immunocytochemistry. The mERα and two mERβ (mERβv1 and mERβv2) cDNA sequences were, therefore, cloned from mouse uterine and ovary tissue, respectively, and ectopically expressed in the two cell lines. Both mERβ variants, but not the mERα, were effectively functionally activated by oestrogens in the BEC cell line 603B. Mouse ERα exhibited functional activity in ductal pancreatic LTPA cells. The reason(s) for the differential activities of the mER subtypes in 603B and LTPA cells are not known but may be due to differences in cell-line dependent cofactor protein expression required for mER transcriptional function. Should this difference extend to human pancreatohepatobiliary tissues, it would suggest that hERβ transcriptional function predominates in BECs.

Although both mERβ variants were functionally active in 603B cells, the mERβv2 exhibited nearly full constitutive activity and required inactivation by the ER antagonist ICI182,780 prior to activation by oestrogen. Compared to the mERβv1, mERβv2 lacks an in-frame exon in the coding region creating a protein lacking 18 amino acids in the ligand binding domain. This deletion might affect the type and affinity of ligands capable of binding to the mERβv2 which could account for the differences in transcriptional activity observed between the two mouse ERβ isoforms. Since constitutive activity of the mERβv2 has not been reported elsewhere, however, it may just be a unique observation in the cell line (603B) in which the receptor was expressed.

Several different splice variants of the hERβ have been described in humans (Sotoca *et al.*, 2012) and interrogation of the NCBI database for the existence of variant hERβ transcripts indicates that at least 7 splice variants have thus far been identified, leading to 5 variant proteins. Clustal alignment of 5 hERβ variant proteins with mERβv1 and mERβv2 (Appendix D) shows that all hERβ proteins lack the 18 amino acid insertion present in mERβv1 and, therefore, hERβ proteins are more likely to respond to oestrogens and xenoestrogens similarly to the mERβv2 protein.

Following development of the mouse-based reporter gene assay, the food additive tartrazine was tested for its ability to interact with the mERs. The sulfonated food dye tartrazine has previously been shown to activate the hERα in reporter gene assays in two independent studies (Datta and Lundin-Schiller, 2008; Axon *et al.*, 2012). I.p. injection of tartrazine at a

dose of 50 mg/kg bw/day (10 daily doses over 14 days, note the ADI is 7.5 mg/kg bw/day) resulted in a mild cholestatic injury in mice (Axon, Thesis 2012). Since oestrogens have been suggested to cause cholestasis via ERα-mediated alterations of hepatic transporter expression (Yamamoto *et al.*, 2006), it was initially hypothesised that the tartrazine-induced cholestatic effects may be associated with activation of the murine ERs. Data in this thesis demonstrate, however, that tartrazine, four of its sulfonated gut-derived metabolites and a major sulfonated contaminant of the food additive failed to activate/antagonise the mERα in the developed mouse-based reporter gene assay.

Tartrazine, its metabolites and the contaminant were also examined for their ability to interact with the mERβ. Data has shown that ERs are unlikely to be expressed in normal BECs but ERβ expression was detectable in human and mouse BECs after time in culture. Similar results have been reported by other researchers which showed that ERs were undetectable in normal liver of humans and at a low level in rat liver (Alvaro *et al.*, 2000a; Alvaro *et al.*, 2004). In a liver disease setting, however, ERβ expression in BECs was found to be markedly increased and thought to influence the proliferation capacity of bile ducts which determines disease progression in cholestatic liver conditions (Alvaro *et al.*, 2000a; Alvaro *et al.*, 2004; Marzioni *et al.*, 2012). Data in this thesis indicate that tartrazine, four of its sulfonated metabolites and a major sulfonated contaminant of the food additive lack mERβv1 and mERβv2 agonist or antagonist activities in the developed reporter gene assay. Therefore, the observed cholestatic effects caused by tartrazine in mice are likely to occur independent of the mERs.

Cholestatic effects of oestrogens in the liver are thought to be mediated by either an ERα-dependent suppression of hepatic transporter expression (Yamamoto *et al.*, 2006) and/or inhibition of hepatic bile acid transporters that leads to impaired bile acid secretion and thus cholestasis and subsequent liver toxicity (Stieger *et al.*, 2000). Given that tartrazine, its metabolites/contaminant did not interact with the mERs, ER-mediated suppression of hepatic transporter expression is unlikely to account for cholestasis caused by tartrazine. Although the effects that tartrazine may have on bile acid transporter activity were not investigated, there is a third possible mechanism by which tartrazine may have caused cholestasis. Previous research has reported that tartrazine inhibited human sulfotransferases (Bamforth *et al.*, 1993). Since sulfation of some bile acids is required for their secretion and excretion (Alnouti, 2009), inhibition of sulfotransferases may result in a build-up of bile acids in the liver and thus cholestasis. Therefore, the effects of tartrazine on murine hepatic sulphotransferase activities were examined. Data demonstrates that tartrazine – and for the first time – that four of its

sulfated metabolites and a major sulfated contaminant inhibited dopamine sulfotransferase in a dose-dependent manner in murine hepatic S9 fractions.

Tartrazine is fairly water soluble and, when exposed to via the oral route as a food additive, not significantly absorbed intact by the gastrointestinal tract. Therefore, tartrazine-mediated cholestatic effects following i.p. injection are likely to be irrelevant in humans, unless the adverse hepatic effects can be attributed to any metabolites of tartrazine that are absorbed. To test the food additive relevance of these observations, tartrazine was orally administered to mice. Since alcohol consumption is associated with an increase in gut permeability, and tartrazine is contained in a variety of alcoholic beverages, the food dye was administered in combination with ethanol to promote its absorption. Tartrazine alone, but not in combination with ethanol caused inflammation in the liver and the gastrointestinal tract without evidence of cholestasis. However, these effects occurred without interaction of tartrazine, its gut-derived metabolites and a contaminant with the mERs and were more likely associated with their inhibitory effects on sulfotransferase enzyme activities. Given the role of sulfotransferases in bile acid excretion, the initiating event leading to adverse hepatic effects through systemic exposure – but not oral exposure – is, therefore, likely to be due to an inhibition of bile acid sulfation and cholestasis. Considering that tartrazine was administered at doses in excess (6.6-fold) of the current ADI, the absence of any cholestatic effects after oral exposure, even on a background of chronic high levels of exposure to alcohol, are unlikely to be of toxicological relevance in respect of its use as a food additive. Since human dopamine sulfotransferase were inhibited by tartrazine at lower concentrations (6.7 µM) (Bamforth *et al.*, 1993) compared to murine sulfotransferase (>100 µM), however, there may be a greater potential for tartrazine to disrupt bile acid metabolism in humans. Combined with the fact that tartrazine is an activator of the hERα, humans may be more sensitive to tartrazine-mediated adverse hepatic effects compared to mice.

The chronic cholestatic liver disease PBC is believed to be triggered in genetically pre-disposed individuals through exposure to an environmental chemical(s)/toxin(s) or infectious agent(s). High incidences of PBC have been reported to occur around toxic waste sites (Ala *et al.*, 2006). Given the ability of oestrogens to cause cholestasis, it was hypothesised that the environment around a waste tip site contains a variety of xenoestrogens. Several waste site soil extracts activated the hERα in a reporter gene assay in MCF-7 cells. Similarly, waste site soil samples activated all three mERs (mERα, mERβv1 and mERβv2) in the initially developed mouse-based reporter gene assay. Soil extracts prepared from soil samples collected from three separate control sites not in proximity to waste sites failed to activate or

had generally low oestrogenic activity in both the human- and mouse-based *in vitro* assays. For the first time, data in this thesis, therefore, demonstrate that xenoestrogens can be extracted from and detected in soil samples. Soil samples collected in close proximity to a waste site contained higher levels of detectable xenoestrogens compared to soil extracts prepared from soil samples collected at control sites not expected to be contaminated with chemicals.

Waste site soil extract-mediated activation of the hERα, mERα and mERβv1 was inhibited by the ER antagonist ICI182,780. Although retaining its sensitivity to antagonism by ICI182,780 when activated by E2 or EE, the ER antagonist failed to inhibit waste site soil extract-dependent activation of the mERβv2. Assuming that xenoestrogens interact with the ligand binding domain of mERβv2 in a similar manner to natural oestrogens, this finding suggests that the dissociation rate of xenoestrogens is significantly reduced compared to E2. Alternatively, xenoestrogens may activate the mERβv2 via a different mechanism such as interacting and binding to the receptor through an alternative binding site which could prevent ICI182,780-mediated antagonism. This finding suggests that soil-based xenoestrogens may have 'super-activating' characteristics with an ERβ variant. Considering that clustal sequence alignments have shown that all hERβ protein variants share a higher degree of sequence homology in their ligand binding domain with the mERβv2 rather than the mERβv1, the hERβ is more likely to respond to xenoestrogens similarly to the mERβv2 protein. Although ERβ expression in BECs under normal conditions is low and its functional role therefore likely to be negligible, ERβ expression is markedly up-regulated in a disease setting (Alvaro *et al.*, 2006b). ERβ is generally known to antagonise the proliferative effects of ERα and Marzioni et al. (2012) reported that an ERβ-selective agonist induced apoptosis in cholangiocarcinoma (Marzioni *et al.*, 2012). Since ERα mediates the proliferative response of BECs, and BEC proliferation is an important hepatic response counter-acting the loss of bile ducts, activation of the ERβ may therefore contribute to cholestatic disease progression. Thus, it is tempting to propose that the role xenoestrogens may play in the development of PBC is via an inhibition of bile duct proliferation and/or promotion of vanishing bile duct syndrome through a sustained activation of ERβ in cholangiocytes. Based on the calculated amount of soil an individual needs to be exposed to (1-50 kg of contaminated soil, see Section 5.5), however, it seems unlikely that an ERβ-targeting EDC alone could be the trigger for a disease such as PBC. If exposure to xenoestrogens is involved in PBC disease progression, it is more likely as a component of a xenobiotic insult, such as PDC-E2 targeting xenobiotics, that triggers PBC.

Overall, work in this thesis demonstrates that if significant exposure to environmental xenoestrogens occurs, they can have adverse hepatic effects and may be part of a trigger process in cholestatic liver diseases. Moreover, work presented in this thesis offers a foundation for future research and provides important information which may help to elucidate potential triggers in cholestatic liver diseases such as PBC. In this context, future work could be aimed at identifying the chemical nature of the compound(s) present in waste site soil extracts in order to find their source and prevent contamination. Provided that enough resources are available, it would further be interesting to examine the effects that chronic exposure to waste site soil extracts may have *in vivo* in mice and to determine the mechanism behind waste site soil extract-mediated hepatic adverse effects (i.e. inhibition of SULTs or ERα-dependent inhibition of bile acid transporters in hepatocytes).

Although it is undoubtedly clear that the development of new medicines and materials for modern products has significantly contributed to improvements of everyday lives, continued production, use and release of novel chemicals into the environment necessitates continued research and strict monitoring to prevent environment contamination and to reduce the risk for development of endocrine disrupters-mediated diseases in wildlife and humans.

References

Aakvaag, A., Utaaker, E., Thorsen, T., Lea, O.A. and Lahooti, H. (1990) 'Growth control of human mammary cancer cells (MCF-7 cells) in culture: effect of estradiol and growth factors in serum-containing medium', *Cancer Research*, 50(24), pp. 7806-7810.

Adachi, M. and Brenner, D.A. (2006) 'Clinical syndromes of alcoholic liver disease', *Digestive Diseases*, 23(3-4), pp. 255-263.

Adachi, Y., Bradford, B.U., Gao, W., Bojes, H.K. and Thurman, R.G. (1994) 'Inactivation of Kupffer cells prevents early alcohol-induced liver injury', *Hepatology*, 20(2), pp. 453-460.

Adachi, Y., Moore, L.E., Bradford, B.U., Gao, W. and Thurman, R.G. (1995) 'Antibiotics prevent liver injury in rats following long-term exposure to ethanol', *Gastroenterology*, 108(1), pp. 218-224.

Ahlbory-Dieker, D.L., Stride, B.D., Leder, G., Schkoldow, J., Trolenberg, S., Seidel, H., Otto, C., Sommer, A., Parker, M.G., Schutz, G. and Wintermantel, T.M. (2009) 'DNA binding by estrogen receptor-alpha is essential for the transcriptional response to estrogen in the liver and the uterus', *Molecular Endocrinology*, 23(10), pp. 1544-1555.

Ajakaiye, M., Jacob, A., Wu, R., Nicastro, J.M., Coppa, G.F. and Wang, P. (2011) 'Alcohol and hepatocyte-Kupffer cell interaction (review)', *Molecular Medicine Reports*, 4(4), pp. 597-602.

Ajmo, J.M., Liang, X., Rogers, C.Q., Pennock, B. and You, M. (2008) 'Resveratrol alleviates alcoholic fatty liver in mice', *American Journal of Physiology - Gastrointestinal and Liver Physiology*, 295(4), pp. G833-G842.

Ala, A., Stanca, C.M., Bu-Ghanim, M., Ahmado, I., Branch, A.D., Schiano, T.D., Odin, J.A. and Bach, N. (2006) 'Increased prevalence of primary biliary cirrhosis near Superfund toxic waste sites', *Hepatology*, 43(3), pp. 525-531.

Ali, S. and Coombes, R.C. (2002) 'Endocrine-responsive breast cancer and strategies for combating resistance', *Nature Reviews Cancer*, 2(2), pp. 101-112.

Alnouti, Y. (2009) 'Bile Acid sulfation: a pathway of bile acid elimination and detoxification', *Toxicological Sciences*, 108(2), pp. 225-246.

Alonso-Magdalena, P., Quesada, I. and Nadal, A. (2011) 'Endocrine disruptors in the etiology of type 2 diabetes mellitus', *Nature Reviews Endocrinology*, 7(6), pp. 346-353.

Alvaro, D., Alpini, G., Onori, P., Franchitto, A., Glaser, S.S., Le Sage, G., Folli, F., Attili, A.F. and Gaudio, E. (2002) 'Alfa and beta estrogen receptors and the biliary tree', *Molecular and Cellular Endocrinology*, 193(1–2), pp. 105-108.

Alvaro, D., Alpini, G., Onori, P., Perego, L., Baroni, G.S., Franchitto, A., Baiocchi, L., Glaser, S.S., Le Sage, G., Folli, F. and Gaudio, E. (2000a) 'Estrogens stimulate proliferation of intrahepatic biliary epithelium in rats', *Gastroenterology*, 119(6), pp. 1681-1691.

Alvaro, D., Barbaro, B., Franchitto, A., Onori, P., Glaser, S.S., Alpini, G., Francis, H., Marucci, L., Sterpetti, P., Ginanni-Corradini, S., Onetti Muda, A., Dostal, D.E., De Santis, A., Attili, A.F., Benedetti, A. and Gaudio, E. (2006a) 'Estrogens and insulin-like growth factor 1 modulate neoplastic cell growth in human cholangiocarcinoma', *American Journal of Pathology*, 169(3), pp. 877-888.

Alvaro, D., Gigliozzi, A. and Attili, A.F. (2000b) 'Regulation and deregulation of cholangiocyte proliferation', *Journal of Hepatology*, 33(2), pp. 333-340.

Alvaro, D., Invernizzi, P., Onori, P., Franchitto, A., De Santis, A., Crosignani, A., Sferra, R., Ginanni-Corradini, S., Grazia Mancino, M., Maggioni, M., Attili, A.F., Podda, M. and Gaudio, E. (2004) 'Estrogen receptors in cholangiocytes and the progression of primary biliary cirrhosis', *Journal of Hepatology*, 41(6), pp. 905-912.

Alvaro, D., Mancino, M.G., Onori, P., Franchitto, A., Alpini, G., Francis, H., Glaser, S. and Gaudio, E. (2006b) 'Estrogens and the pathophysiology of the biliary tree', *World Journal of Gastroenterology*, 12(22), pp. 3537-3545.

Ascenzi, P., Bocedi, A. and Marino, M. (2006) 'Structure-function relationship of estrogen receptor alpha and beta: impact on human health', *Molecular Aspects of Medicine*, 27(4), pp. 299-402.

Atkinson, K.J. and Rao, R.K. (2001) 'Role of protein tyrosine phosphorylation in acetaldehyde-induced disruption of epithelial tight junctions', *American Journal of Physiology-Gastrointestinal and Liver Physiology*, 280(6), pp. G1280-G1288.

Axon, A., Cowie, D.E., Oakley, F., Williams, F.M., Blain, P.G. and Wright, M.C. (2010) 'Acute oestradiol (E2) administration to mice results in liver portal tract inflammation', *Toxicology*, 278(3), p. 349.

Axon, A., May, F.E., Gaughan, L.E., Williams, F.M., Blain, P.G. and Wright, M.C. (2012) 'Tartrazine and sunset yellow are xenoestrogens in a new screening assay to identify modulators of human oestrogen receptor transcriptional activity', *Toxicology*, 298(1-3), pp. 40-51.

Axon, A., Thesis (2012) 'The role of xenoestrogens in the initiation of primary biliary cirrhosis', *Newcastle University ethesis database*.

Bailey, S.A., Zidell, R.H. and Perry, R.W. (2004) 'Relationships between organ weight and body/brain weight in the rat: what is the best analytical endpoint?', *Toxicologic Pathology*, 32(4), pp. 448-466.

Bamforth, K.J., Jones, A.L., Roberts, R.C. and Coughtrie, M.W. (1993) 'Common food additives are potent inhibitors of human liver 17 alpha-ethinyloestradiol and dopamine sulphotransferases', *Biochemical Pharmacology*, 46(10), pp. 1713-1720.

Barkhem, T., Carlsson, B., Nilsson, Y., Enmark, E., Gustafsson, J. and Nilsson, S. (1998) 'Differential response of estrogen receptor alpha and estrogen receptor beta to partial estrogen agonists/antagonists', *Molecular Pharmacology*, 54(1), pp. 105-112.

Barosso, I.R., Zucchetti, A.E., Boaglio, A.C., Larocca, M.C., Taborda, D.R., Luquita, M.G., Roma, M.G., Crocenzi, F.A. and Sanchez Pozzi, E.J. (2012) 'Sequential activation of classic PKC and estrogen receptor alpha is involved in estradiol 17β-D-glucuronide-induced cholestasis', *PLoS One*, 7(11), p. e50711.

Barrett-Connor, E., Mosca, L., Collins, P., Geiger, M.J., Grady, D., Kornitzer, M., McNabb, M.A. and Wenger, N.K. (2006) 'Effects of Raloxifene on Cardiovascular Events and Breast Cancer in Postmenopausal Women', *New England Journal of Medicine*, 355(2), pp. 125-137.

Basuroy, S., Sheth, P., Mansbach, C.M. and Rao, R.K. (2005) 'Acetaldehyde disrupts tight junctions and adherens junctions in human colonic mucosa: protection by EGF and L-glutamine', *American Journal of Physiology-Gastrointestinal and Liver Physiology*, 289(2), pp. G367-G375.

Bay, K., Asklund, C., Skakkebaek, N.E. and Andersson, A.M. (2006) 'Testicular dysgenesis syndrome: possible role of endocrine disrupters', *Best Practice and Research Clinical Endocrinology and Metabolism*, 20(1), pp. 77-90.

Berthois, Y., Katzenellenbogen, J.A. and Katzenellenbogen, B.S. (1986) 'Phenol red in tissue culture media is a weak estrogen: implications concerning the study of estrogen-responsive cells in culture', *Proceedings of the National Academy of Sciences of the United States of America*, 83(8), pp. 2496-2500.

Bertola, A., Mathews, S., Ki, S.H., Wang, H. and Gao, B. (2013) 'Mouse model of chronic and binge ethanol feeding (the NIAAA model)', *Nature Protocols*, 8(3), pp. 627-637.

Bjarnason, I., Ward, K. and Peters, T. (1984) 'The leaky gut of alcoholism: possible route of entry for toxic compounds', *The Lancet*, 323(8370), pp. 179-182.

Bjornstrom, L. and Sjoberg, M. (2005) 'Mechanisms of estrogen receptor signaling: convergence of genomic and nongenomic actions on target genes', *Molecular Endocrinology*, 19(4), pp. 833-842.

Black, L.J., Sato, M., Rowley, E.R., Magee, D.E., Bekele, A., Williams, D.C., Cullinan, G.J., Bendele, R., Kauffman, R.F. and Bensch, W.R. (1994) 'Raloxifene (LY139481 HCI) prevents bone loss and reduces serum cholesterol without causing uterine hypertrophy in ovariectomized rats', *Journal of Clinical Investigation*, 93(1), pp. 63-69.

Bode, C., Kugler, V. and Bode, J.C. (1987) 'Endotoxemia in patients with alcoholic and non-alcoholic cirrhosis and in subjects with no evidence of chronic liver disease following acute alcohol excess', *Journal of Hepatology*, 4(1), pp. 8-14.

Bogdanos, D.P. and Komorowski, L. (2011) 'Disease-specific autoantibodies in primary biliary cirrhosis', *Clinica Chimica Acta*, 412(7-8), pp. 502-512.

Bondesson, M., Hao, R., Lin, C.Y., Williams, C. and Gustafsson, J.A. (2015) 'Estrogen receptor signaling during vertebrate development', *Biochimica et Biophysica Acta (BBA)* 2, pp. 142-151.

Bradford, M.M. (1976) 'A rapid and sensitive method for the quantitation of microgram quantities of protein utilizing the principle of protein-dye binding', *Analytical Biochemistry*, 72(1), pp. 248-254.

Brandon-Warner, E., Schrum, L.W., Schmidt, C.M. and McKillop, I.H. (2012) 'Rodent Models of Alcoholic Liver Disease: Of Mice and Men', *Alcohol* 46(8), pp. 715-725.

Bungert, H.J. (1973) 'Absorption of hemoglobin and hemoglobin iron in alcohol-induced liver injury', *Digestion*, 9(4), pp. 293-308.

Bunone, G., Briand, P.A., Miksicek, R.J. and Picard, D. (1996) 'Activation of the unliganded estrogen receptor by EGF involves the MAP kinase pathway and direct phosphorylation', *The EMBO Journal*, 15(9), pp. 2174-2183.

Burkman, R.T. (2003) 'Hormone replacement therapy. Current controversies', *Minerva Ginecologica*, 55(2), pp. 107-116.

Burra, P. (2013) 'Liver abnormalities and endocrine diseases', *Best Practice & Research Clinical Gastroenterology*, 27(4), pp. 553-563.

Carlsen, H., Moskaug, J.O., Fromm, S.H. and Blomhoff, R. (2002) 'In vivo imaging of NF-kappa B activity', *Journal of Immunology*, 168(3), pp. 1441-1446.

Chu, S. and Fuller, P.J. (1997) 'Identification of a splice variant of the rat estrogen receptor β gene', *Molecular and Cellular Endocrinology*, 132(1), pp. 195-199.

Cohen, J.I., Roychowdhury, S., McMullen, M.R., Stavitsky, A.B. and Nagy, L.E. (2010) 'Complement and alcoholic liver disease: role of C1q in the pathogenesis of ethanol-induced liver injury in mice', *Gastroenterology*, 139(2), pp. 664-674.

Couse, J.F., Lindzey, J., Grandien, K., Gustafsson, J.A. and Korach, K.S. (1997) 'Tissue distribution and quantitative analysis of estrogen receptor-alpha (ERalpha) and estrogen receptor-beta (ERbeta) messenger ribonucleic acid in the wild-type and ERalpha-knockout mouse', *Endocrinology*, 138(11), pp. 4613-4621.

Cowley, S.M., Hoare, S., Mosselman, S. and Parker, M.G. (1997) 'Estrogen receptors alpha and beta form heterodimers on DNA', *The Journal of Biological Chemistry*, 272(32), pp. 19858-19862.

Crocenzi, F.A., Mottino, A.D., Cao, J., Veggi, L.M., Pozzi, E.J., Vore, M., Coleman, R. and Roma, M.G. (2003) 'Estradiol-17beta-D-glucuronide induces endocytic internalization of Bsep in rats', *American Journal of Physiology - Gastrointestinal and Liver Physiology*, 285(2), pp. G449-459.

Cui, J., Shen, Y. and Li, R. (2013) 'Estrogen synthesis and signaling pathways during ageing: from periphery to brain', *Trends in Molecular Medicine*, 19(3), pp. 197-209.

Curtis, S.W., Washburn, T., Sewall, C., DiAugustine, R., Lindzey, J., Couse, J.F. and Korach, K.S. (1996) 'Physiological coupling of growth factor and steroid receptor signaling pathways: estrogen receptor knockout mice lack estrogen-like response to epidermal growth factor', *Proceedings of the National Academy of Sciences*, 93(22), pp. 12626-12630.

D'Souza El-Guindy, N.B., Kovacs, E.J., De Witte, P., Spies, C., Littleton, J.M., de Villiers, W.J.S., Lott, A.J., Plackett, T.P., Lanzke, N. and Meadows, G.G. (2010) 'Laboratory models available to study alcohol-induced organ damage and immune variations; choosing the appropriate model', *Alcoholism, Clinical and Experimental Research*, 34(9), pp. 1489-1511.

Dajani, R., Cleasby, A., Neu, M., Wonacott, A.J., Jhoti, H., Hood, A.M., Modi, S., Hersey, A., Taskinen, J., Cooke, R.M., Manchee, G.R. and Coughtrie, M.W.H. (1999) 'X-ray Crystal Structure of Human Dopamine Sulfotransferase, SULT1A3: Molecular modelling and quantitative structure-activity relationship analysis demonstrate a molecular basis for sulfotransferase substrate specificity ', *Journal of Biological Chemistry*, 274(53), pp. 37862-37868.

Dancygier, H. (2009) *Clinical hepatology: Principles and practice of hepatobiliary diseases*. Springer Science & Business Media.

Datta, P. and Lundin-Schiller, S. (2008) 'Estrogenicity of the synthetic food colorants tartrazine, erythrosin B, and sudan I in an estrogen-responsive human breast cancer cell line', *Journal of the Tennessee Academy of Science*, 83.

DeCarli, L.M. and Lieber, C.S. (1967) 'Fatty liver in the rat after prolonged intake of ethanol with a nutritionally adequate new liquid diet', *Journal of Nutrition*, 91(3), pp. 331-336.

Deleuze, J.F., Jacquemin, E., Dubuisson, C., Cresteil, D., Dumont, M., Erlinger, S., Bernard, O. and Hadchouel, M. (1996) 'Defect of multidrug-resistance 3 gene expression in a subtype of progressive familial intrahepatic cholestasis', *Hepatology*, 23(4), pp. 904-908.

DeMichele, A., Troxel, A.B., Berlin, J.A., Weber, A.L., Bunin, G.R., Turzo, E., Schinnar, R., Burgh, D., Berlin, M., Rubin, S.C., Rebbeck, T.R. and Strom, B.L. (2008) 'Impact of raloxifene or tamoxifen use on endometrial cancer risk: a population-based case-control study', *Journal of Clinical Oncology*, 26(25), pp. 4151-4159.

DeNardo, D.G., Kim, H.T., Hilsenbeck, S., Cuba, V., Tsimelzon, A. and Brown, P.H. (2005) 'Global gene expression analysis of estrogen receptor transcription factor cross talk in breast cancer: identification of estrogen-induced/activator protein-1-dependent genes', *Molecular Endocrinology*, 19(2), pp. 362-378.

Denger, S., Reid, G., Koš, M., Flouriot, G., Parsch, D., Brand, H., Korach, K.S., Sonntag-Buck, V. and Gannon, F. (2001) 'ERα gene expression in human primary osteoblasts: evidence for the expression of two receptor proteins', *Molecular Endocrinology*, 15(12), pp. 2064-2077.

Desmet, V.J., Krstulović, B. and Van Damme, B. (1968) 'Histochemical study of rat liver in alpha-naphthyl isothiocyanate (ANIT) induced cholestasis', *The American Journal of Pathology*, 52(2), pp. 401-421.

Desmet, V.J., van Eyken, P. and Roskams, T. (1998) 'Histopathology of vanishing bile duct diseases', *Advances in Clinical Pathology*, 2(2), pp. 87-99.

Diamanti-Kandarakis, E., Bourguignon, J.P., Giudice, L.C., Hauser, R., Prins, G.S., Soto, A.M., Zoeller, R.T. and Gore, A.C. (2009) 'Endocrine-disrupting chemicals: an Endocrine Society scientific statement', *Endocrinology Reviews*, 30(4), pp. 293-342.

Diel, P. (2002) 'Tissue-specific estrogenic response and molecular mechanisms', *Toxicology Letters*, 127(1-3), pp. 217-224.

Dooley, S. and ten Dijke, P. (2012) 'TGF-β in progression of liver disease', *Cell and Tissue Research*, 347(1), pp. 245-256.

EFSA, E.F.F.I.a.P. (2009) 'Scientific Opinion on the re-evaluation Tartrazine (E 102)', *EFSA Journal 2009*, 7(11), p. 1331 [52 pp].

El-Tanani, M.K. and Green, C.D. (1997) 'Two separate mechanisms for ligand-independent activation of the estrogen receptor', *Molecular Endocrinology*, 11(7), pp. 928-937.

Elhkim, M.O., Heraud, F., Bemrah, N., Gauchard, F., Lorino, T., Lambre, C., Fremy, J.M. and Poul, J.M. (2007) 'New considerations regarding the risk assessment on Tartrazine An update toxicological assessment, intolerance reactions and maximum theoretical daily intake in France', *Regulatory Toxicology and Pharmacology*, 47(3), pp. 308-316.

Enmark, E., Pelto-Huikko, M., Grandien, K., Lagercrantz, S., Lagercrantz, J., Fried, G., Nordenskjold, M. and Gustafsson, J.A. (1997) 'Human estrogen receptor beta-gene structure,

chromosomal localization, and expression pattern', *The Journal of Clinical Endocrinology & Metabolism*, 82(12), pp. 4258-4265.

Enomoto, N., Ikejima, K., Bradford, B., Rivera, C., Kono, H., Brenner, D.A. and Thurman, R.G. (1998) 'Alcohol causes both tolerance and sensitization of rat Kupffer cells via mechanisms dependent on endotoxin', *Gastroenterology*, 115(2), pp. 443-451.

Enomoto, N., Ikejima, K., Yamashina, S., Hirose, M., Shimizu, H., Kitamura, T., Takei, Y., Sato and Thurman, R.G. (2001) 'Kupffer cell sensitization by alcohol involves increased permeability to gut-derived endotoxin', *Alcoholism: Clinical and Experimental Research*, 25(6 Suppl), pp. 51S-54S.

Enomoto, N., Yamashina, S., Kono, H., Schemmer, P., Rivera, C.A., Enomoto, A., Nishiura, T., Nishimura, T., Brenner, D.A. and Thurman, R.G. (1999) 'Development of a new, simple rat model of early alcohol-induced liver injury based on sensitization of Kupffer cells', *Hepatology*, 29(6), pp. 1680-1689.

Etienne, L., Helmut, D., Biao, L., Cheryl, G., Peter, H.W. and Leigh, C.M. (1998) 'Estrogen Receptor β: Mine Is Longer Than Yours?', *The Journal of Clinical Endocrinology & Metabolism*, 83(10), pp. 3754-3755.

Fanning, A.S., Jameson, B.J., Jesaitis, L.A. and Anderson, J.M. (1998) 'The tight junction protein ZO-1 establishes a link between the transmembrane protein occludin and the actin cytoskeleton', *Journal of Biological Chemistry*, 273(45), pp. 29745-29753.

Figtree, G.A., McDonald, D., Watkins, H. and Channon, K.M. (2003) 'Truncated Estrogen Receptor α 46-kDa Isoform in Human Endothelial Cells Relationship to Acute Activation of Nitric Oxide Synthase', *Circulation*, 107(1), pp. 120-126.

Fitzgerald, K.A., Rowe, D.C., Barnes, B.J., Caffrey, D.R., Visintin, A., Latz, E., Monks, B., Pitha, P.M. and Golenbock, D.T. (2003) 'LPS-TLR4 signaling to IRF-3/7 and NF-kappaB involves the toll adapters TRAM and TRIF', *The Journal of Experimental Medicine*, 198(7), pp. 1043-1055.

Flouriot, G., Brand, H., Denger, S., Metivier, R., Kos, M., Reid, G., Sonntag-Buck, V. and Gannon, F. (2000) 'Identification of a new isoform of the human estrogen receptor-alpha (hER-alpha) that is encoded by distinct transcripts and that is able to repress hER-alpha activation function 1', *The EMBO Journal*, 19(17), pp. 4688-4700.

Font de Mora, J. and Brown, M. (2000) 'AIB1 Is a Conduit for Kinase-Mediated Growth Factor Signaling to the Estrogen Receptor', *Molecular and Cellular Biology*, 20(14), pp. 5041-5047.

Freedman, B.J. (1977) 'Asthma induced by sulphur dioxide, benzoate and tartrazine contained in orange drinks', *Clinical & Experimental Allergy*, 7(5), pp. 407-415.

French, S.W. (2001) 'Intragastric ethanol infusion model for cellular and molecular studies of alcoholic liver disease', *Journal of Biomedical Science* 8(1), pp. 20-27.

Fujimoto, M., Uemura, M., Nakatani, Y., Tsujita, S., Hoppo, K., Tamagawa, T., Kitano, H., Kikukawa, M., Ann, T., Ishii, Y., Kojima, H., Sakurai, S., Tanaka, R., Namisaki, T., Noguchi, R., Higashino, T., Kikuchi, E., Nishimura, K., Takaya, A. and Fukui, H. (2000) 'Plasma endotoxin and serum cytokine levels in patients with alcoholic hepatitis: relation to severity of liver disturbance', *Alcoholism: Clinical and Experimental Research*, 24(4 Suppl), pp. 48S-54S.

Fukui, H., Brauner, B., Bode, J.C. and Bode, C. (1991) 'Plasma endotoxin concentrations in patients with alcoholic and non-alcoholic liver disease: reevaluation with an improved chromogenic assay', *Journal of Hepatology*, 12(2), pp. 162-169.

Galey, F.D., Mendez, L.E., Whitehead, W.E., Holstege, D.M., Plumlee, K.H. and Johnson, B. (1993) 'Estrogenic activity in forages: diagnostic use of the classical mouse uterine bioassay', *Journal of Veterinary Diagnostic Investigation*, 5(4), pp. 603-608.

Gamage, N., Barnett, A., Hempel, N., Duggleby, R.G., Windmill, K.F., Martin, J.L. and McManus, M.E. (2006) 'Human Sulfotransferases and Their Role in Chemical Metabolism', *Toxicological Sciences*, 90(1), pp. 5-22.

Gao, W.L., Wu, L.S., Zi, J.H., Wu, B., Li, Y.Z., Song, Y.C. and Cai, D.Z. (2015) 'Measurement of serum estrogen and estrogen metabolites in pre- and postmenopausal women with osteoarthritis using high-performance liquid chromatography-electrospray ionization-tandem mass spectrometry', *Brazilian Journal of Medical and Biological Research*, 48, pp. 146-153.

Gershwin, M.E., Ansari, A.A., Mackay, I.R., Nakanuma, Y., Nishio, A., Rowley, M.J. and Coppel, R.L. (2000) 'Primary biliary cirrhosis: an orchestrated immune response against epithelial cells', *Immunology Reviews*, 174, pp. 210-225.

Gershwin, M.E., Selmi, C., Worman, H.J., Gold, E.B., Watnik, M., Utts, J., Lindor, K.D., Kaplan, M.M. and Vierling, J.M. (2005) 'Risk factors and comorbidities in primary biliary cirrhosis: a controlled interview-based study of 1032 patients', *Hepatology*, 42(5), pp. 1194-1202.

Goldfarb, S., Singer, E.J. and Popper, H. (1962) 'Experimental Cholangitis Due to Alpha-Naphthyl-Isothiocyanate (ANIT)', *The American Journal of Pathology*, 40(6), pp. 685-698.

Gottardis, M.M., Robinson, S.P., Satyaswaroop, P.G. and Jordan, V.C. (1988) 'Contrasting actions of tamoxifen on endometrial and breast tumor growth in the athymic mouse', *Cancer Research*, 48(4), pp. 812-815.

Green, S., Walter, P., Kumar, V., Krust, A., Bornert, J.M., Argos, P. and Chambon, P. (1986) 'Human oestrogen receptor cDNA: sequence, expression and homology to v-erb-A', *Nature*, 320(6058), pp. 134-139.

Greene, G.L., Gilna, P., Waterfield, M., Baker, A., Hort, Y. and Shine, J. (1986) 'Sequence and expression of human estrogen receptor complementary DNA', *Science*, 231(4742), pp. 1150-1154.

Gustafsson, J.-A. (1999) 'Estrogen receptor beta-a new dimension in estrogen mechanism of action', *Journal of Endocrinology*, 163(3), pp. 379-383.

Gustafsson, J.A. (2003) 'What pharmacologists can learn from recent advances in estrogen signalling', *Trends in Pharmacological Sciences*, 24(9), pp. 479-485.

Guzelian, P.S. (1983) 'Research needs for hepatic injury due to environmental agents', *Environmental Health Perspectives*, 48, pp. 65-71.

Hall, J.M. and McDonnell, D.P. (1999) 'The estrogen receptor beta-isoform (ERbeta) of the human estrogen receptor modulates ERalpha transcriptional activity and is a key regulator of the cellular response to estrogens and antiestrogens', *Endocrinology*, 140(12), pp. 5566-5578.

Hammond, G.L. (2011) 'Diverse roles for sex hormone-binding globulin in reproduction', *Biology of Reproduction*, 85(3), pp. 431-441.

Han, D.W. (2002) 'Intestinal endotoxemia as a pathogenetic mechanism in liver failure', *World Journal of Gastroenterology*, 8(6), pp. 961-965.

Hanck, C., Rossol, S., Bocker, U., Tokus, M. and Singer, M.V. (1998) 'Presence of plasma endotoxin is correlated with tumour necrosis factor receptor levels and disease activity in alcoholic cirrhosis', *Alcohol and Alcoholism*, 33(6), pp. 606-608.

Hayashi, S., Sakamoto, T., Inoue, A., Yoshida, N., Omoto, Y. and Yamaguchi, Y. (2003) 'Estrogen and growth factor signaling pathway: basic approaches for clinical application', *The Journal of Steroid Biochemistry and Molecular Biology*, 86(3-5), pp. 433-442.

Heldring, N., Pike, A., Andersson, S., Matthews, J., Cheng, G., Hartman, J., Tujague, M., Strom, A., Treuter, E., Warner, M. and Gustafsson, J.A. (2007) 'Estrogen receptors: how do they signal and what are their targets', *Physiological Reviews*, 87(3), pp. 905-931.

Helguero, L.A., Faulds, M.H., Gustafsson, J.-A. and Haldosen, L.-A. (2005) 'Estrogen receptors alfa (ER[alpha]) and beta (ER[beta]) differentially regulate proliferation and apoptosis of the normal murine mammary epithelial cell line HC11', *Oncogene*, 24(44), pp. 6605-6616.

Herbal Health (2014) *Body FAQ - Where is the liver, why is it aching and more*. Available at: http://www.herbal-health.uk/body-faq-where-is-the-liver-why-is-it-aching-more/ (Accessed: 13 September 2016).

Hernández, J.S., Watson, R.W., Wood, T.C. and Weinshilboum, R.M. (1992) 'Sulfation of estrone and 17 beta-estradiol in human liver. Catalysis by thermostable phenol sulfotransferase and by dehydroepiandrosterone sulfotransferase', *Drug Metabolism and Disposition*, 20(3), pp. 413-422.

Hritz, I., Mandrekar, P., Velayudham, A., Catalano, D., Dolganiuc, A., Kodys, K., Kurt-Jones, E. and Szabo, G. (2008) 'The critical role of toll-like receptor (TLR) 4 in alcoholic liver disease is independent of the common TLR adapter MyD88', *Hepatology*, 48(4), pp. 1224-1231.

Huang, R., Sakamuru, S., Martin, M.T., Reif, D.M., Judson, R.S., Houck, K.A., Casey, W., Hsieh, J.-H., Shockley, K.R., Ceger, P., Fostel, J., Witt, K.L., Tong, W., Rotroff, D.M., Zhao, T., Shinn, P., Simeonov, A., Dix, D.J., Austin, C.P., Kavlock, R.J., Tice, R.R. and Xia, M. (2014) 'Profiling of the Tox21 10K compound library for agonists and antagonists of the estrogen receptor alpha signaling pathway', *Scientific Reports*, 4, p. 5664.

Ignar-Trowbridge, D.M., Nelson, K.G., Bidwell, M.C., Curtis, S.W., Washburn, T.F., McLachlan, J.A. and Korach, K.S. (1992) 'Coupling of dual signaling pathways: epidermal

growth factor action involves the estrogen receptor', *Proceedings of the National Academy of Sciences of the United States of America*, 89(10), pp. 4658-4662.

Ignar-Trowbridge, D.M., Pimentel, M., Parker, M.G., McLachlan, J.A. and Korach, K.S. (1996) 'Peptide growth factor cross-talk with the estrogen receptor requires the A/B domain and occurs independently of protein kinase C or estradiol', *Endocrinology*, 137(5), pp. 1735-1744.

Ignar-Trowbridge, D.M., Teng, C.T., Ross, K.A., Parker, M.G., Korach, K.S. and McLachlan, J.A. (1993) 'Peptide growth factors elicit estrogen receptor-dependent transcriptional activation of an estrogen-responsive element', *Molecular Endocrinology*, 7(8), pp. 992-998.

Inoue, S., Ogawa, S., Horie, K., Hoshino, S., Goto, W., Hosoi, T., Tsutsumi, O., Muramatsu, M. and Ouchi, Y. (2000) 'An estrogen receptor beta isoform that lacks exon 5 has dominant negative activity on both ERalpha and ERbeta', *Biochemical and Biophysical Research Communications*, 279(3), pp. 814-819.

Invernizzi, P., Miozzo, M., Battezzati, P.M., Bianchi, I., Grati, F.R., Simoni, G., Selmi, C., Watnik, M., Gershwin, M.E. and Podda, M. (2004) 'Frequency of monosomy X in women with primary biliary cirrhosis', *Lancet*, 363(9408), pp. 533-535.

Ishida, M., Mitsui, T., Izawa, M. and Arita, J. (2010) 'Absence of ligand-independent transcriptional activation of the estrogen receptor via the estrogen response element in pituitary lactotrophs in primary culture', *The Journal of Steroid Biochemistry and Molecular Biology*, 118(1–2), pp. 93-101.

Isse, K., Specht, S.M., Lunz, J.G., 3rd, Kang, L.I., Mizuguchi, Y. and Demetris, A.J. (2010) 'Estrogen stimulates female biliary epithelial cell interleukin-6 expression in mice and humans', *Hepatology*, 51(3), pp. 869-880.

Ji, C. and Kaplowitz, N. (2003) 'Betaine decreases hyperhomocysteinemia, endoplasmic reticulum stress, and liver injury in alcohol-fed mice', *Gastroenterology*, 124(5), pp. 1488-1499.

Jones, D.E., Watt, F.E., Metcalf, J.V., Bassendine, M.F. and James, O.F. (1999) 'Familial primary biliary cirrhosis reassessed: a geographically-based population study', *Journal of Hepatology*, 30(3), pp. 402-407.

Jones, D.E.J. (2007) 'Pathogenesis of Primary Biliary Cirrhosis', *Gut*, 56(11), pp. 1615-1624.

Jones, R., Ryan, A.J. and Wright, S.E. (1964) 'The metabolism and excretion of tartrazine in the rat, rabbit and man', *Food and Cosmetics Toxicology*, 2, pp. 447-452.

Jordan, V.C. (2003) 'Tamoxifen: a most unlikely pioneering medicine', *Nature Reviews Drug Discovery*, 2(3), pp. 205-213.

Kang, X., Zhong, W., Liu, J., Song, Z., McClain, C.J., Kang, Y.J. and Zhou, Z. (2009) 'Zinc supplementation reverses alcohol-induced steatosis in mice through reactivating hepatocyte nuclear factor-4α and peroxisome proliferator-activated receptor-α', *Hepatology*, 50(4), pp. 1241-1250.

Kaplan, M.M. (2004) 'Novosphingobium aromaticivorans: a potential initiator of primary biliary cirrhosis', *The American Journal of Gastroenterology*, 99(11), pp. 2147-2149.

Kaplan, M.M. and Gershwin, M.E. (2005) 'Primary biliary cirrhosis', *The New England Journal of Medicine*, 353(12), pp. 1261-1273.

Kauffman, F.C., Sharp, S., Allan, B.B., Burchell, A. and Coughtrie, M.W.H. (1998) 'Microsomal steroid sulfatase: interactions with cytosolic steroid sulfotransferases', *Chemico-Biological Interactions*, 109(1–3), pp. 169-182.

Kawamoto, T., Kakizaki, S., Yoshinari, K. and Negishi, M. (2000) 'Estrogen activation of the nuclear orphan receptor CAR (constitutive active receptor) in induction of the mouse Cyp2b10 gene', *Molecular Endocrinology*, 14(11), pp. 1897-1905.

Kerppola, T.K. and Curran, T. (1991) 'DNA bending by Fos and Jun: the flexible hinge model', *Science*, 254(5035), pp. 1210-1214.

Kester, M.H., Bulduk, S., Tibboel, D., Meinl, W., Glatt, H., Falany, C.N., Coughtrie, M.W., Bergman, A., Safe, S.H., Kuiper, G.G., Schuur, A.G., Brouwer, A. and Visser, T.J. (2000) 'Potent inhibition of estrogen sulfotransferase by hydroxylated PCB metabolites: a novel pathway explaining the estrogenic activity of PCBs', *Endocrinology*, 141(5), pp. 1897-1900.

Kirpich, I., Ghare, S., Zhang, J., Gobejishvili, L., Kharebava, G., Barve, S.J., Barker, D., Moghe, A., McClain, C.J. and Barve, S. (2012a) 'Binge Alcohol–Induced Microvesicular Liver Steatosis and Injury are Associated with Down-Regulation of Hepatic Hdac 1, 7, 9, 10, 11 and Up-Regulation of Hdac 3', *Alcoholism: Clinical and Experimental Research*, 36(9), pp. 1578-1586.

Kirpich, I.A., Feng, W., Wang, Y., Liu, Y., Barker, D.F., Barve, S.S. and McClain, C.J. (2012b) 'The Type of Dietary Fat Modulates Intestinal Tight Junction Integrity, Gut Permeability, and Hepatic Toll-Like Receptor Expression in a Mouse Model of Alcoholic Liver Disease', *Alcoholism: Clinical and Experimental Research*, 36(5), pp. 835-846.

Klaassen, C.D. (2007) *Casarett & Doull's Toxicology: The Basic Science of Poisons, Seventh Edition*. McGraw-Hill Education.

Klein-Hitpass, L., Schorpp, M., Wagner, U. and Ryffel, G.U. (1986) 'An estrogen-responsive element derived from the 5' flanking region of the Xenopus vitellogenin A2 gene functions in transfected human cells', *Cell*, 46(7), pp. 1053-1061.

Klinge, C.M. (2000) 'Estrogen receptor interaction with co-activators and co-repressors', *Steroids*, 65(5), pp. 227-251.

Klinge, C.M. (2001) 'Estrogen receptor interaction with estrogen response elements', *Nucleic Acids Research*, 29(14), pp. 2905-2919.

Koh, K.H., Jurkovic, S., Yang, K., Choi, S.Y., Jung, J.W., Kim, K.P., Zhang, W. and Jeong, H. (2012) 'Estradiol induces cytochrome P450 2B6 expression at high concentrations: implication in estrogen-mediated gene regulation in pregnancy', *Biochemical Pharmacology*, 84(1), pp. 93-103.

Koide, A., Zhao, C., Naganuma, M., Abrams, J., Deighton-Collins, S., Skafar, D.F. and Koide, S. (2007) 'Identification of regions within the F domain of the human estrogen receptor α that are important for modulating transactivation and protein-protein interactions', *Molecular Endocrinology*, 21(4), pp. 829-842.

Koike, S., Sakai, M. and Muramatsu, M. (1987) 'Molecular cloning and charcterization of rat estrogen receptor cDNA', *Nucleic Acids Research*, 15(6), pp. 2499-2513.

Kono, H., Rusyn, I., Yin, M., Gäbele, E., Yamashina, S., Dikalova, A., Kadiiska, M.B., Connor, H.D., Mason, R.P., Segal, B.H., Bradford, B.U., Holland, S.M. and Thurman, R.G. (2000) 'NADPH oxidase–derived free radicals are key oxidants in alcohol-induced liver disease', *Journal of Clinical Investigation*, 106(7), pp. 867-872.

Kosters, A. and Karpen, S.J. (2010) 'The role of inflammation in cholestasis – clinical and basic aspects', *Seminars in Liver Disease*, 30(2), pp. 186-194.

Krege, J.H., Hodgin, J.B., Couse, J.F., Enmark, E., Warner, M., Mahler, J.F., Sar, M., Korach, K.S., Gustafsson, J.A. and Smithies, O. (1998) 'Generation and reproductive phenotypes of mice lacking estrogen receptor beta', *Proceedings of the National Academy of Sciences* 95(26), pp. 15677-15682.

Kuiper, G.G., Enmark, E., Pelto-Huikko, M., Nilsson, S. and Gustafsson, J.A. (1996) 'Cloning of a novel receptor expressed in rat prostate and ovary', *Proceedings of the National Academy of Sciences*, 93(12), pp. 5925-5930.

Kuiper, G.G., Lemmen, J.G., Carlsson, B., Corton, J.C., Safe, S.H., van der Saag, P.T., van der Burg, B. and Gustafsson, J.A. (1998) 'Interaction of estrogenic chemicals and phytoestrogens with estrogen receptor beta', *Endocrinology*, 139(10), pp. 4252-4263.

Kumar, R., Zakharov, M.N., Khan, S.H., Miki, R., Jang, H., Toraldo, G., Singh, R., Bhasin, S. and Jasuja, R. (2011) 'The Dynamic Structure of the Estrogen Receptor', *Journal of Amino Acids*, 2011, p. 812540.

Kumar, V. and Chambon, P. (1988) 'The estrogen receptor binds tightly to its responsive element as a ligand-induced homodimer', *Cell*, 55(1), pp. 145-156.

Kuntz, E. and Kuntz, H.-D. (2009) *Hepatology: Textbook and atlas*. Springer Science & Business Media.

Kushner, P.J., Agard, D.A., Greene, G.L., Scanlan, T.S., Shiau, A.K., Uht, R.M. and Webb, P. (2000) 'Estrogen receptor pathways to AP-1', *The Journal of Steroid Biochemistry and Molecular Biology*, 74(5), pp. 311-317.

La Sala, G., Farini, D. and De Felici, M. (2010) 'Estrogenic in vitro assay on mouse embryonic Leydig cells', *The International Journal of Developmental Biology*, 54(4), pp. 717-722.

Lammert, F., Marschall, H.-U., Glantz, A. and Matern, S. (2000) 'Intrahepatic cholestasis of pregnancy: molecular pathogenesis, diagnosis and management', *Journal of Hepatology*, 33(6), pp. 1012-1021.

Lamouille, S., Xu, J. and Derynck, R. (2014) 'Molecular mechanisms of epithelial–mesenchymal transition', *Nature Reviews Molecular Cell Biology*, 15(3), pp. 178-196.

Laws, S.C., Carey, S.A., Ferrell, J.M., Bodman, G.J. and Cooper, R.L. (2000) 'Estrogenic Activity of Octylphenol, Nonylphenol, Bisphenol A and Methoxychlor in Rats', *Toxicological Sciences*, 54(1), pp. 154-167.

Legler, J. and Brouwer, A. (2003) 'Are brominated flame retardants endocrine disruptors?', *Environment International*, 29(6), pp. 879-885.

Lepecq, J.B. and Paoletti, C. (1967) 'Fed Eration of European Biochemical Societies 3rd MeetingA fluorescent complex between ethidium bromide and nucleic acids', *Journal of Molecular Biology*, 27(1), pp. 87-106.

Leung, T.M., Lu, Y., Yan, W., Moron-Concepcion, J.A., Ward, S.C., Ge, X., Conde de la Rosa, L. and Nieto, N. (2012) 'Argininosuccinate synthase conditions the response to acute and chronic ethanol-induced liver injury in mice', *Hepatology*, 55(5), pp. 1596-1609.

Leung, Y.K., Mak, P., Hassan, S. and Ho, S.M. (2006) 'Estrogen receptor (ER)-beta isoforms: a key to understanding ER-beta signaling', *Proceedings of the National Academy of Sciences*, 103(35), pp. 13162-13167.

Leuschner, U., Czygan, P., Liersch, M., Frohling, W. and Stiehl, A. (1977) 'Morphologic studies on the toxicity of sulfated and nonsulfated lithocholic acid in the isolation-perfused rat liver', *Zeitschrift für Gastroenterologie*, 15(4), pp. 246-253.

Levin, E.R. (2002) 'Cellular functions of plasma membrane estrogen receptors', *Steroids*, 67(6), pp. 471-475.

Li, L., Haynes, M.P. and Bender, J.R. (2003) 'Plasma membrane localization and function of the estrogen receptor α variant (ER46) in human endothelial cells', *Proceedings of the National Academy of Sciences*, 100(8), pp. 4807-4812.

Liangpunsakul, S., Rahmini, Y., Ross, R.A., Zhao, Z., Xu, Y. and Crabb, D.W. (2012) 'Imipramine blocks ethanol-induced ASMase activation, ceramide generation, and PP2A activation, and ameliorates hepatic steatosis in ethanol-fed mice', *American Journal of Physiology - Gastrointestinal and Liver Physiology*, 302(Supplement 2), pp. S532–S533.

Lieber, C.S. (2004) 'Alcoholic fatty liver: its pathogenesis and mechanism of progression to inflammation and fibrosis', *Alcohol*, 34(1), pp. 9-19.

Lieber, C.S. and DeCarli, L.M. (1982) 'The feeding of alcohol in liquid diets: two decades of applications and 1982 update', *Alcoholism: Clinical and Experimental Research*, 6(4), pp. 523-531.

Lieber, C.S. and DeCarli, L.M. (1989) 'Liquid diet technique of ethanol administration: 1989 update', *Alcohol and Alcoholism*, 24(3), pp. 197-211.

Lippai, D., Bala, S., Catalano, D., Kodys, K. and Szabo, G. (2014) 'Micro-RNA-155 deficiency prevents alcohol-induced serum endotoxin increase and small bowel inflammation in mice', *Alcoholism: Clinical and Experimental Research*, 38(8), pp. 2217-2224.

Long, S.A., Quan, C., Van de Water, J., Nantz, M.H., Kurth, M.J., Barsky, D., Colvin, M.E., Lam, K.S., Coppel, R.L. and Ansari, A. (2001) 'Immunoreactivity of organic mimeotopes of the E2 component of pyruvate dehydrogenase: connecting xenobiotics with primary biliary cirrhosis', *The Journal of Immunology*, 167(5), pp. 2956-2963.

Lu, B., Leygue, E., Dotzlaw, H., Murphy, L.J. and Murphy, L.C. (2000) 'Functional characteristics of a novel murine estrogen receptor-beta isoform, estrogen receptor-beta 2', *Journal of Molecuar Endocrinology*, 25(2), pp. 229-242.

Lu, B., Leygue, E., Dotzlaw, H., Murphy, L.J., Murphy, L.C. and Watson, P.H. (1998) 'Estrogen receptor-beta mRNA variants in human and murine tissues', *Molecular and Cellular Endocrinology*, 138(1-2), pp. 199-203.

Lubahn, D.B., Moyer, J.S., Golding, T.S., Couse, J.F., Korach, K.S. and Smithies, O. (1993) 'Alteration of reproductive function but not prenatal sexual development after insertional disruption of the mouse estrogen receptor gene', *Proceedings of the National Academy of Sciences*, 90(23), pp. 11162-11166.

Luedde, T. and Schwabe, R.F. (2011) 'NF-κB in the liver - linking injury, fibrosis and hepatocellular carcinoma', *Nature Reviews Gastroenterology & Hepatology*, 8(2), pp. 108-118.

Lundberg, K.S., Shoemaker, D.D., Adams, M.W., Short, J.M., Sorge, J.A. and Mathur, E.J. (1991) 'High-fidelity amplification using a thermostable DNA polymerase isolated from Pyrococcus furiosus', *Gene*, 108(1), pp. 1-6.

Ma, Z.Q., Santagati, S., Patrone, C., Pollio, G., Vegeto, E. and Maggi, A. (1994) 'Insulin-like growth factors activate estrogen receptor to control the growth and differentiation of the human neuroblastoma cell line SK-ER3', *Molecular Endocrinology*, 8(7), pp. 910-918.

Mancuso, M., Leonardi, S., Giardullo, P., Pasquali, E., Borra, F., De Stefano, I., Prisco, M.G., Tanori, M., Scambia, G. and Di Majo, V. (2011) 'The estrogen receptor beta agonist diarylpropionitrile (DPN) inhibits medulloblastoma development via anti-proliferative and pro-apototic pathways', *Cancer Letters*, 308(2), pp. 197-202.

Mandrekar, P., Ambade, A., Lim, A., Szabo, G. and Catalano, D. (2011) 'An essential role for monocyte chemoattractant protein-1 in alcoholic liver injury: regulation of proinflammatory cytokines and hepatic steatosis in mice', *Hepatology*, 54(6), pp. 2185-2197.

Mandrekar, P. and Szabo, G. (2009) 'Signalling pathways in alcohol-induced liver inflammation', *Journal of Hepatology*, 50(6), pp. 1258-1266.

Mann, R.E., Smart, R.G. and Govoni, R. (2003) 'The epidemiology of alcoholic liver disease', *Alcohol Research and Health*, 27, pp. 209-219.

Marzioni, M., Torrice, A., Saccomanno, S., Rychlicki, C., Agostinelli, L., Pierantonelli, I., Rhonnstad, P., Trozzi, L., Apelqvist, T., Gentile, R., Candelaresi, C., Fava, G., Semeraro, R., Benedetti, A., Gaudio, E., Franchitto, A., Onori, P., De Minicis, S., Carpino, G., Kallin, E., Alvaro, D. and Nilsson, S. (2012) 'An oestrogen receptor beta-selective agonist exerts anti-neoplastic effects in experimental intrahepatic cholangiocarcinoma', *Digestive and Liver Disease*, 44(2), pp. 134-142.

Mathews, S., Xu, M., Wang, H., Bertola, A. and Gao, B. (2014) 'Animals models of gastrointestinal and liver diseases. Animal models of alcohol-induced liver disease: pathophysiology, translational relevance, and challenges', *American Journal of Physiology - Gastrointestinal and Liver Physiology*, 306(10), pp. G819-23.

Mathurin, P., Deng, Q.G., Keshavarzian, A., Choudhary, S., Holmes, E.W. and Tsukamoto, H. (2000) 'Exacerbation of alcoholic liver injury by enteral endotoxin in rats', *Hepatology*, 32(5), pp. 1008-1017.

Matthews, J. and Gustafsson, J.A. (2003) 'Estrogen signaling: a subtle balance between ER alpha and ER beta', *Molecular Interventions*, 3(5), pp. 281-292.

Matthews, J., Wihlen, B., Tujague, M., Wan, J., Strom, A. and Gustafsson, J.A. (2006) 'Estrogen receptor (ER) beta modulates ERalpha-mediated transcriptional activation by altering the recruitment of c-Fos and c-Jun to estrogen-responsive promoters', *Molecular Endocrinology*, 20(3), pp. 534-543.

Mattison, D.R., Karyakina, N., Goodman, M. and LaKind, J.S. (2014) 'Pharmaco- and toxicokinetics of selected exogenous and endogenous estrogens: a review of the data and identification of knowledge gaps', *Critical Reviews in Toxicology*, 44(8), pp. 696-724.

Mauss, S., Berg, T., Rockstroh, J., Sarrazin, C., Wedemeyer, H. and Kamps, B.S. (2014) 'Hepatology-A clinical textbook'.

Mauvais-Jarvis, F., Clegg, D.J. and Hevener, A.L. (2013) 'The role of estrogens in control of energy balance and glucose homeostasis', *Endocrine Reviews*, 34(3), pp. 309-338.

Mayo, M.J. (2008) 'Natural history of primary biliary cirrhosis', *Clinical Liver Disease*, 12(2), pp. 277-288.

McDonnell, D.P. and Wardell, S.E. (2010) 'The molecular mechanisms underlying the pharmacological actions of ER modulators: implications for new drug discovery in breast cancer', *Current Opinion in Pharmacology*, 10(6), pp. 620-628.

Mehlem, A., Hagberg, C.E., Muhl, L., Eriksson, U. and Falkevall, A. (2013) 'Imaging of neutral lipids by oil red O for analyzing the metabolic status in health and disease', *Nature Protocols*, 8(6), pp. 1149-1154.

Menasce, L.P., White, G.R., Harrison, C.J. and Boyle, J.M. (1993) 'Localization of the estrogen receptor locus (ESR) to chromosome 6q25.1 by FISH and a simple post-FISH banding technique', *Genomics*, 17(1), pp. 263-265.

Menon, K.V., Gores, G.J. and Shah, V.H. (2001) 'Pathogenesis, diagnosis, and treatment of alcoholic liver disease', *Mayo Clinic Proceedings*, 76(10), pp. 1021-1029.

Metcalf, J.V., Bhopal, R.S., Gray, J., Howel, D. and James, O.F. (1997) 'Incidence and prevalence of primary biliary cirrhosis in the city of Newcastle upon Tyne, England', *International Journal of Epidemiology*, 26(4), pp. 830-836.

Mollerup, S., Jorgensen, K., Berge, G. and Haugen, A. (2002) 'Expression of estrogen receptors alpha and beta in human lung tissue and cell lines', *Lung Cancer*, 37(2), pp. 153-159.

Monga, S.P.S. (2011) *Molecular pathology of liver diseases*. Springer.

Moore, J.T., McKee, D.D., Slentz-Kesler, K., Moore, L.B., Jones, S.A., Horne, E.L., Su, J.L., Kliewer, S.A., Lehmann, J.M. and Willson, T.M. (1998) 'Cloning and characterization of human estrogen receptor beta isoforms', *Biochemical and Biophysical Research Communications*, 247(1), pp. 75-78.

Morales, A., Duarte-Rojo, A., Angeles-Angeles, A., Mery, C.M., Ruiz-Molina, J.M., Diaz-Sanchez, V. and Robles-Diaz, G. (2003) 'The beta form of the estrogen receptor is predominantly expressed in the papillary cystic neoplasm of the pancreas', *Pancreas*, 26(3), pp. 258-263.

Mosselman, S., Polman, J. and Dijkema, R. (1996) 'ER beta: identification and characterization of a novel human estrogen receptor', *FEBS Letters*, 392(1), pp. 49-53.

Mottino, A.D., Cao, J., Veggi, L.M., Crocenzi, F., Roma, M.G. and Vore, M. (2002) 'Altered localization and activity of canalicular Mrp2 in estradiol-17beta-D-glucuronide-induced cholestasis', *Hepatology*, 35(6), pp. 1409-1419.

Mottino, A.D., Crocenzi, F.A., Pozzi, E.J., Veggi, L.M., Roma, M.G. and Vore, M. (2005) 'Role of microtubules in estradiol-17beta-D-glucuronide-induced alteration of canalicular Mrp2 localization and activity', *American Journal of Physiology - Gastrointestinal and Liver Physiology*, 288(2), pp. G327-36.

Naaz, A., Zakroczymski, M., Heine, P., Taylor, J., Saunders, P., Lubahn, D. and Cooke, P.S. (2002) 'Effect of ovariectomy on adipose tissue of mice in the absence of estrogen receptor alpha (ERalpha): a potential role for estrogen receptor beta (ERbeta)', *Hormone and Metabolic Research*, 34(11-12), pp. 758-763.

Nanji, A.A., Jokelainen, K., Fotouhinia, M., Rahemtulla, A., Thomas, P., Tipoe, G.L., Su, G.L. and Dannenberg, A.J. (2001) 'Increased severity of alcoholic liver injury in female rats: role of oxidative stress, endotoxin, and chemokines', *American Journal of Physiology-Gastrointestinal and Liver Physiology*, 281(6), pp. G1348-G1356.

Nanji, A.A., Khettry, U. and Sadrzadeh, S.M.H. (1994) 'Lactobacillus feeding reduces endotoxemia and severity of experimental alcoholic liver (disease)', *Experimental Biology and Medicine*, 205(3), pp. 243-247.

Nath, B., Levin, I., Csak, T., Petrasek, J., Mueller, C., Kodys, K., Catalano, D., Mandrekar, P. and Szabo, G. (2011) 'Hepatocyte-specific hypoxia-inducible factor-1alpha is a determinant of lipid accumulation and liver injury in alcohol-induced steatosis in mice', *Hepatology*, 53(5), pp. 1526-1537.

Nelson, K.G., Takahashi, T., Bossert, N.L., Walmer, D.K. and McLachlan, J.A. (1991) 'Epidermal growth factor replaces estrogen in the stimulation of female genital-tract growth and differentiation', *Proceedings of the National Academy of Sciences*, 88(1), pp. 21-25.

Nelson, L.R. and Bulun, S.E. (2001) 'Estrogen production and action', *Journal of the American Academy of Dermatology*, 45(3 Suppl), pp. S116-124.

Newsome, P.N., Hussain, M.A. and Theise, N.D. (2004) 'Hepatic Oval Cells: Helping Redefine a Paradigm in Stem Cell Biology', in *Current Topics in Developmental Biology*. Academic Press, pp. 1-28.

Newton, C.J., Buric, R., Trapp, T., Brockmeier, S., Pagotto, U. and Stalla, G.K. (1994) 'The unliganded estrogen receptor (ER) transduces growth factor signals', *The Journal of Steroid Biochemistry and Molecular Biology*, 48(5-6), pp. 481-486.

Ng, H.W., Perkins, R., Tong, W. and Hong, H. (2014) 'Versatility or Promiscuity: The Estrogen Receptors, Control of Ligand Selectivity and an Update on Subtype Selective Ligands', *International Journal of Environmental Research and Public Health*, 11(9), pp. 8709-8742.

Nielsen, M., Bjornsdottir, S., Hoyer, P.E. and Byskov, A.G. (2000) 'Ontogeny of oestrogen receptor alpha in gonads and sex ducts of fetal and newborn mice', *Journal of Reproduction and Fertility*, 118(1), pp. 195-204.

Nilsson, S. and Gustafsson, J.-Å. (2000) 'Estrogen receptor transcription and transactivation: Basic aspects of estrogen action', *Breast Cancer Research* 2(5), pp. 360-366.

Nilsson, S., Makela, S., Treuter, E., Tujague, M., Thomsen, J., Andersson, G., Enmark, E., Pettersson, K., Warner, M. and Gustafsson, J.A. (2001) 'Mechanisms of estrogen action', *Physiological Reviews*, 81(4), pp. 1535-1565.

Nomura, M., McKenna, E., Korach, K.S., Pfaff, D.W. and Ogawa, S. (2002) 'Estrogen receptor-beta regulates transcript levels for oxytocin and arginine vasopressin in the

hypothalamic paraventricular nucleus of male mice', *Molecular Brain Research*, 109(1-2), pp. 84-94.

NURSA (2016a) *ESR1*. Available at: https://www.nursa.org/nursa/molecules/nr.jsf?doi=10.1621/E7Q6ROD13W (Accessed: 14 September 2016).

NURSA (2016b) *ESR2*. Available at: https://www.nursa.org/nursa/molecules/nr.jsf?doi=10.1621/X1RBUUJU1Z (Accessed: 14 September 2016).

O'Farrelly, C. and Doherty, D.G. (2007) 'Innate Immune Mechanisms in the Liver', in Gershwin, M.E., Vierling, J.M. and Manns, M.P. (eds.) *Liver Immunology-Principles and Practice*. Totowa, NJ: Humana Press, pp. 41-48.

Ogawa, S., Inoue, S., Watanabe, T., Orimo, A., Hosoi, T., Ouchi, Y. and Muramatsu, M. (1998) 'Molecular cloning and characterization of human estrogen receptor betacx: a potential inhibitor of estrogen action in human', *Nucleic Acids Research*, 26(15), pp. 3505-3512.

Oh, S.H., Hatch, H.M. and Petersen, B.E. (2002) 'Hepatic oval 'stem' cell in liver regeneration', *Seminars in Cell & Developmental Biology*, 13(6), pp. 405-409.

Oude Elferink, R.P., Paulusma, C.C. and Groen, A.K. (2006) 'Hepatocanalicular transport defects: pathophysiologic mechanisms of rare diseases', *Gastroenterology*, 130(3), pp. 908-925.

Ozawa, S., Shimizu, M., Katoh, T., Miyajima, A., Ohno, Y., Matsumoto, Y., Fukuoka, M., Tang, Y.-M., Lang, N.P. and Kadlubar, F.F. (1999) 'Sulfating-Activity and Stability of cDNA-Expressed Allozymes of Human Phenol Sulfotransferase, ST1A3*1 (213Arg) and ST1A3*2 (213His), Both of Which Exist in Japanese as Well as Caucasians', *Journal of Biochemistry*, 126(2), pp. 271-277.

Ozkan, S., Ceylan, Y., Ozkan, O.V. and Yildirim, S. (2015) 'Review of a challenging clinical issue: Intrahepatic cholestasis of pregnancy', *World Journal of Gastroenterology*, 21(23), pp. 7134-7141.

Paige, L.A., Christensen, D.J., Grøn, H., Norris, J.D., Gottlin, E.B., Padilla, K.M., Chang, C.-y., Ballas, L.M., Hamilton, P.T., McDonnell, D.P. and Fowlkes, D.M. (1999) 'Estrogen

receptor (ER) modulators each induce distinct conformational changes in ER α and ER β', *Proceedings of the National Academy of Sciences*, 96(7), pp. 3999-4004.

Parikh-Patel, A., Gold, E.B., Worman, H., Krivy, K.E. and Gershwin, M.E. (2001) 'Risk factors for primary biliary cirrhosis in a cohort of patients from the united states', *Hepatology*, 33(1), pp. 16-21.

Parlesak, A., Schafer, C., Schutz, T., Bode, J.C. and Bode, C. (2000) 'Increased intestinal permeability to macromolecules and endotoxemia in patients with chronic alcohol abuse in different stages of alcohol-induced liver disease', *Journal of Hepatology*, 32(5), pp. 742-747.

Paruthiyil, S., Parmar, H., Kerekatte, V., Cunha, G.R., Firestone, G.L. and Leitman, D.C. (2004) 'Estrogen receptor β inhibits human breast cancer cell proliferation and tumor formation by causing a G2 cell cycle arrest', *Cancer Research*, 64(1), pp. 423-428.

Paul, P., Suwan, J., Liu, J., Dordick, J.S. and Linhardt, R.J. (2012) 'Recent advances in sulfotransferase enzyme activity assays', *Analytical and Bioanalytical Chemistry*, 403(6), pp. 1491-1500.

Peekhaus, N.T., Chang, T., Hayes, E.C., Wilkinson, H.A., Mitra, S.W., Schaeffer, J.M. and Rohrer, S.P. (2004) 'Distinct effects of the antiestrogen Faslodex on the stability of estrogen receptors-alpha and -beta in the breast cancer cell line MCF-7', *Journal of Molecular Endocrinology*, 32(3), pp. 987-995.

Pennington, H.L., Hall, P.D.L.M., Wilce, P.A. and Worrall, S. (1997) 'Ethanol feeding enhances inflammatory cytokine expression in lipopolysaccharide ‐ induced hepatitis', *Journal of Gastroenterology and Hepatology*, 12(4), pp. 305-313.

Penot, G., Le Peron, C., Merot, Y., Grimaud-Fanouillere, E., Ferriere, F., Boujrad, N., Kah, O., Saligaut, C., Ducouret, B., Metivier, R. and Flouriot, G. (2005) 'The human estrogen receptor-alpha isoform hERalpha46 antagonizes the proliferative influence of hERalpha66 in MCF7 breast cancer cells', *Endocrinology*, 146(12), pp. 5474-5484.

Petersen, D.N., Tkalcevic, G.T., Koza-Taylor, P.H., Turi, T.G. and Brown, T.A. (1998) 'Identification of estrogen receptor beta2, a functional variant of estrogen receptor beta expressed in normal rat tissues', *Endocrinology*, 139(3), pp. 1082-1092.

Petrasek, J., Mandrekar, P. and Szabo, G. (2010) 'Toll-Like Receptors in the Pathogenesis of Alcoholic Liver Disease', *Gastroenterology Research and Practice*, 2010(Article ID 710381), p. 7

Pierre M, M., Kathryn B, H., Dale S, R. and McGUIRE, W.L. (1978) 'Phytoestrogen Interaction with Estrogen Receptors in Human Breast Cancer Cells', *Endocrinology*, 103(5), pp. 1860-1867.

Poola, I., Abraham, J., Baldwin, K., Saunders, A. and Bhatnagar, R. (2005) 'Estrogen receptors beta4 and beta5 are full length functionally distinct ERbeta isoforms: cloning from human ovary and functional characterization', *Endocrine*, 27(3), pp. 227-238.

Poola, I., Koduri, S., Chatra, S. and Clarke, R. (2000) 'Identification of twenty alternatively spliced estrogen receptor alpha mRNAs in breast cancer cell lines and tumors using splice targeted primer approach', *The Journal of Steroid Biochemistry and Molecular Biology*, 72(5), pp. 249-258.

Prince, M.I., Chetwynd, A., Diggle, P., Jarner, M., Metcalf, J.V. and James, O.F. (2001) 'The geographical distribution of primary biliary cirrhosis in a well-defined cohort', *Hepatology*, 34(6), pp. 1083-1088.

Probert, P.M.E., Thesis (2014) ' Refining and replacing models of hepatocytes and periportal fibrosis', *Newcastle University ethesis database*.

Probert, P.M.E., Meyer, S.K., Alsaeedi, F., Axon, A.A., Fairhall, E.A., Wallace, K., Charles, M., Oakley, F., Jowsey, P.A., Blain, P.G. and Wright, M.C. (2015) 'An expandable donor-free supply of functional hepatocytes for toxicology', *Toxicology Research*, 4(2), pp. 203-222.

Promega (2016a) *pGL3 Luciferase Reporter Vectors*. Available at: https://www.promega.co.uk/products/reporter-assays-and-transfection/reporter-vectors-and-cell-lines/pgl3-luciferase-reporter-vectors/?activeTab=2 (Accessed: 14 September 2016).

Promega (2016b) *pRL Renilla Luciferase Control Reporter Vectors*. Available at: https://www.promega.co.uk/products/reporter-assays-and-transfection/reporter-vectors-and-cell-lines/prl-renilla-luciferase-control-reporter-vectors/?activeTab=2 (Accessed: 14 September 2016).

Pruett, S.B. and Fan, R. (2009) 'Ethanol inhibits LPS-induced signaling and modulates cytokine production in peritoneal macrophages in vivo in a model for binge drinking', *BMC Immunology*, 10(1), pp. 1-10.

Prusakiewicz, J.J., Harville, H.M., Zhang, Y., Ackermann, C. and Voorman, R.L. (2007) 'Parabens inhibit human skin estrogen sulfotransferase activity: Possible link to paraben estrogenic effects', *Toxicology*, 232(3), pp. 248-256.

Purdom, C.E., Hardiman, P.A., Bye, V.V.J., Eno, N.C., Tyler, C.R. and Sumpter, J.P. (1994) 'Estrogenic effects of effluents from sewage treatment works', *Chemistry and Ecology*, 8(4), pp. 275-285.

Rainville, J., Pollard, K. and Vasudevan, N. (2015) 'Membrane-Initiated Non-Genomic Signaling by Estrogens in the Hypothalamus: Cross-Talk with Glucocorticoids with Implications for Behavior', *Frontiers in Endocrinology*, 6, p. 18.

Rajan, J.P., Simon, R.A. and Bosso, J.V. (2014) 'Prevalence of sensitivity to food and drug additives in patients with chronic idiopathic urticaria', *Journal of Allergy and Clinical Immunology*, 2(2), pp. 168-171.

Ramsey, T.L., Risinger, K.E., Jernigan, S.C., Mattingly, K.A. and Klinge, C.M. (2004) 'Estrogen receptor beta isoforms exhibit differences in ligand-activated transcriptional activity in an estrogen response element sequence-dependent manner', *Endocrinology*, 145(1), pp. 149-160.

Rao, R.K. (1998) 'Acetaldehyde ‐ Induced Increase in Paracellular Permeability in Caco ‐ 2 Cell Monolayer', *Alcoholism: Clinical and Experimental Research*, 22(8), pp. 1724-1730.

Rao, R.K., Seth, A. and Sheth, P. (2004) 'Recent advances in alcoholic liver disease I. Role of intestinal permeability and endotoxemia in alcoholic liver disease', *American Journal of Physiology-Gastrointestinal and Liver Physiology*, 286(6), pp. G881-G884.

Reyes, H. (2008) 'Sex hormones and bile acids in intrahepatic cholestasis of pregnancy', *Hepatology*, 47(2), pp. 376-379.

Riggs, B.L. and Hartmann, L.C. (2003) 'Selective estrogen-receptor modulators -- mechanisms of action and application to clinical practice', *The New England Journal of Medicine*, 348(7), pp. 618-629.

Robinson, G.M., Orrego, H., Israel, Y., Devenyi, P. and Kapur, B.M. (1981) 'Low-molecular-weight polyethylene glycol as a probe of gastrointestinal permeability after alcohol ingestion', *Digestive Diseases and Sciences*, 26(11), pp. 971-977.

Rodrigues, A.D., Lai, Y., Cvijic, M.E., Elkin, L.L., Zvyaga, T. and Soars, M.G. (2014) 'Drug-Induced Perturbations of the Bile Acid Pool, Cholestasis, and Hepatotoxicity: Mechanistic Considerations beyond the Direct Inhibition of the Bile Salt Export Pump', *Drug Metabolism and Disposition*, 42(4), pp. 566-574.

Rodriguez-Garay, E.A. (2003) 'Cholestasis: human disease and experimental animal models', *Annals of Hepatology*, 2(4), pp. 150-158.

Rogers, J.A., Metz, L. and Yong, V.W. (2013) 'Review: Endocrine disrupting chemicals and immune responses: a focus on bisphenol-A and its potential mechanisms', *Molecular Immunology*, 53(4), pp. 421-430.

Roman-Blas, J.A., Castañeda, S., Largo, R. and Herrero-Beaumont, G. (2009) 'Osteoarthritis associated with estrogen deficiency', *Arthritis Research & Therapy*, 11(5), p. 241.

Routledge, E.J., Parker, J., Odum, J., Ashby, J. and Sumpter, J.P. (1998) 'Some alkyl hydroxy benzoate preservatives (parabens) are estrogenic', *Toxicology and Applied Pharmacology*, 153(1), pp. 12-19.

Roxon, J.J., Ryan, A.J. and Wright, S.E. (1967) 'Enzymatic reduction of tartrazine by Proteus vulgaris from rats', *Food and Cosmetics Toxicology*, 5, pp. 645-656.

Rubin, B.L., Dorfman, A.S., Black, L. and Dorfman, R.I. (1951) 'Bioassay of estrogens using the mouse uterine response', *Endocrinology*, 49(4), pp. 429-439.

Ryan, A.J., Welling, P.G. and Roxon, J.J. (1969a) 'Metabolism of a tartrazine analogue by intestinal bacteria', *Food and Cosmetics Toxicology*, 7(4), pp. 297-299.

Ryan, A.J., Welling, P.G. and Wright, S.E. (1969b) 'Further studies on the metabolism of tartrazine and related compounds in the intact rat', *Food and Cosmetics Toxicology*, 7(4), pp. 287-295.

Salaspuro, M. (1996) 'Bacteriocolonic pathway for ethanol oxidation: characteristics and implications', *Annals of Medicine*, 28(3), pp. 195-200.

Saville, B., Wormke, M., Wang, F., Nguyen, T., Enmark, E., Kuiper, G., Gustafsson, J.A. and Safe, S. (2000) 'Ligand-, cell-, and estrogen receptor subtype (alpha/beta)-dependent activation at GC-rich (Sp1) promoter elements', *The Journal of Biological Chemistry*, 275(8), pp. 5379-5387.

Schab, D.W. and Trinh, N.H. (2004) 'Do artificial food colors promote hyperactivity in children with hyperactive syndromes? A meta-analysis of double-blind placebo-controlled trials', *Journal of Developmental & Behavioral Pediatrics*, 25(6), pp. 423-434.

Scharschmidt, B.F., Goldberg, H.I. and Schmid, R. (1983) 'Current concepts in diagnosis. Approach to the patient with cholestatic jaundice', *The New England Journal of Medicine*, 308(25), pp. 1515-1519.

Schon, H.-T. and Weiskirchen, R. (2014) 'Immunomodulatory effects of transforming growth factor-β in the liver', *Hepatobiliary Surgery and Nutrition*, 3(6), pp. 386-406.

Schug, T.T., Janesick, A., Blumberg, B. and Heindel, J.J. (2011) 'Endocrine disrupting chemicals and disease susceptibility', *The Journal of Steroid Biochemistry and Molecular Biology*, 127(3-5), pp. 204-215.

Selmi, C., Balkwill, D.L., Invernizzi, P., Ansari, A.A., Coppel, R.L., Podda, M., Leung, P.S., Kenny, T.P., Van De Water, J. and Nantz, M.H. (2003) 'Patients with primary biliary cirrhosis react against a ubiquitous xenobiotic‐metabolizing bacterium', *Hepatology*, 38(5), pp. 1250-1257.

Selmi, C., Lleo, A., Invernizzi, P. and Eric Gershwin, M. (2007) 'Primary Biliary Cirrhosis and Autoimmune Cholangitis', in Gershwin, M.E., Vierling, J.M. and Manns, M.P. (eds.) *Liver Immunology: Principles and Practice*. Totowa, NJ: Humana Press, pp. 235-247.

Selmi, C., Mayo, M.J., Bach, N., Ishibashi, H., Invernizzi, P., Gish, R.G., Gordon, S.C., Wright, H.I., Zweiban, B., Podda, M. and Gershwin, M.E. (2004) 'Primary biliary cirrhosis in monozygotic and dizygotic twins: genetics, epigenetics, and environment', *Gastroenterology*, 127(2), pp. 485-492.

Shah, K.H. and Verma, R.J. (2011) 'Butyl p-hydroxybenzoic acid induces oxidative stress in mice liver--an in vivo study', *Acta Poloniae Pharmaceutica*, 68(6), pp. 875-879.

Shan, L. (2011) 'Magnetic iron microbeads coupled with HEA-125 monoclonal antibody against epithelial cell adhesion molecule', *Molecular Imaging and Contrast Agent Database*.

Shang, Y. and Brown, M. (2002) 'Molecular determinants for the tissue specificity of SERMs', *Science*, 295(5564), pp. 2465-2468.

Shanle, E.K. and Xu, W. (2011) 'Endocrine disrupting chemicals targeting estrogen receptor signaling: identification and mechanisms of action', *Chemical Research in Toxicology*, 24(1), pp. 6-19.

Shelley, P.M.F., Ali, S.T., Guest, J.R., Oliver, F.W.J., Bassendine, M.F. and Yeaman, S.J. (1990) 'Reactivity of Primary Biliary Cirrhosis Sera with Escherichia coli Dihydrolipoamide Acetyltransferase (E2p): Characterization of the Main Immunogenic Region', *Proceedings of the National Academy of Sciences* 87(10), pp. 3987-3991.

Sherman, K.E. (1991) 'Alanine aminotransferase in clinical practice. A review', *Archives of Internal Medicine*, 151(2), pp. 260-265.

Shibata, H., Spencer, T.E., Onate, S.A., Jenster, G., Tsai, S.Y., Tsai, M.J. and O'Malley, B.W. (1997) 'Role of co-activators and co-repressors in the mechanism of steroid/thyroid receptor action', *Recent Progress in Hormone Research*, 52, pp. 141-164.

Shou, J., Massarweh, S., Osborne, C.K., Wakeling, A.E., Ali, S., Weiss, H. and Schiff, R. (2004) 'Mechanisms of tamoxifen resistance: increased estrogen receptor-HER2/neu cross-talk in ER/HER2-positive breast cancer', *Journal of the National Cancer Institute*, 96(12), pp. 926-935.

Shu, F.J., Sidell, N., Yang, D. and Kallen, C.B. (2010) 'The tri-nucleotide spacer sequence between estrogen response element half-sites is conserved and modulates ERalpha-mediated transcriptional responses', *The Journal of Steroid Biochemistry and Molecular Biology*, 120(4-5), pp. 172-179.

Shukla, S.D., Pruett, S.B., Szabo, G. and Arteel, G.E. (2013) 'Binge Ethanol and Liver: New Molecular Developments', *Alcoholism, clinical and experimental research*, 37(4), pp. 550-557.

Smith, C.L. (1998) 'Cross-talk between peptide growth factor and estrogen receptor signaling pathways', *Biology of Reproduction*, 58(3), pp. 627-632.

Smyk, D., Mytilinaiou, M.G., Rigopoulou, E.I. and Bogdanos, D.P. (2010) 'PBC Triggers in Water Reservoirs, Coal Mining Areas and Waste Disposal Sites: From Newcastle to New York', *Disease Markers*, 29(6), pp. 337-344.

Song, W.C. (2001) 'Biochemistry and reproductive endocrinology of estrogen sulfotransferase', *Annals of the New York Academy of Sciences*, 948, pp. 43-50.

Soto, A.M. and Sonnenschein, C. (2010) 'Environmental causes of cancer: endocrine disruptors as carcinogens', *Nature Reviews Endocrinology*, 6(7), pp. 363-370.

Sotoca, A.M., Vervoort, J., Rietjens, I.M.C.M. and Gustafsson, J. (2012) *Human ERα and ERβ Splice Variants: Understanding Their Domain Structure in Relation to Their Biological Roles in Breast Cancer Cell Proliferation*. InTech.

Staels, B. and Fonseca, V.A. (2009) 'Bile acids and metabolic regulation: mechanisms and clinical responses to bile acid sequestration', *Diabetes Care*, 32 (Suppl 2), pp. S237-245.

Stemerowicz, R., Hopf, U., Moller, B., Wittenbrink, C., Rodloff, A., Reinhardt, R., Freudenberg, M. and Galanos, C. (1988) 'Are antimitochondrial antibodies in primary biliary cirrhosis induced by R(rough)-mutants of enterobacteriaceae?', *Lancet*, 2(8621), pp. 1166-1170.

Stephen, R.H. and Ellis, R.L. (2007) 'Extranuclear Steroid Receptors: Nature and Actions', *Endocrine Reviews*, 28(7), pp. 726-741.

Stieger, B., Fattinger, K., Madon, J., Kullak-Ublick, G.A. and Meier, P.J. (2000) 'Drug- and estrogen-induced cholestasis through inhibition of the hepatocellular bile salt export pump (Bsep) of rat liver', *Gastroenterology*, 118(2), pp. 422-430.

Strautnieks, S.S., Bull, L.N., Knisely, A.S., Kocoshis, S.A., Dahl, N., Arnell, H., Sokal, E., Dahan, K., Childs, S., Ling, V., Tanner, M.S., Kagalwalla, A.F., Nemeth, A., Pawlowska, J., Baker, A., Mieli-Vergani, G., Freimer, N.B., Gardiner, R.M. and Thompson, R.J. (1998) 'A gene encoding a liver-specific ABC transporter is mutated in progressive familial intrahepatic cholestasis', *Nature Genetics*, 20(3), pp. 233-238.

Strober, W. (2001) 'Trypan Blue Exclusion Test of Cell Viability', in *Current Protocols in Immunology*. John Wiley & Sons, Inc.

Strott, C.A. (1996) 'Steroid sulfotransferases', *Endocrine Reviews*, 17(6), pp. 670-697.

Sumpter, J.P. (1995) 'Feminized responses in fish to environmental estrogens', *Toxicology Letters*, 82, pp. 737-742.

Sunami, Y., Leithäuser, F., Gul, S., Fiedler, K., Güldiken, N., Espenlaub, S., Holzmann, K.-H., Hipp, N., Sindrilaru, A., Luedde, T., Baumann, B., Wissel, S., Kreppel, F., Schneider, M., Scharffetter-Kochanek, K., Kochanek, S., Strnad, P. and Wirth, T. (2012) 'Hepatic activation of IKK/NFκB signaling induces liver fibrosis via macrophage-mediated chronic inflammation', *Hepatology*, 56(3), pp. 1117-1128.

Szabo, G. (2015) 'Gut-Liver Axis in Alcoholic Liver Disease', *Gastroenterology*, 148(1), pp. 30-36.

Szabo, G. and Bala, S. (2010) 'Alcoholic liver disease and the gut-liver axis', *World Journal of Gastroenterology*, 16(11), pp. 1321-1329.

Takeda, K. and Akira, S. (2004) 'TLR signaling pathways', *Seminars in Immunology*, 16(1), pp. 3-9.

Talwalkar, J.A. and Lindor, K.D. (2003) 'Primary biliary cirrhosis', *Lancet*, 362(9377), pp. 53-61.

Thomas, P. and Dong, J. (2006) 'Binding and activation of the seven-transmembrane estrogen receptor GPR30 by environmental estrogens: a potential novel mechanism of endocrine disruption', *The Journal of Steroid Biochemistry and Molecular Biology*, 102(1-5), pp. 175-179.

Thomas, P. and Smart, T.G. (2005) 'HEK293 cell line: a vehicle for the expression of recombinant proteins', *Journal of Pharmacological and Toxicological Methods*, 51(3), pp. 187-200.

Torrice, A., Alvaro, D., Onori, P., Franchitto, A., Mancino, M.G., Alpini, G., Jefferson, D.M., Angelico, M., Strazzabosco, M., Attili, A.F., Battisti, G. and Gaudio, E. (2006) 'Estrogens and IGF1 promote the proliferation of hepatic cyst epithelium in autosomal dominant polycystic kidney disease (ADPKD)', *Journal of Hepatology*, 44, pp. S42-S43.

Toth, C.A. and Thomas, D. (1992) 'Liver endocytosis and Kupffer cells', *Hepatology*, 16(1), pp. 255-266.

Trauner, M. and Boyer, J.L. (2003) 'Bile salt transporters: molecular characterization, function, and regulation', *Physiological Reviews*, 83(2), pp. 633-671.

Tremblay, G.B., Tremblay, A., Copeland, N.G., Gilbert, D.J., Jenkins, N.A., Labrie, F. and Giguere, V. (1997) 'Cloning, chromosomal localization, and functional analysis of the murine estrogen receptor beta', *Molecular Endocrinology*, 11(3), pp. 353-365.

Tsai, M.J. and O'Malley, B.W. (1994) 'Molecular mechanisms of action of steroid/thyroid receptor superfamily members', *Annual Review of Biochemistry*, 63, pp. 451-486.

Tsuchiya, Y., Nakajima, M. and Yokoi, T. (2005) 'Cytochrome P450-mediated metabolism of estrogens and its regulation in human', *Cancer Letters*, 227(2), pp. 115-124.

Tsukamoto, H., Reidelberger, R.D., French, S.W. and Largman, C. (1984) 'Long-term cannulation model for blood sampling and intragastric infusion in the rat', *American Journal of Physiology*, 247(3 Pt 2), pp. R595-599.

Uebi, T., Umeda, M. and Imai, T. (2015) 'Estrogen induces estrogen receptor alpha expression and hepatocyte proliferation in the livers of male mice', *Genes to Cells*, 20(3), pp. 217-223.

Ueno, A., Lazaro, R., Wang, P.Y., Higashiyama, R., Machida, K. and Tsukamoto, H. (2012) 'Mouse intragastric infusion (iG) model', *Nature Protocols*, 7(4), pp. 771-781.

Uesugi, T., Froh, M., Arteel, G.E., Bradford, B.U. and Thurman, R.G. (2001) 'Toll-like receptor 4 is involved in the mechanism of early alcohol-induced liver injury in mice', *Hepatology*, 34(1), pp. 101-108.

Uesugi, T., Froh, M., Arteel, G.E., Bradford, B.U., Wheeler, M.D., Gabele, E., Isayama, F. and Thurman, R.G. (2002) 'Role of lipopolysaccharide-binding protein in early alcohol-induced liver injury in mice', *Journal of Immunology*, 168(6), pp. 2963-2969.

Van de Water, J., Ishibashi, H., Coppel, R.L. and Gershwin, M.E. (2001) 'Molecular mimicry and primary biliary cirrhosis: Premises not promises', *Hepatology*, 33(4), pp. 771-775.

Vinas, R. and Watson, C.S. (2013) 'Mixtures of xenoestrogens disrupt estradiol-induced non-genomic signaling and downstream functions in pituitary cells', *Environmental Health*, 12(26), pp. 12-26.

Vogel, C.L. (2003) 'Update on the current use of hormonals as therapy in advanced breast cancer', *Anti-Cancer Drugs*, 14(4), pp. 265-273.

Vore, M. (1987) 'Estrogen cholestasis. Membranes, metabolites, or receptors?', *Gastroenterology*, 93(3), pp. 643-649.

Wagner, M., Zollner, G. and Trauner, M. (2009) 'New molecular insights into the mechanisms of cholestasis', *Journal of Hepatology*, 51(3), pp. 565-580.

Wakeling, A.E., Dukes, M. and Bowler, J. (1991) 'A Potent Specific Pure Antiestrogen with Clinical Potential', *Cancer Research*, 51(15), pp. 3867-3873.

Walker, P., Germond, J.E., Brown-Luedi, M., Givel, F. and Wahli, W. (1984) 'Sequence homologies in the region preceding the transcription initiation site of the liver estrogen-responsive vitellogenin and apo-VLDLII genes', *Nucleic Acids Research*, 12(22), pp. 8611-8626.

Wallace, K., Burt, A.D. and Wright, M.C. (2008) 'Liver fibrosis', *Biochemical Journal*, 411(1), pp. 1-18.

Wang, Z., Zhang, X., Shen, P., Loggie, B.W., Chang, Y. and Deuel, T.F. (2005) 'Identification, cloning, and expression of human estrogen receptor-alpha36, a novel variant of human estrogen receptor-alpha66', *Biochemical and Biophysical Research Communications*, 336(4), pp. 1023-1027.

Wang, Z., Zhang, X., Shen, P., Loggie, B.W., Chang, Y. and Deuel, T.F. (2006) 'A variant of estrogen receptor-α, hER-α36: transduction of estrogen- and antiestrogen-dependent membrane-initiated mitogenic signaling', *Proceedings of the National Academy of Sciences*, 103(24), pp. 9063-9068.

Warner, M. and Gustafsson, J.-Å. (2010) 'The role of estrogen receptor β (ERβ) in malignant diseases - A new potential target for antiproliferative drugs in prevention and treatment of cancer', *Biochemical and Biophysical Research Communications*, 396(1), pp. 63-66.

Watanabe, N., Suzuki, J. and Kobayashi, Y. (1996) 'Role of calcium in tumor necrosis factor-α production by activated macrophages', *Journal of Biochemistry*, 120(6), pp. 1190-1195.

Weber, R.W., Hoffman, M., Raine, D.A., Jr. and Nelson, H.S. (1979) 'Incidence of bronchoconstriction due to aspirin, azo dyes, non-azo dyes, and preservatives in a population of perennial asthmatics', *Journal of Allergy and Clinical Immunology*, 64(1), pp. 32-37.

Weinshilboum, R.M., Otterness, D.M., Aksoy, I.A., Wood, T.C., Her, C. and Raftogianis, R.B. (1997) 'Sulfation and sulfotransferases 1: Sulfotransferase molecular biology: cDNAs and genes', *The FASEB Journal*, 11(1), pp. 3-14.

White, R., Lees, J.A., Needham, M., Ham, J. and Parker, M. (1987) 'Structural organization and expression of the mouse estrogen receptor', *Molecular Endocrinology*, 1(10), pp. 735-744.

Wiseman, L.R., Johnson, M.D., Wakeling, A.E., Lykkesfeldt, A.E., May, F.E.B. and Westley, B.R. (1993) 'Type I IGF receptor and acquired tamoxifen resistance in oestrogen-responsive human breast cancer cells', *European Journal of Cancer*, 29(16), pp. 2256-2264.

Woolbright, B.L., Dorko, K., Antoine, D.J., Clarke, J.I., Gholami, P., Li, F., Kumer, S.C., Schmitt, T.M., Forster, J., Fan, F., Jenkins, R.E., Park, B.K., Hagenbuch, B., Olyaee, M. and Jaeschke, H. (2015) 'Bile acid-induced necrosis in primary human hepatocytes and in patients with obstructive cholestasis', *Toxicology and Applied Pharmacology*, 283(3), pp. 168-177.

Woolbright, B.L. and Jaeschke, H. (2012) 'Novel insight into mechanisms of cholestatic liver injury', *World Journal of Gastroenterology*, 18(36), pp. 4985-4993.

Worthington, B.S., Meserole, L. and Syrotuck, J.A. (1978) 'Effect of daily ethanol ingestion on intestinal permeability to macromolecules', *The American Journal of Digestive Diseases*, 23(1), pp. 23-32.

Wu, D., Wang, X., Zhou, R., Yang, L. and Cederbaum, A.I. (2012) 'Alcohol steatosis and cytotoxicity: The role of cytochrome P4502E1 and autophagy', *Free Radical Biology and Medicine*, 53(6), pp. 1346-1357.

Xenbase (2016) *pcDNA3.1*. Available at: http://www.xenbase.org/common/showImage.do?imageId=40928&printer=true (Accessed: 14 September 2016).

Xia, X., Jung, D., Webb, P., Zhang, A., Zhang, B., Li, L., Ayers, S.D., Gabbi, C., Ueno, Y., Gustafsson, J.A., Alpini, G., Moore, D.D. and Lesage, G.D. (2012) 'Liver X receptor beta and peroxisome proliferator-activated receptor delta regulate cholesterol transport in murine cholangiocytes', *Hepatology*, 56(6), pp. 2288-2296.

Yamada, S., Mochida, S., Ohno, A., Hirata, K., Ogata, I., Ohta, Y. and Fujiwara, K. (1991) 'Evidence for enhanced secretory function of hepatic macrophages after long‐term ethanol feeding in rats', *Liver*, 11(4), pp. 220-224.

Yamamoto, Y., Moore, R., Hess, H.A., Guo, G.L., Gonzalez, F.J., Korach, K.S., Maronpot, R.R. and Negishi, M. (2006) 'Estrogen receptor alpha mediates 17alpha-ethynylestradiol causing hepatotoxicity', *The Journal of Biological Chemistry*, 281(24), pp. 16625-16631.

Yang, J., Singleton, D.W., Shaughnessy, E.A. and Khan, S.A. (2008) 'The F-domain of estrogen receptor-alpha inhibits ligand induced receptor dimerization', *Molecular and Cellular Endocrinology*, 295(1-2), pp. 94-100.

Yang, L., Rozenfeld, R., Wu, D., Devi, L.A., Zhang, Z. and Cederbaum, A. (2014) 'Cannabidiol protects liver from binge alcohol-induced steatosis by mechanisms including inhibition of oxidative stress and increase in autophagy', *Free Radical Biology and Medicine*, 68, pp. 260-267.

Yi, P., Driscoll, M.D., Huang, J., Bhagat, S., Hilf, R., Bambara, R.A. and Muyan, M. (2002) 'The effects of estrogen-responsive element- and ligand-induced structural changes on the recruitment of cofactors and transcriptional responses by ER alpha and ER beta', *Molecular Endocrinology*, 16(4), pp. 674-693.

Yin, M., Wheeler, M.D., Kono, H., Bradford, B.U., Gallucci, R.M., Luster, M.I. and Thurman, R.G. (1999) 'Essential role of tumor necrosis factor α in alcohol-induced liver injury in mice', *Gastroenterology*, 117(4), pp. 942-952.

Yoon, K., Kwack, S.J., Kim, H.S. and Lee, B.-M. (2014) 'Estrogenic Endocrine-Disrupting Chemicals: Molecular Mechanisms of Actions on Putative Human Diseases', *Journal of Toxicology and Environmental Health*, 17(3), pp. 127-174.

Zhao, C., Toresson, G., Xu, L., Koehler, K.F., Gustafsson, J.-Å. and Dahlman-Wright, K. (2005) 'Mouse Estrogen Receptor β Isoforms Exhibit Differences in Ligand Selectivity and Coactivator Recruitment', *Biochemistry*, 44(22), pp. 7936-7944.

Zhong, W., McClain, C.J., Cave, M., Kang, Y.J. and Zhou, Z. (2010) 'The role of zinc deficiency in alcohol-induced intestinal barrier dysfunction', *American Journal of Physiology - Gastrointestinal and Liver Physiology*, 298(5), pp. 625-633.

Ziegler, R.G., Fuhrman, B.J., Moore, S.C. and Matthews, C.E. (2015) 'Epidemiologic studies of estrogen metabolism and breast cancer', *Steroids*, 99(Pt A), pp. 67-75.

Appendix A.

Alignment of mouse ERα (mERa) mRNA sequence with sequencing results of the mERα insert cloned into the destination vector pcDNA3.1 (Cloned mERa). The clustal alignment software (http://www.ebi.ac.uk/Tools/msa/clustalo/) was used. *, identical amino acid between sequences.

```
CLUSTAL O(1.2.1) multiple sequence alignment


Cloned mERa   ATGACCATGACCCTTCACACCAAAGCCTCGGGAATGGCCTTGCTGCACCAGATCCAAGGG
mERa mRNA     ATGACCATGACCCTTCACACCAAAGCCTCGGGAATGGCCTTGCTGCACCAGATCCAAGGG
              ************************************************************

Cloned mERa   AACGAGCTGGAGCCCCTCAACCGCCCGCAGCTCAAGATGCCCATGGAGAGGGCCCTGGGC
mERa mRNA     AACGAGCTGGAGCCCCTCAACCGCCCGCAGCTCAAGATGCCCATGGAGAGGGCCCTGGGC
              ************************************************************

Cloned mERa   GAGGTATACGTGGACAACAGCAAGCCCACTGTGTTCAACTACCCCGAGGGCGCCGCCTAC
mERa mRNA     GAGGTATACGTGGACAACAGCAAGCCCACTGTGTTCAACTACCCCGAGGGCGCCGCCTAC
              ************************************************************

Cloned mERa   GAGTTCAACGCCGCCGCCGCCGCCGCCGCCGCCGCCTCGGCGCCGGTCTACGGCCAGTCG
mERa mRNA     GAGTTCAACGCCGCCGCCGCCGCCGCCGCCGCCTCGGCGCCGGTCTACGGCCAGTCG
              ************************************************************

Cloned mERa   GGCATCGCCTACGGCCCCGGGTCGGAGGCGGCCGCCTTCAGTGCCAACAGCCTGGGGGCT
mERa mRNA     GGCATCGCCTACGGCCCCGGGTCGGAGGCGGCCGCCTTCAGTGCCAACAGCCTGGGGGCT
              ************************************************************

Cloned mERa   TTCCCCCAGCTCAACAGCGTGTCGCCTAGCCCGCTGATGCTGCTGCACCCGCCGCCGCAG
mERa mRNA     TTCCCCCAGCTCAACAGCGTGTCGCCTAGCCCGCTGATGCTGCTGCACCCGCCGCCGCAG
              ************************************************************

Cloned mERa   CTGTCTCCTTTCCTGCACCCGCACGGCCAGCAGGTGCCCTACTACCTGGAGAACGAGCCC
mERa mRNA     CTGTCTCCTTTCCTGCACCCGCACGGCCAGCAGGTGCCCTACTACCTGGAGAACGAGCCC
              ************************************************************

Cloned mERa   AGCGCCTACGCCGTGCGCGACACCGGCCCTCCCGCCTTCTACAGGTCTAATTCTGACAAT
mERa mRNA     AGCGCCTACGCCGTGCGCGACACCGGCCCTCCCGCCTTCTACAGGTCTAATTCTGACAAT
              ************************************************************

Cloned mERa   CGACGCCAGAATGGCCGAGAGAGACTGTCCAGCAGTAACGAGAAAGGAAACATGATCATG
mERa mRNA     CGACGCCAGAATGGCCGAGAGAGACTGTCCAGCAGTAACGAGAAAGGAAACATGATCATG
              ************************************************************

Cloned mERa   GAGTCTGCCAAGGAGACTCGCTACTGTGCCGTGTGCAATGACTATGCCTCTGGCTACCAT
mERa mRNA     GAGTCTGCCAAGGAGACTCGCTACTGTGCCGTGTGCAATGACTATGCCTCTGGCTACCAT
              ************************************************************

Cloned mERa   TATGGGGTCTGGTCCTGCGAAGGCTGCAAGGCTTTCTTTAAGAGAAGCATTCAAGGACAC
mERa mRNA     TATGGGGTCTGGTCCTGCGAAGGCTGCAAGGCTTTCTTTAAGAGAAGCATTCAAGGACAC
              ************************************************************

Cloned mERa   AATGACTACATGTGTCCAGCTACAAACCAATGCACCATTGACAAGAACCGGAGGAAGAGT
mERa mRNA     AATGACTACATGTGTCCAGCTACAAACCAATGCACCATTGACAAGAACCGGAGGAAGAGT
              ************************************************************

Cloned mERa   TGCCAGGCCTGTCGGCTGCGCAAGTGTTACGAAGTGGGCATGATGAAAGGCGGCATACGG
mERa mRNA     TGCCAGGCCTGTCGGCTGCGCAAGTGTTACGAAGTGGGCATGATGAAAGGCGGCATACGG
              ************************************************************

Cloned mERa   AAAGACCGCCGAGGAGGGAGAATGTTGAAGCACAAGCGTCAGAGAGATGACTTGGAAGGC
mERa mRNA     AAAGACCGCCGAGGAGGGAGAATGTTGAAGCACAAGCGTCAGAGAGATGACTTGGAAGGC
              ************************************************************
```

```
Cloned mERa   CGAAATGAAATGGGTGCTTCAGGAGACATGAGGGCTGCCAACCTTTGGCCAAGCCCTCTT
mERa mRNA     CGAAATGAAATGGGTGCTTCAGGAGACATGAGGGCTGCCAACCTTTGGCCAAGCCCTCTT
              ************************************************************

Cloned mERa   GTGATTAAGCACACTAAGAAGAATAGCCCTGCCTTGTCCTTGACAGCTGACCAGATGGTC
mERa mRNA     GTGATTAAGCACACTAAGAAGAATAGCCCTGCCTTGTCCTTGACAGCTGACCAGATGGTC
              ************************************************************

Cloned mERa   AGTGCCTTGTTGGATGCTGAACCGCCCATGATCTATTCTGAATATGATCCTTCTAGACCC
mERa mRNA     AGTGCCTTGTTGGATGCTGAACCGCCCATGATCTATTCTGAATATGATCCTTCTAGACCC
              ************************************************************

Cloned mERa   TTCAGTGAAGCCTCAATGATGGGCTTATTGACCAACCTAGCAGATAGGGAGCTGGTTCAT
mERa mRNA     TTCAGTGAAGCCTCAATGATGGGCTTATTGACCAACCTAGCAGATAGGGAGCTGGTTCAT
              ************************************************************

Cloned mERa   ATGATCAACTGGGCAAAGAGAGTGCCAGGCTTTGGGGACTTGAATCTCCATGATCAGGTC
mERa mRNA     ATGATCAACTGGGCAAAGAGAGTGCCAGGCTTTGGGGACTTGAATCTCCATGATCAGGTC
              ************************************************************

Cloned mERa   CACCTTCTCGAGTGTGCCTGGCTGGAGATTCTGATGATTGGTCTCGTCTGGCGCTCCATG
mERa mRNA     CACCTTCTCGAGTGTGCCTGGCTGGAGATTCTGATGATTGGTCTCGTCTGGCGCTCCATG
              ************************************************************

Cloned mERa   GAACACCCGGGGAAGCTCCTGTTTGCTCCTAACTTGCTCCTGGACAGGAATCAAGGTAAA
mERa mRNA     GAACACCCGGGGAAGCTCCTGTTTGCTCCTAACTTGCTCCTGGACAGGAATCAAGGTAAA
              ************************************************************

Cloned mERa   TGTGTGGAAGGCATGGTGGAGATCTTTGACATGTTGCTGGCTACGTCAAGTCGGTTCCGC
mERa mRNA     TGTGTGGAAGGCATGGTGGAGATCTTTGACATGTTGCTGGCTACGTCAAGTCGGTTCCGC
              ************************************************************

Cloned mERa   ATGATGAACCTGCAGGGAGAAGAGTTTGTGTGCCTCAAATCCATCATTTTGCTTAATTCC
mERa mRNA     ATGATGAACCTGCAGGGAGAAGAGTTTGTGTGCCTCAAATCCATCATTTTGCTTAATTCC
              ************************************************************

Cloned mERa   GGAGTGTACACGTTTCTGTCCAGCACCTTGAAGTCTCTGGAAGAGAAGGACCACATCCAC
mERa mRNA     GGAGTGTACACGTTTCTGTCCAGCACCTTGAAGTCTCTGGAAGAGAAGGACCACATCCAC
              ************************************************************

Cloned mERa   CGTGTCCTGGACAAGATCACAGACACTTTGATCCACCTGATGGCCAAAGCTGGCCTGACT
mERa mRNA     CGTGTCCTGGACAAGATCACAGACACTTTGATCCACCTGATGGCCAAAGCTGGCCTGACT
              ************************************************************

Cloned mERa   CTGCAGCAGCAGCATCGCCGCCTAGCTCAGCTCCTTCTCATTCTTTCCCATATCCGGCAC
mERa mRNA     CTGCAGCAGCAGCATCGCCGCCTAGCTCAGCTCCTTCTCATTCTTTCCCATATCCGGCAC
              ************************************************************

Cloned mERa   ATGAGTAACAAAGGCATGGAGCATCTCTACAACATGAAATGCAAGAACGTTGTGCCCCTC
mERa mRNA     ATGAGTAACAAAGGCATGGAGCATCTCTACAACATGAAATGCAAGAACGTTGTGCCCCTC
              ************************************************************

Cloned mERa   TATGACCTGCTCCTGGAGATGTTGGATGCCCACCGCCTTCATGCCCCAGCCAGTCGCATG
mERa mRNA     TATGACCTGCTCCTGGAGATGTTGGATGCCCACCGCCTTCATGCCCCAGCCAGTCGCATG
              ************************************************************

Cloned mERa   GGAGTGCCCCCAGAGGAGCCCAGCCAGACCCAGCTGGCCACCACCAGCTCCACTTCAGCA
mERa mRNA     GGAGTGCCCCCAGAGGAGCCCAGCCAGACCCAGCTGGCCACCACCAGCTCCACTTCAGCA
              ************************************************************

Cloned mERa   CATTCCTTACAAACCTACTACATACCCCCGGAAGCAGAGGGCTTCCCCAACACGATCTGA
mERa mRNA     CATTCCTTACAAACCTACTACATACCCCCGGAAGCAGAGGGCTTCCCCAACACGATCTGA
              ************************************************************
```

Appendix B.

Alignment of mouse ERβ variant 1 (mERbv1) mRNA sequence with sequencing results of the mERβv1 insert cloned into the destination vector pcDNA3.1 (Cloned mERbv1). The clustal alignment software (http://www.ebi.ac.uk/Tools/msa/clustalo/) was used. *, identical amino acid between sequences.

```
CLUSTAL O(1.2.1) multiple sequence alignment

mERbv1 mRNA     ------------------------------------------------------------
Cloned mERbv1   ATACTCAAGCTATGCATCAAGCTTGGTACCGAGCTCGGATCCACTAGTAACGGCCGCCAG

mERbv1 mRNA     ----------------CCGTGAGTCTCTGAGAGCATCATGTCCATCTGTGCCTCTTCTCA
Cloned mERbv1   TGTGCTGGAATTCAGGCCGTGAATTCCAGAGAGCATCATGTCCATCTGTGCCTCTTCTCA
                      ******.*  *:********************************

mERbv1 mRNA     CAAGGATTTTTCTCAGCTGAGACCTACGCAAGACATGGAGATCAAAAACTCACCATCAAG
Cloned mERbv1   CAAGGATTTTTCTCAGCTGAGACCTACGCAAGACATGGAGATCAAAAACTCACCATCAAG
                ************************************************************

mERbv1 mRNA     CCTTACTTCCCCTGCTTCTTATAACTGTAGCCAGTCCATCCTACCCTTGGAGCATGGTCC
Cloned mERbv1   CCTTACTTCCCCTGCTTCTTATAACTGTAGCCAGTCCATCCTACCCTTGGAGCATGGTCC
                ************************************************************

mERbv1 mRNA     CATCTATATCCCTTCCTCCTATGTAGAGAGCCGTCACGAATACTCAGCCATGACATTCTA
Cloned mERbv1   CATCTATATCCCTTCCTCCTATGTAGAGAGCCGTCACGAATACTCAGCCATGACATTCTA
                ************************************************************

mERbv1 mRNA     CAGTCCTGCTGTGATGAACTACAGTGTTCCCAGCAGCACCGGTAACCTGGAAGGTGGGCC
Cloned mERbv1   CAGTCCTGCTGTGATGAACTACAGTGTTCCCAGCAGCACCGGTAACCTGGAAGGTGGGCC
                ************************************************************

mERbv1 mRNA     TGTTCGCCAGACTGCAAGCCCAAATGTGCTATGGCCAACTTCTGGACACCTCTCTCCTTT
Cloned mERbv1   TGTTCGCCAGACTGCAAGCCCAAATGTGCTATGGCCAACTTCTGGACACCTCTCTCCTTT
                ************************************************************

mERbv1 mRNA     AGCCACCCACTGCCAATCATCGCTTCTCTATGCAGAACCTCAAAAGAGTCCTTGGTGTGA
Cloned mERbv1   AGCCACCCACTGCCAATCATCGCTTCTCTATGCAGAACCTCAAAAGAGTCCTTGGTGTGA
                ************************************************************

mERbv1 mRNA     AGCAAGATCACTAGAACACACCTTGCCTGTAAACAGAGAGACCCTGAAGAGGAAGCTTGG
Cloned mERbv1   AGCAAGATCACTAGAACACACCTTGCCTGTAAACAGAGAGACCCTGAAGAGGAAGCTTGG
                ************************************************************

mERbv1 mRNA     CGGGAGCGGTTGTGCCAGCCCTGTTACTAGTCCAAGCGCCAAGAGGGATGCTCACTTCTG
Cloned mERbv1   CGGGAGCGGTTGTGCCAGCCCTGTTACTAGTCCAAGCGCCAAGAGGGATGCTCACTTCTG
                ************************************************************

mERbv1 mRNA     CGCCGTCTGCAGTGATTATGCATCTGGGTATCATTACGGTGTCTGGTCCTGTGAAGGATG
Cloned mERbv1   CGCCGTCTGCAGTGATTATGCATCTGGGTATCATTACGGTGTCTGGTCCTGTGAAGGATG
                ************************************************************

mERbv1 mRNA     TAAGGCCTTTTTTAAAAGAAGCATTCAAGGACATAATGACTATATCTGTCCAGCCACGAA
Cloned mERbv1   TAAGGCCTTTTTTAAAAGAAGCATTCAAGGACATAATGACTATATCTGTCCAGCCACGAA
                ************************************************************

mERbv1 mRNA     TCAGTGTACCATAGACAAGAACCGGCGTAAAAGCTGCCAGGCCTGCCGACTTCGCAAGTG
Cloned mERbv1   TCAGTGTACCATAGACAAGAACCGGCGTAAAAGCTGCCAGGCCTGCCGACTTCGCAAGTG
                ************************************************************

mERbv1 mRNA     TTACGAAGTAGGAATGGTCAAGTGTGGATCCAGGAGAGAAAGGTGTGGGTACCGAATAGT
Cloned mERbv1   TTACGAAGTAGGAATGGTCAAGTGTGGATCCAGGAGAGAAAGGTGTGGGTACCGAATAGT
                ************************************************************
```

```
mERbv1 mRNA     ACGAAGACAGAGAAGTGCCAGCGAGCAGGTGCATTGCCTGAACAAAGCCAAGAGAACCAG
Cloned mERbv1   ACGAAGACAGAGAAGTGCCAGCGAGCA-GTGCATTGCCTGAACAAAGCCAAGAGAACCAG
                *************************** ******************************


mERbv1 mRNA     TGGGCACACACCCCGGGTGAAGGAGCTACTGCTGAACTCTCTGAGTCCCGAGCAGCTGGT
Cloned mERbv1   TGGGCACACACCCCGGGTGAAGGAGCTACTGCTGAACTCTCTGAGTCCCGAGCAGCTGGT
                ************************************************************

mERbv1 mRNA     GCTCACCCTGCTGGAAGCTGAGCCACCCCAATGTGCTAGTGAGCCGTCCCAGCATGCCCTT
Cloned mERbv1   GCTCACCCTGCTGGAAGCTGAGCCACCCCAATGTGCTAGTGAGCCGTCCCAGCATGCCCTT
                ************************************************************

mERbv1 mRNA     CACCGAGGCCTCCATGATGATGTCCCTCACGAAGCTGGCTGACAAGGAACTGGTGCACAT
Cloned mERbv1   CACCGAGGCCTCCATGATGATGTCCCTCACGAAGCTGGCTGACAAGGAACTGGTGCACAT
                ************************************************************

mERbv1 mRNA     GATTGGCTGGGCCAAGAAAATCCCTGGCTTTGTGGAGCTCAGCCTGTTGGACCAAGTCCG
Cloned mERbv1   GATTGGCTGGGCCAAGAAAATCCCTGGCTTTGTGGAGCTCAGCCTGTTGGACCAAGTCCG
                ************************************************************

mERbv1 mRNA     CCTCTTGGAAAGCTGCTGGATGGAGGTGCTGATGGTGGGGCTGATGTGGCGCTCCATCGA
Cloned mERbv1   CCTCTTGGAAAGCTGCTGGATGGAGGTGCTGATGGTGGGGCTGATGTGGCGCTCCATCGA
                ************************************************************

mERbv1 mRNA     CCACCCCGGCAAGCTCATCTTTGCTCCAGACCTCGTTCTGGACAGGTCCTCAGAAGACCC
Cloned mERbv1   CCACCCCGGCAAGCTCATCTTTGCTCCAGACCTCGTTCTGGACAGGTCCTCAGAAGACCC
                ************************************************************

mERbv1 mRNA     TCACTGGCACGTTGCGCAGACGAAGAGTGCTGTCCCAAGGGATGAGGGGAAGTGCGTGGA
Cloned mERbv1   TCACTGGCACGTTGCGCAGACGAAGAGTGCTGTCCCAAGGGATGAGGGGAAGTGCGTGGA
                ************************************************************

mERbv1 mRNA     AGGGATTCTGGAAATCTTTGACATGCTCCTGGCGACGACGGCACGGTTCCGTGAGTTAAA
Cloned mERbv1   AGGGATTCTGGAAATCTTTGACATGCTCCTGGCGACGACGGCACGGTTCCGTGAGTTAAA
                ************************************************************

mERbv1 mRNA     ACTGCAGCACAAAGAATATCTGTGTGTGAAGGCCATGATTCTCCTCAACTCCAGTATGTA
Cloned mERbv1   ACTGCAGCACAAAGAATATCTGTGTGTGAAGGCCATGATTCTCCTCAACTCCAGTATGTA
                ************************************************************

mERbv1 mRNA     CCCCTTGGCTACCGCAAGCCAGGAAGCAGAGAGTAGCCGGAAGCTGACACACCTATTGAA
Cloned mERbv1   CCCCTTGGCTACCGCAAGCCAGGAAGCAGAGAGTAGCCGGAAGCTGACACACCTATTGAA
                ************************************************************

mERbv1 mRNA     CGCAGTGACAGATGCCCTGGTCTGGGTGATTTCGAAGAGTGGAATCTCTTCCCAGCAGCA
Cloned mERbv1   CGCAGTGACAGATGCCCTGGTCTGGGTGATTTCGAAGAGTGGAATCTCTTCCCAGCAGCA
                ************************************************************

mERbv1 mRNA     GTCAGTCCGTCTGGCCAACCTCCTGATGCTTCTTTCTCATGTCAGGCACATCAGTAACAA
Cloned mERbv1   GTCAGTCCGTCTGGCCAACCTCCTGATGCTTCTTTCTCATGTCAGGCACATCAGTAACAA
                ************************************************************

mERbv1 mRNA     GGGCATGGAACATCTGCTCAGCATGAAGTGCAAAAATGTGGTCCCGGTGTACGACCTGCT
Cloned mERbv1   GGGCATGGAACATCTGCTCAGCATGAAGTGCAAAAATGTGGTCCCGGTGTACGACCTGCT
                ************************************************************

mERbv1 mRNA     GCTGGAGATGCTGAATGCTCACACGCTTCGAGGGTACAAGTCCTCAATCTCGGGGTCTGA
Cloned mERbv1   GCTGGAGATGCTGAATGCTCACACGCTTCGAGGGTACAAGTCCTCAATCTCGGGGTCTGA
                ************************************************************

mERbv1 mRNA     GTGCTGCTCGACAGAGGACAGTAAGAGCAAAGAGGGCTCCCAGAACCTCCAGTCACAGTG
Cloned mERbv1   GTGCTGCTCGACAGAGGACAGTAAGAGCAAAGAGGGCTCCCAGAACCTCCAGTCACAGTG
                ************************************************************

mERbv1 mRNA     ACGGCCAGGCTGGAGGCGGA
Cloned mERbv1   ACGGCCAGGCTGGAGGCGGA
                ********************
```

Appendix C.

Alignment of mouse ERβ variant 2 (mERbv2) mRNA sequence with sequencing results of the mERβv1 insert cloned into into the destination vector pcDNA3.1 (Cloned mERbv2). The clustal alignment software (http://www.ebi.ac.uk/Tools/msa/clustalo/) was used. *, identical amino acid between sequences.

```
CLUSTAL O(1.2.2) multiple sequence alignment


mERbv2_mRNA         CCCGTGAGTCTCTGAGAGCATCATGTCCATCTGTGCCTCTTCTCACAAGGATTTTTCTCA
Cloned_mERbv2       ---CAGAATTCCTGAGAGCATCATGTCCATCTGTGCCTCTTCTCACAAGGATTTTTCTCA
                         ** *  **************************************************

mERbv2_mRNA         GCTGAGACCTACGCAAGACATGGAGATCAAAAACTCACCATCAAGCCTTACTTCCCCTGC
Cloned_mERbv2       GCTGAGACCTACGCAAGACATGGAGATCAAAAACTCACCATCAAGCCTTACTTCCCCTGC
                    ************************************************************

mERbv2_mRNA         TTCTTATAACTGTAGCCAGTCCATCCTACCCTTGGAGCATGGTCCCATCTATATCCCTTC
Cloned_mERbv2       TTCTTATAACTGTAGCCAGTCCATCCTACCCTTGGAGCATGGTCCCATCTATATCCCTTC
                    ************************************************************

mERbv2_mRNA         CTCCTATGTAGAGAGCCGTCACGAATACTCAGCCATGACATTCTACAGTCCTGCTGTGAT
Cloned_mERbv2       CTCCTATGTAGAGAGCCGTCACGAATACTCAGCCATGACATTCTACAGTCCTGCTGTGAT
                    ************************************************************

mERbv2_mRNA         GAACTACAGTGTTCCCAGCAGCACCGGTAACCTGGAAGGTGGGCCTGTTCGCCAGACTGC
Cloned_mERbv2       GAACTACAGTGTTCCCAGCAGCACCGGTAACCTGGAAGGTGGGCCTGTTCGCCAGACTGC
                    ************************************************************

mERbv2_mRNA         AAGCCCAAATGTGCTATGGCCAACTTCTGGACACCTCTCTCCTTTAGCCACCCACTGCCA
Cloned_mERbv2       AAGCCCAAATGTGCTATGGCCAACTTCTGGACACCTCTCTCCTTTAGCCACCCACTGCCA
                    ************************************************************

mERbv2_mRNA         ATCATCGCTTCTCTATGCAGAACCTCAAAAGAGTCCTTGGTGTGAAGCAAGATCACTAGA
Cloned_mERbv2       ATCATCGCTTCTCTATGCAGAACCTCAAAAGAGTCCTTGGTGTGAAGCAAGATCACTAGA
                    ************************************************************

mERbv2_mRNA         ACACACCTTGCCTGTAAACAGAGAGACCCTGAAGAGGAAGCTTGGCGGGAGCGGTTGTGC
Cloned_mERbv2       ACACACCTTGCCTGTAAACAGAGAGACCCTGAAGAGGAAGCTTGGCGGGAGCGGTTGTGC
                    ************************************************************

mERbv2_mRNA         CAGCCCTGTTACTAGTCCAAGCGCCAAGAGGGATGCTCACTTCTGCGCCGTCTGCAGTGA
Cloned_mERbv2       CAGCCCTGTTACTAGTCCAAGCGCCAAGAGGGATGCTCACTTCTGCGCCGTCTGCAGTGA
                    ************************************************************

mERbv2_mRNA         TTATGCATCTGGGTATCATTACGGTGTCTGGTCCTGTGAAGGATGTAAGGCCTTTTTTAA
Cloned_mERbv2       TTATGCATCTGGGTATCATTACGGTGTCTGGTCCTGTGAAGGATGTAAGGCCTTTTTTAA
                    ************************************************************

mERbv2_mRNA         AAGAAGCATTCAAGGACATAATGACTATATCTGTCCAGCCACGAATCAGTGTACCATAGA
Cloned_mERbv2       AAGAAGCATTCAAGGACATAATGACTATATCTGTCCAGCCACGAATCAGTGTACCATAGA
                    ************************************************************

mERbv2_mRNA         CAAGAACCGGCGTAAAAGCTGCCAGGCCTGCCGACTTCGCAAGTGTTACGAAGTAGGAAT
Cloned_mERbv2       CAAGAACCGGCGTAAAAGCTGCCAGGCCTGCCGACTTCGCAAGTGTTACGAAGTAGGAAT
                    ************************************************************

mERbv2_mRNA         GGTCAAGTGTGGATCCAGGAGAGAAAGGTGTGGGTACCGAATAGTACGAAGACAGAGAAG
Cloned_mERbv2       GGTCAAGTGTGGATCCAGGAGAGAAAGGTGTGGGTACCGAATAGTACGAAGACAGAGAAG
                    ************************************************************

mERbv2_mRNA         TGCCAGCGAGCAGGTGCATTGCCTGAACAAAGCCAAGAGAACCAGTGGGCACACACCCCG
Cloned_mERbv2       TGCCAGCGAGCAGGTGCATTGCCTGAACAAAGCCAAGAGAACCAGTGGGCACACACCCCG
                    ************************************************************
```

```
mERbv2_mRNA         GGTGAAGGAGCTACTGCTGAACTCTCTGAGTCCCGAGCAGCTGGTGCTCACCCTGCTGGA
Cloned_mERbv2       GGTGAAGGAGCTACTGCTGAACTCTCTGAGTCCCGAGCAGCTGGTGCTCACCCTGCTGGA
                    ************************************************************

mERbv2_mRNA         AGCTGAGCCACCCAATGTGCTAGTGAGCCGTCCCAGCATGCCCTTCACCGAGGCCTCCAT
Cloned_mERbv2       AGCTGAGCCACCCAATGTGCTAGTGAGCCGTCCCAGCATGCCCTTCACCGAGGCCTCCAT
                    ************************************************************

mERbv2_mRNA         GATGATGTCCCTCACGAAGCTGGCTGACAAGGAACTGGTGCACATGATTGGCTGGGCCAA
Cloned_mERbv2       GATGATGTCCCTCACGAAGCTGGCTGACAAGGAACTGGTGCACATGATTGGCTGGGCCAA
                    ************************************************************

mERbv2_mRNA         GAAAATCCCTGGCTTTGTGGAGCTCAGCCTGTTGGACCAAGTCCGCCTCTTGGAAAGCTG
Cloned_mERbv2       GAAAATCCCTGGCTTTGTGGAGCTCAGCCTGTTGGACCAAGTCCGCCTCTTGGAAAGCTG
                    ************************************************************

mERbv2_mRNA         CTGGATGGAGGTGCTGATGGTGGGGCTGATGTGGCGCTCCATCGACCACCCCGGCAAGCT
Cloned_mERbv2       CTGGATGGAGGTGCTGATGGTGGGGCTGATGTGGCGCTCCATCGACCACCCCGGCAAGCT
                    ************************************************************

mERbv2_mRNA         CATCTTTGCTCCAGACCTCGTTCTGGACAGGGATGAGGGGAAGTGCGTGGAAGGGATTCT
Cloned_mERbv2       CATCTTTGCTCCAGACCTCGTTCTGGACAGGGATGAGGGGAAGTGCGTGGAAGGGATTCT
                    ************************************************************

mERbv2_mRNA         GGAAATCTTTGACATGCTCCTGGCGACGACGGCACGGTTCCGTGAGTTAAAACTGCAGCA
Cloned_mERbv2       GGAAATCTTTGACATGCTCCTGGCGACGACGGCACGGTTCCGTGAGTTAAAACTGCAGCA
                    ************************************************************

mERbv2_mRNA         CAAAGAATATCTGTGTGTGAAGGCCATGATTCTCCTCAACTCCAGTATGTACCCCTTGGC
Cloned_mERbv2       CAAAGAATATCTGTGTGTGAAGGCCATGATTCTCCTCAACTCCAGTATGTACCCCTTGGC
                    ************************************************************

mERbv2_mRNA         TACCGCAAGCCAGGAAGCAGAGAGTAGCCGGAAGCTGACACACCTATTGAACGCAGTGAC
Cloned_mERbv2       TACCGCAAGCCAGGAAGCAGAGAGTAGCCGGAAGCTGACACACCTATTGAACGCAGTGAC
                    ************************************************************

mERbv2_mRNA         AGATGCCCTGGTCTGGGTGATTTCGAAGAGTGGAATCTCTTCCCAGCAGCAGTCAGTCCG
Cloned_mERbv2       AGATGCCCTGGTCTGGGTGATTTCGAAGAGTGGAATCTCTTCCCAGCAGCAGTCAGTCCG
                    ************************************************************

mERbv2_mRNA         TCTGGCCAACCTCCTGATGCTTCTTTCTCATGTCAGGCACATCAGTAACAAGGGCATGGA
Cloned_mERbv2       TCTGGCCAACCTCCTGATGCTTCTTTCTCATGTCAGGCACATCAGTAACAAGGGCATGGA
                    ************************************************************

mERbv2_mRNA         ACATCTGCTCAGCATGAAGTGCAAAAATGTGGTCCCGGTGTACGACCTGCTGCTGGAGAT
Cloned_mERbv2       ACATCTGCTCAGCATGAAGTGCAAAAATGTGGTCCCGGTGTACGACCTGCTGCTGGAGAT
                    ************************************************************

mERbv2_mRNA         GCTGAATGCTCACACGCTTCGAGGGTACAAGTCCTCAATCTCGGGGTCTGAGTGCTGCTC
Cloned_mERbv2       GCTGAATGCTCACACGCTTCGAGGGTACAAGTCCTCAATCTCGGGGTCTGAGTGCTGCTC
                    ************************************************************

mERbv2_mRNA         GACAGAGGACAGTAAGAGCAAAGAGGGCTCCCAGAACCTCCAGTCACAGTGACGG
Cloned_mERbv2       GACAGAGGACAGTAAGAGCAAAGAGGGCTCCCAGAACCTCCAGTCACAGTGACGG
                    ********************************************************
```

Appendix D.

Alignment of mouse ERβ variant 1 (ERb_v1) and variant 2 (ERb_v2) amino acid sequences with 5 hERβ amino acid sequences using clustal alignment software (http://www.ebi.ac.uk/Tools/msa/clustalo/). *, identical amino acid in all sequences. Unique ERβ variant 1 domain is shown in red.

```
CLUSTAL O(1.2.2) multiple sequence alignment


mERb_v1      MSICASSHKDFSQLRPTQDMEIKNSPSSLTSPASYNCSQSILPLEHGPIYIPSSYVESRH
mERb_v2      MSICASSHKDFSQLRPTQDMEIKNSPSSLTSPASYNCSQSILPLEHGPIYIPSSYVESRH
hERb_v1      -------------------MDIKNSPSSLNSPSSYNCSQSILPLEHGSIYIPSSYVDSHH
hERb_v5      -------------------MDIKNSPSSLNSPSSYNCSQSILPLEHGSIYIPSSYVDSHH
hERb_v3      -------------------MDIKNSPSSLNSPSSYNCSQSILPLEHGSIYIPSSYVDSHH
hERb_v2      -------------------MDIKNSPSSLNSPSSYNCSQSILPLEHGSIYIPSSYVDSHH
hERb_v6      -------------------MDIKNSPSSLNSPSSYNCSQSILPLEHGSIYIPSSYVDSHH
                               * ******** ** ************** ******** * *

mERb_v1      EYSAMTFYSPAVMNYSVPSSTGNLEGGPVRQTASPNVLWPTSGHLSPLATHCQSSLLYAE
mERb_v2      EYSAMTFYSPAVMNYSVPSSTGNLEGGPVRQTASPNVLWPTSGHLSPLATHCQSSLLYAE
hERb_v1      EYPAMTFYSPAVMNYSIPSNVTNLEGGPGRQTTSPNVLWPTPGHLSPLVVHRQLSHLYAE
hERb_v5      EYPAMTFYSPAVMNYSIPSNVTNLEGGPGRQTTSPNVLWPTPGHLSPLVVHRQLSHLYAE
hERb_v3      EYPAMTFYSPAVMNYSIPSNVTNLEGGPGRQTTSPNVLWPTPGHLSPLVVHRQLSHLYAE
hERb_v2      EYPAMTFYSPAVMNYSIPSNVTNLEGGPGRQTTSPNVLWPTPGHLSPLVVHRQLSHLYAE
hERb_v6      EYPAMTFYSPAVMNYSIPSNVTNLEGGPGRQTTSPNVLWPTPGHLSPLVVHRQLSHLYAE
             ** ************** **   ****** *** ******** ******  * * * ****

mERb_v1      PQKSPWCEARSLEHTLPVNRETLKRKLGGSGCASPVTSPSAKRDAHFCAVCSDYASGYHY
mERb_v2      PQKSPWCEARSLEHTLPVNRETLKRKLGGSGCASPVTSPSAKRDAHFCAVCSDYASGYHY
hERb_v1      PQKSPWCEARSLEHTLPVNRETLKRKVSGNRCASPVTGPGSKRDAHFCAVCSDYASGYHY
hERb_v5      PQKSPWCEARSLEHTLPVNRETLKRKVSGNRCASPVTGPGSKRDAHFCAVCSDYASGYHY
hERb_v3      PQKSPWCEARSLEHTLPVNRETLKRKVSGNRCASPVTGPGSKRDAHFCAVCSDYASGYHY
hERb_v2      PQKSPWCEARSLEHTLPVNRETLKRKVSGNRCASPVTGPGSKRDAHFCAVCSDYASGYHY
hERb_v6      PQKSPWCEARSLEHTLPVNRETLKRKVSGNRCASPVTGPGSKRDAHFCAVCSDYASGYHY
             *************************  *  ****** *  ******************

mERb_v1      GVWSCEGCKAFFKRSIQGHNDYICPATNQCTIDKNRRKSCQACRLRKCYEVGMVKCGSRR
mERb_v2      GVWSCEGCKAFFKRSIQGHNDYICPATNQCTIDKNRRKSCQACRLRKCYEVGMVKCGSRR
hERb_v1      GVWSCEGCKAFFKRSIQGHNDYICPATNQCTIDKNRRKSCQACRLRKCYEVGMVKCGSRR
hERb_v5      GVWSCEGCKAFFKRSIQGHNDYICPATNQCTIDKNRRKSCQACRLRKCYEVGMVKCGSRR
hERb_v3      GVWSCEGCKAFFKRSIQGHNDYICPATNQCTIDKNRRKSCQACRLRKCYEVGMVKCGSRR
hERb_v2      GVWSCEGCKAFFKRSIQGHNDYICPATNQCTIDKNRRKSCQACRLRKCYEVGMVKCGSRR
hERb_v6      GVWSCEGCKAFFKRSIQGHNDYICPATNQCTIDKNRRKSCQACRLRKCYEVGMVKCGSRR
             ************************************************************

mERb_v1      ERCGYRIVRRQRSASEQVHCLNKAKRTSGHTPRVKELLLNSLSPEQLVLTLLEAEPPNVL
mERb_v2      ERCGYRIVRRQRSASEQVHCLNKAKRTSGHTPRVKELLLNSLSPEQLVLTLLEAEPPNVL
hERb_v1      ERCGYRLVRRQRSADEQLHCAGKAKRSGGHAPRVRELLLDALSPEQLVLTLLEAEPPHVL
hERb_v5      ERCGYRLVRRQRSADEQLHCAGKAKRSGGHAPRVRELLLDALSPEQLVLTLLEAEPPHVL
hERb_v3      ERCGYRLVRRQRSADEQLHCAGKAKRSGGHAPRVRELLLDALSPEQLVLTLLEAEPPHVL
hERb_v2      ERCGYRLVRRQRSADEQLHCAGKAKRSGGHAPRVRELLLDALSPEQLVLTLLEAEPPHVL
hERb_v6      ERCGYRLVRRQRSADEQLHCAGKAKRSGGHAPRVRELLLDALSPEQLVLTLLEAEPPHVL
             ****** ******* ** **  ****  ** *** ****  *************** **

mERb_v1      VSRPSMPFTEASMMMSLTKLADKELVHMIGWAKKIPGFVELSLLDQVRLLESCWMEVLMV
mERb_v2      VSRPSMPFTEASMMMSLTKLADKELVHMIGWAKKIPGFVELSLLDQVRLLESCWMEVLMV
hERb_v1      ISRPSAPFTEASMMMSLTKLADKELVHMISWAKKIPGFVELSLFDQVRLLESCWMEVLMM
hERb_v5      ISRPSAPFTEASMMMSLTKLADKELVHMISWAKKIPGFVELSLFDQVRLLESCWMEVLMM
hERb_v3      ISRPSAPFTEASMMMSLTKLADKELVHMISWAKKIPGFVELSLFDQVRLLESCWMEVLMM
hERb_v2      ISRPSAPFTEASMMMSLTKLADKELVHMISWAKKIPGFVELSLFDQVRLLESCWMEVLMM
hERb_v6      ISRPSAPFTEASMMMSLTKLADKELVHMISWAKKIPGMYPLVTATQDADSSRKLAHLLNA
              **** ********************** *******   *    *           *
```

```
mERb_v1      GLMWRSIDHPGKLIFAPDLVLDRSSEDPHWHVAQTKSAVPRDEGKCVEGILEIFDMLLAT
mERb_v2      GLMWRSIDHPGKLI-----------------FAPDLVLDRDEGKCV-EGILEIFDMLLAT
hERb_v1      GLMWRSIDHPGKLI-----------------FAPDLVLDRDEGKCV-EGILEIFDMLLAT
hERb_v5      GLMWRSIDHPGKLI-----------------FAPDLVLDRDEGKCV-EGILEIFDMLLAT
hERb_v3      GLMWRSIDHPGKLI-----------------FAPDLVLDRDEGKCV-EGILEIFDMLLAT
hERb_v2      GLMWRSIDHPGKLI-----------------FAPDLVLDRDEGKC-VEGILEIFDMLLAT
hERb_v6      V------TDALVWV-----------------IAKSGISSQQQSMRLANLLMLLSHVRHAS
                                              *                        *

mERb_v1      TARFRELKLQHKEYLCVKAMILLNSSMYPLATASQEAESSRKLTHLLNAVTDALVWVISK
mERb_v2      TARFRELKLQHKEYLCVKAMILLNSSMYPLATASQEAESSRKLTHLLNAVTDALVWVISK
hERb_v1      TSRFRELKLQHKEYLCVKAMILLNSSMYPLVTATQDADSSRKLAHLLNAVTDALVWVIAK
hERb_v5      TSRFRELKLQHKEYLCVKAMILLNSSMYPLVTATQDADSSRKLAHLLNAVTDALVWVIAK
hERb_v3      TSRFRELKLQHKEYLCVKAMILLNSSMYPLVTATQDADSSRKLAHLLNAVTDALVWVIAK
hERb_v2      TSRFRELKLQHKEYLCVKAMILLNSSMYPLVTATQDADSSRKLAHLLNAVTDALVWVIAK
hERb_v6      NKGMEH----LLNMKCKNVVP-----VYDLLLEMLNAHVLRG---CKSSIT---------
                          *          * *      *   *         *

mERb_v1      SGISSQQQSVRLANLLMLLSHVRHISNKGMEHLLSMKCKNVVPVYDLLLEMLNAHTLRGY
mERb_v2      SGISSQQQSVRLANLLMLLSHVRHISNKGMEHLLSMKCKNVVPVYDLLLEMLNAHTLRGY
hERb_v1      SGISSQQQSMRLANLLMLLSHVRHASNKGMEHLLNMKCKNVVPVYDLLLEMLNAHVLRGC
hERb_v5      SGISSQQQSMRLANLLMLLSHVRHARSCVYK-----------------------------
hERb_v3      SGISSQQQSMRLANLLMLLSHVRHARWGEKQFIHLKLS----------------------
hERb_v2      SGISSQQQSMRLANLLMLLSHVRHARAEKASQTLTSFG------MKMETLLPEATMEQ--
hERb_v6      -GS-----ECSPAED-----------------SKSKEG------SQNPQSQ---------
              *          *

mERb_v1      KSSISGSECCSTEDSKSKEGSQNLQSQ
mERb_v2      KSSISGSECCSTEDSKSKEGSQNLQSQ
hERb_v1      KSSITGSECSPAEDSKSKEGSQNPQSQ
hERb_v5      ---------------------------
hERb_v3      ---------------------------
hERb_v2      ---------------------------
hERb_v6      ---------------------------
```